FAA-RD-83/26

Project Report
ATC-121

An Experimental GPS Navigation Receiver for General Aviation: Design and Measured Performance

S. D. Campbell
R. R. LaFrey

27 September 1983

Lincoln Laboratory
MASSACHUSETTS INSTITUTE OF TECHNOLOGY
LEXINGTON, MASSACHUSETTS

Prepared for the Federal Aviation Administration,
Washington, D.C. 20591

Technical Report Documentation Page

1. Report No.	2. Government Accession No.	3. Recipient's Catalog No.
FAA-RD-83/26		

4. Title and Subtitle	5. Report Date / 6. Performing Organization Code
An Experimental GPS Navigation Receiver for General Aviation: Design and Measured Performance	5. Report Date: 27 September 1983 6. Performing Organization Code:
7. Author(s)	**8. Performing Organization Report No.**
Steven D. Campbell and Raymond R. LaFrey	ATC-121
9. Performing Organization Name and Address	**10. Work Unit No.** / **11. Contract or Grant No.**
Massachusetts Institute of Technology Lincoln Laboratory, M.I.T. P.O. Box 73 Lexington, MA 02173-0073	10. Work Unit No.: 11. Contract or Grant No.: DOT-FA79-WAI-091
12. Sponsoring Agency Name and Address	**13. Type of Report and Period Covered** / **14. Sponsoring Agency Code**
Department of Transportation Federal Aviation Administration Systems Research and Development Service Washington, DC 20591	13. Type of Report and Period Covered: Project Report 14. Sponsoring Agency Code:

15. Supplementary Notes

The work reported in this document was performed at Lincoln Laboratory, a center for research operated by Massachusetts Institute of Technology, under Air Force Contract F19628-80-C-0002.

16. Abstract

This report describes work performed by M.I.T. Lincoln Laboratory, between 1 October 1979 and 1 March 1983, to evaluate the use of the Global Positioning System (GPS) for low-cost civil air navigation.

The report describes a GPS Test and Evaluation System developed jointly by M.I.T. Lincoln Laboratory, Stanford Telecommunications, Inc., and Intermetrics, Inc., using techniques that could lead to low-cost commercial avionics. System performance results obtained in the laboratory and during flight tests are provided which demonstrate compliance with current and future navigation accuracy requirements for enroute, terminal and non-precision approach flight paths. The report also includes functional specifications for a low-cost GPS navigation system for civil aircraft.

The GPS Test and Evaluation system design was based on two important features: 1) automatic tracking of all visible satellites (rather than a minimum set of four) and 2) a dual-channel GPS C/A code receiver. Tracking all visible satellites allows the system to maintain continuous navigation when a satellite sets or is momentarily masked during aircraft maneuvers. The dual-channel receiver dedicates one channel to pseudo-range measurements, and the other channel to acquiring new satellites as they become visible. These two features, validated by flight test, allow the system to provide continuous navigation updates during critical aircraft maneuvers, such as non-precision approaches, and during satellite constellation changes.

17. Key Words	18. Distribution Statement
NAVSTAR GPS global positioning system air navigation civil aviation general aviation C/A code receiver dual-channel receiver	Document is available to the public through the National Technical Information Service, Springfield, Virginia 22151

19. Security Classif. (of this report)	20. Security Classif. (of this page)	21. No. of Pages	22. Price
Unclassified	Unclassified	254	

CONTENTS

CONTENTS (CONT'D)

ILLUSTRATIONS

ILLUSTRATIONS (CONT'D)

ILLUSTRATIONS (CONT'D)

ILLUSTRATIONS (CONT'D)

TABLES

TABLES (CONT'D)

1.0 INTRODUCTION AND SUMMARY

This report describes the work performed by M.I.T. Lincoln Laboratory, between 1 October 1979 and 1 March 1983 to evaluate the use of the Global Positioning System (GPS) for low-cost civil air navigation. The effort was supported by the Federal Aviation Administration through Interagency Agreement DOT-FA79WAI-091 between the FAA and the United States Air Force.

M.I.T. Lincoln Laboratory was tasked by the FAA to develop a GPS Test and Evaluation System and to flight test the system in a typical general aviation aircraft. The system was required to meet FAA accuracy requirements for area navigation systems and to use techniques that could lead to low-cost commercial avionics. This report describes the system design, and provides system performance results from laboratory and flight tests. The report also includes functional specifications for a low-cost GPS navigation system based on validated design concepts.

The GPS Test and Evaluation system design was based on two important features: 1) automatic tracking of all visible satellites (rather than a minimum set of four) and 2) a dual-channel GPS C/A code receiver. Tracking all visible satellites allows the system to maintain continuous navigation when a satellite sets or is momentarily masked during aircraft maneuvers. The dual-channel receiver dedicates one channel to pseudo-range measurements, and the other channel to acquiring new satellites as they become visible. These two features allow the system to provide continuous navigation updates during aircraft maneuvers such as non-precision approaches and during satellite constellation changes.

The major elements of the GPS Test and Evaluation System are:

- Dual Channel Receiver - a unit developed by Stanford Telecommunications, Inc. that sequentially tracks satellites on one channel while the other channel acquires new satellites and demodulates data; provides pseudo-range estimates and satellite data to the Position Processor.

- Position Processor - a microcomputer with software developed by Intermetrics, Inc. that manages the receiver channels and computes geodetic position estimates.

- Navigation Processor - a microcomputer that translates geodetic estimates into displays suitable for pilot navigation.

- Pilot Displays - a standard Course Deviation Indicator/Omni-Bearing Selector (CDI/OBS) and a Control and Display Unit (CDU), designed to provide navigation data to the pilot in a format consistent with current civil navigation practices.

The system also includes extensive instrumentation and data recording capabilities for post-flight data analysis.

The performance of the GPS Test and Evaluation System was measured during laboratory tests and during flight tests in a typical twin-engine general aviation aircraft, a Rockwell Aero Commander. The laboratory test showed that the typical static RMS horizontal position error was 93 feet. The flight tests showed a RMS horizontal error of 189 feet and a 95% confidence horizontal error of 333 feet in typical general aviation operations. As shown below, the measured accuracy was well within the requirements of FAA Advisory Circular 90-45A for two-dimensional area navigation and essentially met the proposed 328 ft., 95% Federal Navigation Plan requirement for non-precision approach.

Navigation Accuracy Summary

	Horizontal (95%) (ft)
FAA Advisory Circular 90-45A Approach, ascent/descent	1824.
Federal Radionavigation Plan Non-precision approach	328.
Accuracy Achieved Level and turning mix	333.

Operation of the GPS Test and Evaluation System was evaluated in areas of mountainous terrain, at a large urban airport and in typical general aviation operations. The system was shown to provide continuous navigation service during 30° bank-angle turns and was able to track satellites with elevation angles as low as 5°. Finally, the system appeared to be compatible with existing air-traffic control procedures and air-crew practices.

Although the experimental GPS was found to perform well as a practical general aviation navigation system, it was physically large. This was necessary in order that the system be constructed from readily available components and that it provide for experimental flexibility. However, the increasing use of VLSI digital techniques is likely to result in a system design which can be produced in an avionics package comparable in size to that of present day commercially available area navigation equipment. The cost, as estimated by ARINC Research, Inc., of a GPS navigator based on the Lincoln design was $8500 in 1982 dollars assuming the use of circa-1990 integrated-circuit technology.

The remainder of this report is divided into four sections. Section 2.0 provides an overview of the project and details the performance requirements and goals. Section 3.0 describes the system design, including the hardware characteristics and software architecture. Section 4.0 provides the system performance results, including ground and flight test measurements. Section 5.0 gives functional requirements of a general aviation GPS navigation system as determined from the results of this project.

2.0 PROJECT OVERVIEW

2.1 Background and Objectives

The NAVSTAR Global Positioning System (GPS) is a satellite-based system currently being developed by the Department of Defense to provide position information to suitably equipped military users. Such users will receive world-wide, continuous, real-time, all weather, precision navigation data from a constellation of 18 satellites in 12 hour orbits (Ref. 1). Six satellites have been placed in orbit and ground support facilities have been developed to support user equipment development.

Previous studies (Refs. 2, 3) suggested that a GPS navigator meeting FAA performance requirements could be developed at a cost consistent with general aviation use. However, the performance of low cost GPS receiver designs had not been fully determined by field measurement. To fill this gap, M.I.T. Lincoln Laboratory was tasked by the Federal Aviation Adminstration to a) develop GPS Test and Evaluation Equipment functionally consistent with a low cost design and FAA two-dimensional (2-D) navigation requirements, b) evaluate the design by field measurement, and c) develop a functional specification for a general aviation GPS receiver. Lincoln Laboratory contracted with Stanford Telecommunications, Inc., to develop a dual channel receiver, and Intermetrics, Inc., to develop receiver management and position estimation software. To establish cost, the FAA tasked ARINC Research, Inc., to estimate the cost of a commercial version of the design developed at Lincoln Laboratory; the results of that cost study have been reported by ARINC Research in a separate document (Ref. 4).

2.2 Current Civil Navigation Requirements

In order that a navigation system be acceptable for civil aviation it must satisfy needs within four major areas of concern: accuracy, reliability integrity, and compatibility.

2.2.1 Accuracy

The basic output of the typical GPS navigation system is a geodetic (latitude-longitude) position estimate. This is to be contrasted with low cost VOR/DME navigation receivers which produce rho-theta (range-bearing) estimates with respect to a ground facility. The relevant specifications from FAA Advisory Circular 90-45A, (Ref. 5) for GPS are shown summarized in Table 2-1.

Position accuracy should not be considered apart from update rate. Equipment intended for use in non-precision approaches should provide navigation information that is essentially continuous with interruptions no longer than would result from switching from one pre-programmed waypoint to another. Also, navigation service should be continuously available during flight in any direction/climb/descend profile approved by the aircraft manufacturer. The navigation service shall, per AC90-45A, be restored (if temporarily lost due to bank-induced fades) within 5 seconds after the completion of any allowable maneuver. Also, the time lag between data measurements and displayed position must not be operationally significant.

TABLE 2-1

AC90-45A 2-D NAVIGATION REQUIREMENTS

	Position Accuracy Requirements - 95% Conf. (Averaged Over One Update Cycle)	
	Cross-Track	Along-Track
Flight Technical Error[1] (FTE)		
Enroute[2]	2.0 nmi	--
Terminal[3]	1.0 nmi	--
Non-Precision Approach[4]	0.5 nmi	--
Navigation Equipment Error		
Enroute	1.5 nmi	1.5 nmi
Terminal	1.1 nmi	1.1 nmi
Non-Precision Approach	0.3 nmi	0.3 nmi
Total Error[5]		
Enroute	2.5 nmi	1.5 nmi
Terminal	1.5 nmi	1.1 nmi
Non-Precision Approach	0.6 nmi	0.3 nmi

1. FTE accounts for deviations due to display interpretation, pilot response and aircraft response.

2. Enroute = Cruising flight between terminal areas.

3. Terminal = Between enroute and approach; normally below 18000 feet and within 50 miles of the airport.

4. Non-Precision Approach = Between final approach waypoint and airport.

5. Total Error = RSS combination of FTE and navigation equipment errors.

As part of the test and evaluation equipment design development, the accuracy and update specifications in Table 2-2 were established. The dynamic requirement is the Non-Precision Approach approach tolerance of AC90-45A. The static requirement is derived from a generic low-cost receiver model. An additional requirement, Time-to-First-Fix, was established based on the typical time between first turn-on of the avionics and when the general aviation aircraft is positioned near the departure runway.

2.2.2 Reliability

The GPS navigation system encompassing the user equipment, satellite vehicles and ground support equipment, must have a combined reliability equal to or surpassing that of alternative navigation systems. The GPS user equipment must therefore provide navigation data without operationally significant outages due to fades or multipath, assuming that the NAVSTAR constellation provides acceptable coverage.

2.2.3 Integrity

The GPS navigation system must not provide misleading information under any conditions of operational significance. It is therefore necessary that the GPS receiver continually monitor its own performance and indicate to the pilot when the navigation information displayed is no longer in compliance with the accuracy requirements.

Further, provisions must be incorporated to allow the pilot to verify that the navigation information is accurate using either built-in test equipment, an auxiliary test system, or a procedural check.

2.2.4 Compatibility

The GPS navigation system must provide a pilot interface which is compatible with existing air navigation systems. This requirement stems from the way that pilots are accustomed to using aircraft navigation systems.

2.3 Future Civil Navigation Requirements

To anticipate the more stringent navigation requirements likely in the future, the accuracy and update rate goals in Table 2-3 were established for the GPS Test and Evaluation (T and E) equipment.

Later, after the GPS T and E Equipment specifications were frozen in procurement specifications, the Federal Radio Navigation Plan (FRP) (Ref. 6) was completed and published. The FRP established new future navigation requirements that are summarized in Table 2-4.

The rationale for increasing the accuracy is to provide a service equivalent to that provided by on-airport VOR's which now exist at approximately 30% of all U.S. airfields.

TABLE 2-2

GPS TEST AND EVALUATION EQUIPMENT ACCURACY AND UPDATE REQUIREMENTS

Horizontal Dynamic Position Error[1]	0.3 NM, 95%
Horizontal Static Position Error[2]	335 ft., 95%
Update Rate	0.5 Hz, min
Time to First Fix[3]	6 minutes, max

Assumptions:

Velocity < 200 KTS

Acceleration < 0.5g

L1 C/A only

No artifical degradation of the GPS navigation message data or intentional electromagnetic interference

1. For HDOP* < 5, bank angle > 30°.
2. For HDOP < 2.0 and a 2 minute integration.
3. From power-on until cockpit display of position fix.

*Horizontal Dilution of Precision.

TABLE 2-3

GPS TEST AND EVALUATION EQUIPMENT PERFORMANCE GOALS

Horizontal Position Error[1]	
Level Flight	500 ft., 95%
Turning Flight	1000 ft., 95%
Vertical Position Error[2]	
Enroute level flight	163 ft., 95%
Terminal level flight	163 ft., 95%
Approach level flight	88 ft., 95%
Enroute Ascend/Descent	275 ft., 95%
Terminal Ascend/Descent	205 ft., 95%
Approach Ascend/Descent	116 ft., 95%
Update Rate	1 Hz, min

1. For HDOP < 5, bank angle < 30°, ground speed < 200 KTS.
2. From AC90-45A (Total error less FTE, Table B, Appendix A); same conditions as Horizontal Goals.

TABLE 2-4

FRP NAVIGATION ACCURACY TO MEET PROJECTED FUTURE REQUIREMENTS

Phase	Altitude	Horizontal Position Error
Enroute	500 ft. to FL 180*	1000 meters (2 drms) (3280 ft.)
Terminal	500 ft. to FL 180	500 meters (95%) (1650 ft.)
Non-Precision Approach	250 to 3000 ft. above surface	100 meters (95%) (328 ft.)

*FL 180 means flight level 18,000 feet.

2.4 Assumptions

The following assumptions were made for the development and testing of the GPS T and E Equipment:

a. The satellites will radiate the L1 signal such that the received signal at the civil users GPS antenna input will meet or exceed the levels specified in the space segment User Interface ICD, (Ref. 7).

b. The radiated signals from the GPS satellites will not be artifically degraded to reduce accuracy.

c. The T and E Equipment will not be exposed to intentional radio frequency interference.

2.5 General Approach

2.5.1 Development

The development of the GPS T and E Equipment was, in part, based on past work (Ref. 7) and on the DOD GPS user equipment developments that suggested:

a. Designs which tracked all satellites in view (a significant advantage) could be realized at reasonable cost,

b. Designs which convert functions from hardware to firmware using microcomputers would reduce cost, and

c. An L1 C/A-only receiver would be able to provide acceptable accuracy for civil general aviation users.

The need for continuous navigation service, especially during non-precision approaches, led to the requirement that the T and E Equipment contain two independent channels. The need to evaluate performance under a variety of stressing situations resulted in the requirement for extensive instrumentation. The requirement to evaluate operational issues lead to the definition of a general purpose cockpit display consistent with current civil navigation procedures.

It was assumed that during the initial general aviation use of GPS, the pilot interface would be consistent with the VOR/DME system, with RNAV features as added options. This implied that the following features would be available on initial GPS receivers and therefore should be part of the T and E Equipment:

a. Automatic Operation. The receiver should automatically acquire and track satellites, estimate position and continually monitor performance without operator intervention.

b. Course Deviation Indicator (CDI) Interface. The receiver should accept desired course bearing from an Omni Bearing Selector (OBS) and provide signals to drive the Course-Deviation Indicator (CDI).

c. Magnetic Bearing. A map should be provided to apply local magnetic variation corrections (to within ± 1 degree); the map to be stored in a non-volatile memory.

d. Way Points. The system should accept way points in the form of unambiguous designators such as the current letter codes. The receiver could then maintain several thousand waypoints with their associated geographical coordinates in a non-volatile memory.

The concern for integrity led to the inclusion of performance monitoring and fail-soft techniques. Tests such as satellite health checks, pseudo-range consistency tests, position estimate variance tests and geometry tests were provided.

Finally, low cost was emphasized by designing to requirements that are consistent with civil aviation navigation and by using technology which can be expected to become inexpensive in the current decade.

The design and construction of the equipment was accomplished during 1980-82. As mentioned previously, Standard Telecommunications, Inc., developed the dual channel receiver and Intermetrics, Inc., developed software which managed the receivers and estimated position. Lincoln Laboratory developed the navigation software, instrumentation, Control and Display Unit (CDU), and ground support facilities, conducted ground and flight measurements, and evaluated system performance.

2.5.2 Evaluation

In keeping with the principal concerns, field evaluation of the GPS T and E equipment focused on a) link margins and position estimation techniques, b) performance monitoring and fail-soft techniques, and c) operational performance in typical general aviation flight operations with emphasis on non-precision approaches.

Link margins were evaluated by determining the effects of:

a) the number and location of available satellites,
b) received signal strength,
c) multipath and terrain blockage,
d) electromagnetic interference (EMI),
e) antenna shielding, and
f) receiver acquisition and tracking

on the acquisition time, positional accuracy and update reliability. Accuracy was measured using truth derived from a ground tracker while flying the T and E Equipment in a general aviation aircraft. The position estimation technique, including its smoothing filter, was evaluated to assess the effect of signal margin and aircraft dynamics on the position estimate variance.

Performance monitoring and fail-soft features were evaluated within the limitations of the current GPS constellation.

Operational evaluation flights were conducted using a limited set of cross-country, terminal and non-precision approach flight plans in the New England area. The cockpit was configured to allow the test pilot to simultaneously observe the GPS CDU and CDI, and a conventional VOR-driven CDI.

3.0 GPS TEST AND EVALUATION EQUIPMENT DESIGN

3.1 System Design

The GPS T and E Equipment is shown in Fig. 3-1. This design provides high rate (5 Hz) sequential processing of all visible GPS satellites in order to support a position estimate update rate of 1.0 Hz. Two channels are provided in order for one channel to be dedicated to high rate sequential pseudo-range processing while the other is available to demodulate satellite navigation messages. This assures continuous navigation service during non-precision approaches.

The key features of the system design are:

a. Automatic Operation. The receiver automatically acquires all satellites in view and provides a first fix to the pilot in less than 6 minutes. If required (after being powered-off for more than 30 days), it automatically acquires fresh almanac data, which increases the time-to-first fix (TTFF) to 16 minutes. The receiver normally requires no operator intervention during use other than such navigation functions as waypoint entry.

b. Performance Monitoring. The receiver continually monitors satellite data, pseudo-range estimates, receiver parameters, and position solution estimates in order to determine compliance with FAA navigation requirements.

c. Microprocessor Based Design. The receiver makes extensive use of microprocessor technology to synthesize receiver loops, manage receiver operations and compute own position.

d. Intelligent Control and Display Unit. The control and display unit is managed by a separate Z80 microprocessor in order to allow developmental flexibility in the pilot display interface design without affecting the receiver design.

e. Operational Compatibility. The design incorporates modes of operation consistent with current VOR enroute terminal and non-precision approach procedures. In addition, it includes direct routing area navigation (RNAV) modes.

3.1.1 System Timing

The typical sequence of events following power-on is illustrated in Fig. 3-2. During a brief initialization period, built-in diagnostics test microprocessor and receiver functions, and the age of the stored almanac are checked. The position software uses the last stored position and almanac data to select four space vehicles (SV's) for initial acquisition. The first SV is then assigned to both channels, one searching the 1023 chip code in a 1500 Hz

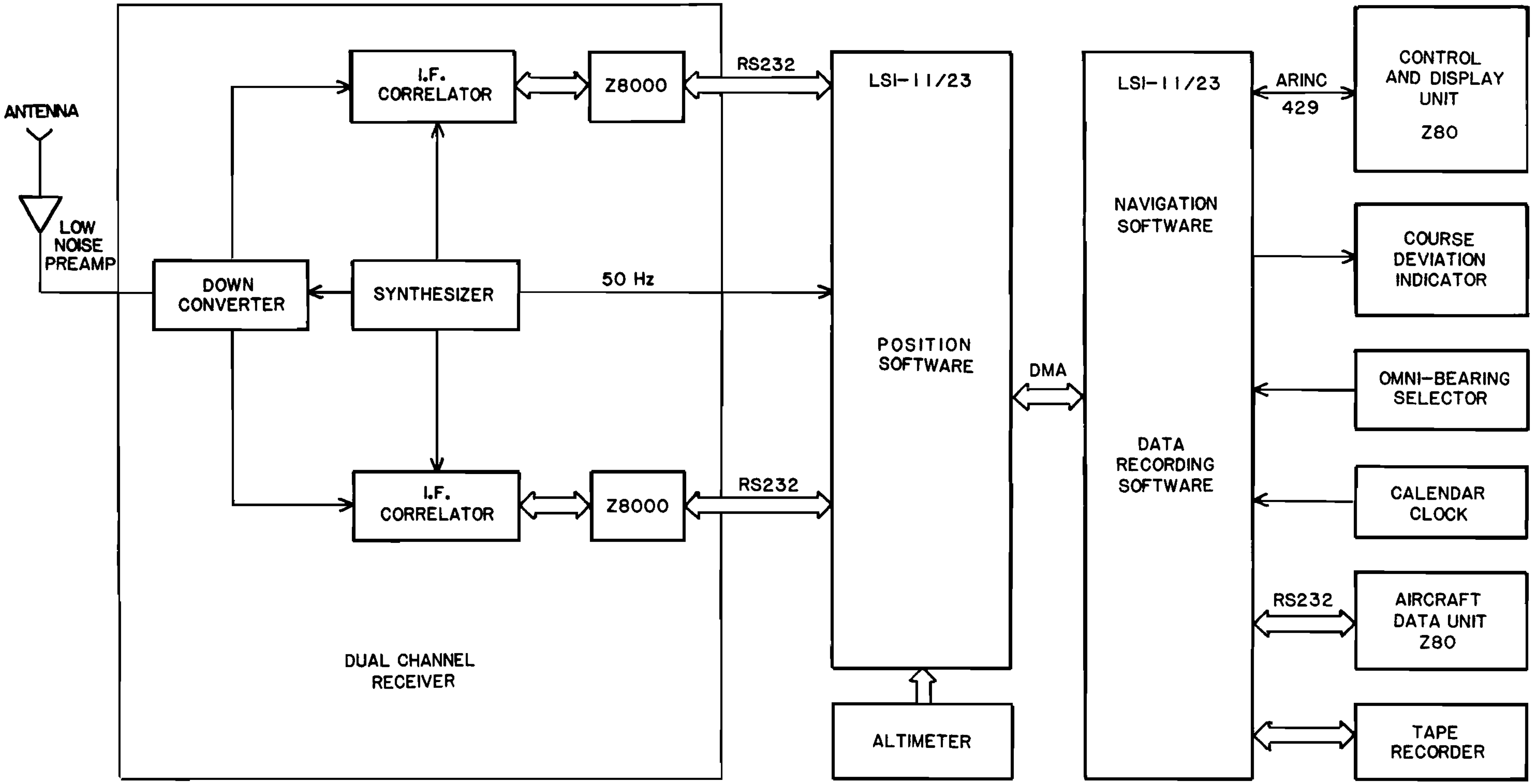

Fig. 3-1. **GPS TEST AND EVALUATION SYSTEM**

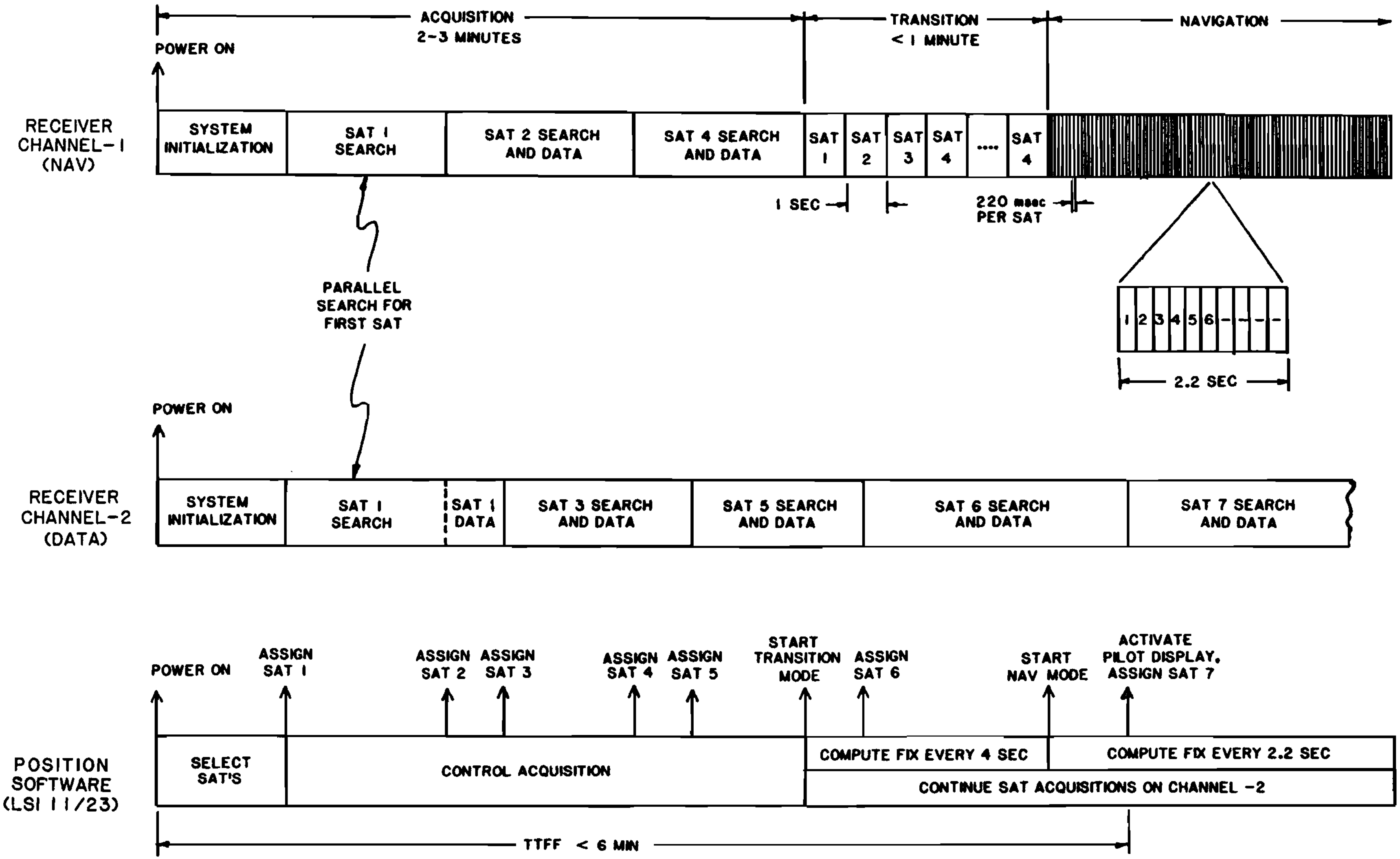

FIG. 3-2. SYSTEM TIMING

bin centered on the expected frequency, and the second searching in an adjacent 1500 Hz bin. As shown in the example of Fig. 3-2, Channel 2 acquired SV-1 first and proceeded to demodulate the 1500 bit navigation message. Concurrently, the receiver management software directed Channel 1 to search for SV-2.

When four SV's are acquired, Channel 1 is then placed in the transition mode. On entry to the transition mode, the satellites have ± 17 chip code phase and ± 750 Hz frequency uncertainties. After several four-second transition cycles, the code and frequency uncertainties narrow to ± 0.16 chips and ± 200 Hz. Channel 1 is then assigned to the navigation mode where SVs 1-4 are sequentially accessed at 220 msec per SV. The navigation mode operates on a ten slot cycle lasting 2.2 seconds. As additional SVs are acquired by Channel 2, they are immediately transferred to a slot in the Channel 1 navigation mode cycle.

When six SVs have been acquired or six minutes has passed, a smoothed position estimate, based on a batch processed least-squares linearization algorithm, is transferred to the pilot display. It is important to attempt to have acquired at least six SVs prior to activation of the pilot display in order to have two backup SVs during aircraft takeoff maneuvers. Typically six or more SVs will have been acquired within six minutes.

3.1.2 Alternative Startup Modes

The startup sequence discussed in the previous section assumed that the current time (± 1 minute) and location (± 3 miles) are available (i.e., were recorded prior to the previous power shutdown) and that a stored almanac exists whose age is less than 30 days. Should own position be unknown, or the battery supporting the built-in calendar clock be low, one of the alternative startup modes shown in Table 3-1 will be automatically selected.

Should the almanac be old (age > 30 days), an additional 12.5 minutes is necessary to acquire a new almanac from any of the available SVs.

3.2 Antenna

An important aspect of the low-cost GPS receiver development is the definition of the required gain versus elevation angle characteristic for the aircraft antenna. Results of a study to determine this characteristic are summarized below.

3.2.1 General Considerations

It is convenient to consider the above-horizon and below-horizon portion of the GPS antenna gain characteristic separately. The above horizon characteristic depends on the satellite slant ranges at low and high elevation angles. Since the free space path loss is 2 dB greater at 5° elevation than at zenith, the antenna gain should be 2 dB greater at low elevations than at high elevations. The boundary between these two regimes is taken as 30°, where the free space path loss is 1 dB greater than at 5°.

TABLE 3-1

ALTERNATIVE START-UP MODES

MODE	CONDITIONS	ASSUMPTIONS	CHARACTERISTICS
Cold Start	• Full range and L.O. frequency uncertainty • User position uncertainty	• Prestored almanac (may be old) • Stationary user	• Trial-and-error SV visibility determination • Wide frequency searches • Full code searches • Constellation review and 2nd acquisition pass following first fix • TTFF ~ 10-36 mins
"Time only" starts	• Know time to ± 1 min • Know coarse position (± 6.75°) • Full L.O. frequency uncertainty	• Prestored almanac • Stationary user	• Predicted SV visibility • Wide 1st SV frequency search - narrowed subsequently • Full code searches • TTFF ~ 4-7.5 mins
Time-and position wideband start	• Know time to ± 1 min • Know position to ± 1° • Full L.O. freq uncertainty (3×10^{-6})	• Prestored almanac • User motion: 200 knot velocity 0.5_g acceleration 30 deg banks	• Predicted SV visibility • Wide 1st SV frequency search - narrowed subsequently • Full code searches • TTFF ~ 3-4 mins
Time-and position narrow-band start	• Know time to ± 1 min • Know position to ± 3 miles • Know L.O. frequency to $\pm 5 \times 10^{-7}$		• Predicted SV visibility • Narrow frequency searches • Full code 1st SV search - limited subsequently • TTFF ~ 3-4 mins

The below-horizon characteristic depends upon the effect of multipath on the GPS receiver. Two types of effect result from multipath. The first effect is that deep fading of the GPS signal can result from the destructive interference of the direct and multipath signals. The magnitude of this effect is largely dependent on the GPS signal fade margin. In general, a deep fade will mean either a temporary loss of the signal or a delay in signal acquisition.

The second effect of multipath on the receiver is to cause an error in the delay-lock-loop pseudo-range tracking. The nature of this error depends upon whether the multipath delay is greater or less than 1.5 C/A code chips. The dependence of the multipath delay upon elevation angle and aircraft altitude is shown in Fig. 3-3. As seen in the figure, the multipath delay always exceeds 1.5 code chips for altitudes greater than 8600 feet and elevation angles greater than 5°. In general, tracking errors due to multipath delays greater than 1.5 chips can be removed by software tests, whereas errors due to delays less than 1.5 chips cause tracking bias errors which cannot be removed. These effects are discussed more fully in the following paragraphs.

3.2.2 Multipath Delay Greater Than 1.5 Microseconds

If the multipath delay is greater than 1.5 μsec (1.5 C/A code chips), the delay-lock-loop (DLL) discriminator characteristic can develop a second stable operating point, as shown in Fig. 3-4. In this case, the DLL may track the pseudo-range of the multipath signal rather than the direct signal, resulting in a large (> 1500 ft) pseudo-range error. However, since the receiver is sequential, reacquiring each satellite once per second, this error is likely to be manifested as an occasional false lock with accompanying large range change. Thus, the receiver control software can eliminate this type of error by tracking the pseudo-range and rejecting any unrealistically large range changes.

3.2.3 Multipath Delay Less Than 1.5 Microseconds

In the case where the multipath delay is less than 1.5 chips the effect on the DLL performance is more serious. Figure 3-5 shows that the effect of multipath in this case is not to create a second stable operating point, but rather to introduce a bias into the original operating point. This bias, furthermore, may not be discernable by the position software. The magnitude of this error depends upon both the magnitude of the multipath relative to the direct signal and magnitude of the multipath delay.

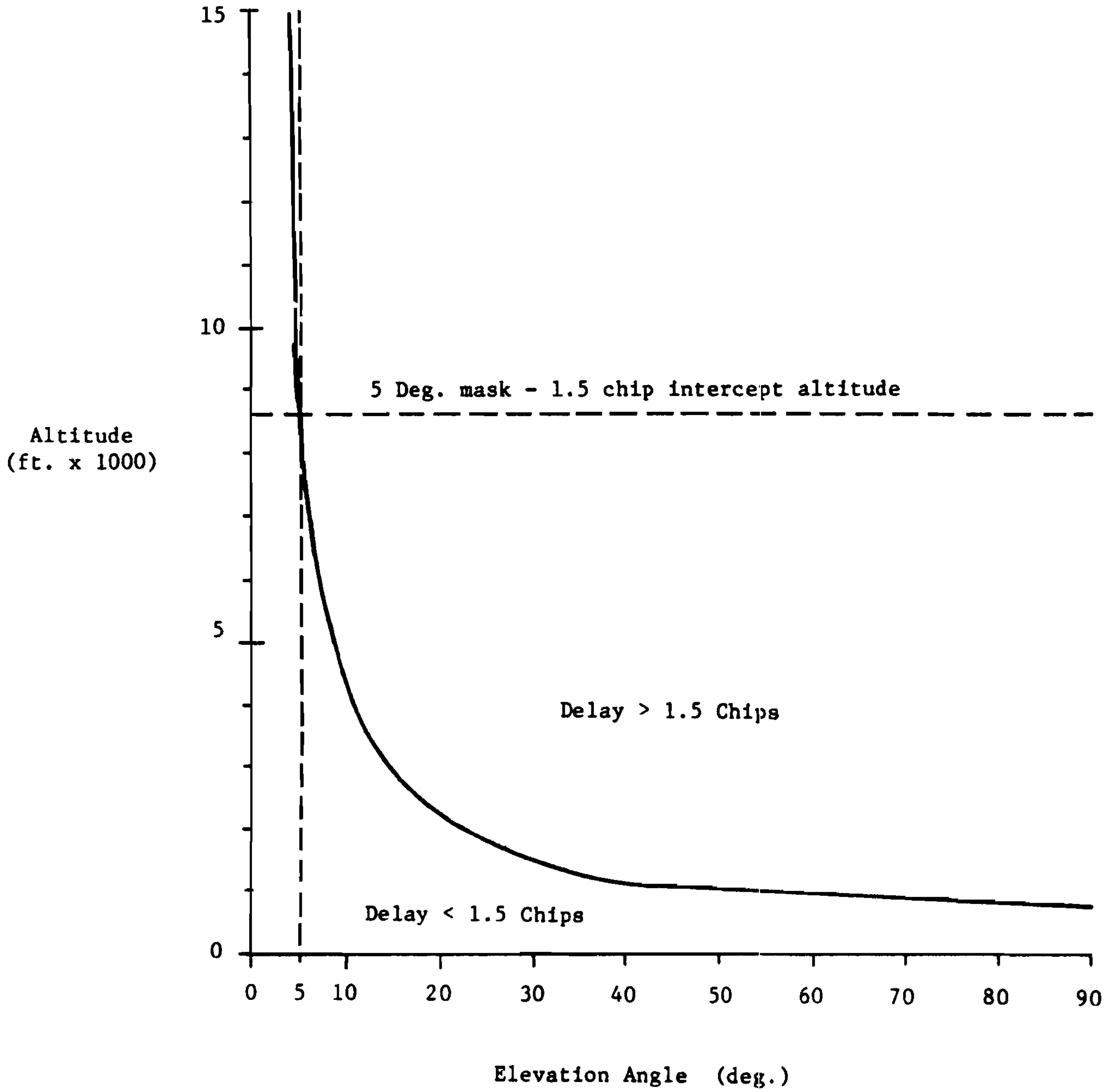

FIG. 3-3. Altitude vs Elevation Angle For 1.5 Chip Multipath Delay

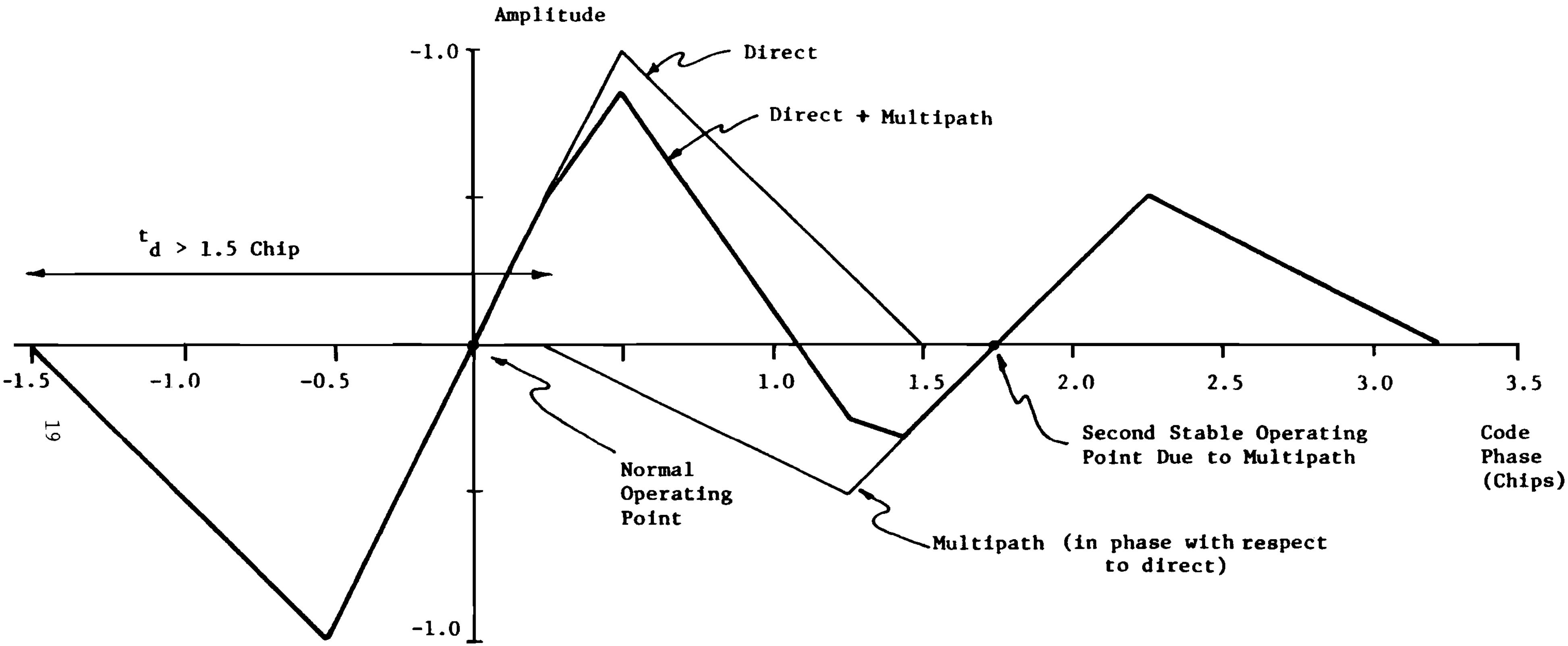

FIG. 3-4. Effect of Multipath Delay Greater than 1.5 Chips.

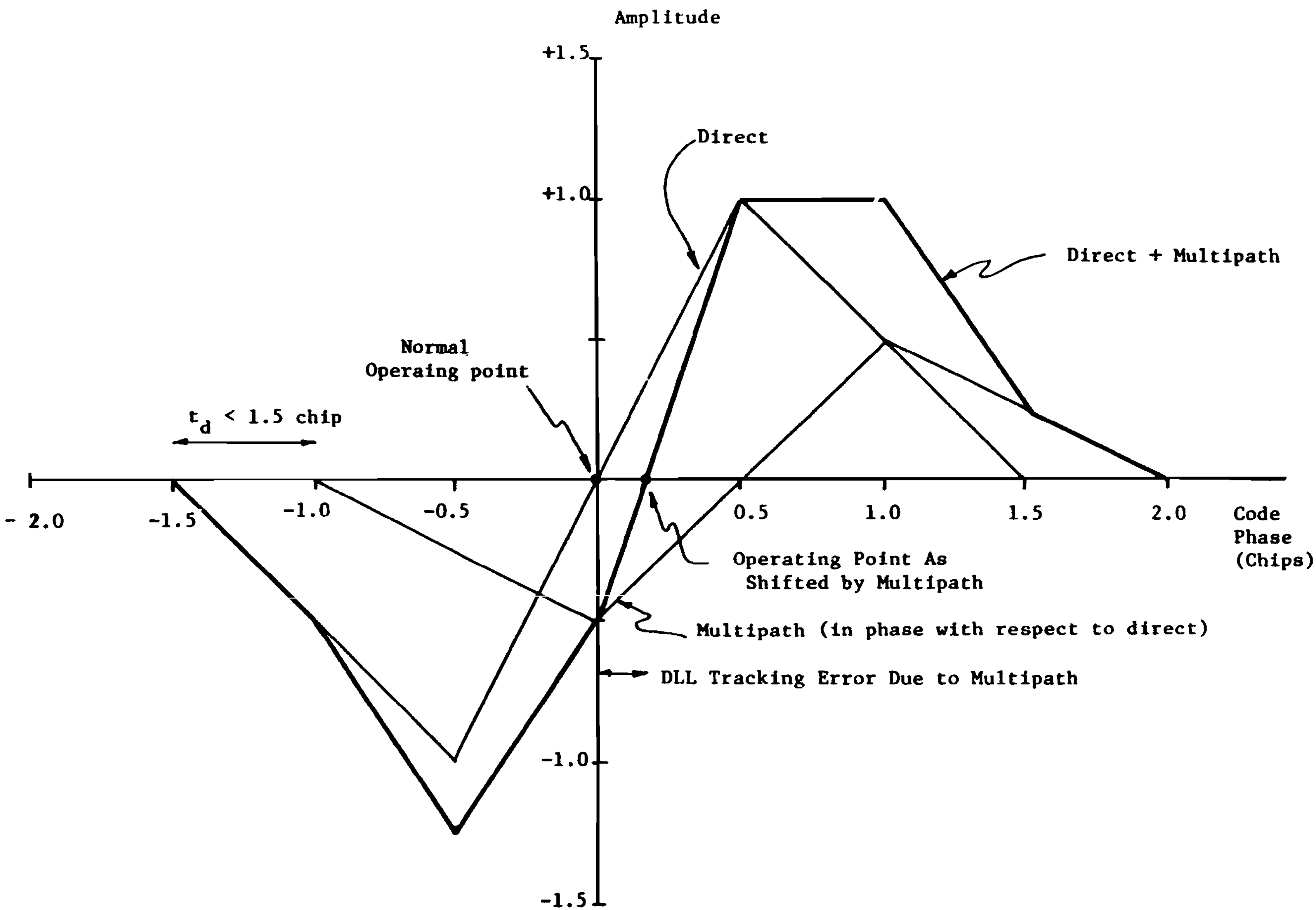

FIG. 3-5. Effect of Multipath Delay Less Than 1.5 Chips.

Hagerman (Ref. 9) has studied the effect of multipath on both the coherent and noncoherent Delay Lock Loop. Two regions of DLL operation in the presence of multipath have been defined. In Region I, the DLL is tracking the direct signal, whereas in Region II the DLL is tracking the multipath signal. The results of Hagerman's analysis for the noncoherent DLL are shown in Figs. 3-6 and 3-7. (Note: Hagerman's results are in terms of the P-code and thus must be multiplied by 10 for the C/A code). Although the Region II errors are much larger than the Region I errors, they are less probable, especially in the case of a non-coherent delay lock loop. The worst-case error therefore can be taken from the results for Region I.

It is seen from these results that the worst-case error depends on the relative multipath amplitude. If the multipath amplitude can be limited to 0.2, then the expected (mean) tracking error is 10 feet and the rms error is 50 feet. The multipath amplitude depends in turn on the antenna gain vs. elevation characteristic and the reflection coefficient of the surface. According to Figure 3-8 (Ref. 10) the worst case reflection coefficient at 5° is 0.7. If the antenna gain is 0 dBIC at 5°, then the required antenna gain at -5° can be calculated from:

$$\text{Relative multipath amplitude at } 5^\circ = \frac{\text{Antenna Gain } (+5^\circ)}{\text{Antenna Gain } (-5^\circ)} \times \text{Reflection coefficient at } 5^\circ$$

If it is assumed that the antenna gain at 5° is at least 0 dBIC, then the required antenna gain at -5° should be no greater than -5.5 dB.

The results of the foregoing discussion are summarized in Table 3-2.

TABLE 3-2

Initial Antenna Gain vs. Elevation Angle Requirement

Elevation Angle	Antenna Gain
30° to 90°	> -2 dBIC
5° to 30°	> 0 dBIC
-90° to -5°	< -5.5 dBIC

This characteristic is illustrated in Fig. 3-9. Also shown is the specification developed by General Dynamics (Ref. 11). The single difference between the two characteristics is that General Dynamics specifies < -7 dBIC below 10°, perhaps due to the difficulty of achieving -5.5 dBIC at 5°. The receiver performance characteristics, however, will be essentially equivalent for both specifications.

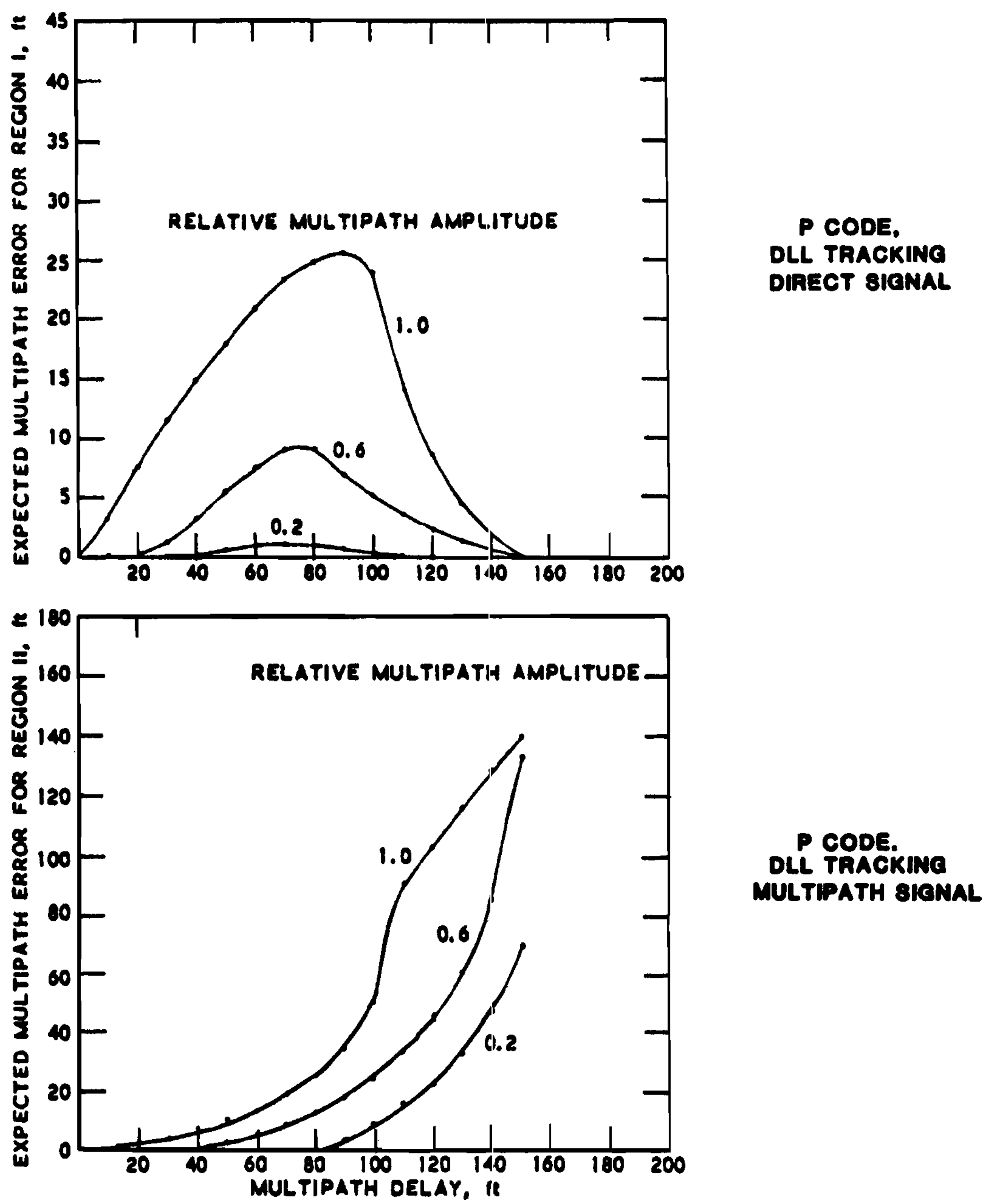

FIG. 3-6. Expected Noncoherent DLL Tracking Error, 20 dB Carrier Tracking Margin (Ref. 8)

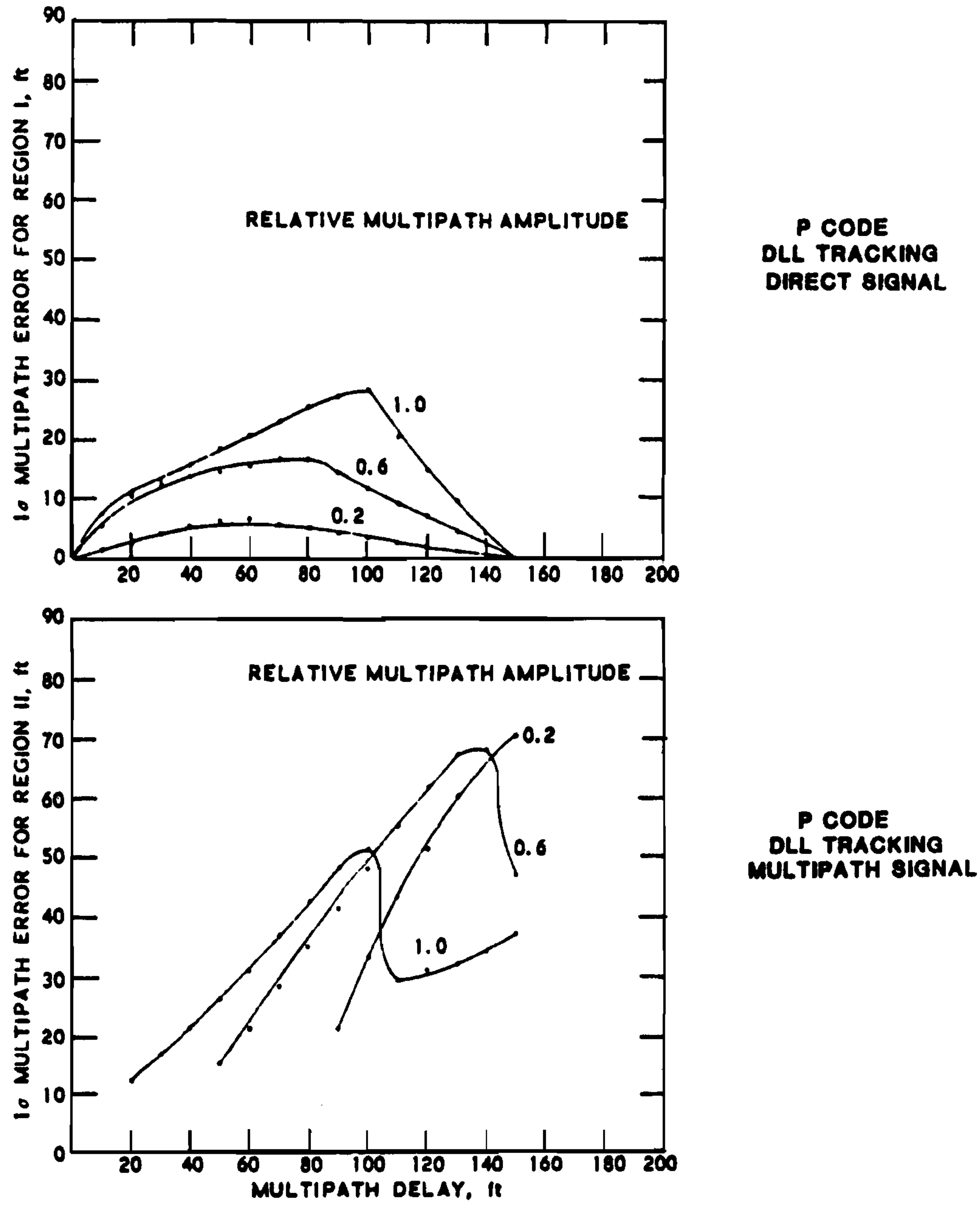

FIG. 3-7. 1σ Noncoherent DLL Tracking Error, 20 dB Carrier Tracking Margin (Ref. 8)

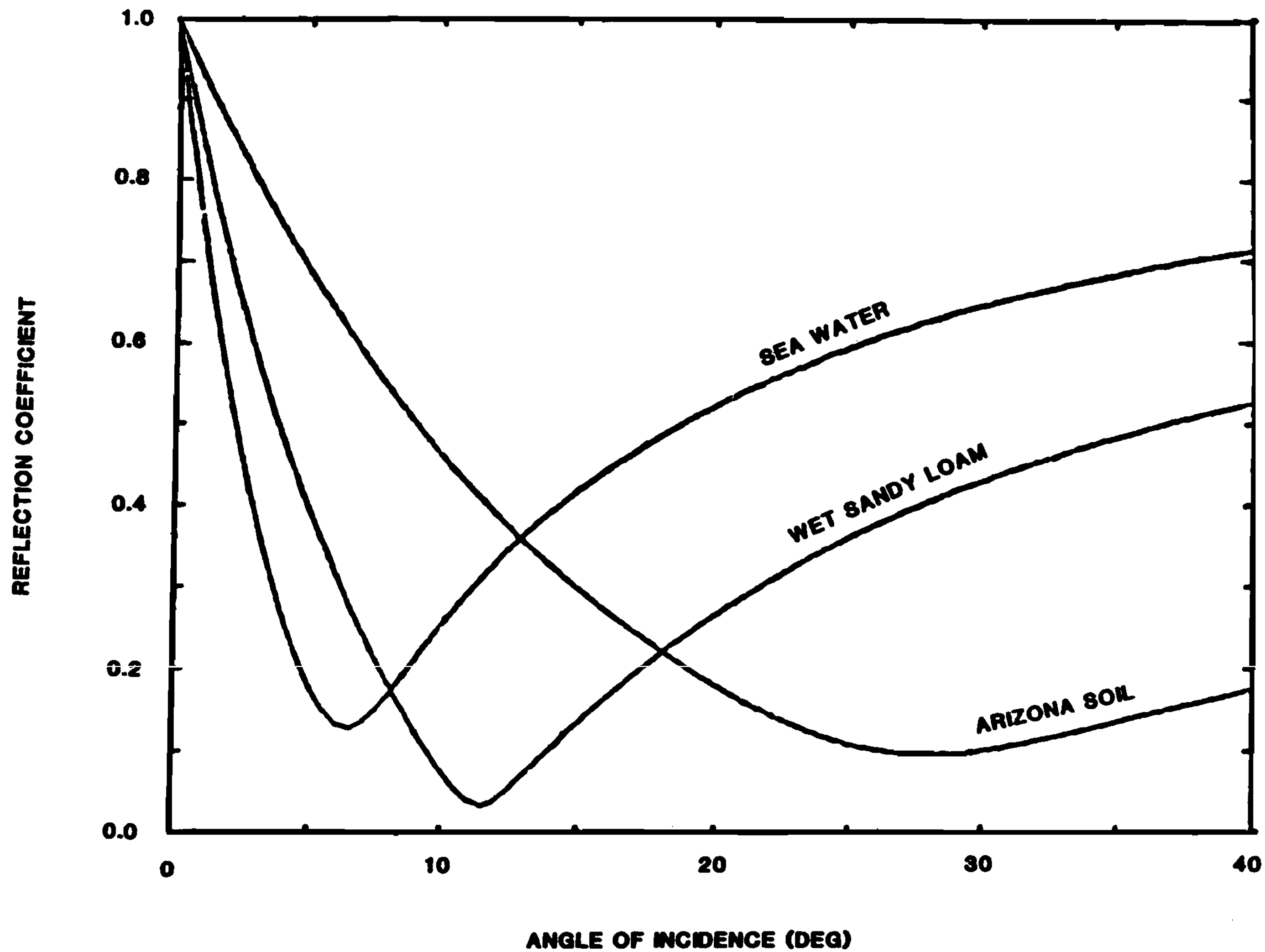

FIG. 3-8. Typical Vertically Polarized Signal Reflection Characteristics (Ref. 2).

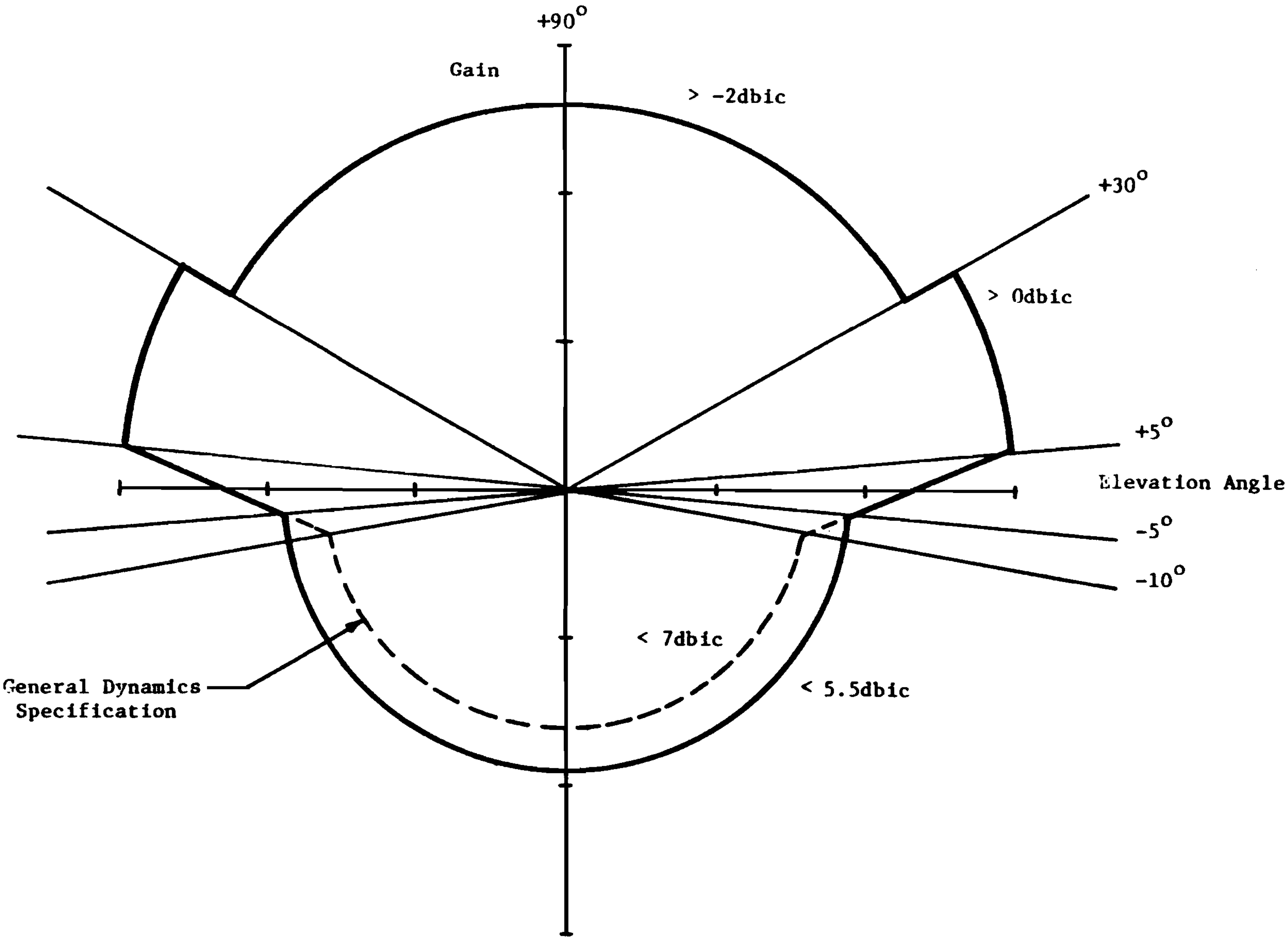

FIG. 3-9. INITIAL ANTENNA GAIN VS ELEVATION ANGLE REQUIREMENT

However, the way in which groups of pseudo-range measurements (up to 10 measurements, from as many satellites) are batch processed in the position computation makes the gain characteristic for multipath suppression less stringent. The batch least-squares position estimation method reduces the sensitivity of the position solution to an individual multipath-corrupted pseudo-range measurement. With least-squares fit processing it was determined that it is possible to redesign for a random error of 120 feet, as long as the associated bias error was limited to 50 feet, worst case. The below-horizon antenna gain requirements were recalculated to meet this revised multipath-induced range error bias limit assuming a ground bounce reflection coefficient of 0.7, maximum.

The revised specifications are depicted in Table 3-3 and in Fig. 3-10. Note that the below-horizon gain for elevation angles in the range minus 5 to minus 30 degrees need only be 2 dB less than the gain over the above-horizon 5 to 30 degree sector.

TABLE 3-3. REVISED GPS ANTENNA SPECIFICATION

Elevation Angle, (θ)	Antenna Gain, G(θ)
30° to 90°	$>$ -2 dBIC
5° to 30°	$>$ 0 dBIC
-5° to 5°	$<$ 0 dBIC
-30° to -5°	$<$ -2 dBIC
-90° to -30°	$<$ -4 dBIC

The measured performance of an antenna (Fig. 3-11) purchased from Chu Associates using the revised specifications is reported in Section 4.2.1.

3.3 Preamplifier

The receiver preamplifier specification was based on considerations of noise figure and out-of-band rejection. A nominal link budget, based on reasonable fade margins, resulted in the need for a 4 dB receiver noise figure. Since 3 dB must be allocated to the preamplifier and 1 dB to losses associated with filters and connectors, it is necessary that the preamplifier be located at the antenna. The dual-channel receiver developed by STI further assumed a nominal gain of 50 dB with 10 dB cable loss between the amplifier and receiver.

A commercial amplifier, an Avantek AM-1664M, was purchased with the following specifications:

f_o	1575.42 MHz
Bandwidth	20 MHz (3 dB)
Gain	52 dB
Noise Figure	2 dB

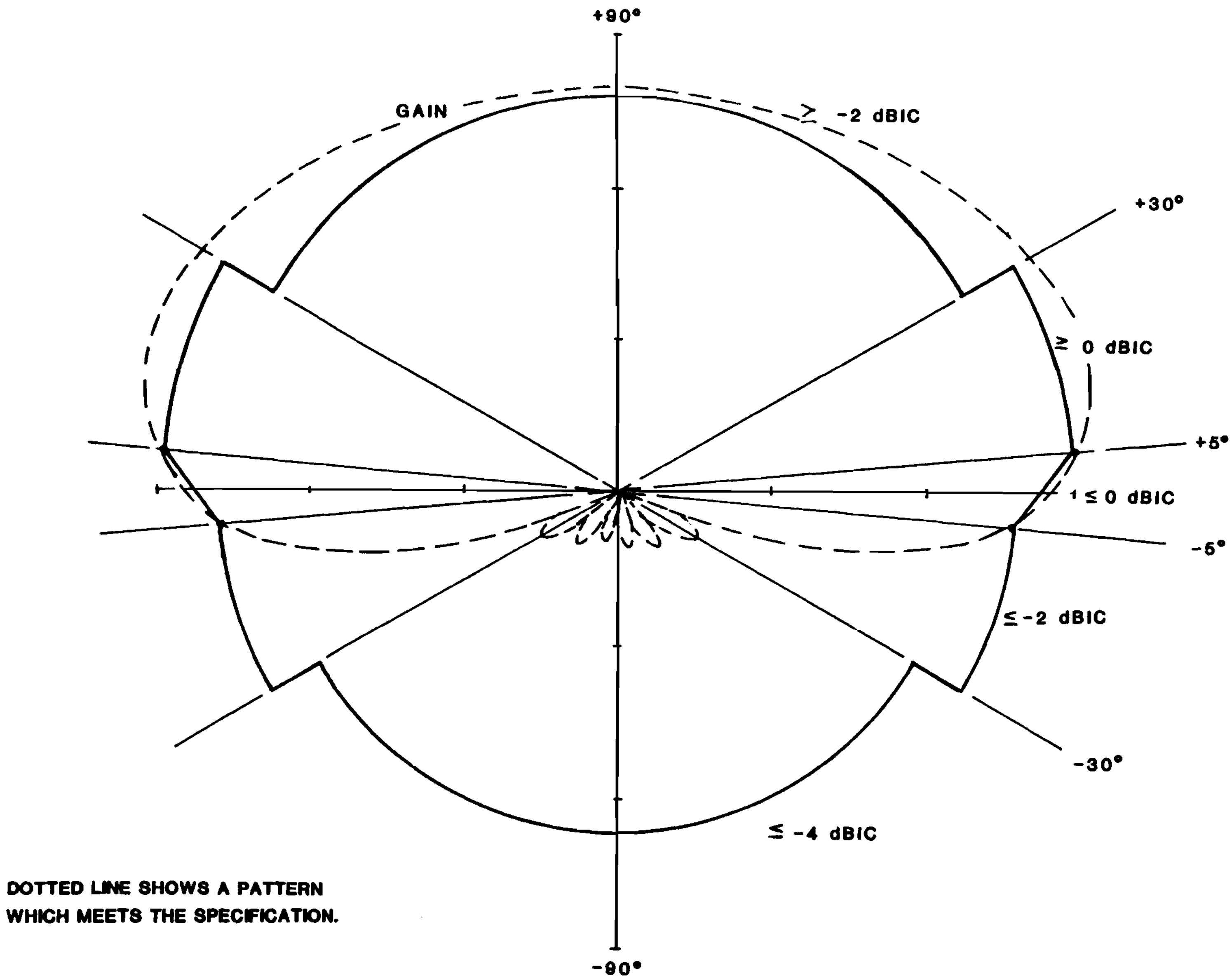

FIG. 3-10. REVISED GPS ANTENNA CHARACTERISTIC

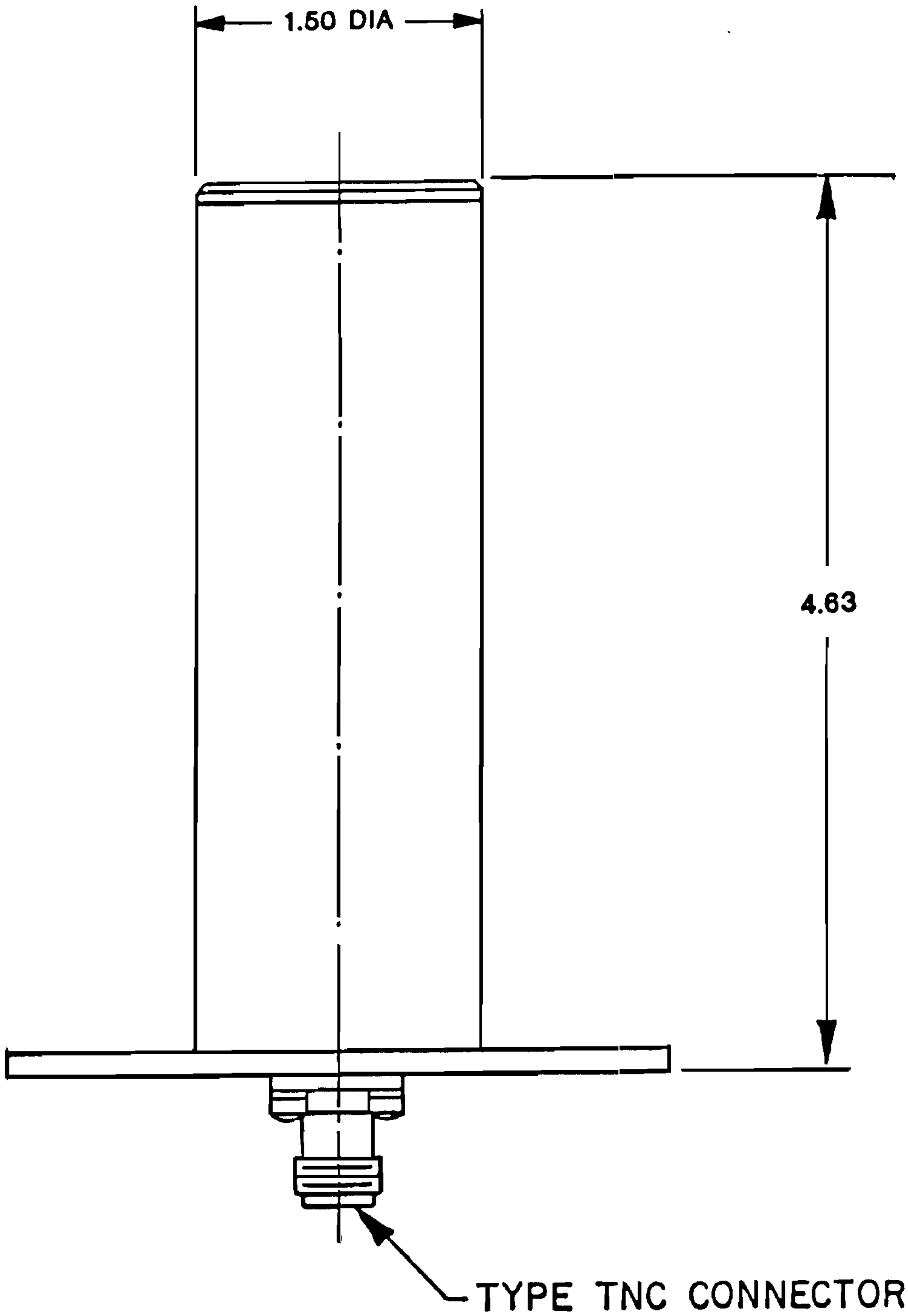

FIG. 3-11. GPS ANTENNA, OUTLINE DIMENSIONS

3.4 Dual Channel Receiver Hardware

3.4.1 Architecture and Design Features

The receiver, developed by Stanford Telecommunications, Inc. for Lincoln Laboratory, consists of two identical channels fed by a common down-converter and timer/synthesizer as shown in Fig. 3-12. Each channel performs digital functions in Z8000 microprocessors. The functional schematic of Fig. 3-13 provides further detail for one of the two channels with analog (hardware) and digital (software) functions to the left and right of the dashed vertical line. Software switches SW1 and SW2 are programmed so that during acquisition SW1 is in the "selected frequency" position and SW2 in "code search". During the navigation mode a steady state condition will occur in which SW1 is programmed to "AFC" and SW2 to the "DLL" Position. The allocation of receiver functions between the Z8000 microcomputers and the position software in the LSI 11/23 is shown in Table 3-4.

The IF noise bandwidth, B_{IF}, is determined by the integrate and dump (I and D) circuits and by the digital accumulators according to the expression

$$B_{IF} = \frac{1}{2\,T\,M}$$

where T is the sampling period and M the number of samples accumulated. The output of the low-pass filter is sampled at a 2 KHz rate. Additional filtering is provided by the post-detection integrator (PDI).

The code select circuitry can operate in the punctual mode (P) for code search and data extraction, or in the early-late dither mode to control the delay locked loop (DLL). Characteristics of the search detector, and the AFC, code and AGC loops are shown in Table 3-5.

Figure 3-14 shows the AFC lock detector and the carrier and noise ratio estimator embodied in each STI receiver channel. Characteristics of these circuits are given in Table 3-6.

3.4.2 Receiver States

When a receiver channel is provided with commands and initialization data by receiver management software in the LSI 11/23 it responds by executing one of the following Z8000 programs:

- initialization
- acquisition
- transition
- navigation
- data demodulation

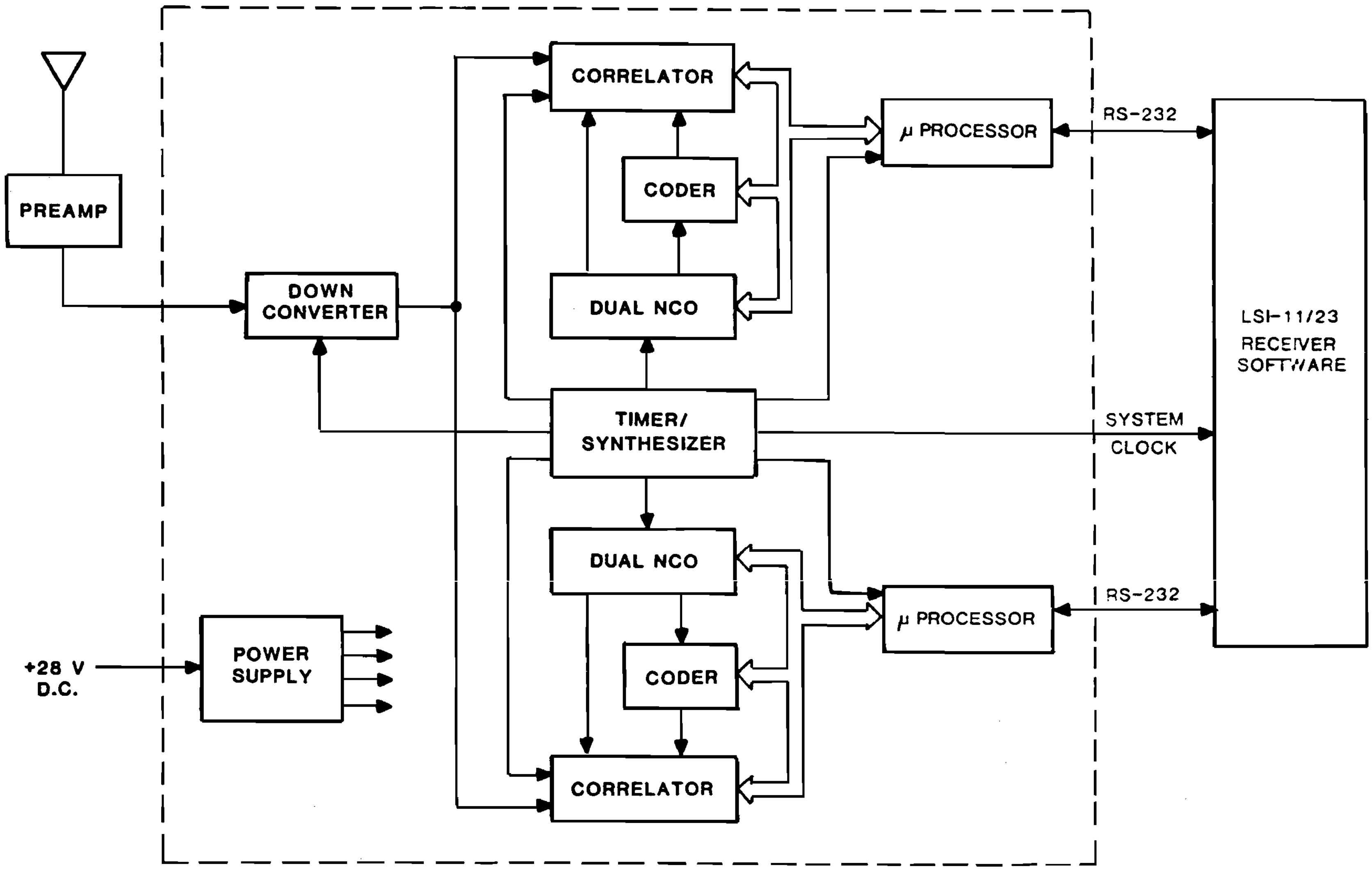

FIG. 3-12. EXPERIMENTAL DUAL CHANNEL RECEIVER

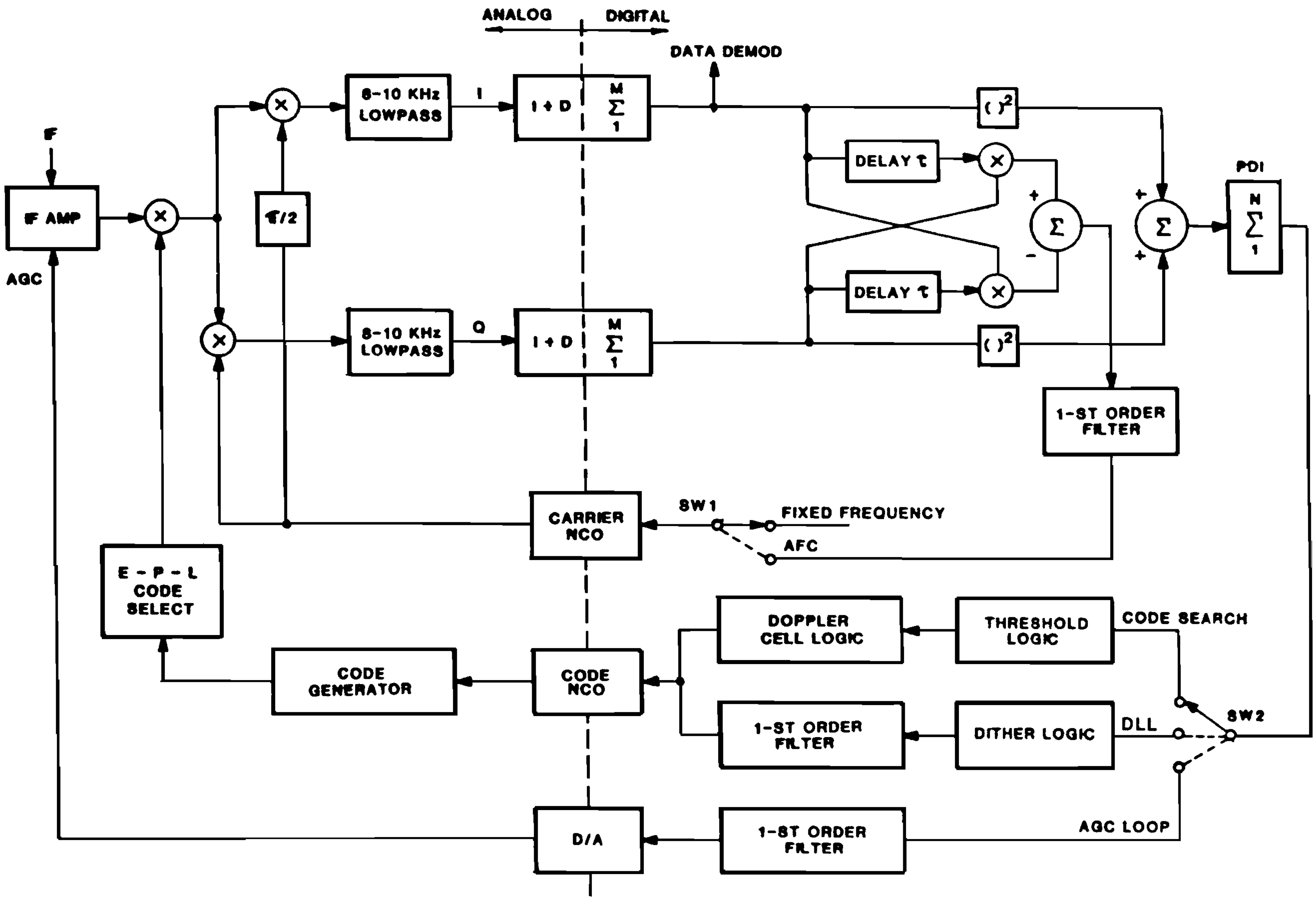

FIG. 3-13. FUNCTIONAL SCHEMATIC OF RECEIVER

TABLE 3-4

RECEIVER CHANNEL - POSITION SOFTWARE FUNCTIONAL ALLOCATION

REQUIREMENT	Z8000 RECEIVER CHANNEL SOFTWARE	LSI 11/23 POSITION SOFTWARE
Acquistion	Sequential detection Pull-in and track Data synchronization	SV selection Acquisition prepositioning Search control Acquisition sequence control
Sequential Track	Limited sequential detection Pull-in and track Dwell sequencing Inter-dwell prepositioning	SV constellation revision New SV prepositioning Sequence monitoring and control
Pseudo-range	Code state sampling	Pseudo-range construction Ambiguity resolution Ionispheric and tropospheric compensation
Data Demodulation	Bit demodulation Word recovery Parity checking	Data synchronization (single channel) Data unpacking Demodulation monitoring and control

TABLE 3-5

RECEIVER LOOP CHARACTERISTICS

SEARCH DETECTOR	AFC LOOP	CODE LOOP	AGC
Square law power detector	Delayed cross product detector $\approx \sin 2\pi\Delta f\,\tau$	± 0.5 chips early/late power detector	Maintains constant power
Open loop operation	1st order loop	Carrier (AFC or PLL) loop aided	Deals with up to 10 satellite signals.
AGC sets noise floor	Variable loop bandwidth	Variable loop bandwidth	Variable loop bandwidth
Two search rates: 50 chips/sec 83.3 chips/sec	Primary loop bandwidth 5 Hz and 10 Hz	Primary loop bandwidth 5 Hz and 10 Hz	Primary loop bandwidth 1 Hz (for 1st satellite acquisition only), 10 Hz otherwise
Multiple freq. cell search	Operates with early/late code		Supplies power reference to lock detectors
Upon detection does false alarm check			

TABLE 3-6

RECEIVER AFC LOCK DETECTOR AND C/N_0 ESTIMATOR CHARACTERISTICS

AFC Lock Detector	C/N_0 Estimator
Detector output $\approx \cos 2\pi\Delta f\tau$	Measures AGC normalized power
Uses narrow band IF (B_{IF}=50 Hz) for narrow frequency discrimination	Output monotonic with C/N_0
AGC compensated to be insensitive to noise and gain variations	Estimate for each satellite
Also serves as code sync detector	Filtered over multiple intervals
Detection bandwidth adjustable from 5 Hz up	Detection bandwidth 5 Hz

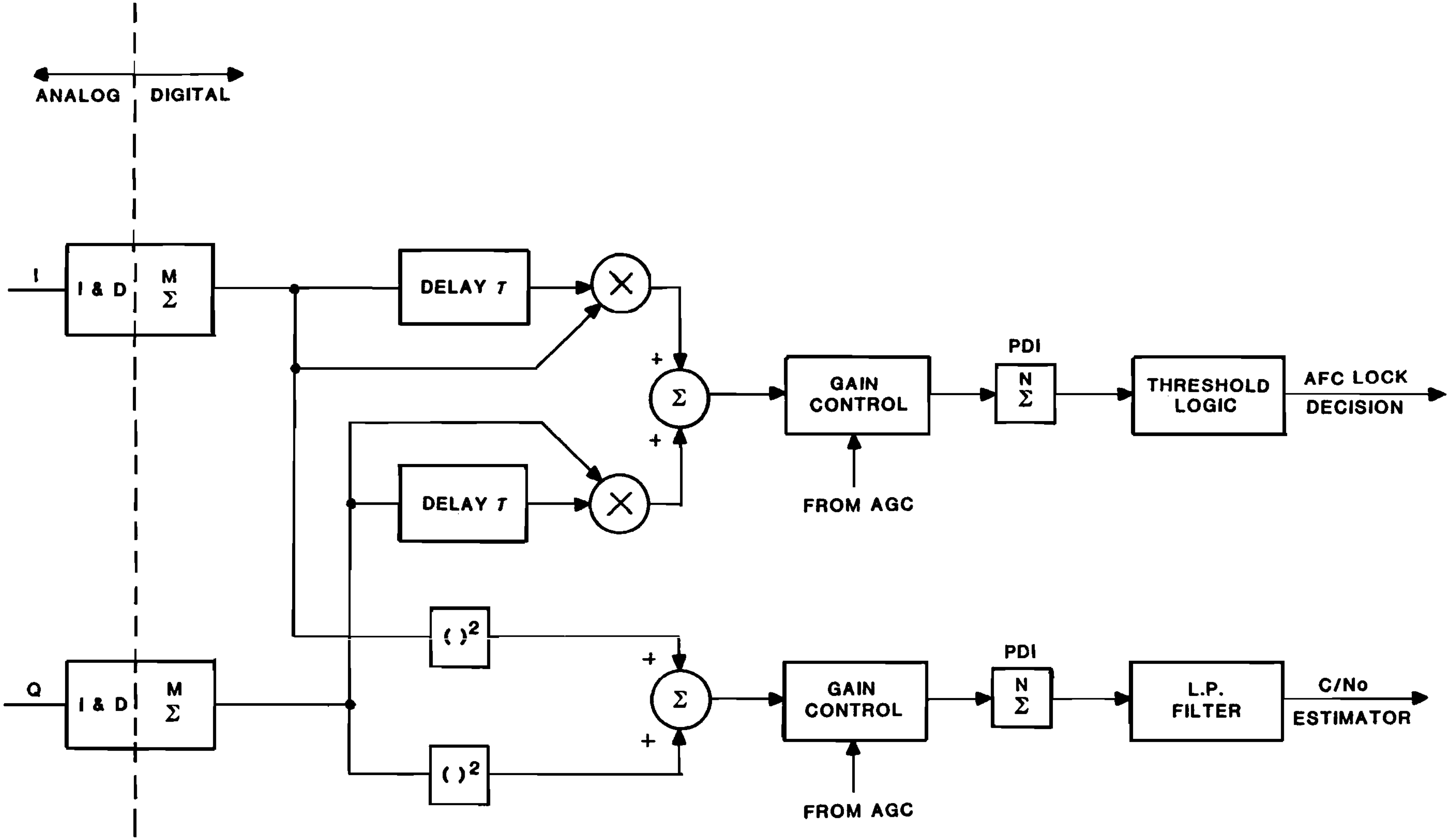

FIG. 3-14. AFC AND C/N_0 ESTIMATOR

The initialization routine establishes operating parameters and checks status. The acquisition routine is illustrated in Fig. 3-15. Note that the IF bandwidth, B_{IF}, is changed several times during the acquisition sequence, which illustrates the significant advantage of software realizations of receiver detection algorithms.

Figures 3-16 and 3-17 show the transition and navigation state diagrams.

Figure 3-18 shows the detailed events that occur during each 220 millisecond dwell internal in navigation mode. The prepositioning data will have a ± 0.16 chip uncertainty for an SV entering the dwell from phase transition. Should lock fail to occur twice, the receiver will automatically commence a ± 1 chip search. If two additional failures occur, a ± 2 chip search is initiated. After a total of 6 failures, the receiver management software (in the LSI 11/23) will command a broader search by relocation of the search window. After several subsequent unsuccessful attempts the SV will be declared to be potentially faded and less aggressive techniques will be applied to reacquire it.

During normal operation new SVs will become visible. Figure 3-19 shows the state diagrams for the acquisition and data demodulation of a new SV.

The receiver hardware was physically assembled in an ATR Chassis as shown in Figs. 3-20 through 3-22. The receiver modules are mounted in a multibus-type chassis, and consist of a mixture of off-the-shelf commercial and custom-built boards. It should be noted that the actual size of a commercial equivalent will be significantly (~8-10 times) smaller because:

a) An extra board to provide the 9K byte ROM memory for each Z8000 was included (the Z8000 boards provided only 8K of local ROM).

b) LSI devices are currently being developed for the C/A Coder and NCO functions and,

c) much of the board area is not populated.

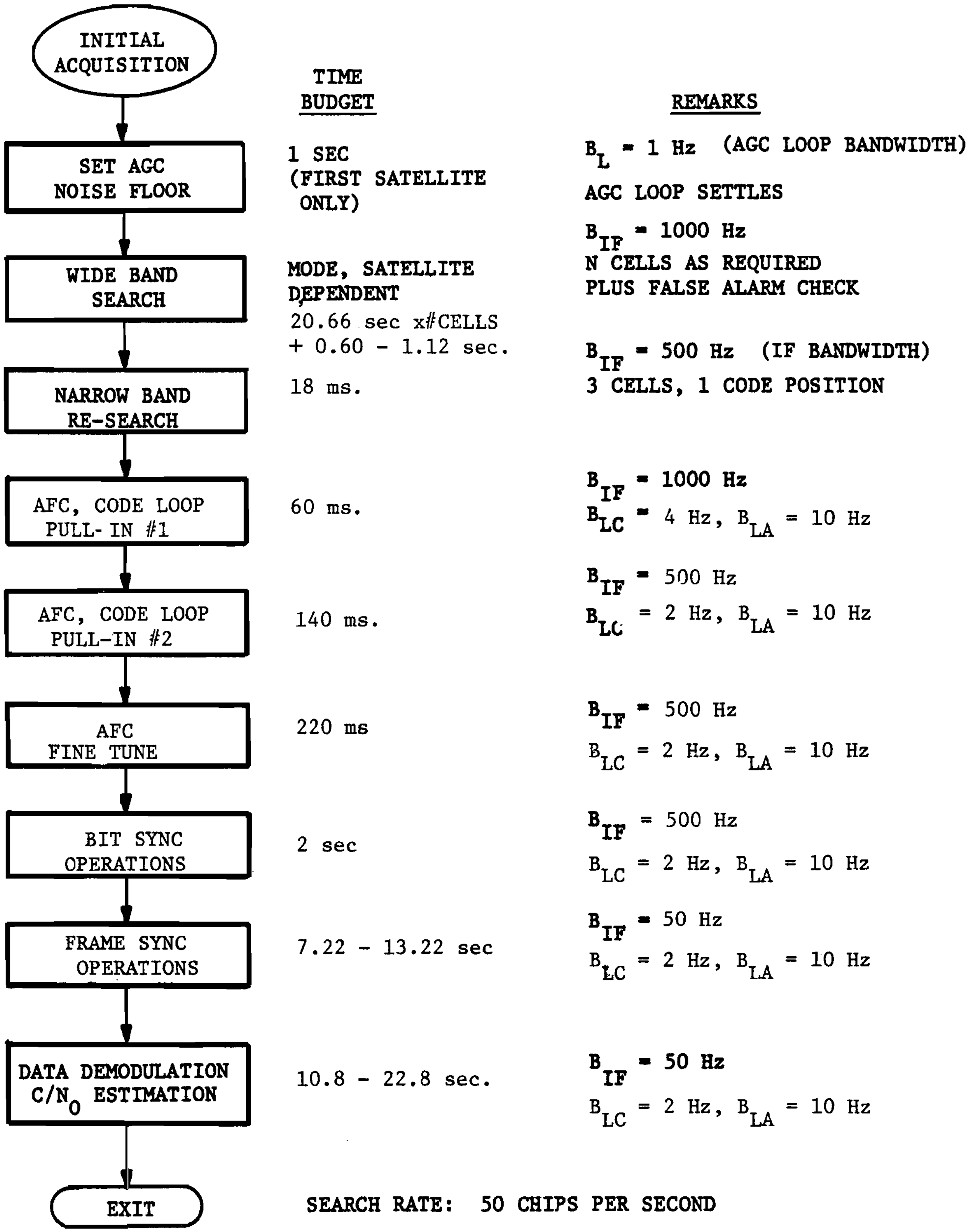

FIG. 3-15. Receiver Acquisition State Diagram.

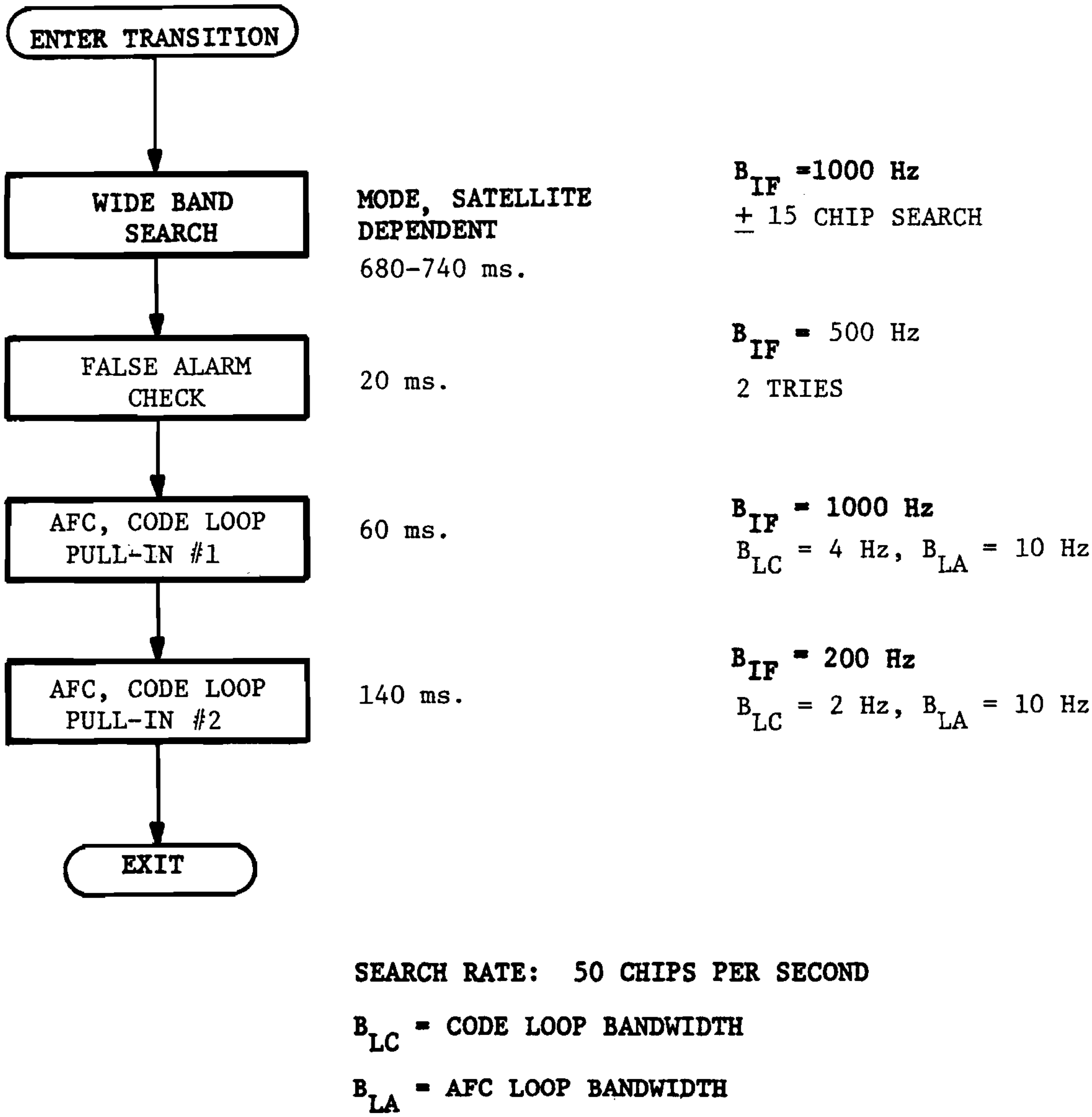

FIG. 3-16. Receiver Transition State Diagram.

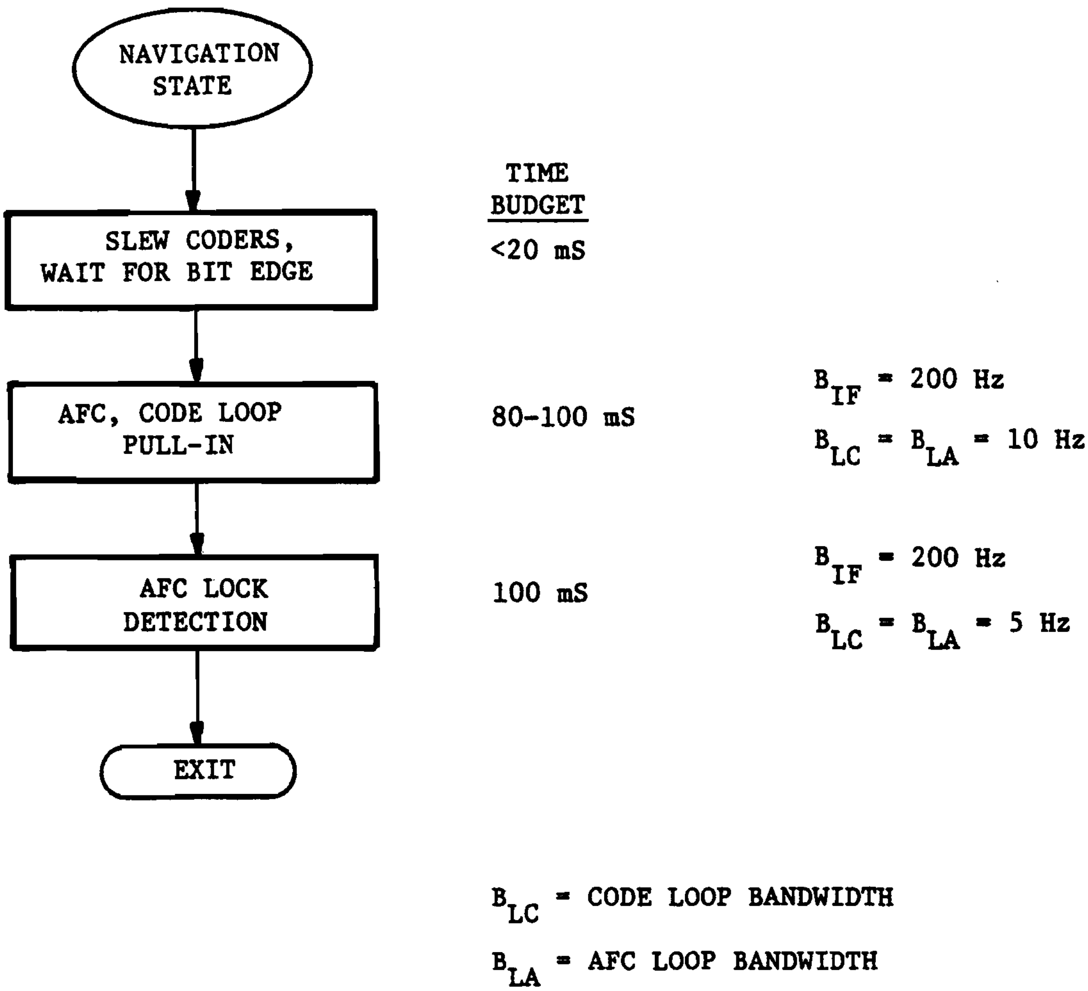

FIG. 3-17. Receiver Navigation State Diagram.

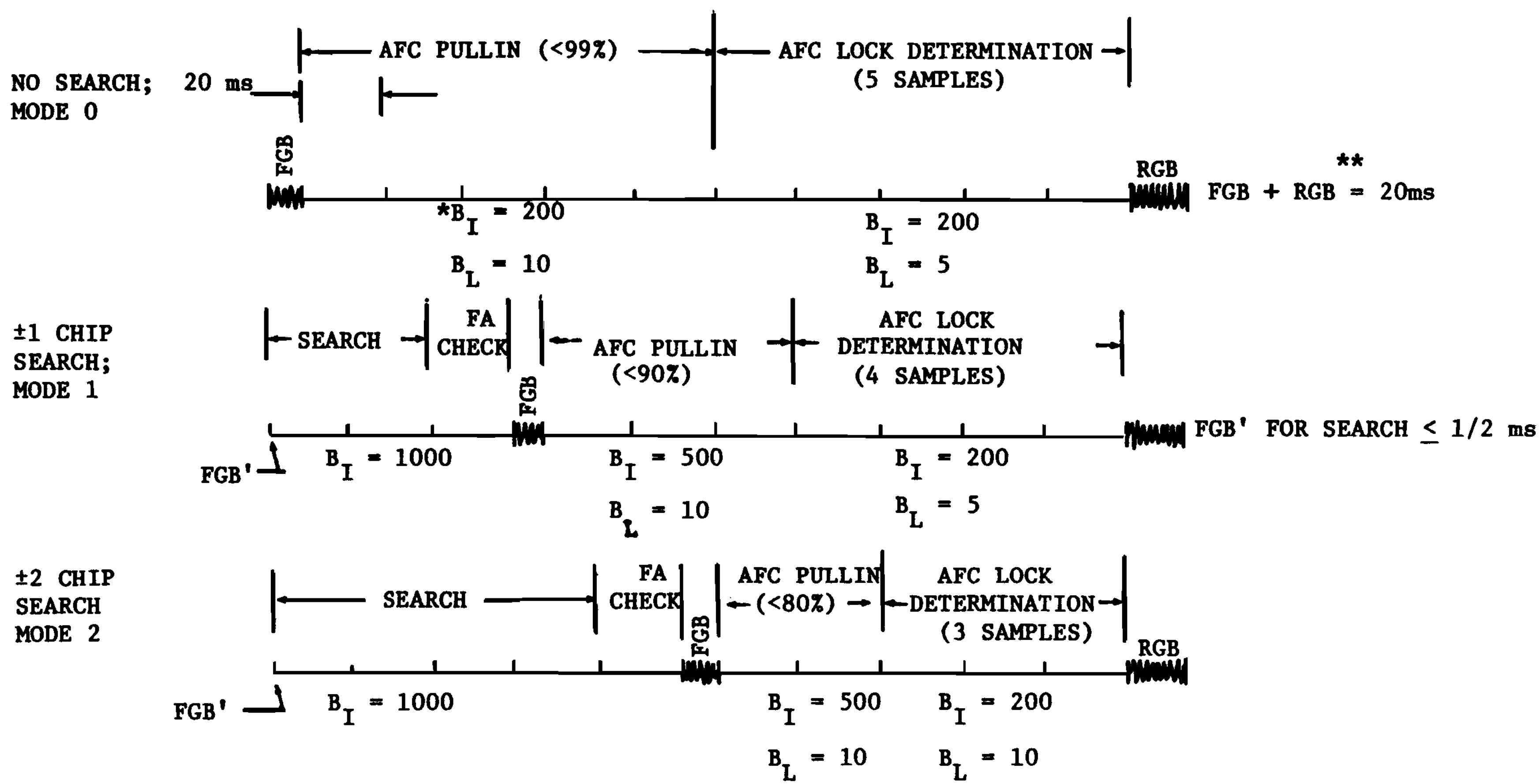

Search Rate: 50 Chips per second

*B_I Is Single-Sided

** FGB Is The Front Guard Band
RGB Is The Rear Guard Band

FIG. 3-18. NAVIGATION STATE 220 MS INTERVAL MODES AND TIME LINES

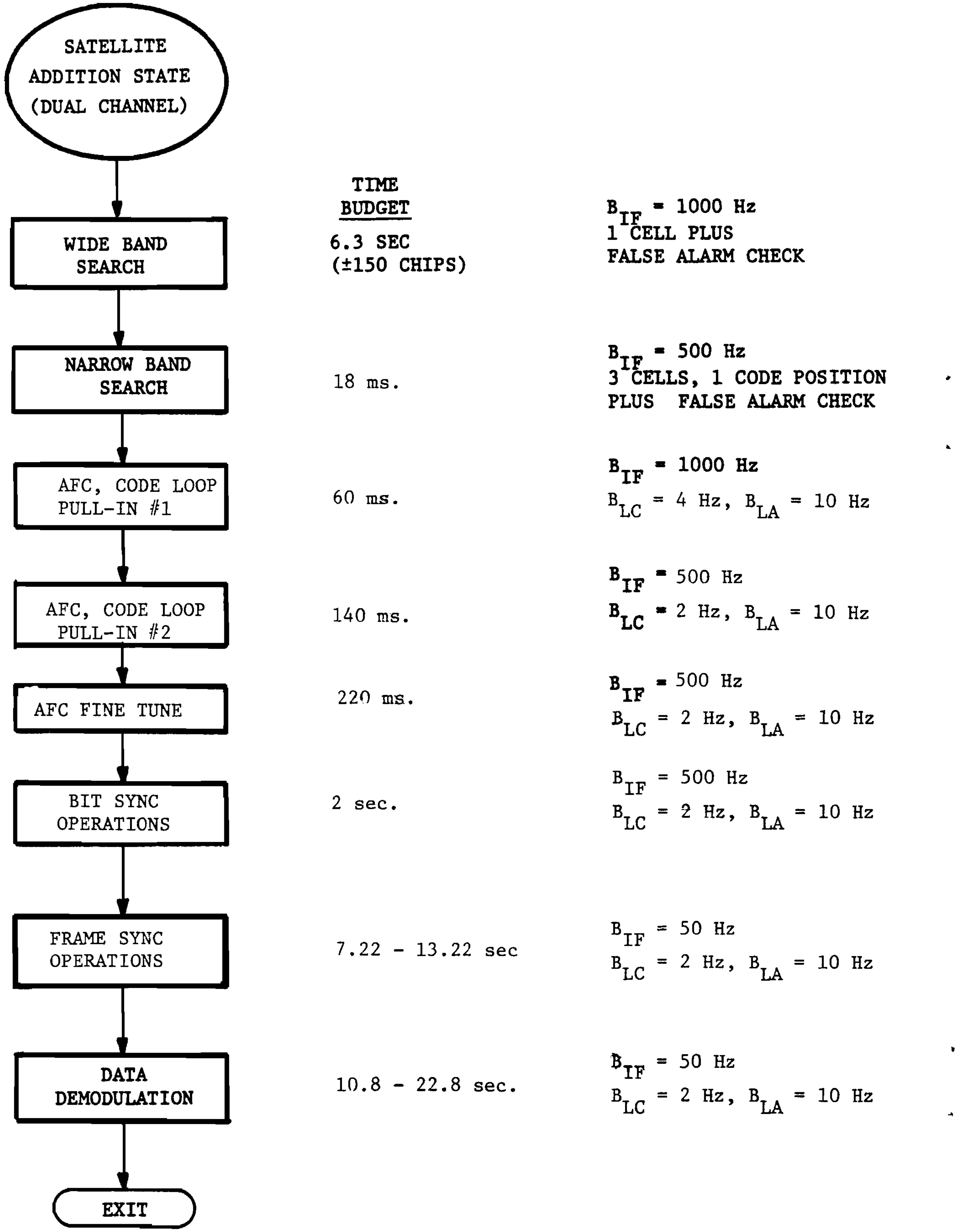

FIG. 3-19. Satellite Addition State Diagram.

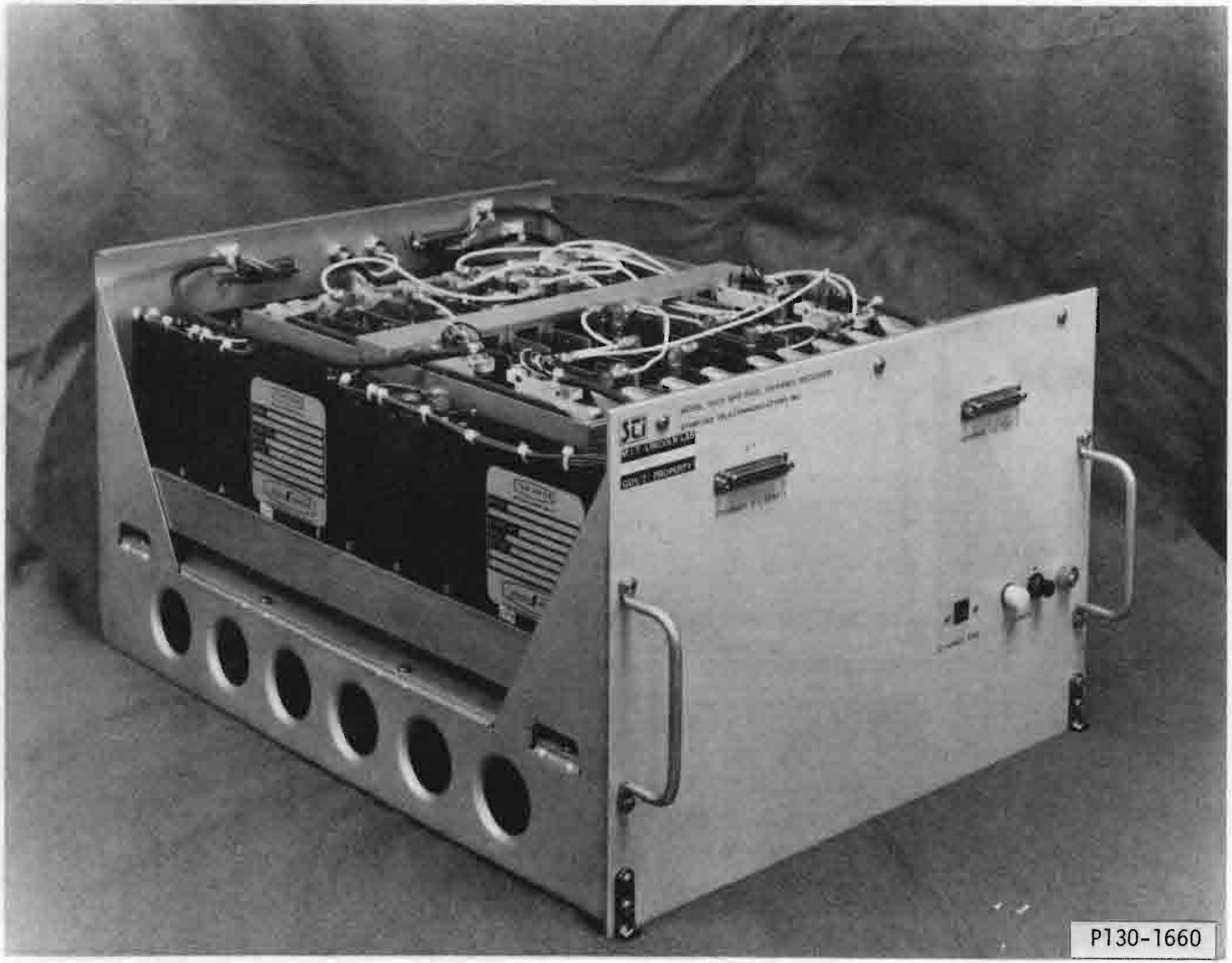

FIG. 3-20. DUAL CHANNEL RECEIVER

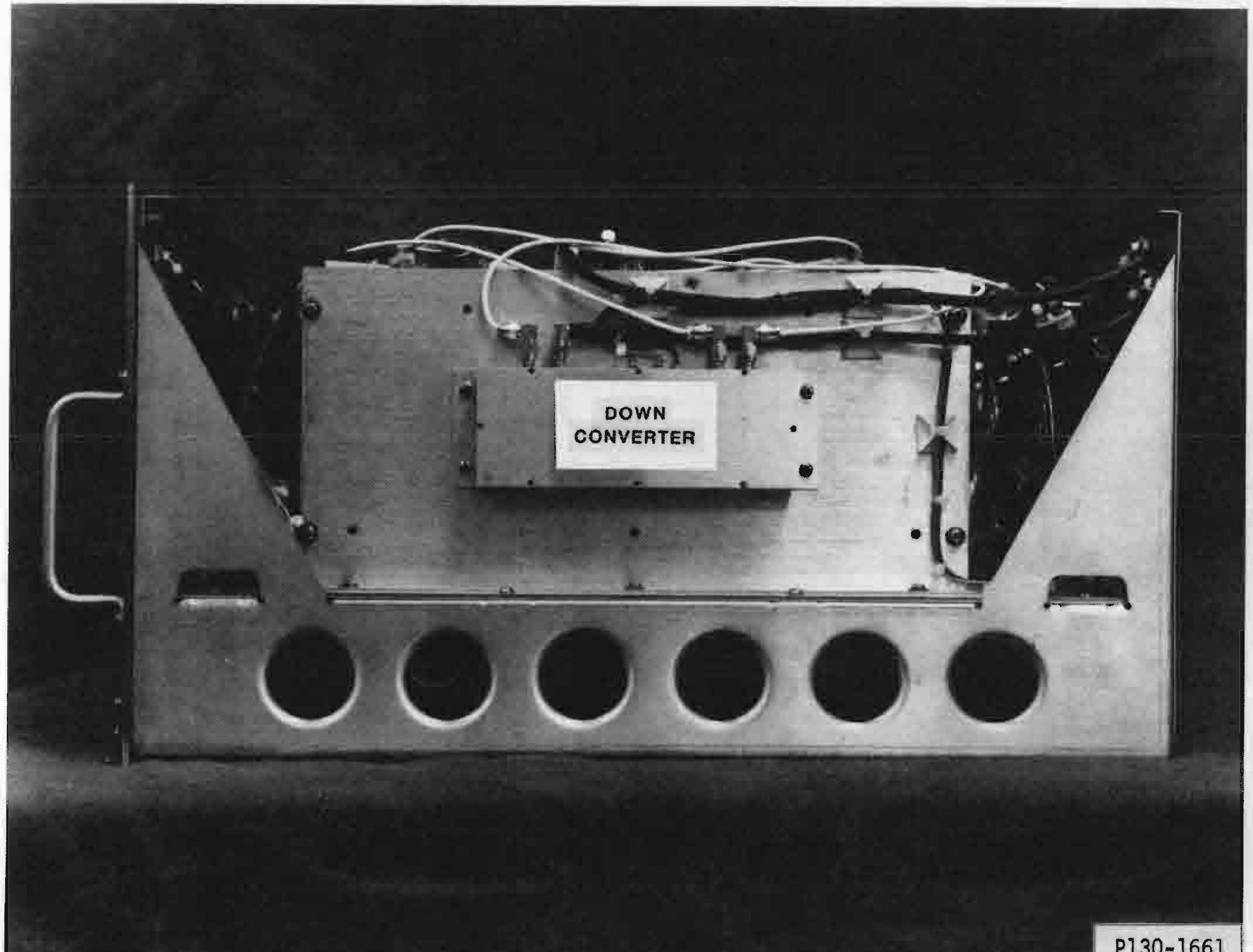

FIG. 3-21. DUAL CHANNEL RECEIVER - DOWN CONVERTER

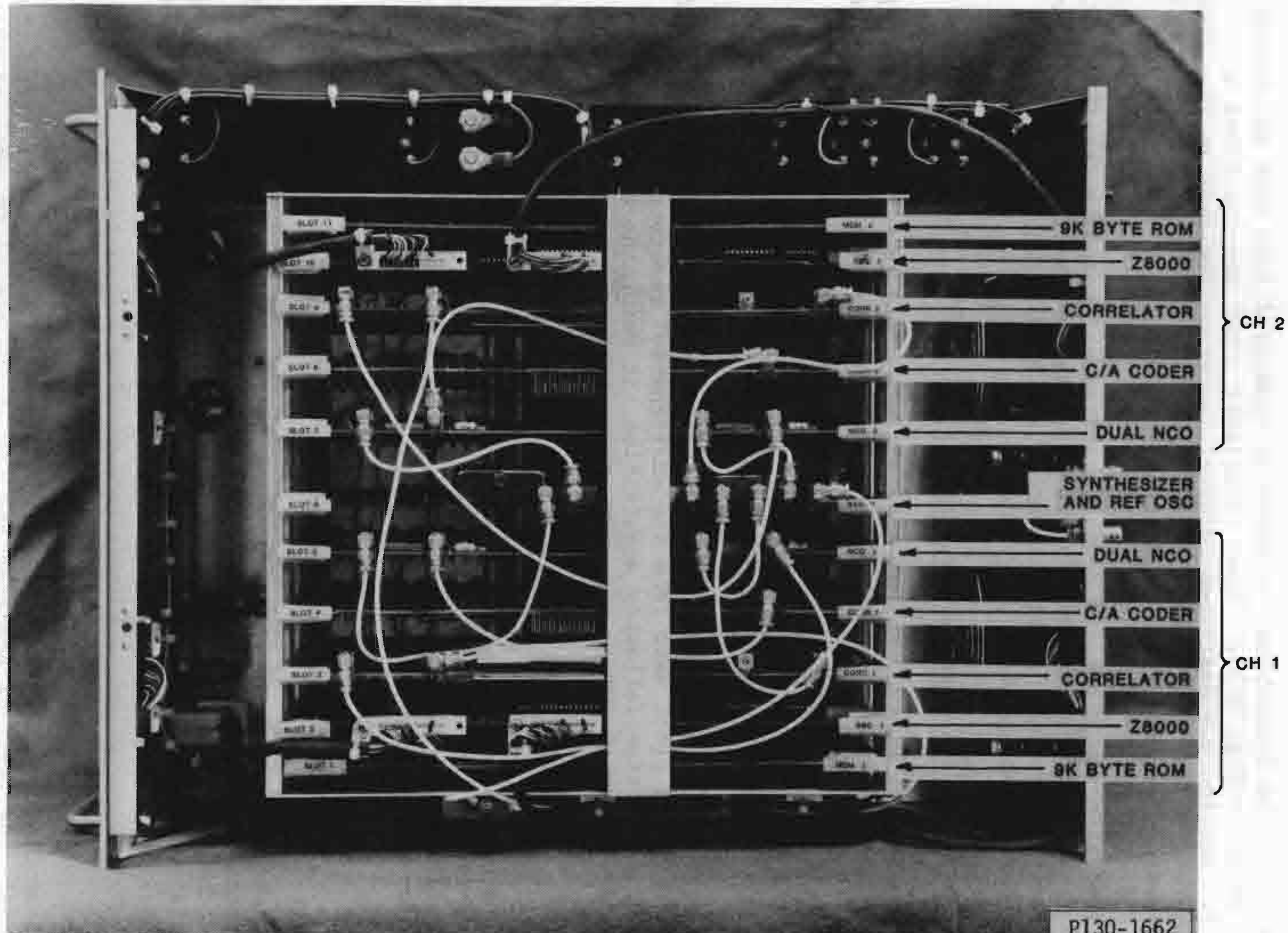

FIG. 3-22. DUAL CHANNEL RECEIVER - TOP VIEW

3.5 Position Software

3.5.1 Overview

The GPS T and E Equipment software is organized into four functional areas as shown in Fig. 3-23. These functional areas are described in Table 3-7. Section 3.4 described receiver functions resident in the Z8000 microcomputers. The Navigation, Instrumentation and Control and Display Unit software designs are described in Sections 3.6-3.8.

This section describes the position software located in the LSI-11/23 Position Processor. The position software, developed by Intermetrics, Inc., is organized into several functional areas as shown in Fig. 3-24. The following paragraphs describe each module:

3.5.1.1 System Mode Control

This module maintains control over all other modules. It controls the receiver channel modes, prepositions the receiver channels in frequency and code phase, and updates the SV list as visibilities change with time and aircraft altitude.

3.5.1.2 System Time Management

The system time management module establishes and maintains system time based on the 50 Hz clock sent from the dual channel receiver. After correction to GPS time following acquisition, it maintains time for data tagging and display of GMT to the operator or pilot.

3.5.1.3 Satellite Selection

This module makes use of a stored almanac, stored current position, and a battery-operated calendar clock to select four SVs for initial acquisition. It also will implement a search strategy should less orbital information be available or the clock have failed. While in operation it also maintains a list of up to 10 visible SVs.

3.5.1.4 Receiver Management

The functional task breakdown between the position software and the dual channel receiver was shown in Table 3-4. A high level flow chart which describes the major receiver states from the point of view of the receiver firmware is provided in Fig. 3-25. The detailed activities of this module during acquisition were shown in Fig. 3-2.

3.5.1.5 GPS Navigation Data Management

This module receives parity-checked navigation message words from the dual channel receiver. It monitors the age of the stored SV ephemeris data, requests updates, monitors data collection and maintains a full data almanac for all SVs.

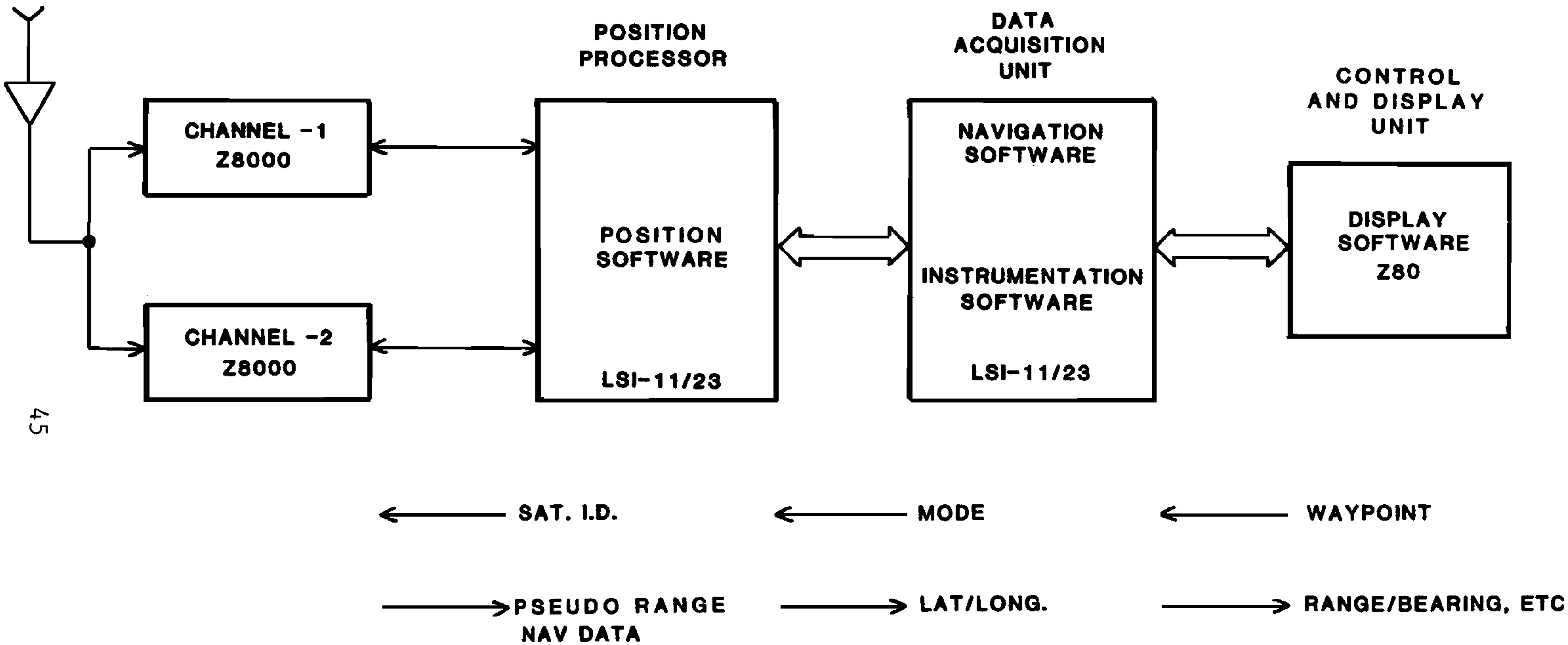

FIG. 3-23. SYSTEM SOFTWARE

TABLE 3-7

SOFTWARE FUNCTIONAL AREAS

- Receiver Firmware (Z8000)

  Directs detailed acquisition of SVs, maintains receiver feedback loops (AFC, DLL, etc.), computes pseudo-range, demodulates navigation data and maintains dwell tracking. Is under the control of Receiver Software.

- Position Software (LSI-11/23)

  Selects satellites, controls Z8000 receiver activities, computes position estimates in latitude-longitude coordinates and monitors performance.

- Navigation and Instrumentation Software (LSI-11/23)

  Accepts position estimates from the receiver management software and waypoint definitions from the cockpit display. Computes bearing, distance and time estimates, controls course deviation indicator and provides data to the control and display unit software. Collects, distributes and records data.

- Control and Display Unit Software (Z80)

  Establishes specific formats and protocol for data entry and display on the cockpit display and control unit.

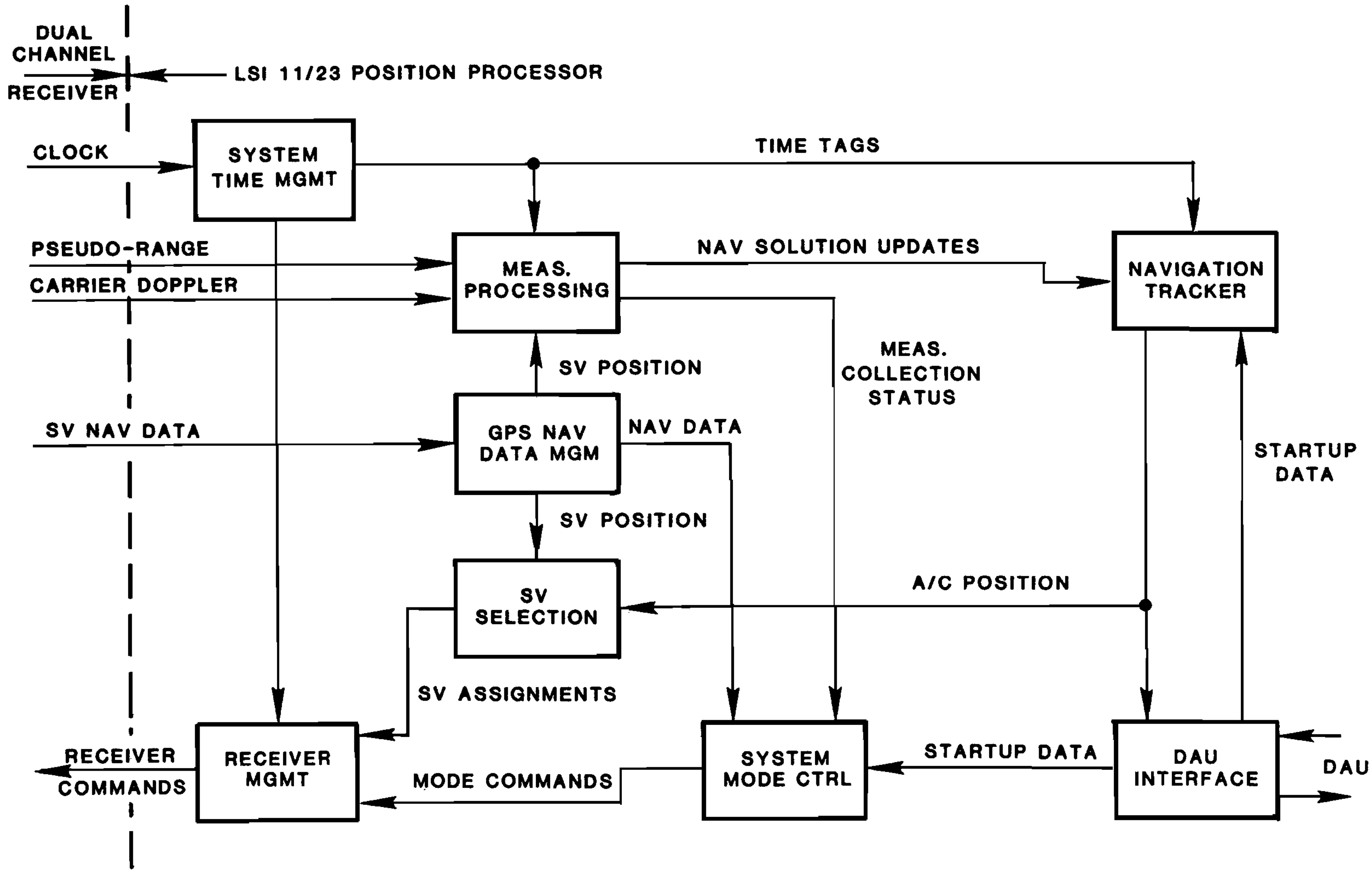

FIG. 3-24. POSITION SOFTWARE SYSTEM BLOCK DIAGRAM

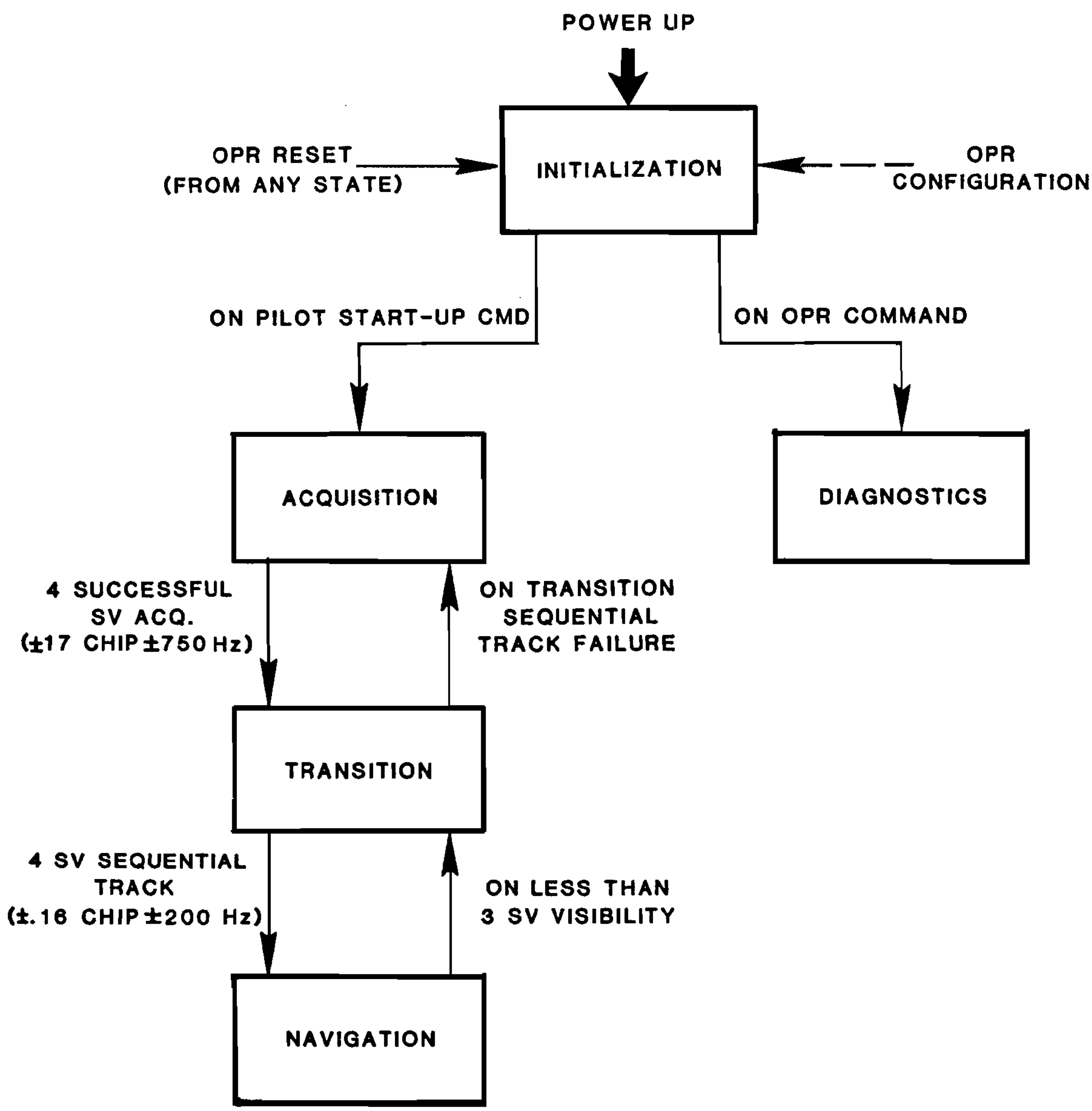

FIG. 3-25. RECEIVER MODES

3.5.1.6 Measurement Processing

This module collects measurements from the receiver channels, resolves measurement ambiguities, compensates for deterministic error effects such as tropospheric delay, and computes a position and time fix every 2.2 seconds.

3.5.1.7 Navigation Tracker

This module maintains a current estimate of the aircraft position, smooths position fixes using an alpha-beta tracker and interpolates the data to provide 1-second updates to the navigation software.

3.5.1.8 DAU Interface

This module provides linkage with the the Data Acquisition Unit (DAU). It accepts inputs during system start up (position and time if required), and transfers smoothed navigation estimates (in latitude-longitude coordinates) and aircraft velocity estimates to the navigation software in the DAU. The DAU interface also accepts receiver channel configuration commands from the DAU, and provides receiver data to the DAU for recording on magnetic tape. The DAU also provides a limited data display capability while in flight. The interface to the DAU is a DMA hardware interface since the DAU resides in a separate LSI-11/23.

The implementation of the receiver software is under the Digital Equipment Corporation RSX-11S operating system. The software was written in RATFOR, a structured FORTRAN language. A top-down design approach was used to achieve developmental flexibility and modular, well documented, maintainable software.

3.5.2 Acquisition Strategy

The basic acquisition strategy was described in Section 3.1. This section provides additional detail regarding satellite selection, receiver channel control and preparation for entry into the transition mode.

While provisions for the cold start mode were incorporated in the design, the typical situation as described here will be a narrow or wide band start as defined in Table 3-1. Both assume that a battery operated clock provides GMT to $\pm$ 1 minute, and that the present location and an almanac less than 30 days old are available from a non-volatile memory.

A satellite selection algorithm is used in the acquisition mode in order to a) select a reasonable set of up to 6 satellites to provide good geometry and shadowing protection during departure if one or two satellites fade during turns, and b) present an acceptable fix to the CDU within 6 minutes. Later, in the navigation mode, selection is unnecessary as all satellites in view are tracked.

Initially, a set of four satellites are selected based on maximizing the sum of the azimuth and elevation differences between all pairs, and providing at least 30° elevation angle to all satellites, if possible. Additional satellites, if available, are selected for subsequent acquisition in order to enter the navigation mode with up to 6 in track. Eventually all satellites in view are acquired and placed in the navigation mode.

The time to acquire the first satellite was shown by Intermetrics to have a smaller variance if both channels searched in parallel for the first satellite than if each channel searched independently for different satellites. Therefore, initial acquisition is done by both channels searching cooperatively for a single satellite. When the first satellite is acquired, the local clock is corrected to a value within 20 milliseconds of GPS time and the reference oscillator frequency error is logged to reduce the frequency search during the remaining satellite acquisition.

The acquisition strategy includes reacquiring all previously acquired satellites following each new acquisition (a detail not shown in Fig. 3-2) because of the need for recent code phase and doppler estimates in order to preposition the receiver channel for the transition mode. If acquisition is completed but only three satellites are located, the barometric altitude is substituted and the initial position fix is computed.

3.5.3 Transition Strategy

When four satellites have been successfully acquired (or if necessary, three plus barometric altitude), the position software commands one of the receiver channels into the transition mode. In this mode, each satellite is acquired and tracked for 1 second. At the end of each four second schedule a fix is attempted. When two successive fixes are successful, the receiver software computes prepositioning data in preparation for the navigation mode.

3.5.4 Navigation Strategy

When the position software determines that two successive fixes have been successful, the transition mode is terminated and the receiver channel placed in the navigation mode. Once started the receiver channel Z8000 is able to sustain the 0.22 second per satellite sequential detection of up to ten satellites without further assistance from the position software. The position software does, however, have to synchronously request and accept pseudo-range, code phase, and status data from the navigation mode channel every 0.22 seconds.

Once one receiver channel is placed in the navigation mode, the second channel is used to acquire and track additional satellites in order to place them in a navigation mode slot, and to update ephemeris and almanac data. As new satellites rise, a satellite visibility algorithm (run every 3 minutes) enables SV acquisitions by the second channel and allows new SVs to be placed in navigation slots in the first channel.

The ten navigation slots are all filled if less than ten satellites are in view, by repeating satellites in the extra slots as necessary. This simplifies several algorithms and provides additional margin for satellites that are fading but are assigned to more than one slot.

A pseudo-range measurement is declared valid by the receiver channel if AFC lock occurred during the last dwell interval, and it is within 1000 feet of a predicted value based on a predicted position. When a valid measurement is not received for a particular satellite, the algorithm in Fig. 3-26 is invoked.

Valid pseudo-range measurements for each 2.2 second scheduling cycle are propagated to a common solution time using measured doppler and presented to the position estimation algorithm described in Section 3.5.5.

3.5.5 Position Estimation

A batch-processed linearization (BPL) position fixing algorithm was selected following a study of alternative techniques. The principal advantages of the BPL algorithm are that a) it uses all available pseudo-range measurements in every position fix, b) it is a minimum least-squares error estimate, and c) it can be easily implemented. A description of the position fixing algorithm is provided in Appendix A.

A separate analysis of tracking filters was conducted which compared alpha-beta, least-squares second order, and Kalman filters. The functions of the filter are to a) accept new position fixes every 2.2 seconds, b) compute new smoothed position estimates at a 1 Hz rate, and c) coast the output for up to 8 seconds* when new position estimates do not occur. Should no estimates be available for 8 seconds, the NAV flag is shown to the pilot indicating unacceptable performance.

The emphasis on low cost and limited aircraft dynamics (200 KTS, 0.5g) led to the selection of a fixed gain alpha-beta filter which had, in simulation, acceptable dynamic performance and the lowest computational requirements. The relationship between the position fixing algorithm and the navigation tracker is illustrated in Fig. 3-27. A more detailed discussion of the navigation tracker is provided in Appendix B.

3.5.6 Performance Monitoring

Performance monitoring features are provided in each receiver channel and in the position software. Table 3-8 lists the various parameters that are monitored in each receiver channel.

* Selected to limit the horizontal position error to 500 feet.

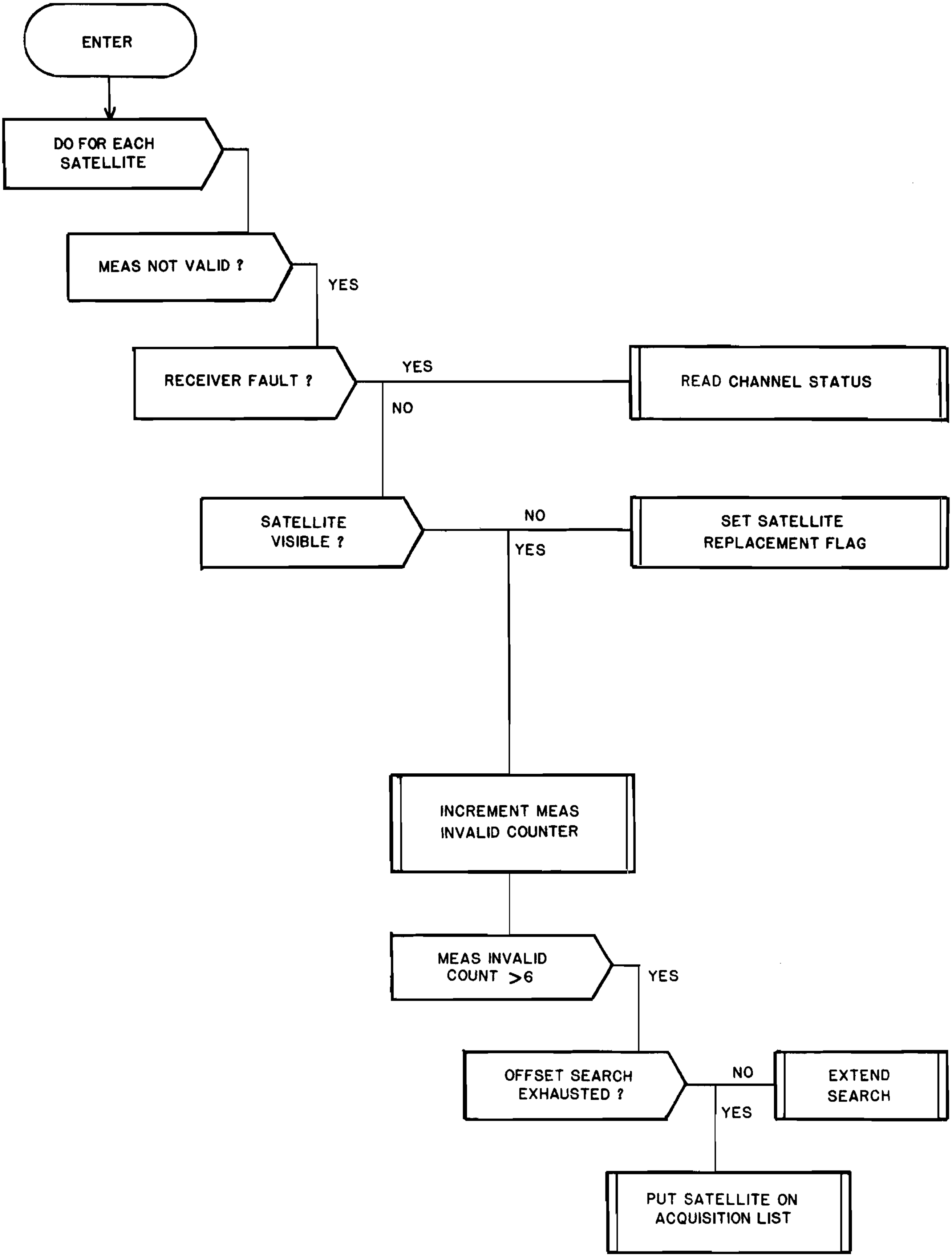

FIG. 3-26. LOSS OF LOCK ALGORITHM

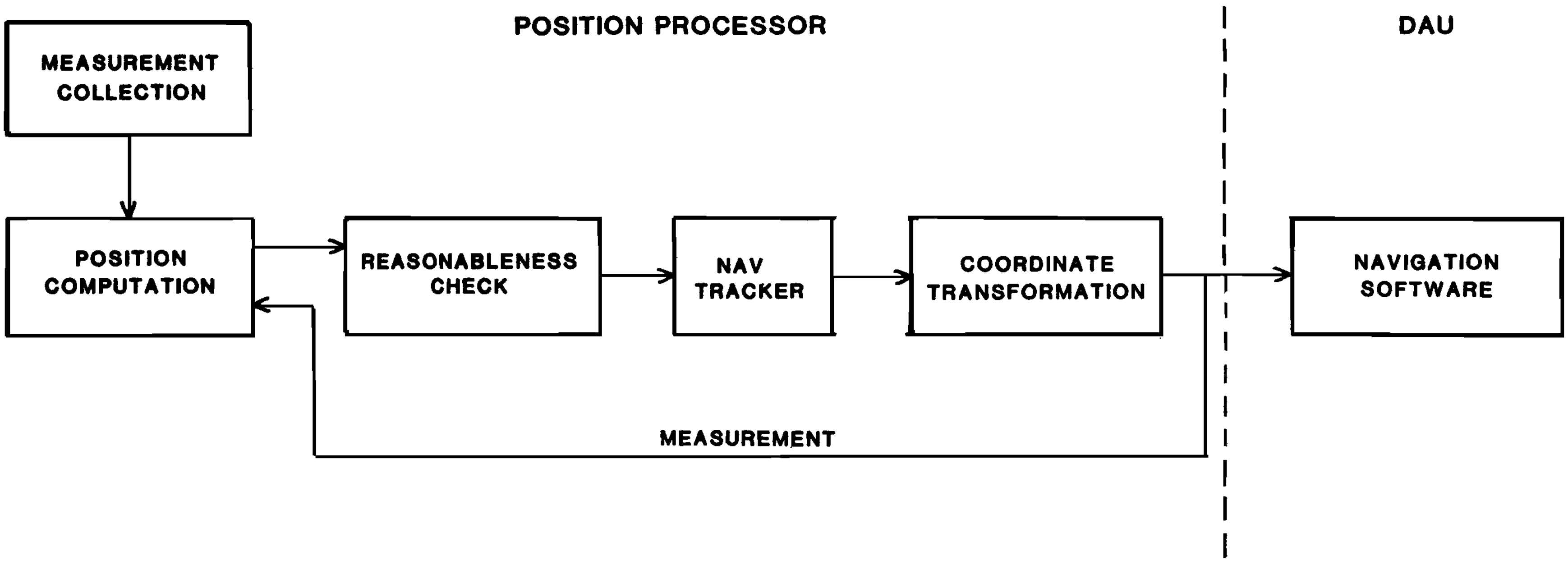

FIG. 3-27. POSITION SOLUTION AND MEASUREMENT PROCESSING

TABLE 3-8

PERFORMANCE MONITOR PARAMETERS

Receiver Channel Fault Indicators

- AGC gain out of range
- C/A coder
- Loss of phase lock on synthesizer interrupt
- 20-msec system clock not present
- NCO frequency word greater than maximum limit
- Correlator power not in range
- Correlator 2-KHz interrupt not present
- CPU fault

Receiver Channel - Position Software Interface Fault Indicators

- Command incorrectly received
- Command inconsistent with current mode
- Time-out requirement not met

The basic performance monitoring algorithm in the position software is shown in Fig. 3-28 and 3-29.

The position software also tests the navigation data for inconsistent values such as sudden change in clock bias. Slow drifts are, however, more likely and may be difficult to detect if operating with a minimum number of satellites and high GDOP.

3.5.7 Fail-Soft Techniques

Several fail-soft techniques were developed. If during any mode one of the two receiver channels fails, a design was developed in which the remaining healthy channel provides reduced rate navigation service to the pilot displays. The single channel case operates in one of two modes:

a) A mode identical to the high rate navigation mode of the dual channel case.

b) A mixed mode, illustrated in figure 3-30, which allows data demodulation to occur for one satellite and six satellites to be tracked on a 2.4 second cycle.

The latter mode requires a satellite selection algorithm to select the six satellites for the navigation dwells. The mixed mode has been fully implemented and validated in the receiver channels, and designed but not implemented in the position software.

As indicated in the description of the position fixing algorithm, Section 3.5.5, the position software monitors HDOP and the number of satellites in track. As a result it takes the actions summarized in Table 3-9.

Another fail-soft technique addressed the problem of rapid recovery following a momentary power outage. An algorithm was designed which restored navigation service within one minute of the end of a power outage lasting less than 30 seconds. The technique requires that receiver data be remembered and that a battery backup be provided for the reference oscillator (to sustain the oscillator and system clock for 30 seconds). This technique was not implemented due to other higher priority work and because it appeared to be straightforward.

3.6 Navigation Software

The navigation software is organized as shown in Fig. 3-31. It receives smoothed position estimates from the position software at a once-per-second rate. The Area Navigation Computation (RNAV) module uses the position estimates to compute navigation data for display to the pilot. As shown in Fig. 3-32, this includes distance-to-waypoint (DIST), bearing to waypoint (BRG) and cross-track deviation (XTK). The cross-track deviation is displayed to the pilot via the course deviation indicator shown in Fig. 3-33; the other parameters are displayed via the CDU front panel.

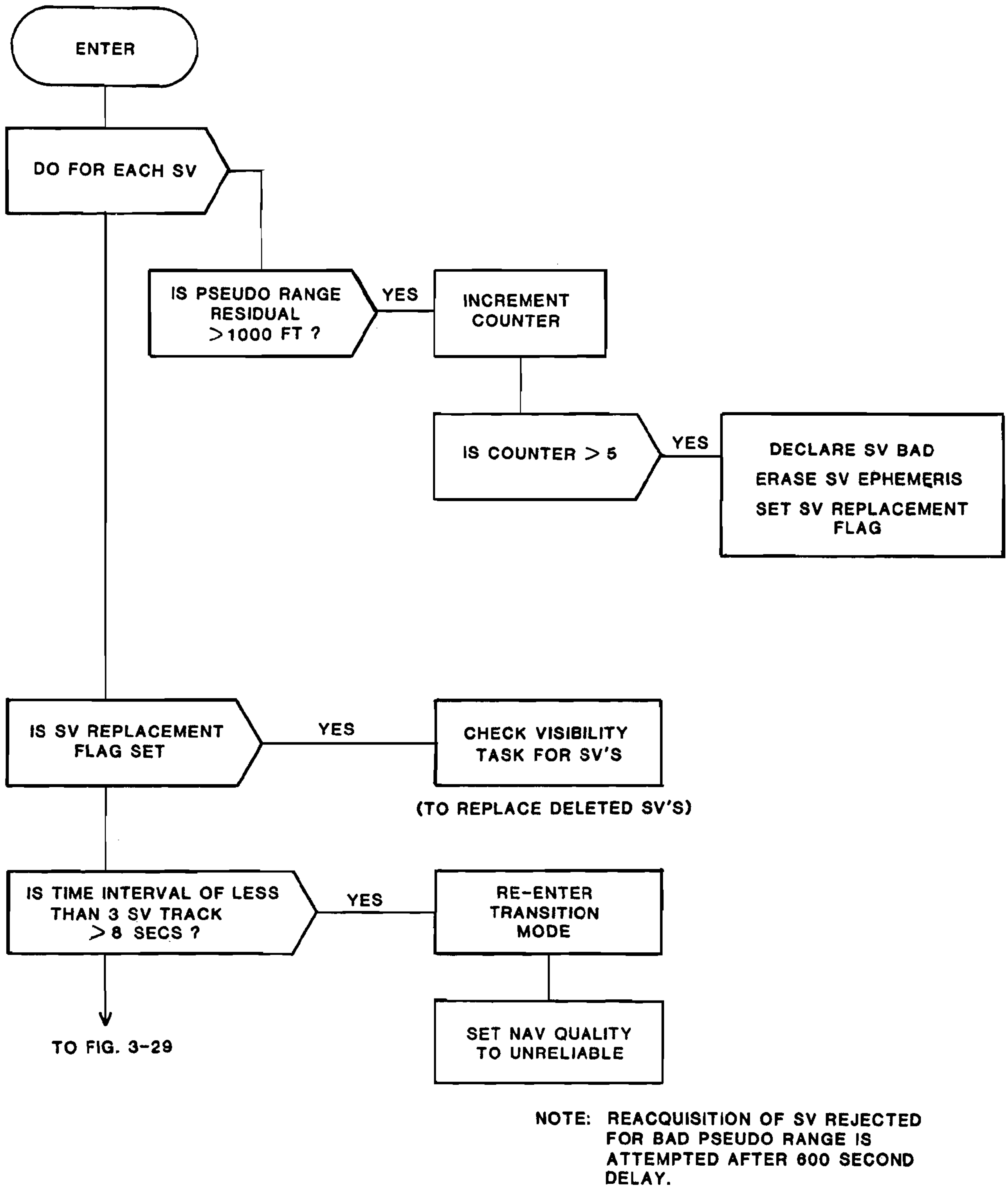

FIG. 3-28. POSITION SOFTWARE PERFORMANCE MONITOR

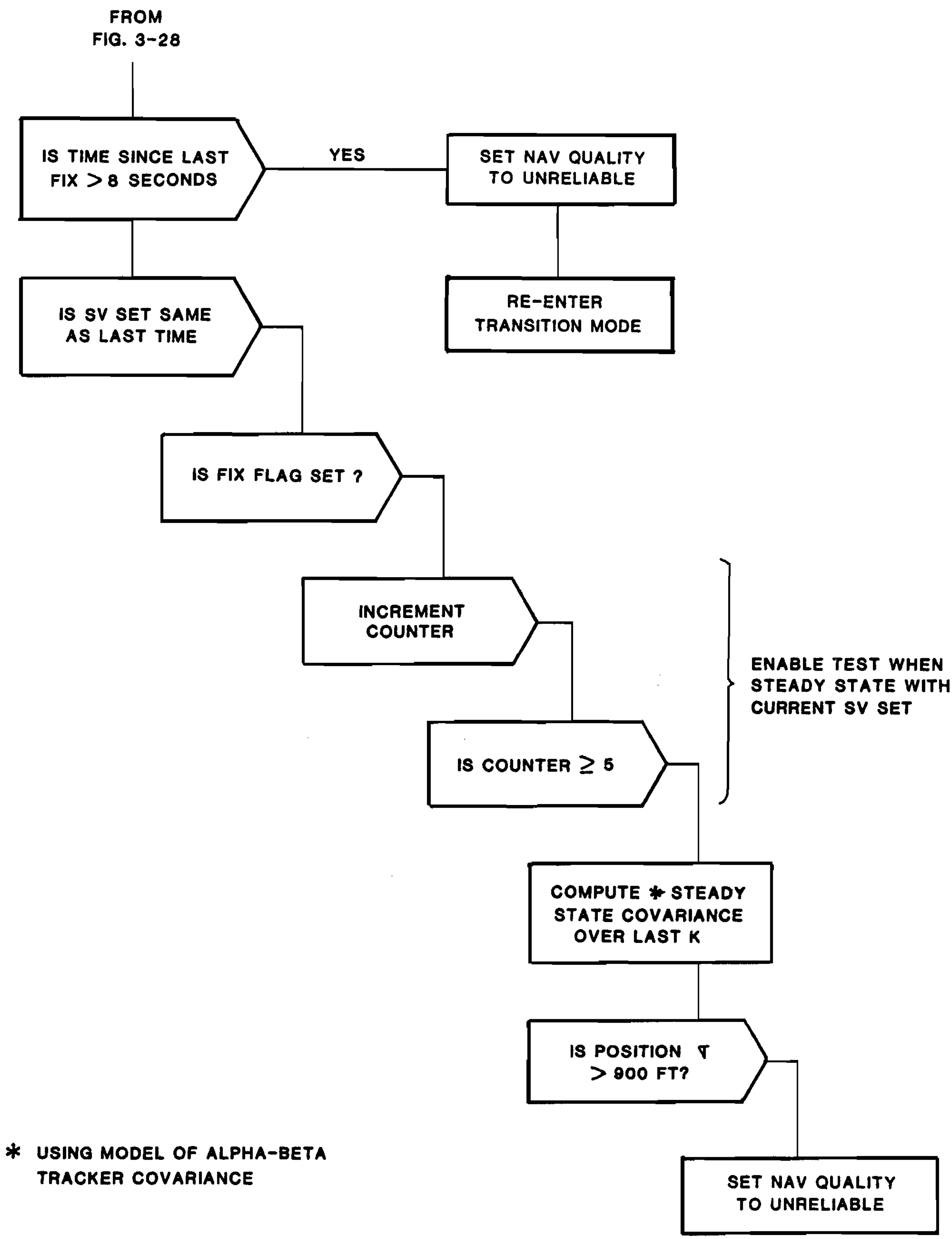

FIG. 3-29. POSITION SOFTWARE PERFORMANCE MONITOR

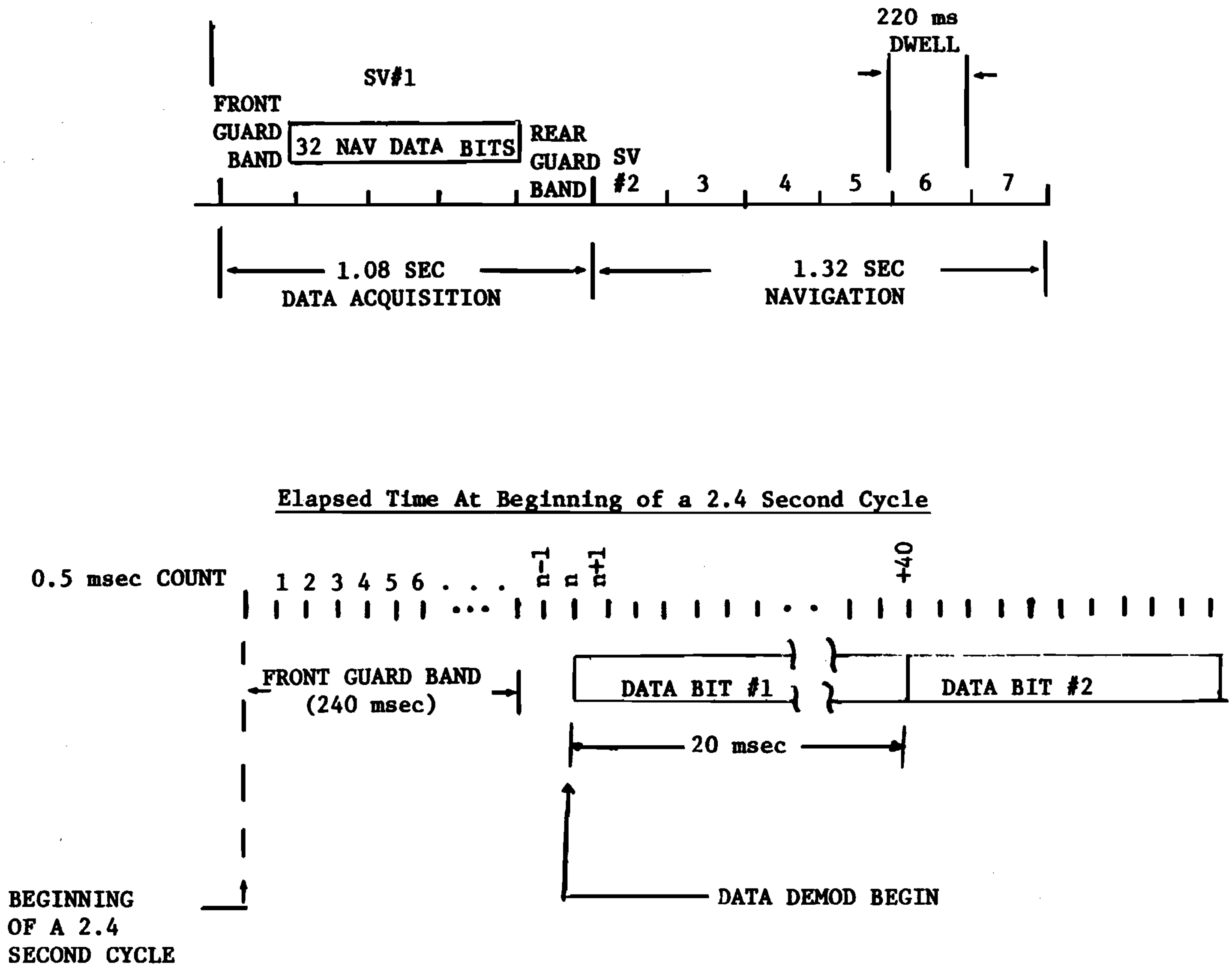

FIG. 3-30. Timing Diagram for a 2.4 Second Cycle Single Channel System.

TABLE 3-9

FAIL SOFT TECHNIQUES.

Number of Satellites in Track	HDOP	Action
0,1,2	--	Declare Failure; Go to Acquisition Mode.
3	> 10	Use coasted altitude (Pseudo-baro).
3	< 10	Substitute Baromentric Altitude.

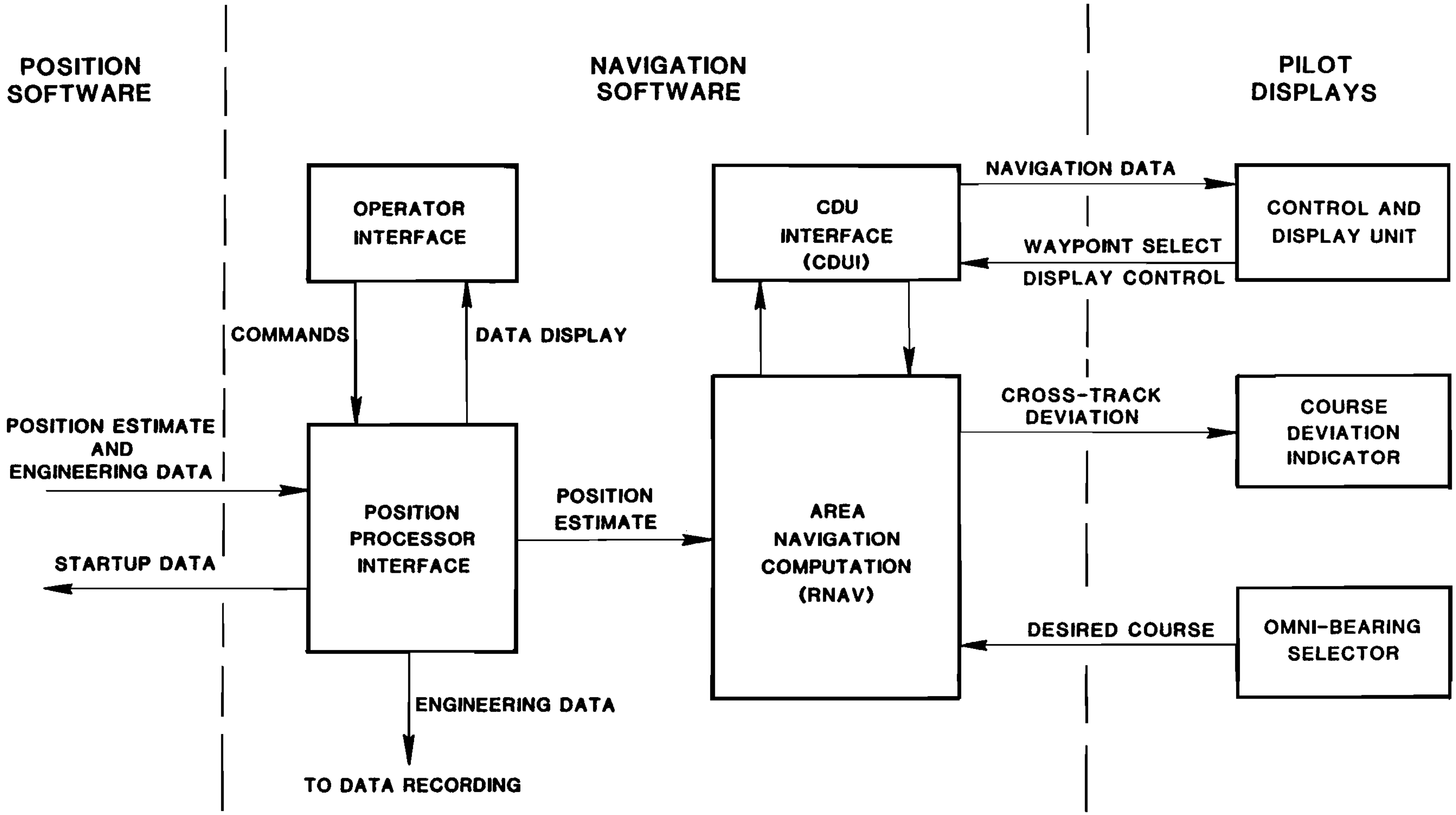

FIG. 3-31. NAVIGATION SOFTWARE, FUNCTIONAL BLOCK DIAGRAM

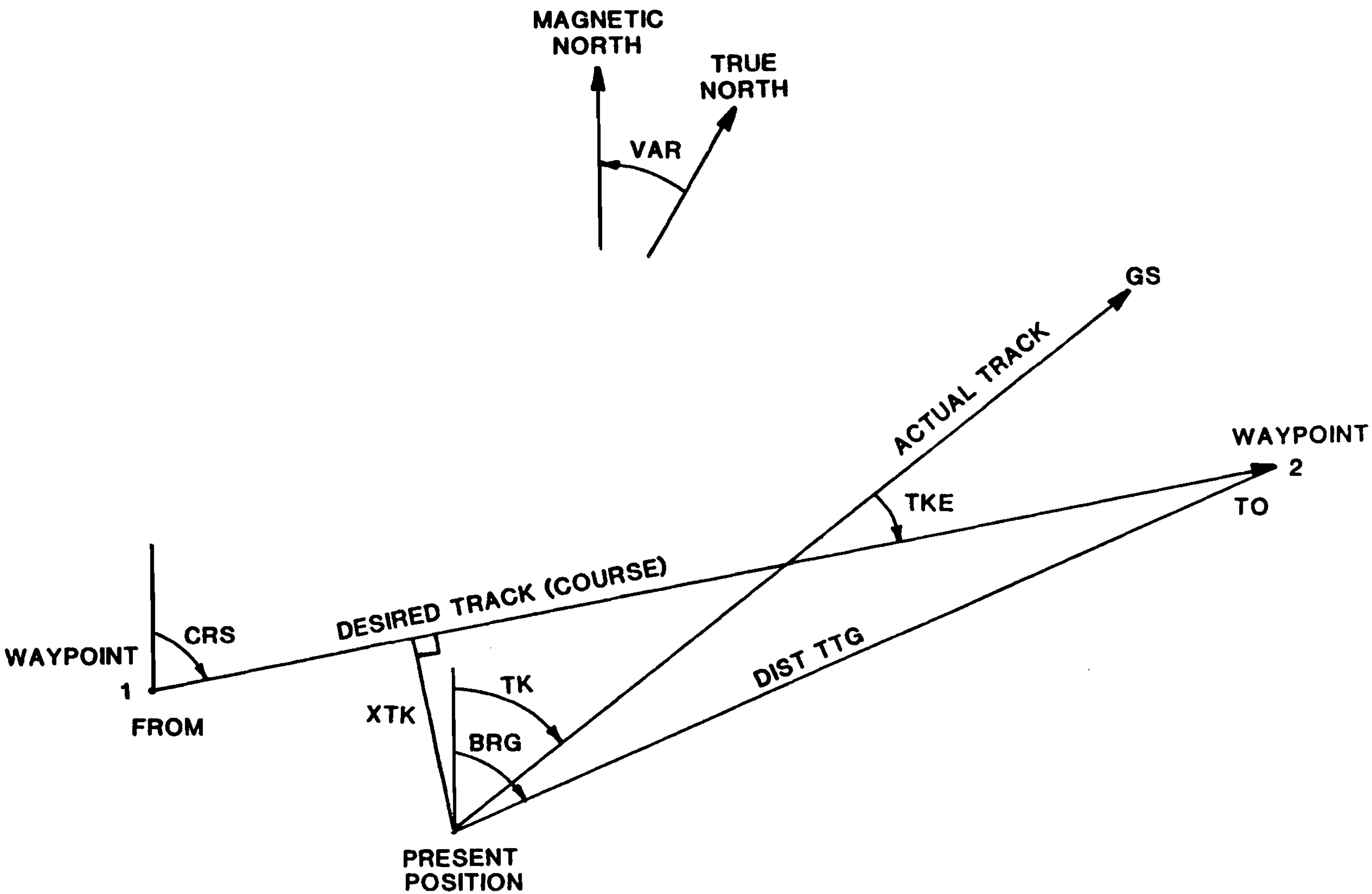

FIG. 3-32. RNAV GEOMETRY

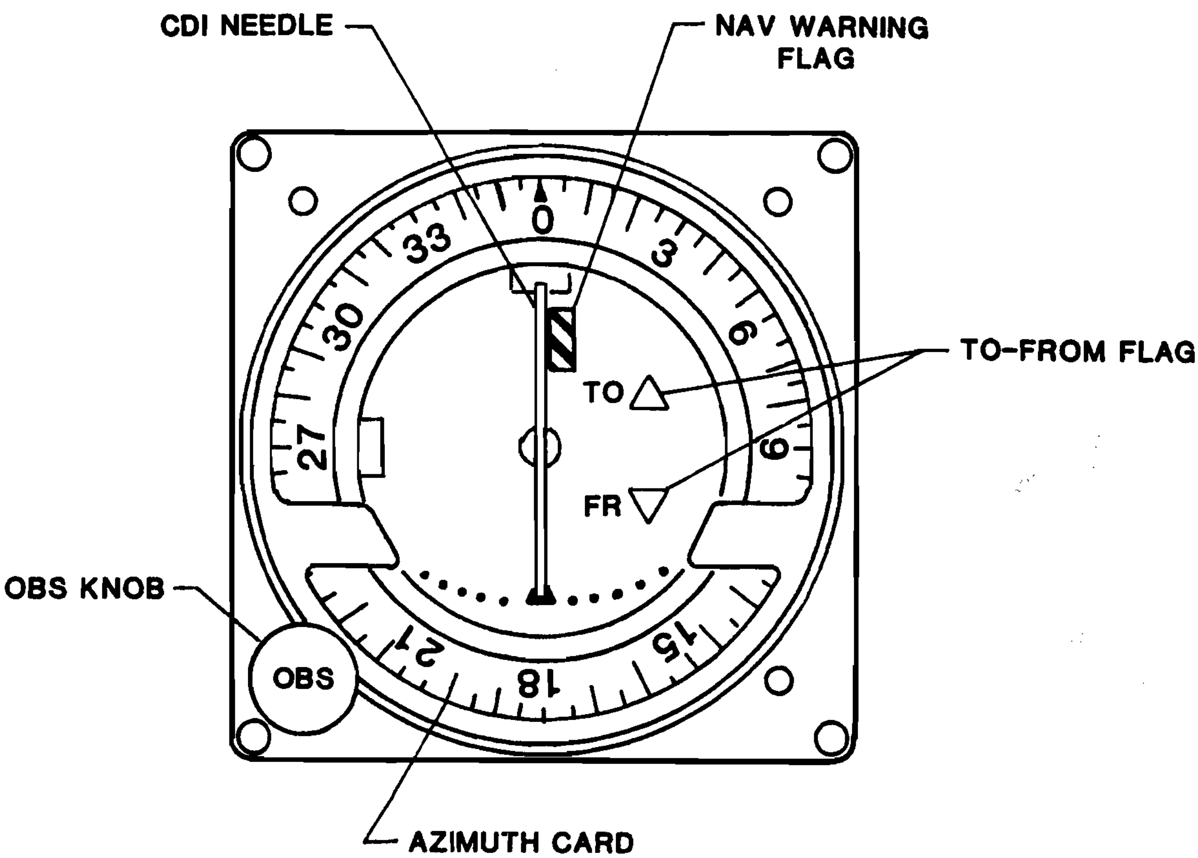

FIG. 3-33. COURSE DEVIATION INDICATOR/OMNI-BEARING SELECTOR

The CDU interface (CDUI) module receives navigation data from the RNAV module and passes the data to the CDU for front panel display. CDUI also receives pilot data from the CDU consisting of such data as startup mode, CDI sensitivity, and active waypoint number. The RNAV module passes the cross-track deviation to the CDI and reads the desired course from the OBS.

3.7 Control and Display Unit

The function of the Control and Display Unit (CDU) is to interface the pilot to the test and evaluation equipment. The CDU front panel layout is shown in Fig. 3-34. The front panel consists of an alphanumeric display with two lines of 16 characters per line, a 32 position keyboard and three control switches. The alphanumeric displays are of the LED lighted-segment type and are 0.25 inches high. These displays are bright, easily read at a distance of five feet, and feature a wide viewing angle ($\pm$ 55°). The keypads are compact, off-the-shelf, units with 0.5 inch button spacing; control switches are standard rotary types.

CDU functions can be divided into two groups: flight plan data entry and navigation data display. Flight plan entry occurs before takeoff while the GPS receiver is still in the acquisition mode and has not yet obtained an initial position fix. The pilot uses this time to enter the desired flight plan via the CDU keyboard, with appropriate prompting messages from the alphanumeric display. The flight plan data is passed to the Navigation Software via an ARINC 429 interface, as shown in Fig. 3-35. A sample flight plan for a trip from Atlantic City, NJ to Hanscom Field, MA is illustrated in Fig. 3-36. The flight plan data is entered in the form of waypoints along the planned flight path. The data file generated by this data entry process is termed the Stored Waypoint data file.[1] The Stored Waypoint data file for the sample flight plan is shown in Table 3-10.

The waypoints along the flight plan can be of several types: VOR, intersection, latitude/longitude or artificial. VOR and intersection waypoints are entered by three-and five-letter labels, respectively. Artificial waypoints are specified in terms of range and bearing from a VOR, intersection or latitude/longitude. As the waypoints are entered, they are accumulated in the Stored Waypoint data file. The navigation software determines the latitude and longitude of each waypoint using look-up tables and calculations as required. The Stored Waypoint data file also includes the courses to and from each waypoint. These courses can be entered by the pilot or computed by the navigation software.

The other function of the CDU is to display navigation data while the aircraft is in flight. The data required to support the navigation display is termed the Active Waypoint data file. This data file is maintained by the navigation software and passed to the CDU via the ARINC interface. The Active Waypoint data file must be updated at a rate such that the CDU navigation display is always current (i.e., every second).

---

1. Due to schedule constraints, the flight plan data entry function was not implemented in the navigation software. Instead, the stored waypoint file was predefined in the navigation softw[illegible] to include a set of waypoints for the test flight area. The effect was the same as if the pilot had entered the waypoints manually.

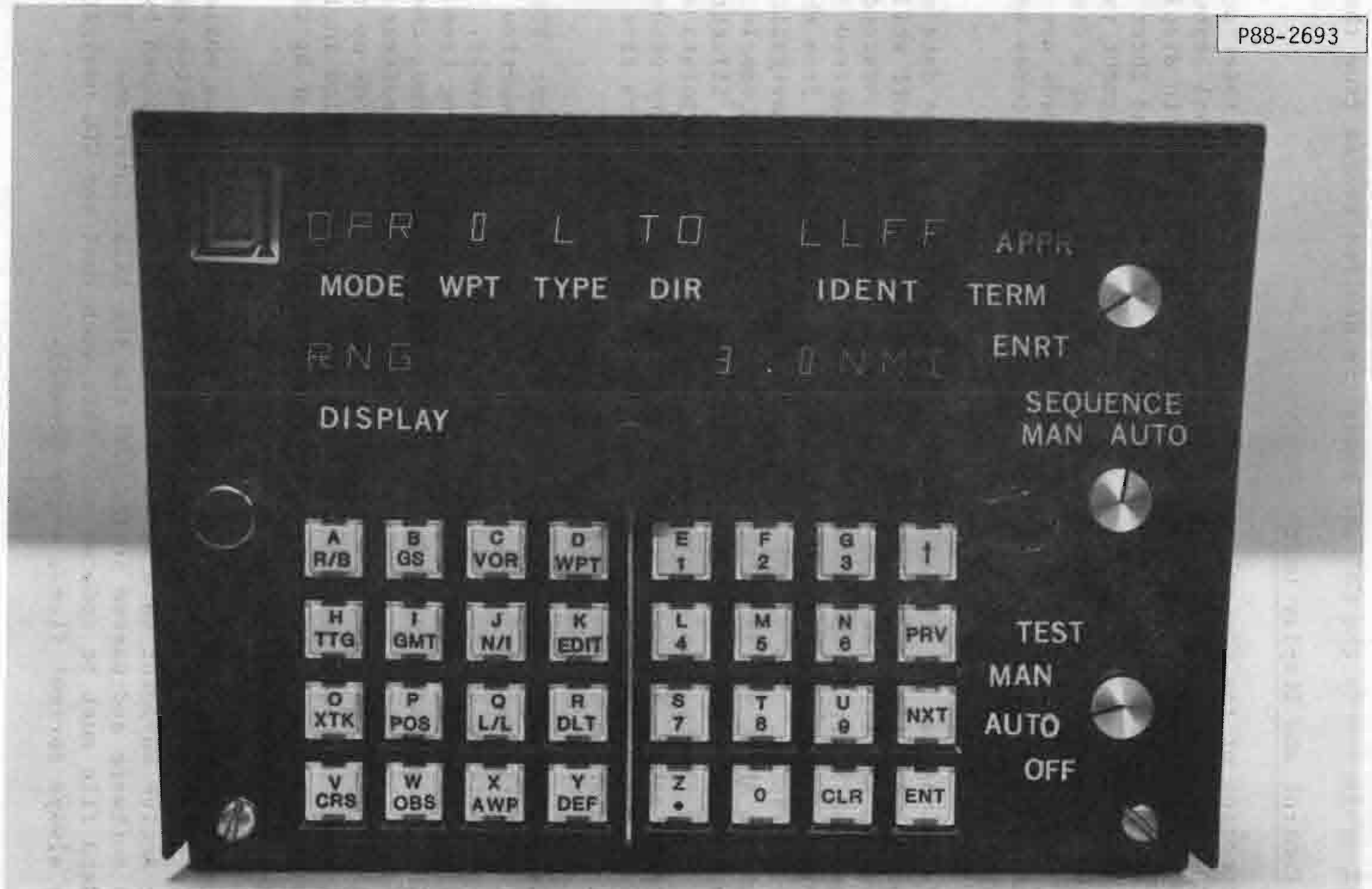

FIG. 3-34. CONTROL AND DISPLAY UNIT (CDU)

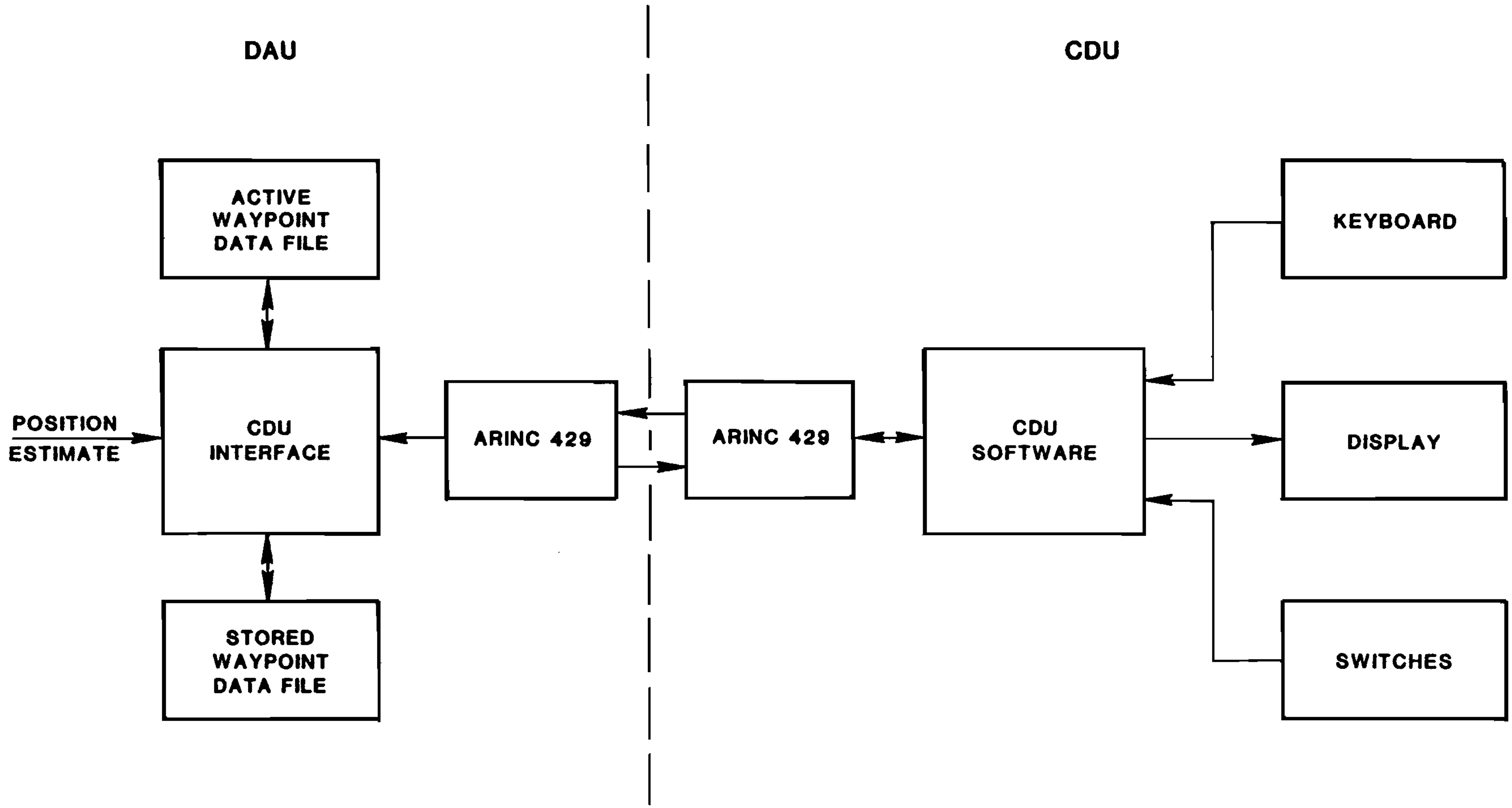

FIG. 3-35. DAU-CDU INTERFACE

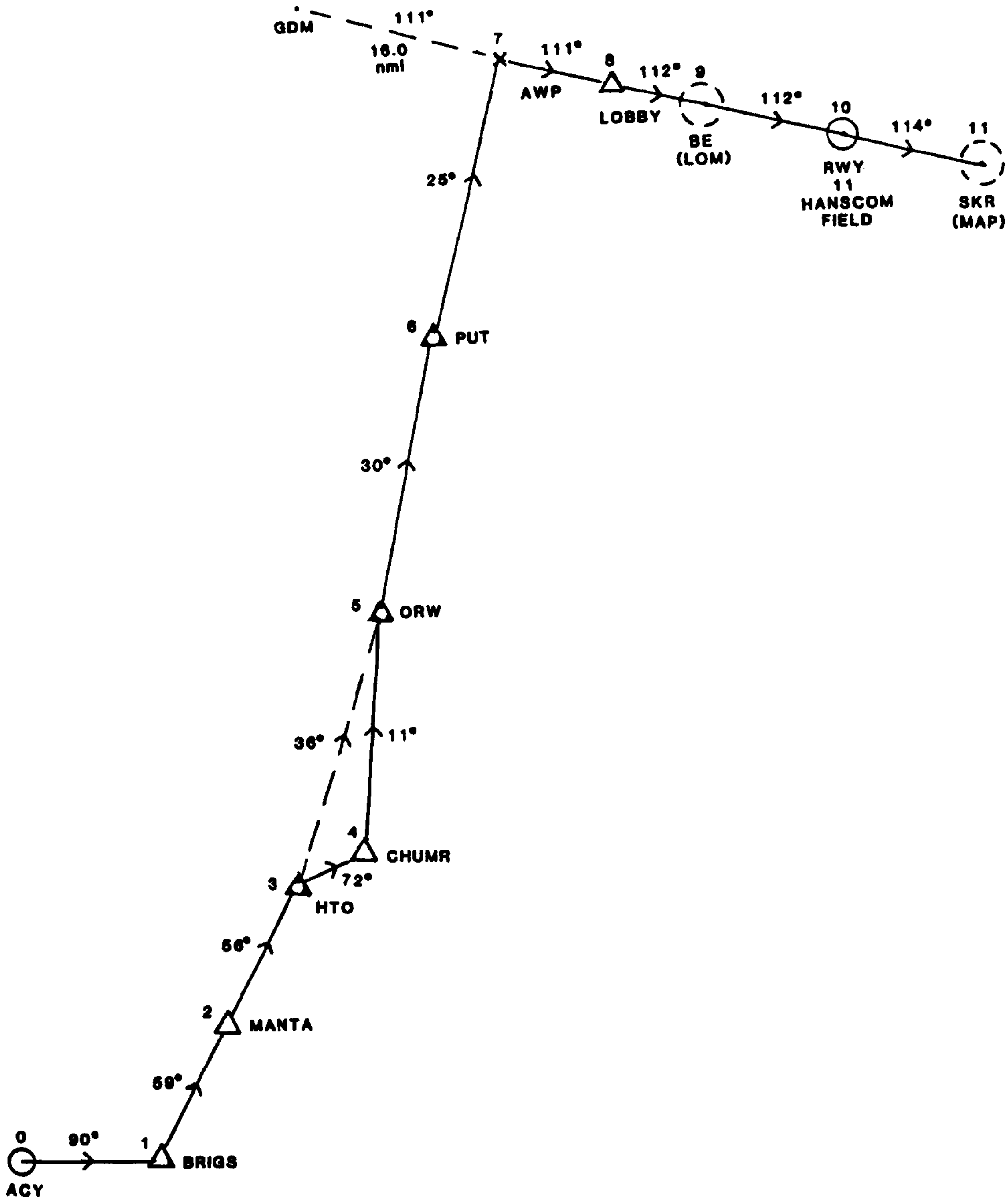

FIG. 3-36. SAMPLE FLIGHT PLAN: ATLANTIC CITY TO HANSCOM FIELD

TABLE 3-10

STORED WAYPOINT DATA FILE: ATLANTIC CITY TO HANSCOM FIELD

WPT	TYPE[1]	IDENT	TO	FROM	LATITUDE	LONGITUDE	OFFSET
0	L/L	ACY[2]	-	90°	39°27.4'N	74°34.7'W	None
1	INT	BRIGS	90	59	Lookup	Lookup	"
2	INT	MANTA	59	56	"	"	"
3	VOR	HTO	56	72	"	"	"
4	INT	CHUMR	72	11	"	"	"
5	VOR	ORW	11	30	"	"	"
6	VOR	PUT	30	25	"	"	"
7	AWP	V431[2]	25	111	Calculate	Calculate	GDM 111° 16.0 nmi
8	INT	LOBBY	111	113	Lookup	Lookup	None
9	NDB	BE	112	112	"	"	"
10	L/L	BED[2]	112	114	42°28.2'N	71°17.4'W	None
11	NDB	SKR	114	294	Lookup	Lookup	None

Note 1: L/L = Latitude/Longitude
INT = Intersection
AWP = Artificial Waypoint
NDB = Non-directional Beacon

Note 2: IDENT Optional for L/L and AWP types.

The contents of the Active Waypoint data file are shown in Table 3-11. This data includes such information as the range and bearing to the active waypoint, i.e., the waypoint the aircraft is currently heading to or from. The active waypoints can be selected by the pilot via the CDU keyboard or can be automatically incremented as the waypoints along the flight plan are overflown. The specific data displayed is selected by keyboard entries as summarized in Table 3-12. The navigation data appears in the "DISPLAY" field of the CDU display.

A typical CDU navigation display is shown in Fig. 3-37. The display indicates that the CDU mode is "OPERATE", the active waypoint is number 6 (Putnam VOR), and that the aircraft is 19.2 nmi away from the waypoint and traveling toward it. Alternate data can be obtained by pushing one of the keys in the leftmost three columns. For example, pushing "TTG" would display the time-to-go to the active waypoint. The active waypoint could be changed to number 5 by pushing "WPT", "5" and "ENT".

The uppermost rotary switch selects the CDI sensitivity desired. The three settings are for Enroute, Terminal and Approach, in order of least to most sensitive. The sequencing switch controls whether or not the active waypoint will increment automatically as the waypoints are overflown. A software check is implemented such that the pilot must rotate the OBS knob to the appropriate course before the active waypoint number is incremented. The bottom rotary switch controls the initial start-up mode of the GPS receiver. In Auto Start mode, the system assumes that the GPS receiver has not moved substantially since the last time the GPS set was turned on. In this case, the system uses the position fix stored in non-volatile memory from the last flight as the assumed initial location of the receiver. In the Manual Start mode, the operator must enter the initial position of the receiver to the nearest degree in latitude and longitude.

The CDU design is based on the Z80 microprocessor, and employs the STD BUS form factor and bus structure.

3.8 Instrumentation

The GPS T and E equipment was equipped with instrumentation to record:

a) receiver channel and position software activity and outputs,

b) received carrier to noise ratios on each satellite,

c) pilot (CDU, CDI, OBS) activity, and

d) aircraft attitude (roll, pitch, heading).

Receiver channel and position software activity is monitored by recording inter-task messages. Table 3-13 shows the general content of the various messages recorded on magnetic tape during a typical flight. Tables 3-14 through 3-21 show the message formats frequently used in assessing status and position estimation performance. Table 3-22 defines the aircraft attitude data.

TABLE 3-11

ACTIVE WAYPOINT DATA FILE

NAME	DESCRIPTION	ACCURACY	KEY	UPDATE INTERVAL
PLAT	Present Latitude	0.1'	POS	2 sec
PLNG	Present Longitude	0.1'	POS	2 sec
GS	Ground Speed	1.0kt	GS	2 sec
TK	Actual Track (Magnetic)	1.0 deg	GS	2 sec
WPT	Active Waypoint	N/A	WPT	2 sec
DIST	Distance to Active Waypoint	0.1 nm	R/B	2 sec
BRG	Bearing to Active Waypoint	1.0 deg	R/B	2 sec
DTK	Desired Track	1.0 deg	CRS	2 sec
NTK	Next Desired Track	1.0 deg	CRS	2 sec
TTG	Time-to-go	0.1 min	TTG	2 sec
XTK	Cross-track Deviation	0.01 nmi	XTK	2 sec
TKE	Track Angle Error	0.1 deg	XTK	2 sec
VAR	Magnetic Variation	1.0 deg	GMT	2 sec
GMT	Greenwich Mean Time	1 sec	GMT	1 sec
OBS	Current OBS Setting	1 deg	OBS	1 sec
CSE	Course Selection Error	0.1 deg	OBS	1 sec
TDIST	Total distance flown from Waypoint 0.	1.0 nmi	TTG	2 sec

TABLE 3-12

DISPLAY FIELD BY KEY ENTRY (OPR MODE ONLY)

KEY	DISPLAY (Note 1)	EXPLANATION
R/B	WPT RNG 19.2 NMI	Range to active waypoint
R/B	WPT BRG 207 MAG	Bearing to active waypoint
TTG	WPT TTG 12.1 MIN	Time to go to active waypoint
TTG	TOT TIME 2:31 HRS	Total time in air from waypoint 0.
XTK	XTK DEV 0.02 NMI	Cross-track deviation
XTK	TRK ERR 14.1 DEG	Track Angle Error (DTK-TK)
CRS	CRS TO 205 MAG	Course to active waypoint (Note 2)
CRS	CRS FROM 241 MAG	Course from active waypoint (Note 2)
GS	GS 135 KTS	Ground Speed
GS	TK 206 MAG	Actual Track
GMT	GMT 1453:11 HRS	Greenwich Mean Time
GMT	MAG VAR 15 DEG	Magnetic Variation
POS	LAT 42DG 17.0'	Present Latitude
POS	LONG 71DG 43.6'	Present Longitude
OBS	OMNIBRG 170 DEG	OBS Setting
OBS	OBS ERR 2.1 DEG	Course Selection Error (DTK - OBS)
VOR	***INVALID ENTRY	Not used in OPR Mode
INT	***INVALID ENTRY	Not used in OPR Mode
L/L	WLAT 41DG 23.6'	Active waypoint latitude
L/L	WLNG 72DG 42.1'	Active waypoint longitude
AWP	ART WP: GDM VOR	Reference ident and type
AWP	111.0MAG 16.0 NMI	Bearing and range from reference

Note 1: The first display listed for each key appears the first time the key is struck, (except CRS key, see Note 2.) Subsequent keystrokes cause the two display lines to alternate.

Note 2: The first strike of CRS Key causes "CRS TO" to be displayed if current direction is "TO" active waypoint. Otherwise, "CRS FROM" is displayed. Subsequent keystrokes cause lines to alternate.

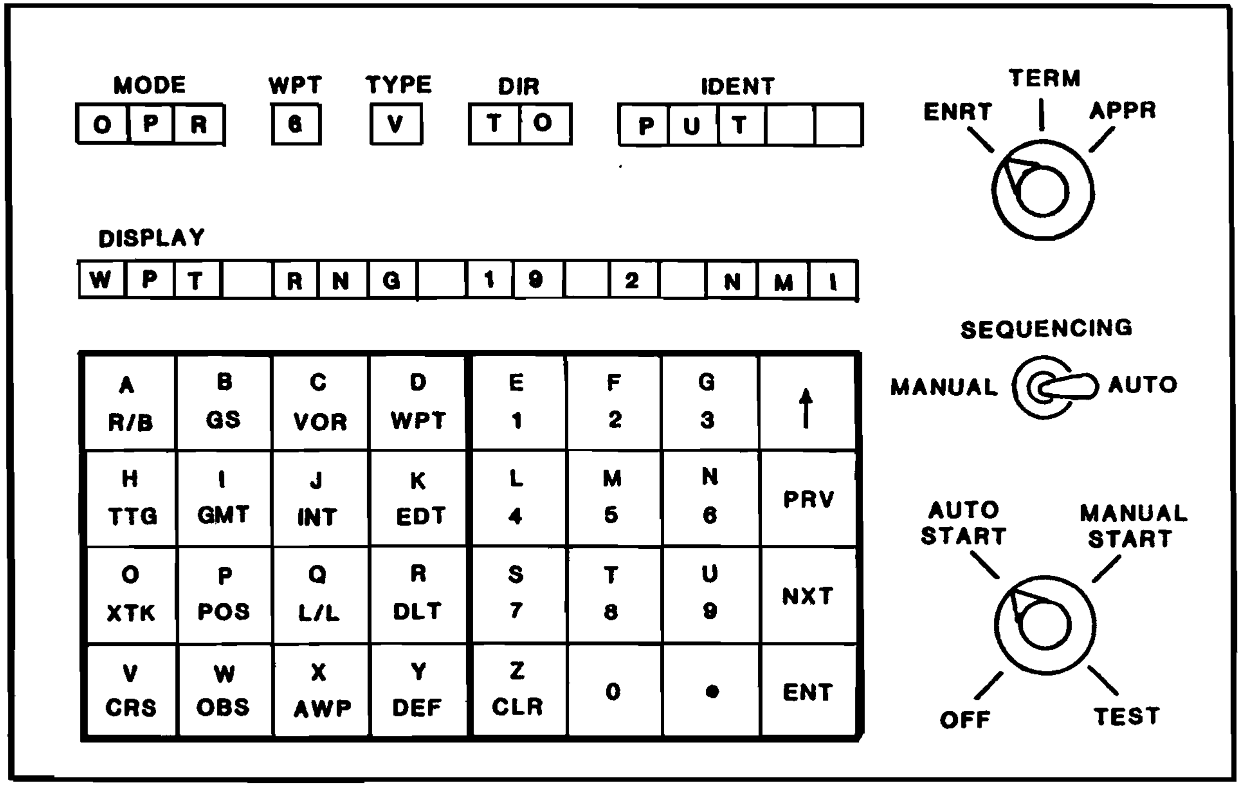

FIG. 3-37. GPS CDU FRONT PANEL

TABLE 3-13

DATA RECORDING MESSAGES

Message Block Number	Source	Content	Frequency
0	DAU	System Reset	Startup
10	DAU	Receiver Configuration Data	Startup
15	NSW	PNP-DAU Time Synchronization	Startup
20	PSW	Position Estimate Sent to NSW	1/sec
25	DAU	Operator Startup Data (if defined)	Startup
30	PSW	Raw GPS Satellite Nav Data (1 word)	Variable
40	PSW	Acquisition Command	As Required
50	PSW	Phased Transition Command	As Required
60	PSW	Navigation Command	As Required
70	PSW	Measurement Command Data	1-5/sec
80	PSW	Satellite Reassignment Command	As Required
90	PSW	Nav Plus Data Command	Single Channel
110	PSW	Ephemeric, Clock and Almanac	Infrequent
120	PSW	PSW Error Message	
130	NSW	Receiver Startup Data to PSW	Startup
140	PSW	PNP Status to DAU	3/Minute
150	PSW	Raw Position Fix	1/2.2 sec Typical
160	PSW	Tracked Position Fix	1/sec
170	NSW	Pilot Flight Plan Waypoint Data	As Required
180	NSW	CDU, CDI, OBS Data	1/sec
190	NSW	Pilot Startup Data From CDU	Startup
200	NSW	Displayed Waypoint Data Type	When Changed
210	NSW	OBS Data	1/sec
220	NSW	Displayed Waypoint Data	1/sec
230	NSW	Clock Status Sent to CDUI	Startup
400	ADU	RAS Data	1/sec
410	ADU	DME Data	Variable
420	ADU	ADU Status	Variable
430	ADU	ADU Error	Variable

DAU Data Acquisition Unit
NSW Navigation Software
PSW Position Software
ADU Aircraft Data Unit
RAS Real Time Aircraft State

TABLE 3-14

BLOCK #10 RECEIVER CHANNEL CONFIGURATION DATA

Byte	Definition	Format	Units	LSB Scale
1	Block ID (=10)	constant	N/A	1
2	Block Length (=14)	constant	words	1
3	Dual/Single Channel = 0 Dual = 377_8 Single	binary, unsigned	N/A	1
4	Statistics Collect (1 = collect)			
5-6	AGC Loop Corner Frequencys	byte	N/A	1
7-8	Nominal AGC Gains	byte	N/A	1
9-12	Search Thresholds	integer	N/A	1
13	Re-search Frequency offset	integer	Hz	1
14-16	AFC Loop Noise Bandwidths	byte	Hz	1
17-18	Code Loop Noise Bandwidths	byte	Hz	1
19-26	AFC Lock Gains	integer	N/A	1
27-28	Bit Sync Histogram Threshold	byte	N/A	1

TABLE 3-15

BLOCK #30 RAW GPS NAV MESSAGE DATA WORD

Byte	Definition	Format	Units	LSB Scale
1	Block ID (=30)	constant	N/A	1
2	Block Length = (13)	constant	bytes	1
3-10	GPS Time	real	seconds	-
11-14	Mission Time	integer	millisecs.	20 ms.
15	Channel Status	see block #70		
16	SV ID	binary, unsigned 6 LSBs	N/A	1
17	Subframes ID	binary, 3 LSBs	N/A	1
18	Word count (1-10) within subframe	binary, 4 LSBs	N/A	1
19	Parity check flag: 0 = data valid 1 = parity fail	binary, LSB	N/A	1
20	Least significiant byte of demodulated parity stripped data word	binary	N/A	-
21	2nd byte of demoudlated, parity stripped data word	binary	N/A	-
22	Most significant byte of demodulated parity stripped data word	binary	N/A	-
23-24	Wide Band Power	see block #70		
25-26	Narrow Band Power	see block #70		

TABLE 3-16

BLOCK #40 ACQUISITION COMMAND DATA

Byte	Definition	Format	Units	LSB Scale
1	Block ID (=40)	constant	N/A	1
2	Block Length (=12)	constant	bytes	1
3-10	GPS Time	real	seconds	-
11-14	Mission Time	binary, unsigned	milli-seconds	20 ms.
15	SV ID Assignment (1-31)	binary, unsigned 6 LSB's	N/A	1
16-17	Carrier frequency prepositioning estimate (Note 1) 16 - LSByte 17 - MSByte	binary, 2's complement	Hz	4.064
18	Sub-chip phase code prepositioning estimate (0-9)	binary, unsigned 4 LSB'S	C/A code chip	0.1
19	Chip phase code prepositioning estimate, (0-1022) least significant byte	binary, unsigned	C/A code chip	1
20	Chip phase code prepositioning estimate, 2 MSB's	binary, unsigned, 2 LSB's	C/A code chip	256
21	Epoch phase code prepositioning estimate (0-19)	binary,unsigned, 6 LSB's	C/A epochs	1
22	Search and Acquisition Strategy	(Note 2)	(Note 2)	(Note 2)
23-24	Bit Count (0-299) (Note 3) 23 - LSByte 24 - MSByte	binary, unsigned binary, unsigned 1 LSB	quanta quanta	1 256

TABLE 3-16. (CONT'D)

Notes:

(1) All prepositioning estimates are valid at the trailing edge of the particular 20 msec system clock pulse defining the beginning of acquisition of an SV.

(2) Search and Acquisition Strategy Byte, contains:

- Bit 7 (MSB)is DATA DEMOD FLAG
  - 0: channel to demodulate data
  - 1: channel not to demodulate data

- Bit 6 is SYNC FLAG
  - 0: channel to perform Bit/Subframe Sync operations
  - 1: channel to use PNP given BIT COUNT (Bytes 10 and 11) to drive Subframe Sync

(DATA DEMOD FLAG = 1 SYNC FLAG = 0 is illegal combination)

- Bit 5-0 is HALF SEARCH APERTURE CODE (HSAC) (format: binary, unsigned) related to half search aperture as follows

HSAC	Half Search Aperture (chips)
0	8
1	16
2	24
.	.
.	.
.	.
63	512

$$\text{i.e., HSAC} = \frac{\text{Half Search Aperture (chips)}}{8} - 1$$

(3) Bit Count is valid only if SYNC FLAG = 1

TABLE 3-17

BLOCK #70 MEASUREMENT DATA

Byte	Definition	Format	Units	LSB Scale
1	Block ID (=70)	constant	N/A	1
2	Block Length (=15)	constant	words	1
3-10	GPS Time	real	seconds	--
11-14	Mission Time	binary, unsigned	milli-seconds	20 ms.
15	Channel Status (Note 2)			
16	SV ID (1-31)	binary, unsigned, 6 LSB's	N/A	1
17	Least significant byte of receiver channel estimated carrier frequency (Note 2)	binary 2'comple-ment	mHz	6.35
18	Second byte of receiver channel estimated carrier frequency			
19	Most significant byte of receiver channel estimated carrier frequency			
20	Sub-chip code phase, valid at dwell ending (0-31)	binary, unsigned, 4 LSB's	C/A code chips	0.1
21	Chip code phase, least significant byte. Valid at dwell ending (0-1022)	binary, unsigned	C/A code chips	1
22	Chip code phase, 2 MSB's	binary, unsigned, 2 LSB's	C/A code chips	256
23	Epoch code phase valid at dwell ending (-127 to +128) (Note 3)	binary, 2'comple-ment	C/A code epoch	1
24-25	Wideband Power 24 - LSByte 25 - MSByte	binary, unsigned	quanta	
26-27	Narrow Band Power 26 - LSByte 27 - MSByte	binary, unsigned	quanta	
28	Data word count (0-9) within sub-frame at dwell ending	binary, unsigned, 4 LSB	N/A	1
29	Data bit count (0-29) within sub-frame at dwell ending	binary, unsigned, 5 LSB	N/A	1

TABLE 3-17. (CONT'D)

Notes:

(1) During navigation mode, this data is valid at the leading edge of the particular 20 msec system clock pulse that defines satellite transition.

(2) Channel status byte

7 6 5 4	3 2 1	0

*Bit 0	Set when receiver fault sensed
Bit 1	Init Mode or Configuration Mode Complete, Carrier Lock, or Measurement Valid
**Bit 2	Frame Synch Complete/In Data Demod
Bit 3	1 Pass of Search Completed
Bits 4-7	Receiver State (coded)

0 = Idle
1 = In Limited Search (± 15 chip)
2 = In ± 2 chip Search
3 = In ± 1 chip Search
4 = In False Alarm Check
5 = In Re-search
6 = In AFC Pull-in #1 (Pre Bit Sync)
7 = In AFC Pull-in #2 (Pre Bit Sync)
8 = AFC Lock
9 = In AFC Pull-in #1 (Post Bit Sync)
10 = In AFC Pull-in #2 (Post Bit Sync)
11 = Fine-Time
12 = Bit Synch Operations
13 = Frame Synch Operations
14 = Data Demodulation
15 = Statistics Done

(3) Pseudo-range can roll over a bit edge (overflow or underflow), therefore it can be larger than 20msec, or it can be negative; referenced to the initial position value.

(4) Wide band (WBP) and narrowband (NBP) power quantities are used in the following equation to compute the C/N_o estimate:

$$C/N_o = 10 \log_{10} 2000 \frac{(NBP - WBP)}{(40\ WBP - NBP)} \text{ dB Hz}$$

Note: 6 dB must be added to C/N_o estimate if data is not being demodulated.

*Pseudo-Range is valid if Bit 1 is set in Acquisition, Transition or Navigation Phase. Bit 1 is set when mode is complete when in Initialization or Configuration Modes.

**Bit 2 is set when frame synch is achieved and data is being demodulated, unless Frame Sync is not required. Then it indicates data demodulation.

TABLE 3-18

BLOCK #150 RAW POSITION FIX DATA

Byte	Definition	Format	Units	LSB Scale
1	Block ID (=150)	constant	N/A	1
2	Block Length (=60)	constant	words	1
3-10	GPS Time	double real	seconds	-
11-14	Mission Time	integer	milli-seconds	20 ms.
15-22	Position (ECEF) X	double real	feet	-
23-30	Y	double real	feet	-
31-38	Z	double real	feet	-
39-42	Velocity (ECEF) X-dot	real	feet/sec	-
44-46	Y-dot	real	feet/sec	-
47-50	Z-dot	real	feet/sec	-
51-58	Clock phase	double real	seconds	-
59-66	Clock frequency	double real	sec/sec	-
67	Baro Altimeter Flag (1000 0000=used)	integer	-	-
68	Spare			
69-72	Baro Altimeter Measurement	real	feet	-
73-76	Computed Altitude	real	feet	-
77-88	Unit vector for Baro and Pseudo-Baro measurements (3 elements)	real	-	-
89-90	Pseudo-Baro Flag (1000 0000 = used)	integer	-	-
91-94	Position fix (ECEF) ΔX	real	feet	-
95-98	ΔY	real	feet	-
99-102	ΔZ	real	feet	-
103-106	Δclock	real	seconds	-
107-116	Diagonal elements of fix matrix (4 elements)	real	-	-
117-120	Spare			

TABLE 3-19

BLOCK #160 TRACKED POSITION FIX DATA

Byte	Definition	Format	Units	LSB Scale
1	Block ID (=160)	constant	-	1
2	Block length (=63)	constant	words	1
3-10	GPS Time	double real	seconds	-
11-14	Mission Time	integer	milli sec.	-
15-22	Position (ECEF) X	double real	feet	-
23-30	Y	double real	feet	-
31-38	Z	double real	feet	-
39-42	Velocity (ECEF) X-dot	real	feet/sec	-
43-46	Y-dot	real	feet/sec	-
47-50	Z-dot	real	feet/sec	-
51-58	Position (Geodetic) latitude	double real	radians	-
59-66	longitude	double real	radians	-
67-74	altitude	double real	feet	-
75-78	Velocity (Local-level) North	real	feet/sec	-
79-82	East	real	feet/sec	-
83-86	Vertical	real	feet/sec	-
87-94	clock phase offset	double real	seconds	-
95-102	clock frequency offset	double real	sec/sec	-
103-110	time of tracker update	double real	seconds	-
111-114	Tracker update (ECEF) ΔX	real	feet	-
115-118	ΔY	real	feet	-
119-122	ΔZ	real	feet	-
123-126	Δclock	real	seconds	-

TABLE 3-20

ACTIVE WAYPOINT DATA BLOCK #200 (FROM CDU)

WORD	DEFINITION	FORMAT	UNITS	LSB SCALE
1	Block ID (= 200)	constant	-	1
2	Block Length (=14)	constant	words	1
3-4	Mission Time	positive integer	milliseconds	20 ms.
5(bits 8-15)	Active Waypoint number (0 to 19)	integer	-	1
5(bits 2,1,0)	CDI Sensitivity 0 = Enroute 1 = Terminal 2 = Approach	integer	-	1
6-9	Active Waypoint Latitude	double real	radians	-
10-13	Active Waypoint Longitude	double real	radians	-
14(bits 0-5)	RNAV Parameter Number (11 through 32) 11 = Range-to-Waypoint 12 = Bearing-to-Waypoint 13 = Time-to-go 14 = Not used 15 = Cross-track deviation 16 = Track angle error 17 = Course to waypoint 18 = Course from waypoint 19 = Groundspeed 20 = Track angle 21 = Greenwich Mean-Time 22 = Not used 23 = Present latitude 24 = Present Longitude 25 = OBS setting 26 = Not used 27 = Artificial Waypoint reference type 28 = Artificial waypoint reference ident. 29 = Artificial waypoint offset range 30 = Artificial waypoint offset bearing 31 = Waypoint latitude 32 = Waypoint longitude	integer	-	1

TABLE 3-21

AREA NAVIGATION DATA BLOCK #220 (TO CDU)

WORD	DEFINITION	FORMAT	UNITS	LSB SCALE
1	Block ID (=220)	constant	-	1
2	Block length (=20)	constant	16-bit words	1
3-4	Mission Time	positive integer	milliseconds	20 ms.
5(bit 8)	NAV flag 0 = okay 1 = not OK	integer	-	-
5(bits 1,0)	To/From flag 0 = from 1 = to 2 = neither	integer	-	-
6(bits10,9,8)	Solution Quality 0 = OPR 1 = UNR 2 = LCH 3 = BAD 4 = STR	integer	-	-
6 (bits 0→5)	RNAV Parameter No. (see block #200)	integer	-	1
7-8	RNAV Parameter	real	-	
9-10	OBS Setting	real	radians	-
11-12	CDI Deflection	real	dots	1
13-16	Present Latitude	double real	radians	-
17-20	Present Longitude	double real	radians	-

TABLE 3-22

REAL-TIME AIRCRAFT STATE DATA

Parameter	Value of LSB	Range Min	Max
Heading	(360°/512)	0	360° (binary 512)
Roll	1°	-31° (binary 0)	+32° (binary 63)
Pitch	1°	-31° (binary 63)	+32° (binary 0)
Outside air Temperature	0.625°C	-40°C (binary 0	+39.375°C (binary 127)
Indicated Air Speed	1 mm H_2O	0 (binary 0)	1023 (binary 1023)
Rate of Climb	24 mm H_2O/min	-768 (binary 0)	+744 (binary 63)

Note: Pitch reading is not linear for pitch angles greater than 20 degrees.

The receiver carrier-to-noise-density ratio (C/N_0) is estimated using the wide-band energy detected by the AGC loop and the narrow-band detector shown in Fig. 3-14. Scaled estimates are recorded for each measurement in blocks 30 and 70. C/N_0 is then calculated using the formula in Note (4), Table 3-17.

Aircraft altitude is measured using standard aircraft instruments which have been connected via a digital interface to a Z80-based Aircraft Data Unit assembly (ADU). The ADU in turn communicates via a serial RS232 interface to the DAU, nominally once per second. The altitude parameters are defined in Table 3-19.

Pilot activity is monitored by recording request and response messages between the DAU and CDU using the formats shown in Tables 3-20 and 3-21.

4.0 MEASURED PERFORMANCE

4.1 Test Facilities

4.1.1 Ground Test Laboratory

During integration of the GPS T and E system a tower-mounted antenna was employed. Initial evaluation of the hardware and software functions were completed in the laboratory before flight tests commenced.

4.1.2 Aircraft Installtion

The GPS T and E equipment was installed in a Rockwell Aerocommander 500A, as shown in Figs. 4-1 through 4-4. The T and E equipment was configured as shown in Figs. 4-5 and 4-6. The CDU and CDI are installed as shown in Fig. 4-7. The traditional difficulty of pushing buttons on a vertically mounted cockpit device was relieved for the CDU because the engine controls provide a convenient stabilizing hand rest for most power settings. The performance envelope for the Aerocommander is shown in Table 4-1.

4.1.3 Mode S Experimental Facility

Position truth was established using the Mode S Experimental Facility (MODSEF) operated at Lincoln Laboratory. It includes a monopulse surveillance system capable of interrogating ATCRBS and Mode S Transponders. Its principal characteristics are provided in Table 4-2.

During GPS tests Mode S Experimental Facility surveillance accuracy was verified using a calibration transponder located 6 miles from the Mode S Experimental Facility. The aircrafts altimeter calibration was also verified. Since most of the Hanscom runways are visible to the Mode S Experimental Facility sensor, a test was conducted in which the aircraft parked at a taxi way reference point, to verify surveillance range/altitude.

The Mode S Experimental Facility surveillance data for the GPS test aircraft was recorded and identified based on either an ATCRBS discrete code or Mode S ID (both transponders were available on the Aerocommander).

FIG. 4-1. AEROCOMMANDER TEST AIRCRAFT

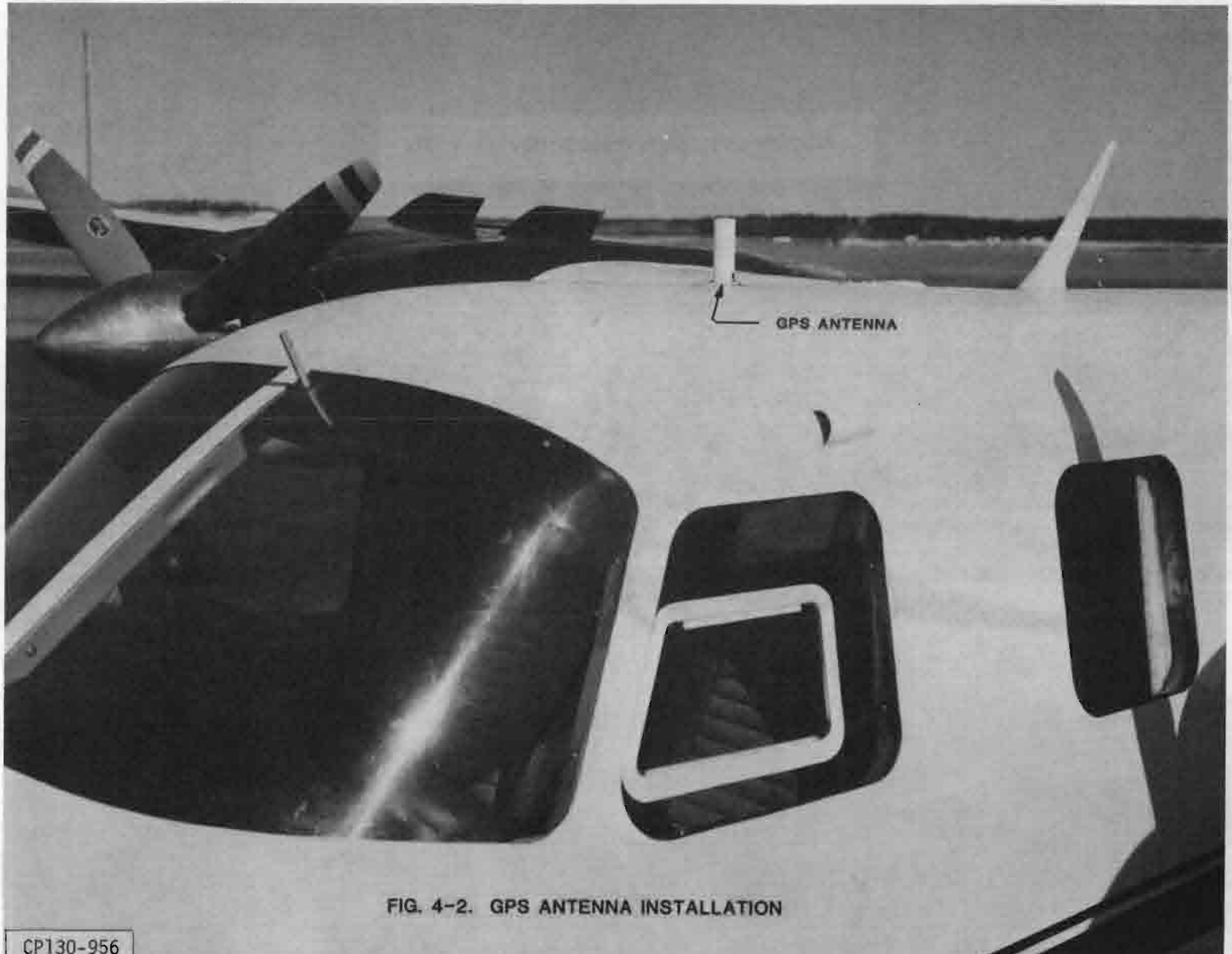

FIG. 4-2. GPS ANTENNA INSTALLATION

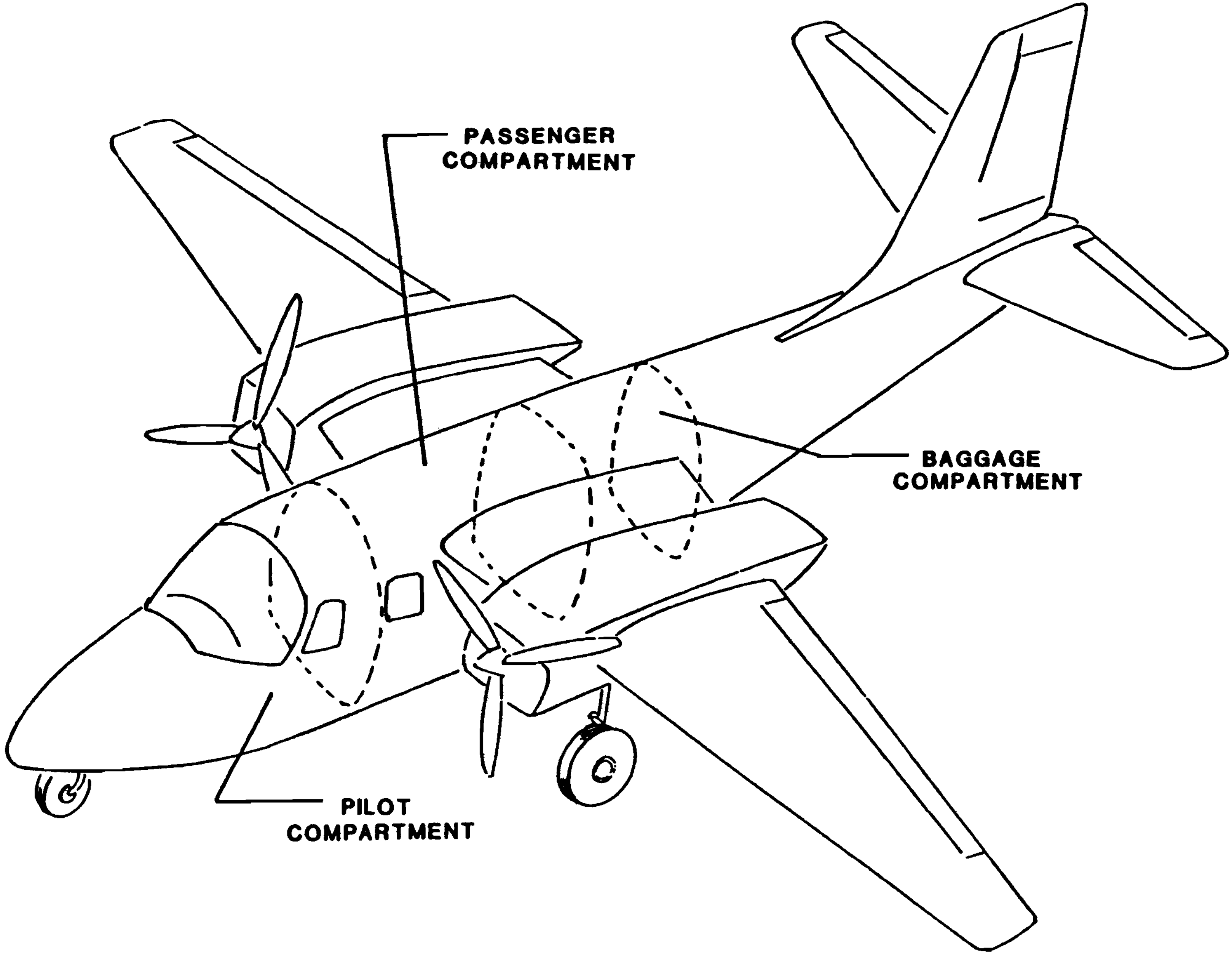

FIG. 4-3. GPS TEST AIRCRAFT INTERNAL LAYOUT

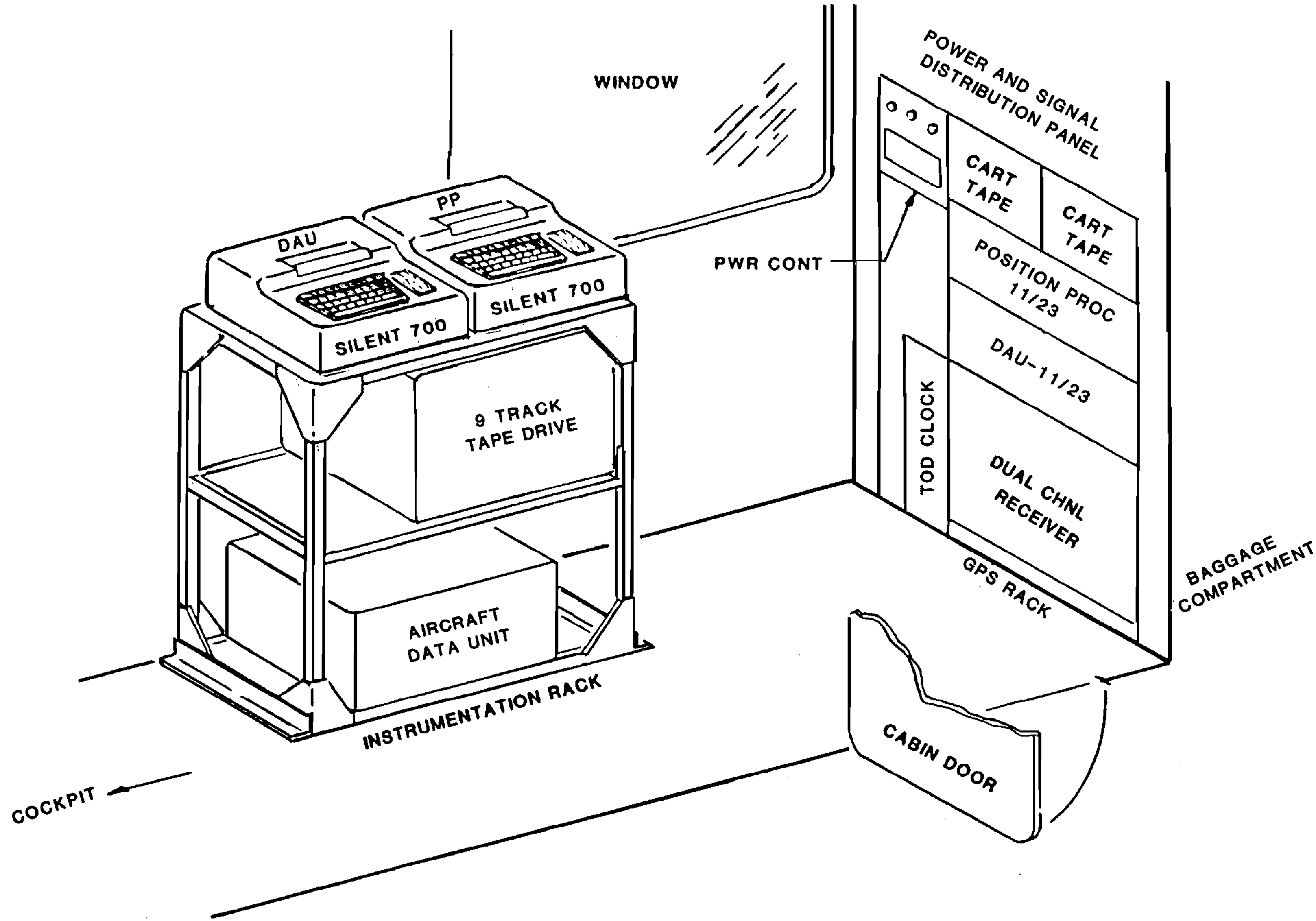

FIG. 4-4. GPS FLIGHT SYSTEM IN PASSENGER COMPARTMENT
OF AEROCOMMANDER AIRCRAFT

FIG. 4-5. INSTRUMENTATION RACK

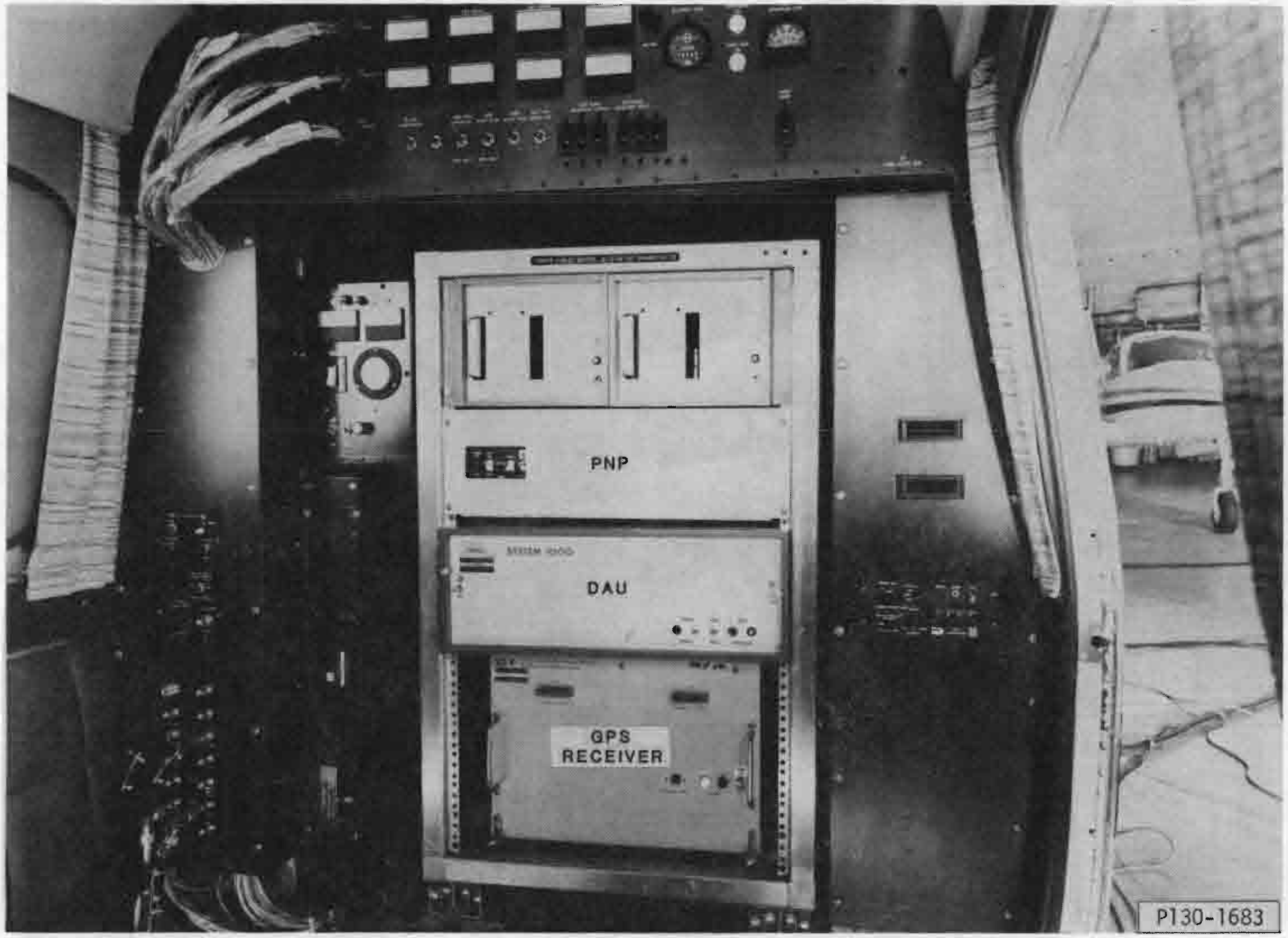

FIG. 4-6. RECEIVER RACK

FIG. 4-7. AEROCOMMANDER N333BE, COCKPIT VIEW

TABLE 4-1

AEROCOMMANDER FLIGHT CHARACTERISTICS

	Complete System	Without Instrumentation
Cruise Speed	160 KIAS	160 KIAS
Ceiling	10 Kft.	10 Kft.
Time at 10 Kft.	1.5 Hours	2.5 Hours

Assumptions

2 Pilots
1 Operator

TABLE 4-2

MODE S EXPERIMENTAL FACILITY SURVEILLANCE CHARACTERISTICS

Antenna	4° monopulse
Transmit	150 watts with SLS
Receiver	Phase monopulse 10 dB noise figure RSLS
Nominal Range	75 nmiles
Surveillance Accuracy	
Range	40 feet 1σ
Azimuth	0.05 deg 1σ
Calibration	Test transponder at surveyed site 6 miles north of The Mode S Experimental Facility
Display	TPX 42 display

4.1.4 Analysis Software

The data recorded on the aircraft, and at the Mode S Experimental Facility were processed as shown in Fig. 4-8 to produce a basic surveillance data base and error statistics.

The difference between the GPS and Mode S Experimental Facility position estimates was determined by using every ungarbled Mode S Experimental Facility report (unsmoothed, occurring at 4 second rate), and the two adjacent GPS position estimates as shown in Fig. 4-9. Conversion from the Mode S Experimental Facility R, θ, H position estimate to the aircraft's XYZ in earth centered earth fixed ECEF coordinates was done using matrix transformations* which account for the WGS-72 ellipsoid of revolution earth model.

Plots of XY versus time, GPS position error with respect to the Mode S Experimental Facility versus time, and error statistics were developed.

GDOP was independently estimated using Z STARS, a Lincoln program which provides visibility to current satellites. Using Z STARS, GDOP was calculated based on all satellites actually in track.

4.2 Laboratory Tests

4.2.1. Antenna

The Chu Associates, Inc., model CA-3224 volute antenna was tested while mounted on a 5-foot by 5-foot aluminum plate shaped to simulate the local Aero Commander fuselage as shown in Fig. 4-10. Anechoic chamber azimuth gain measurements were made at various elevation angles. The results, shown in Figs. 4-11, -12 and -13, show that the specification was met or exceeded over most elevation angles except within the range 5-10° where the gain was 2-dB lower than specified. Measurements above 50° elevation were not possible due to mechanical conflicts between the fuselage plate and the anechoic chamber mount. It is assumed that a gain of 0 ± 1 dBi in the region 50°-90° has been provided.

The elevation gain profile, Fig. 4-14, was developed by computing the mean azimuth gain at each elevation angle from samples taken every 10° in azimuth. The standard deviations in azimuth gain were also computed, as shown by the dotted lines.

* See Appendix C for details.

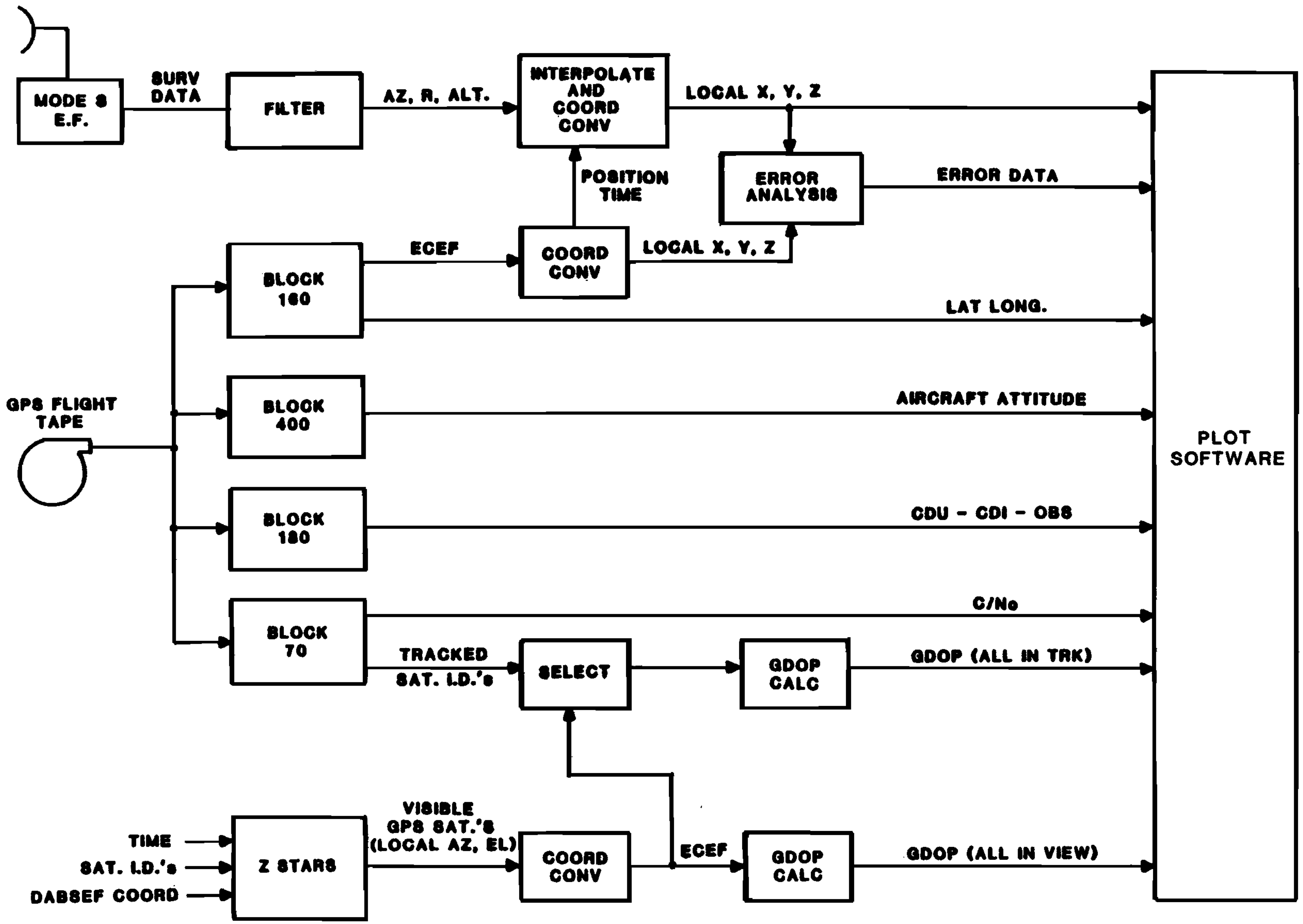

FIG. 4-8. POST FLIGHT ANALYSIS SOFTWARE

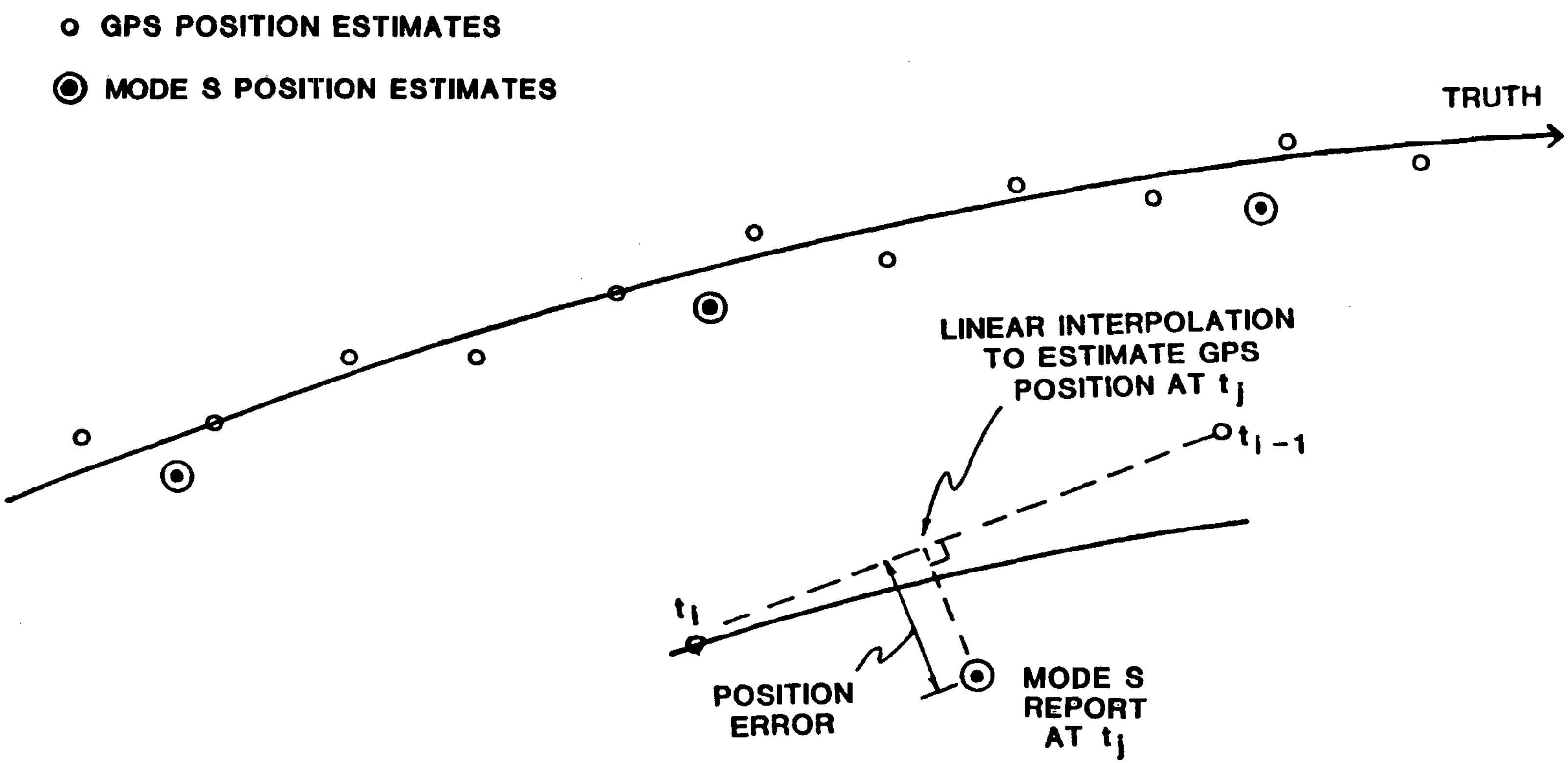

FIG. 4-9. GPS POSITION ESTIMATION ERROR ALGORITHM

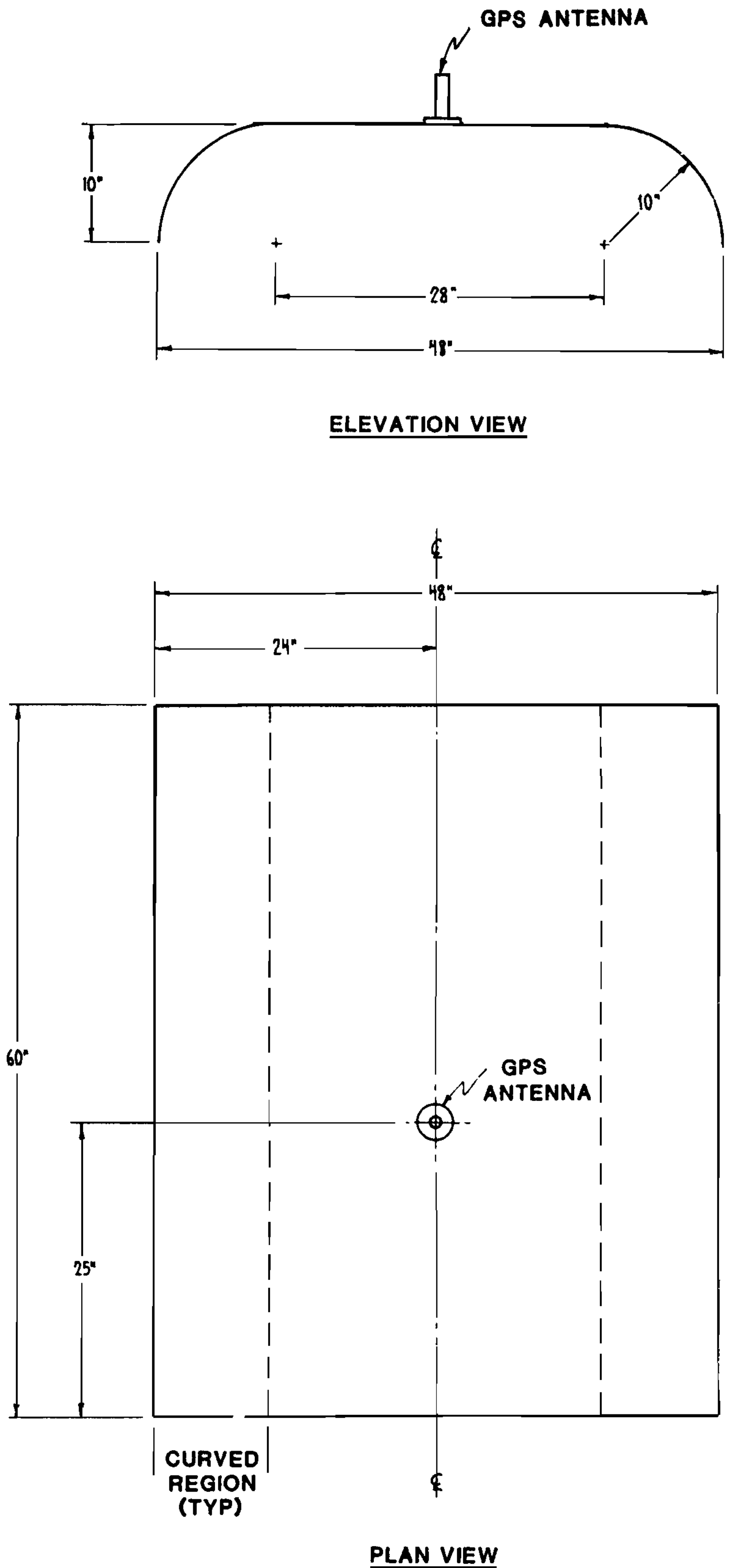

FIG. 4-10. CURVED GROUNDPLANE

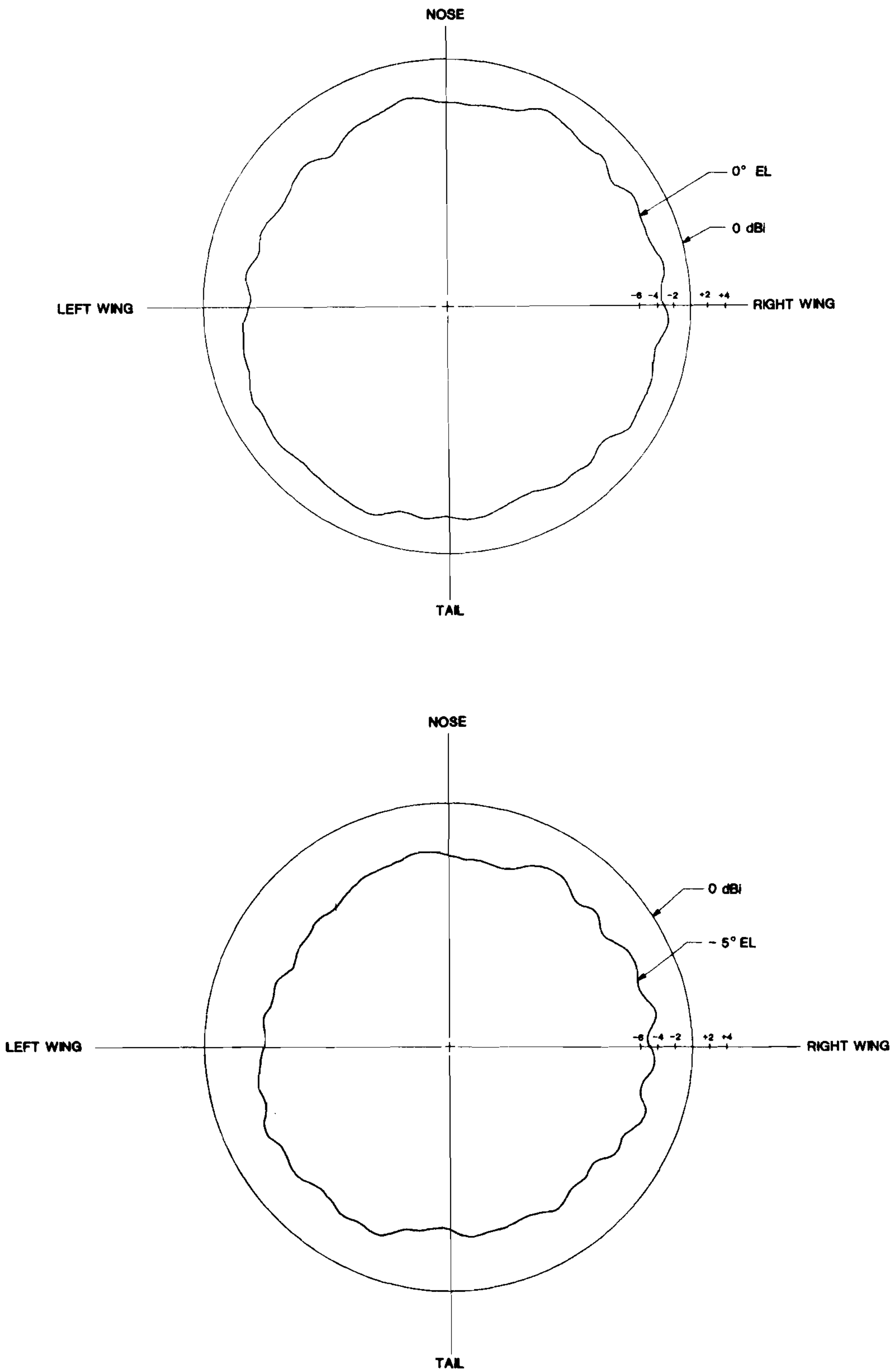

FIG. 4-11. Gain vs. Azimuth for Elevation Cuts at -5° and 0°; Chu Model CA-3224 Volute Antenna.

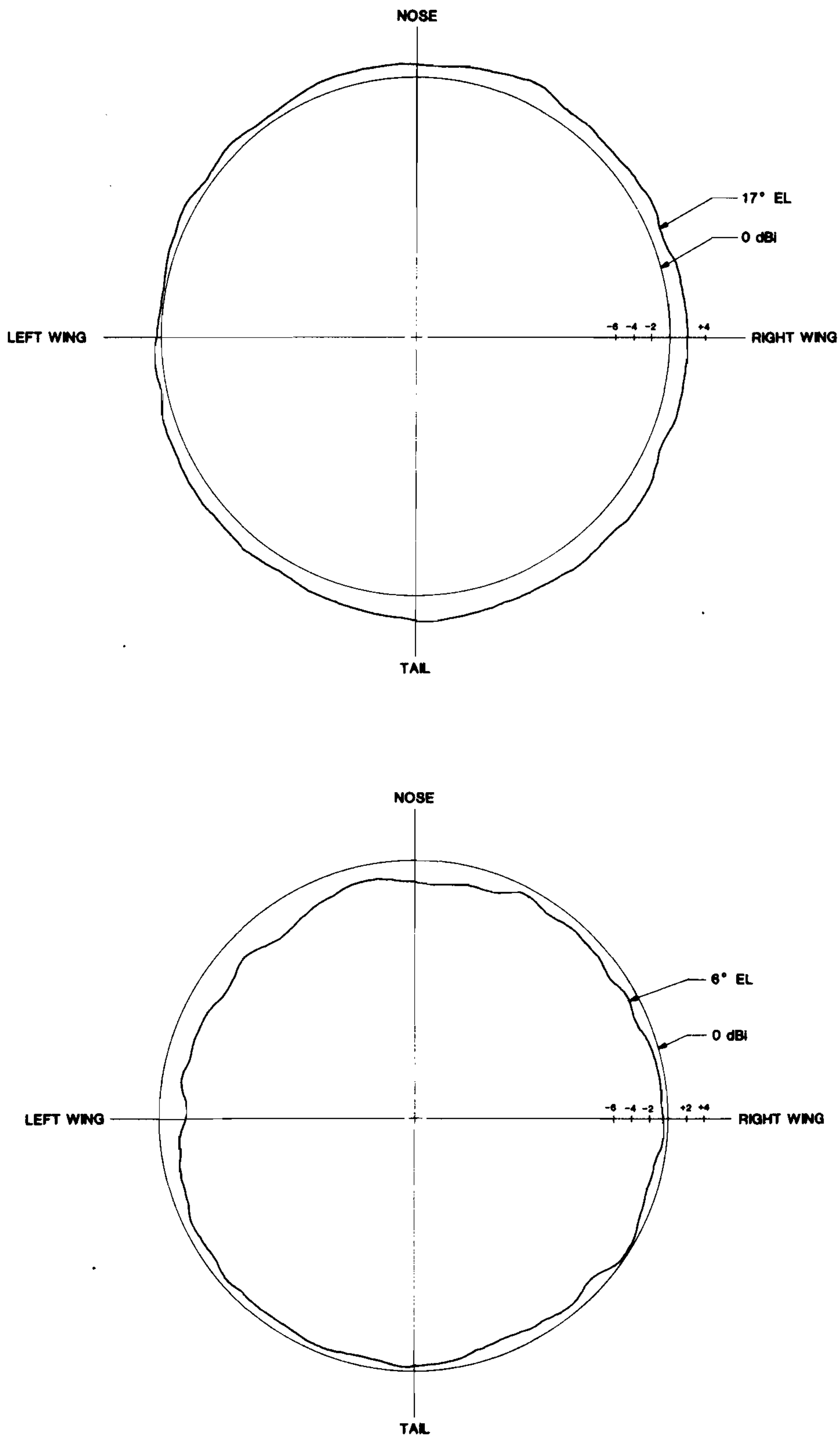

FIG. 4-12. Gain vs. Azimuth for Elevation Cuts at +6° and +17°; Chu Model CA-3224 Volute Antenna.

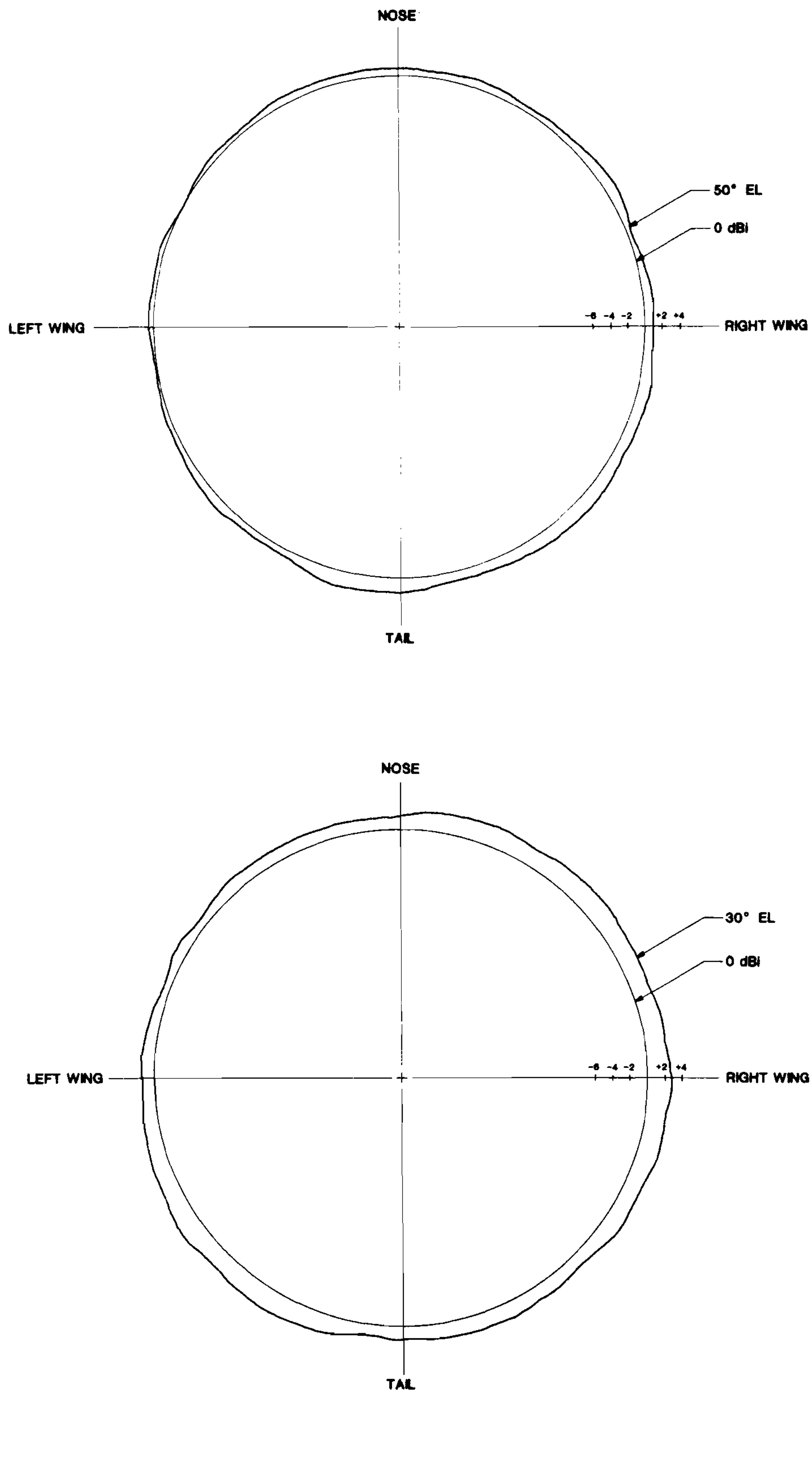

FIG. 4-13. Gain vs. Azimuth for Elevation Cuts at +30° and +50°; Chu Model CA-3224 Volute Antenna.

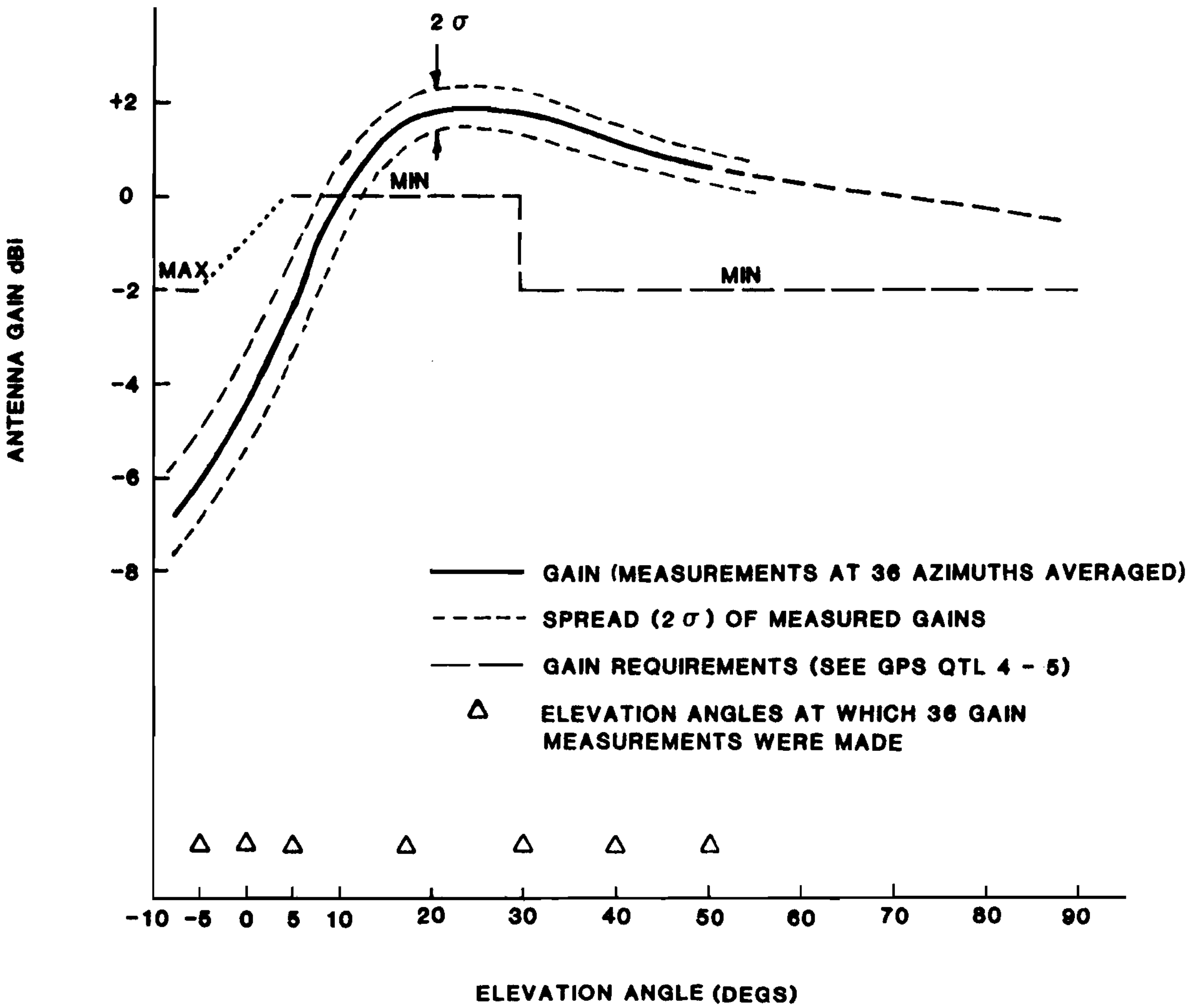

FIG. 4-14. VOLUTE ANTENNA GAIN, ELEVATION PROFILE

4.2.2 Receiver Channel Performance

The receiver factory acceptance tests, conducted using the equipment configuration shown in Fig. 4-15, verified compliance with all receiver specifications including:

a) Receiver Hardware - PNP Software Interface.
b) Acquisition time versus doppler and C/N_0.
c) Data error rate versus C/N_0.
d) Transition performance versus C/N_0.
e) Navigation performance versus C/N_0.
f) Nav plus Data performance versus C/N_0.
g) AFC error performance.
h) Pseudo-range accuracy.
i) C/N_0 measurement accuracy.

During the acceptance tests, acquisition of all satellite codes now in use with doppler offsets up to > 1000 Hz (> 750 Hz requirement) was demonstrated. Tests of the Transition, Navigation and Navigation plus Data modes were accomplished by phase-locking the receiver oscillator to the satellite simulator oscillator and manually entering prepositioning code and doppler data into the PNP simulator. CPU activity monitoring verified that the receiver Z8000 microcomputer task execution times did not exceed their allotted times in any mode. Finally, all visible satellites were successfully acquired using a roof antenna. All tests were conducted on both channels.

Following shipment of the receiver to Lincoln Laboratory, the acceptance tests were repeated in a laboratory using the same test configuration as in Fig. 4-15 except that a volute antenna identical to that installed on the Aerocommander was used.

Table 4-3 summarizes the major requirements and performance measured during the factory acceptance tests and during the post-acceptance evaluation. Results of specific measurements are shown in Figs. 4-16 through 4-24, and the results of a test in which a GPS satellite was tracked for 5 hours are shown in Fig. 4-25.

The measured receiver performance was also evaluated with respect to theoretical predictions. The results, shown in Figs. 4-26, -27, and in Table 4-4, show good agreement.

To assess the 5-hour tracking test data, the expected receive C/N_0 was calculated as shown in Table 4-5. Worst-case RF power (C/A code only) at the user antenna is seen to be -160 dBw. Note that the receiver preamp is assumed to be located at the antenna for minimum cabling loss.

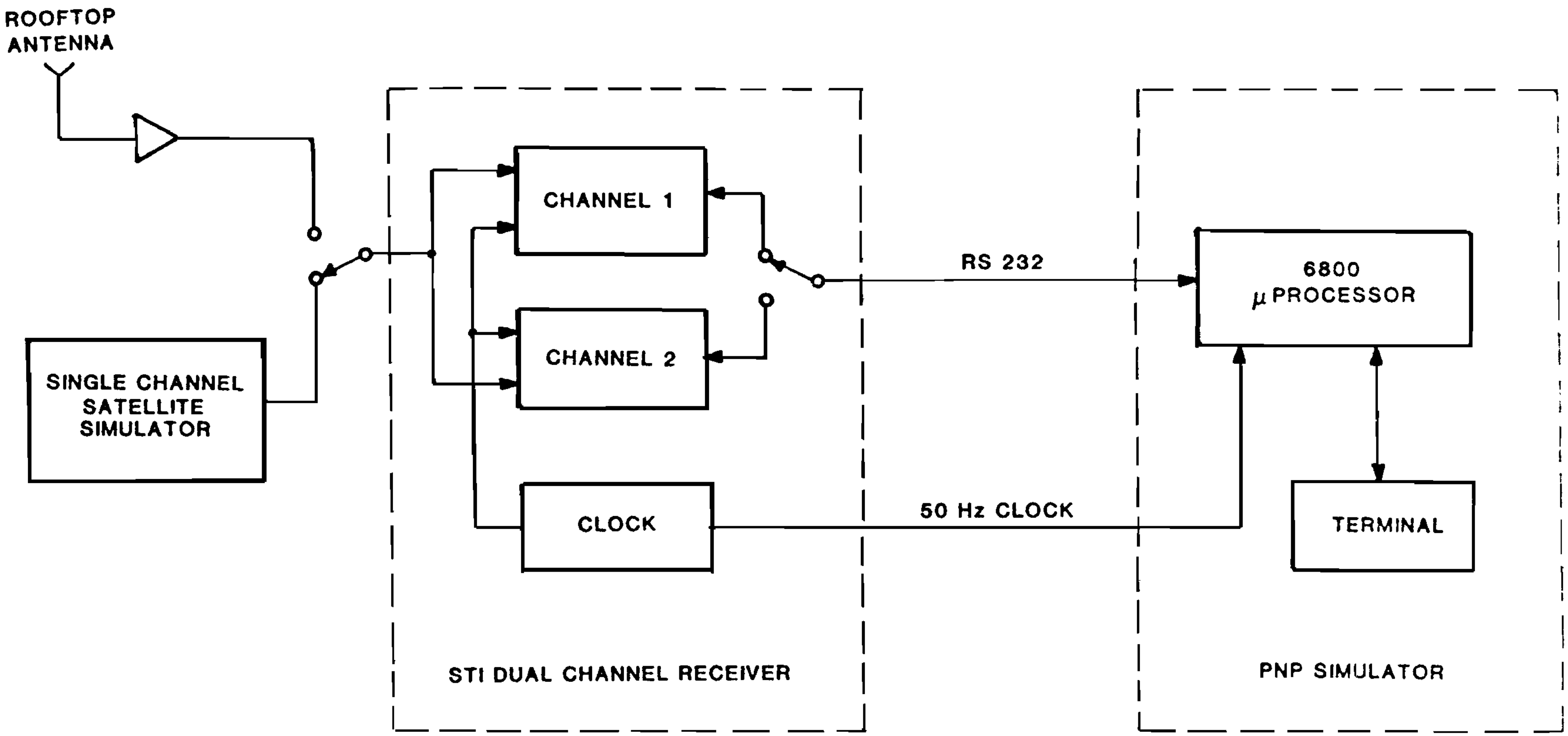

FIG. 4-15. DUAL CHANNEL RECEIVER ACCEPTANCE TEST CONFIGURATION

TABLE 4-3

RECEIVER HARDWARE PERFORMANCE

Parameter	Requirement	Measured Performance
Acquisition		
Time to acquire	25 sec (based on 6 min TTFF)	25 sec, $P > .9$
AFC errors	$\Delta_f < 10$ Hz for data demodulation	$\sigma_f < 1.4$ Hz for $C/N_o > 36$ dBHz
Bit Error Rate	$< 10^{-5}$	$< 10^{-5}$
C/N_o Error	$\pm$ 1 dB	$\sigma_{C/No} < 0.7$ dB
Phased Transition		
AFC Error	Not specified	$\sigma_f < 5$ Hz
Pseudo Range Error	Not specified	$\sigma_\tau < 45$ ns for $C/N_o > 36$ dBHz
C/N_o Error	$\pm$ 1 dB	$\sigma_{C/No} < .85$ dB
Navigation		
AFC Error	Not specified	$\sigma_f < 7$ Hz
Pseudo Range Error	$\sigma_\tau < 50$ ns	$\sigma_\tau < 47$ ns for $C/N_o > 36$ dBHz
C/N_o	$\pm$ 1 dB	$\sigma_{C/No} < 1.0$ dB
Nav Plus Data		
Same as Navigation and Acquisition	Same as Navigation and Acquisition	Same as Navigation and Acquisition
Acquisition Link Margin*	At least 4 dB	4.5 dB at 5° elevation, 10 dB at 40° elevation, for the volute antenna.

*Assuming 4 dB noise figure. See Table 4-5.

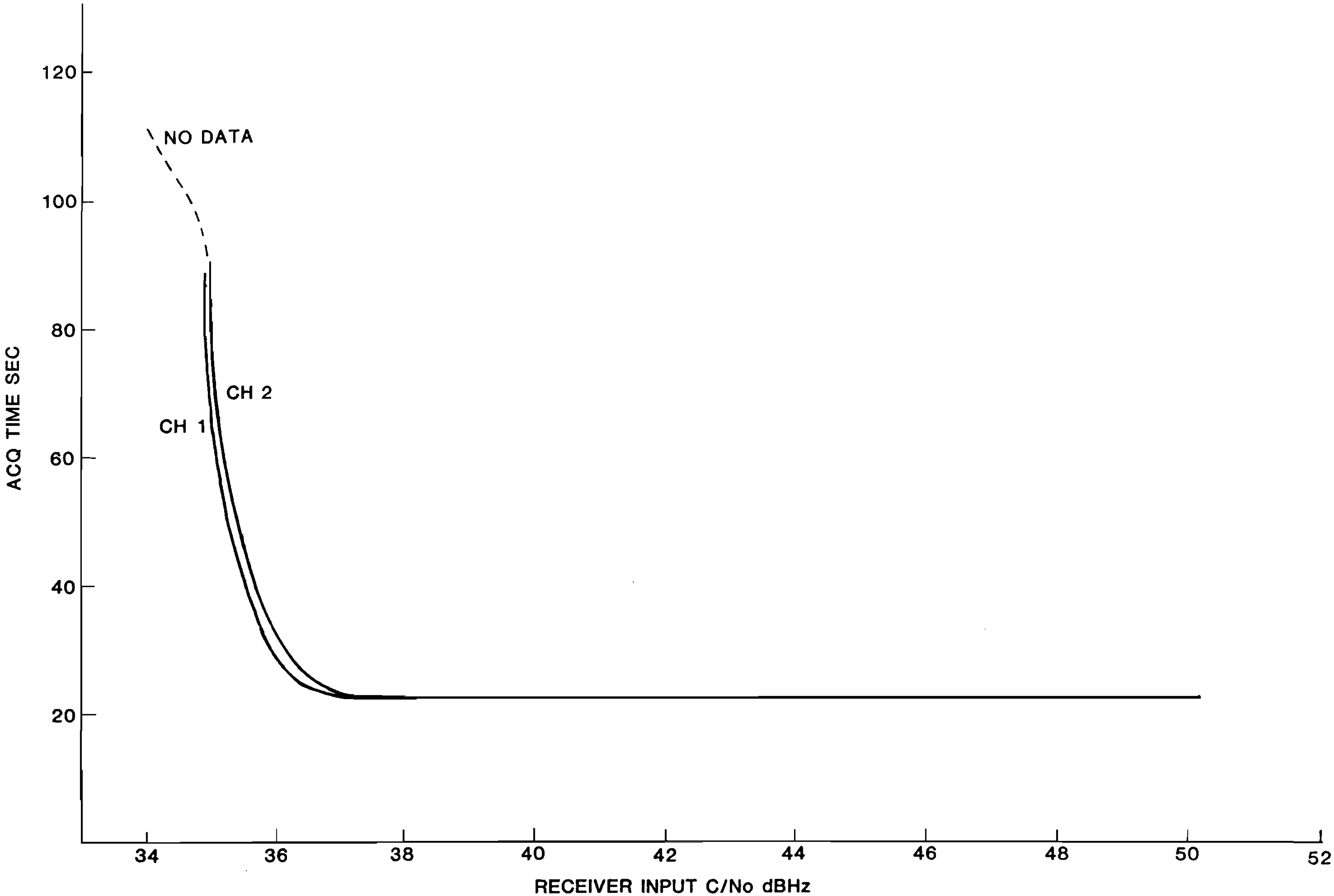

FIG. 4-16. ACQUISITION TIMES OF A SINGLE SATELLITE

C42-2188

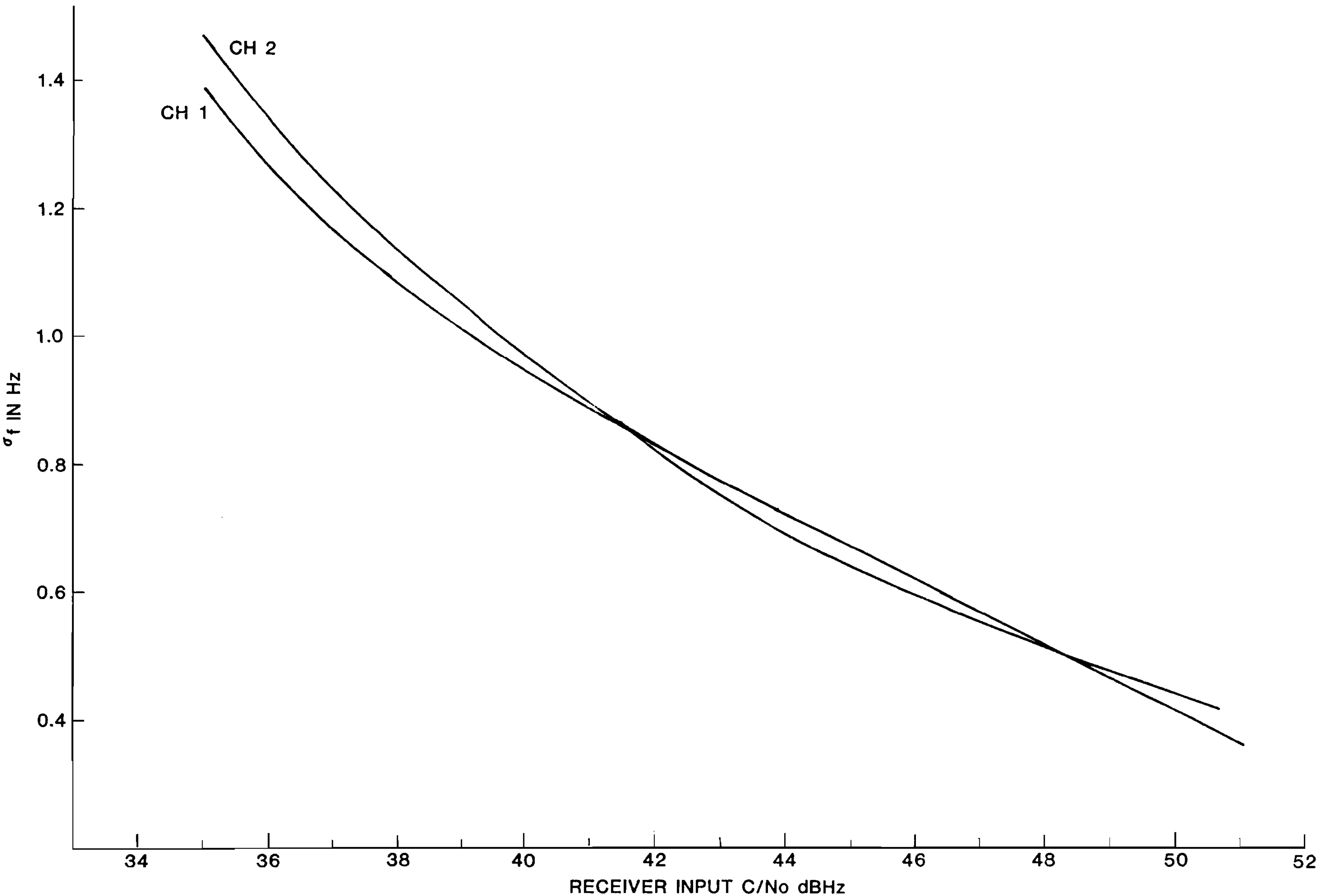

FIG. 4-17. RECEIVER AFC PERFORMANCE IN ACQUISITION PHASE

C42-2189

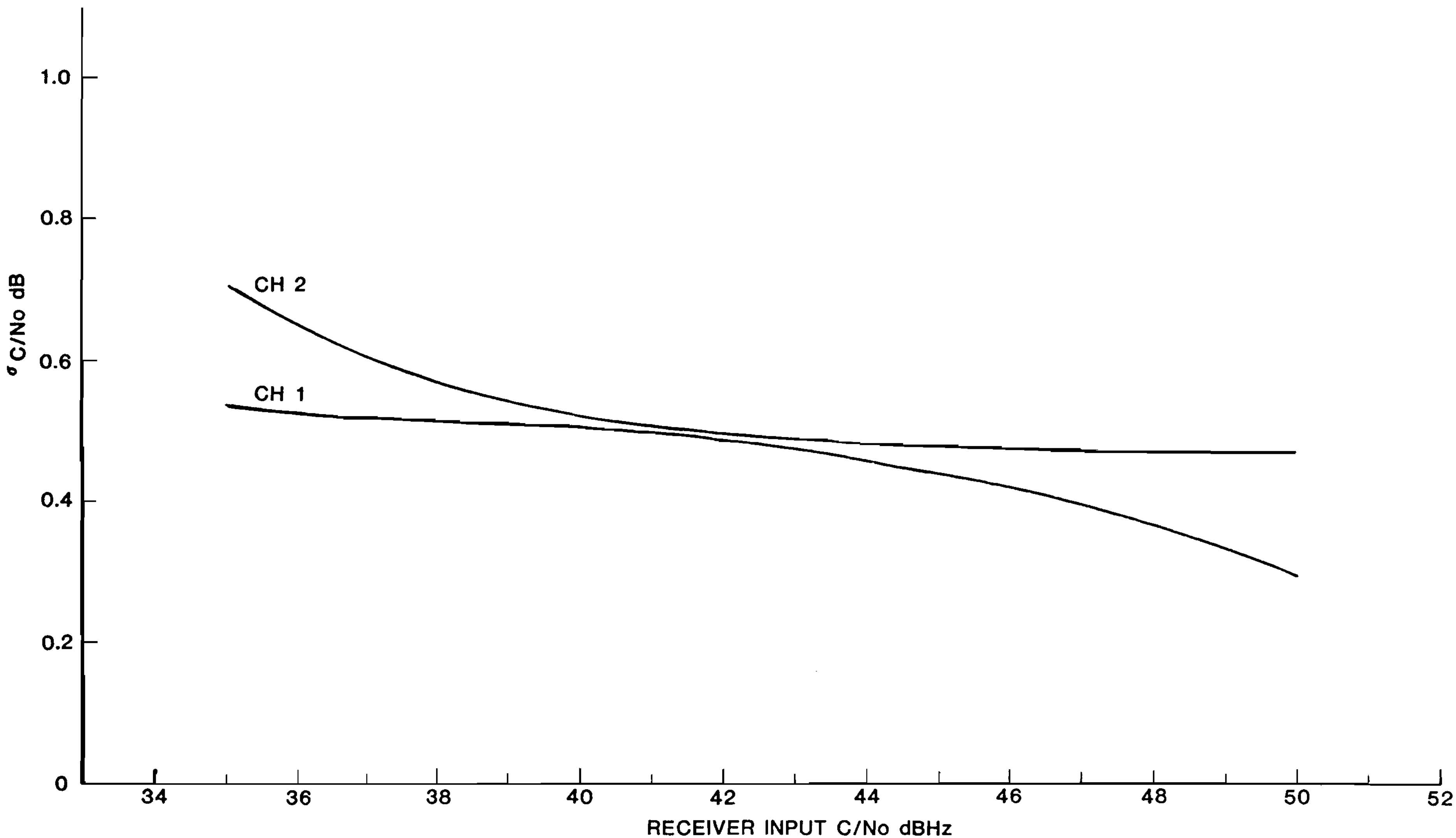

FIG. 4-18. RECEIVER C/No ESTIMATOR PERFORMANCE IN ACQUISITION PHASE

C42-2190

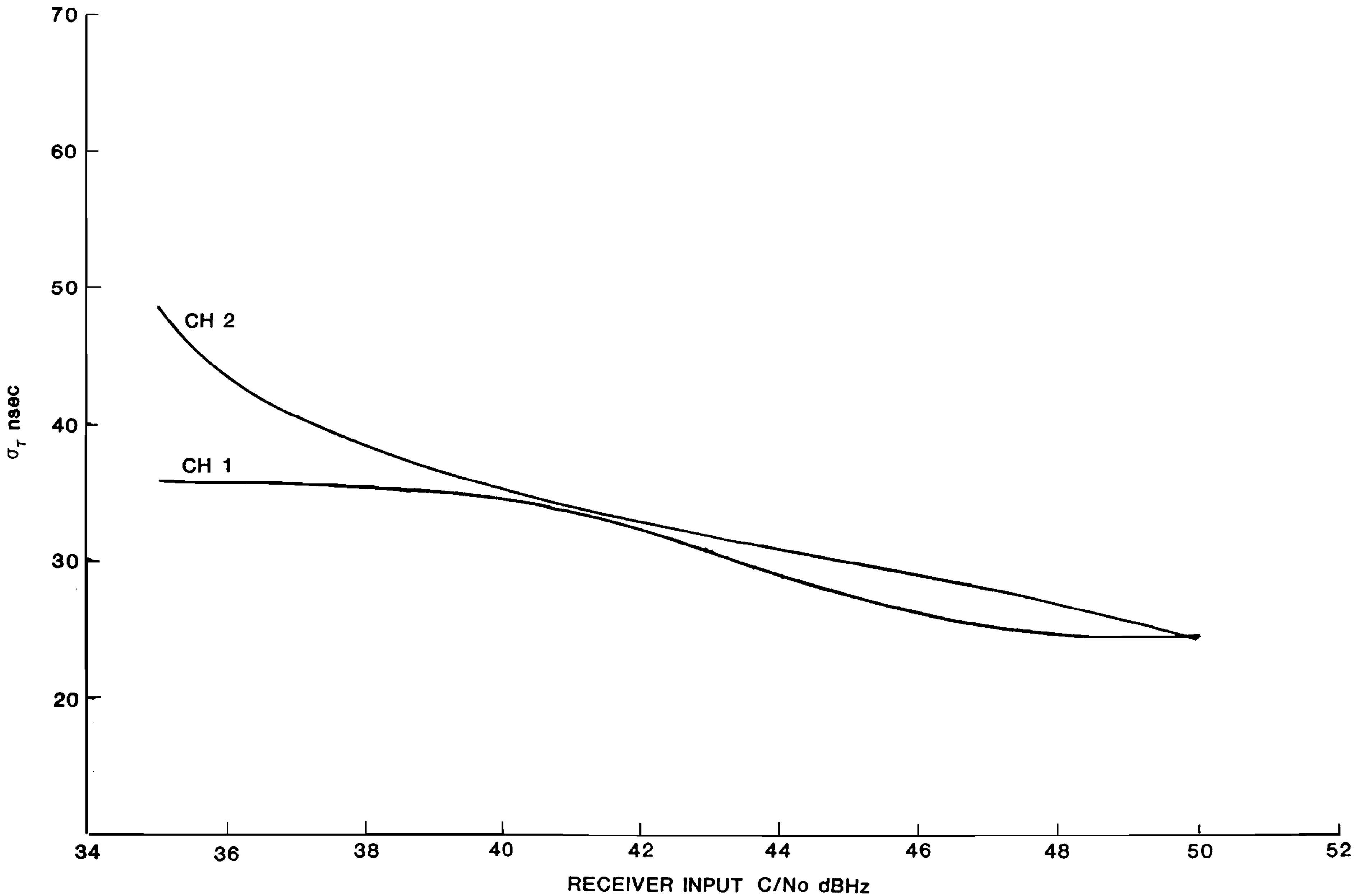

FIG. 4-19. RECEIVER PSEUDO RANGE PERFORMANCE IN PHASED TRANSITION

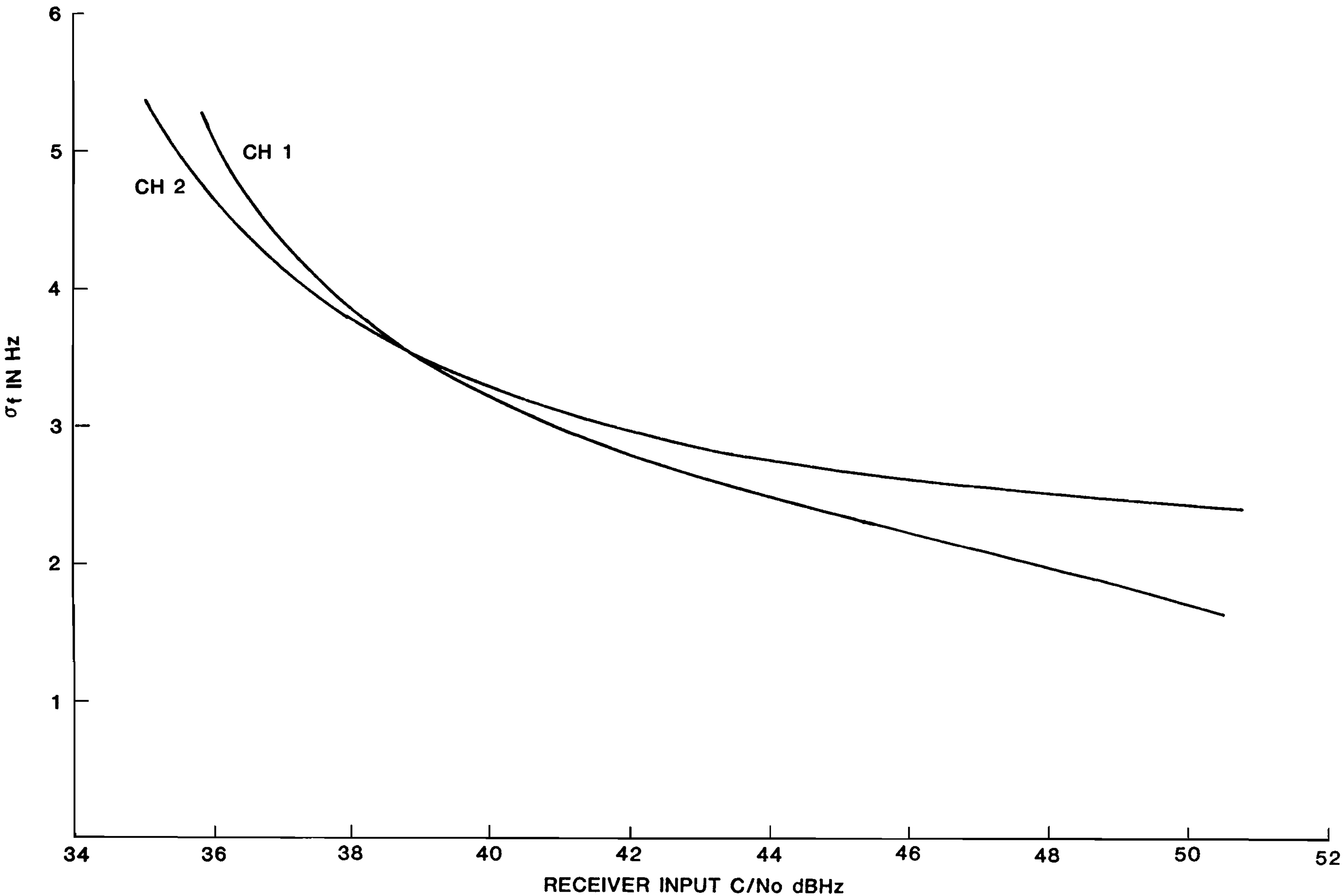

FIG. 4-20. RECEIVER AFC PERFORMANCE IN PHASED TRANSITION

C42-2186

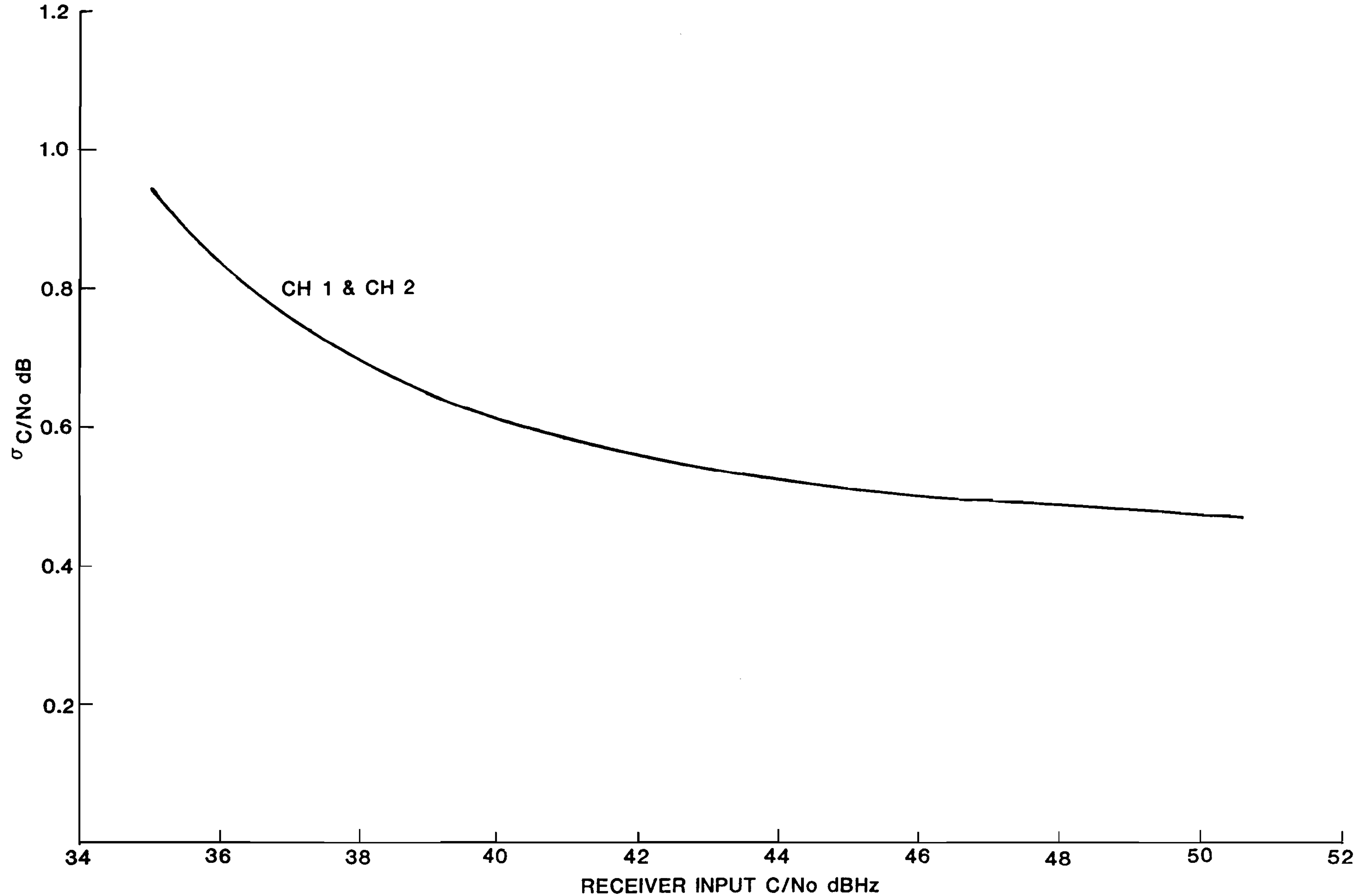

FIG. 4-21. RECEIVER C/No ESTIMATOR PERFORMANCE IN PHASED TRANSITION

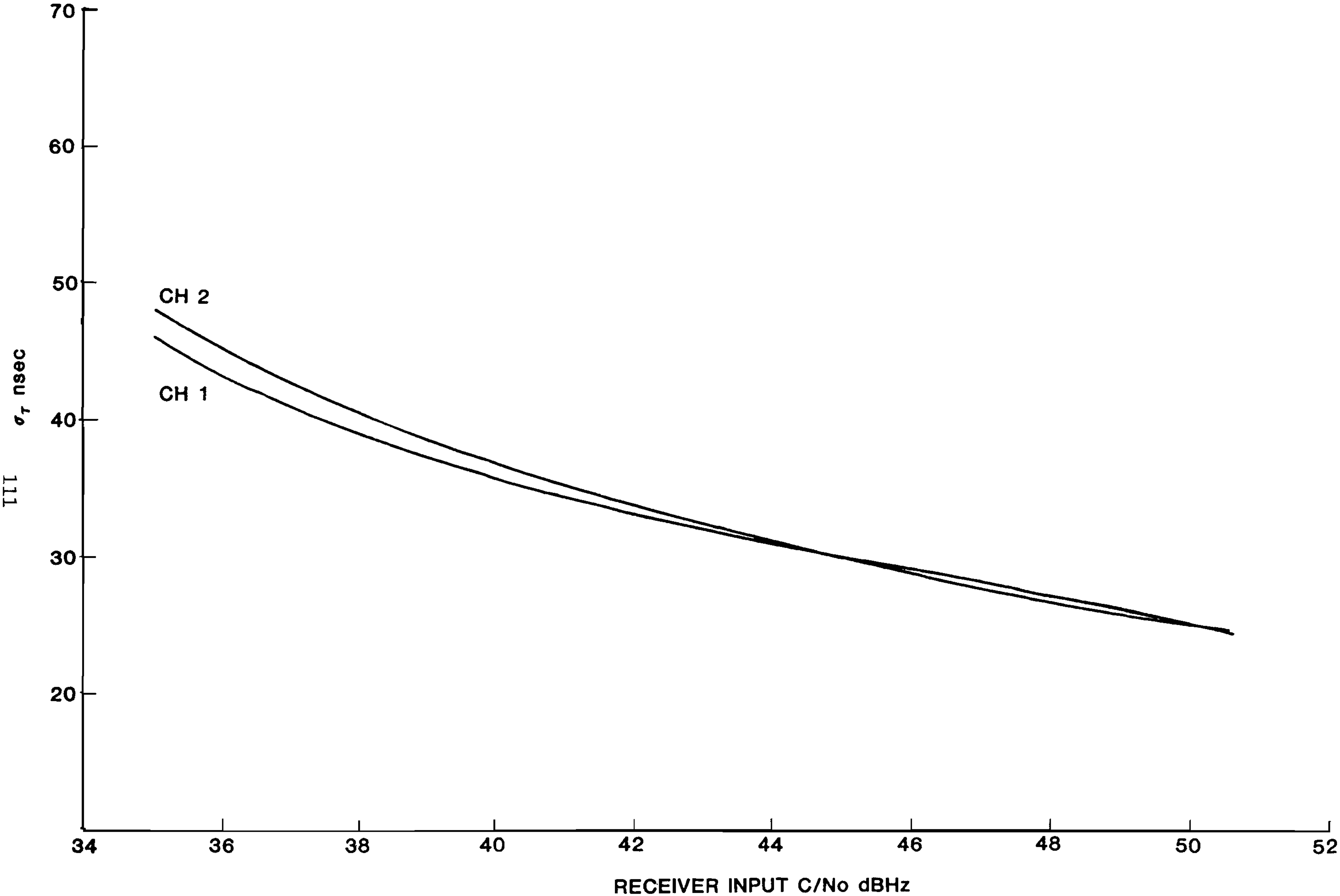

FIG. 4-22. RECEIVER PSEUDO RANGE PERFORMANCE IN THE NAVIGATION STATE

C42-2185

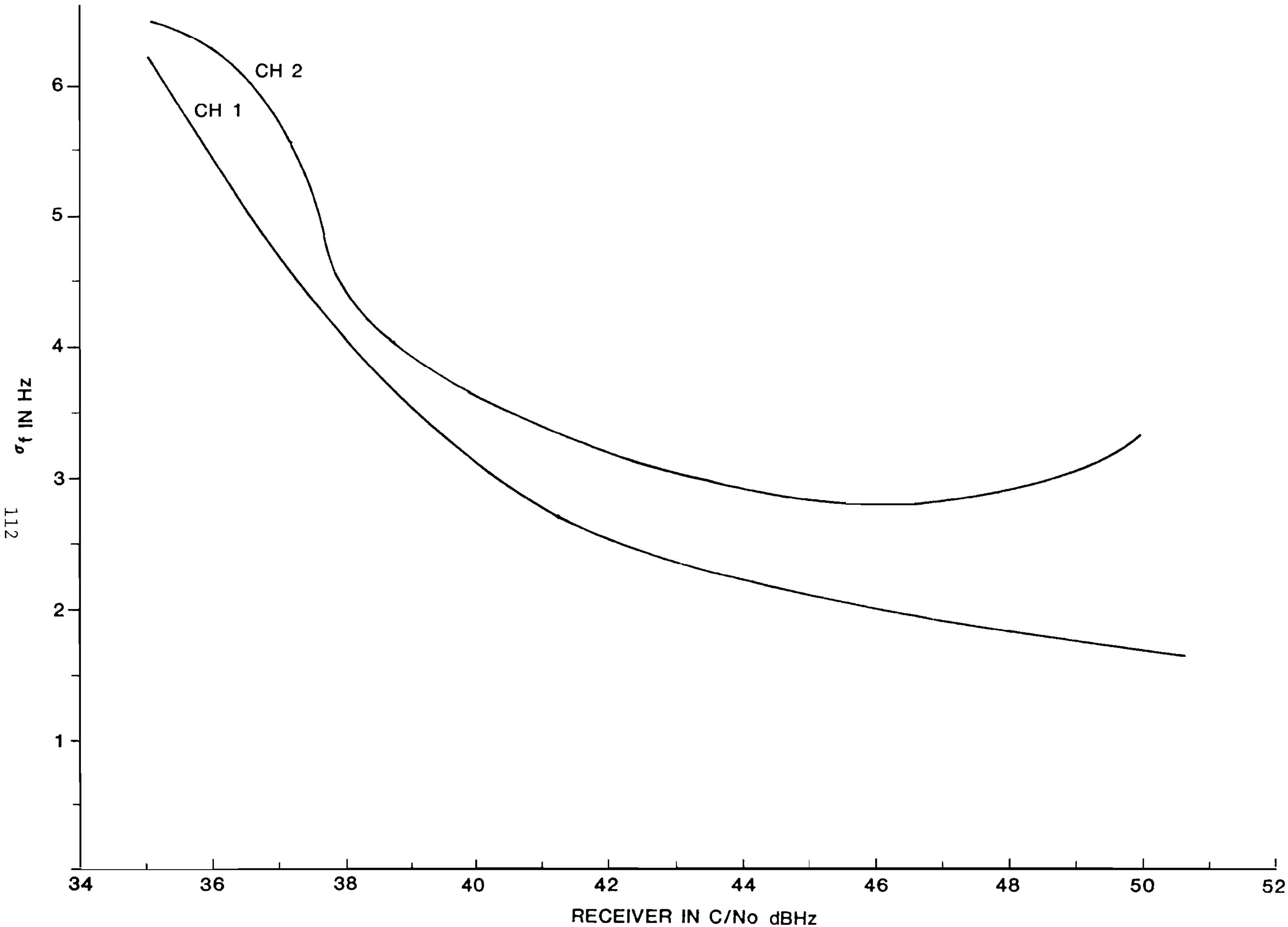

FIG. 4-23. RECEIVER AFC PERFORMANCE IN THE NAVIGATION STATE

C42-2183

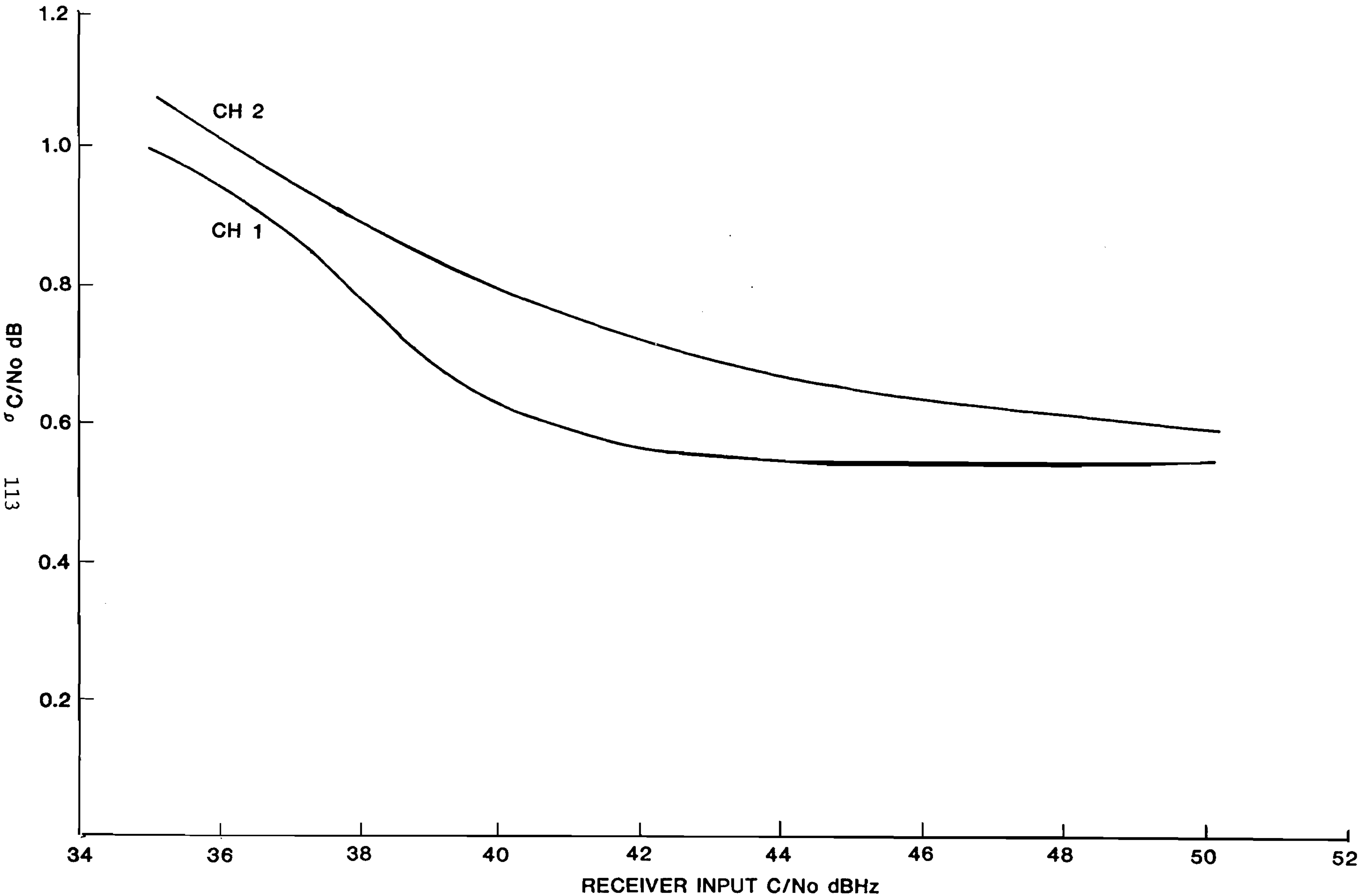

FIG. 4-24. RECEIVER C/No ESTIMATOR PERFORMANCE IN NAVIGATION STATE

C42-2184

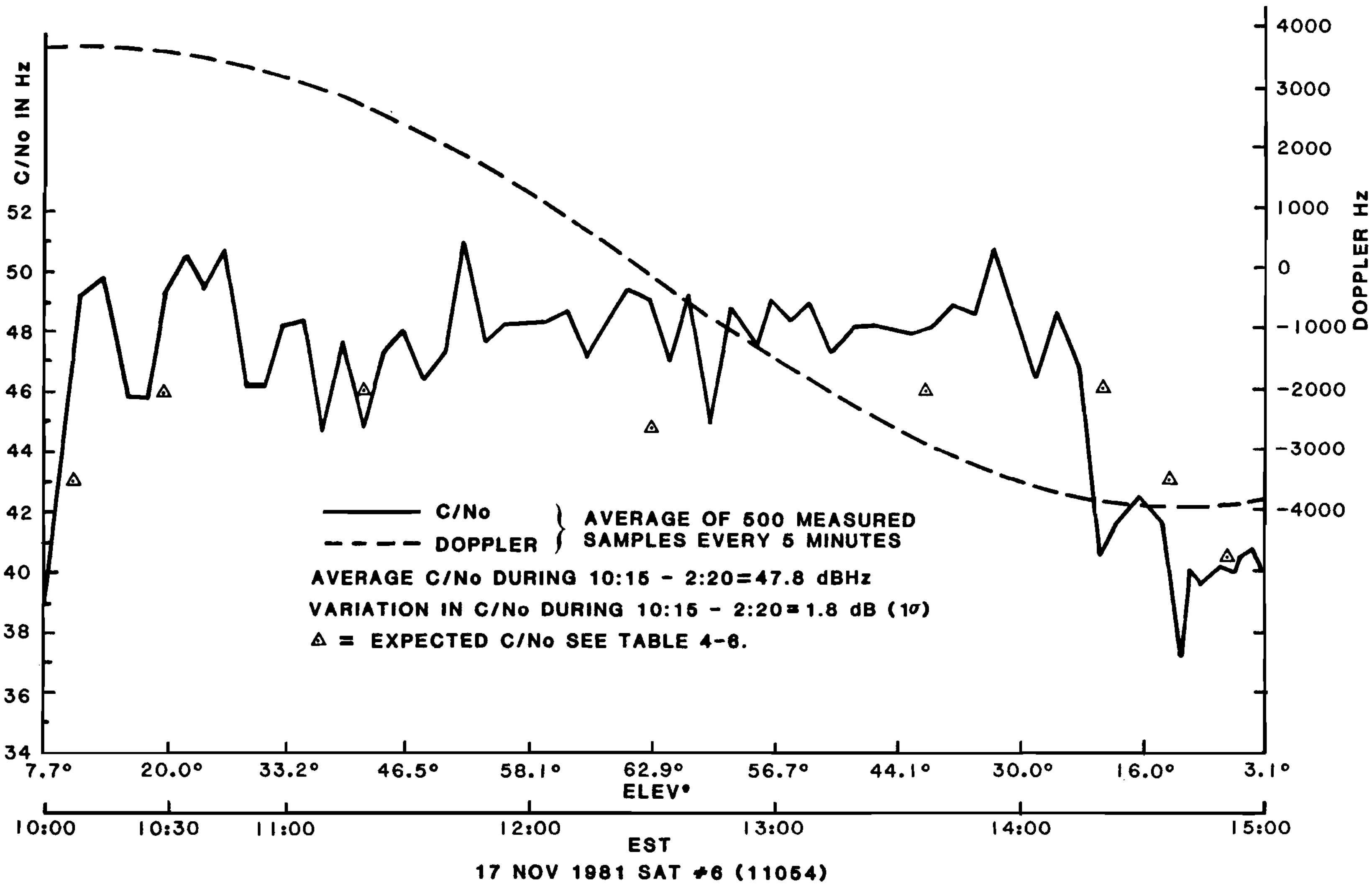

FIG. 4-25. RECEIVER PERFORMANCE DURING SATELLITE PASS

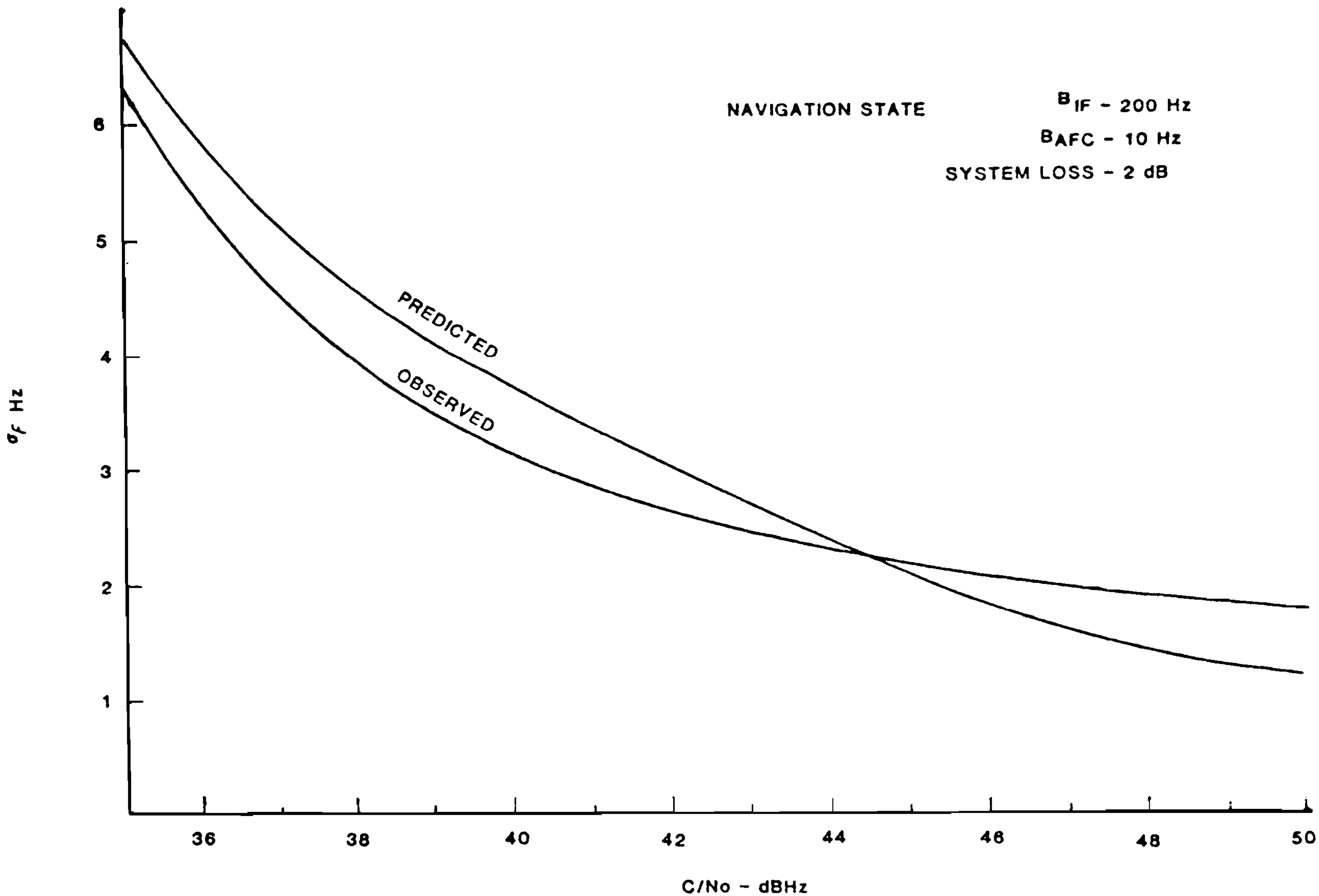

FIG. 4-26. COMPARISON OF THEORETICAL AND MEASURED RECEIVER FREQUENCY TRACKING PERFORMANCE

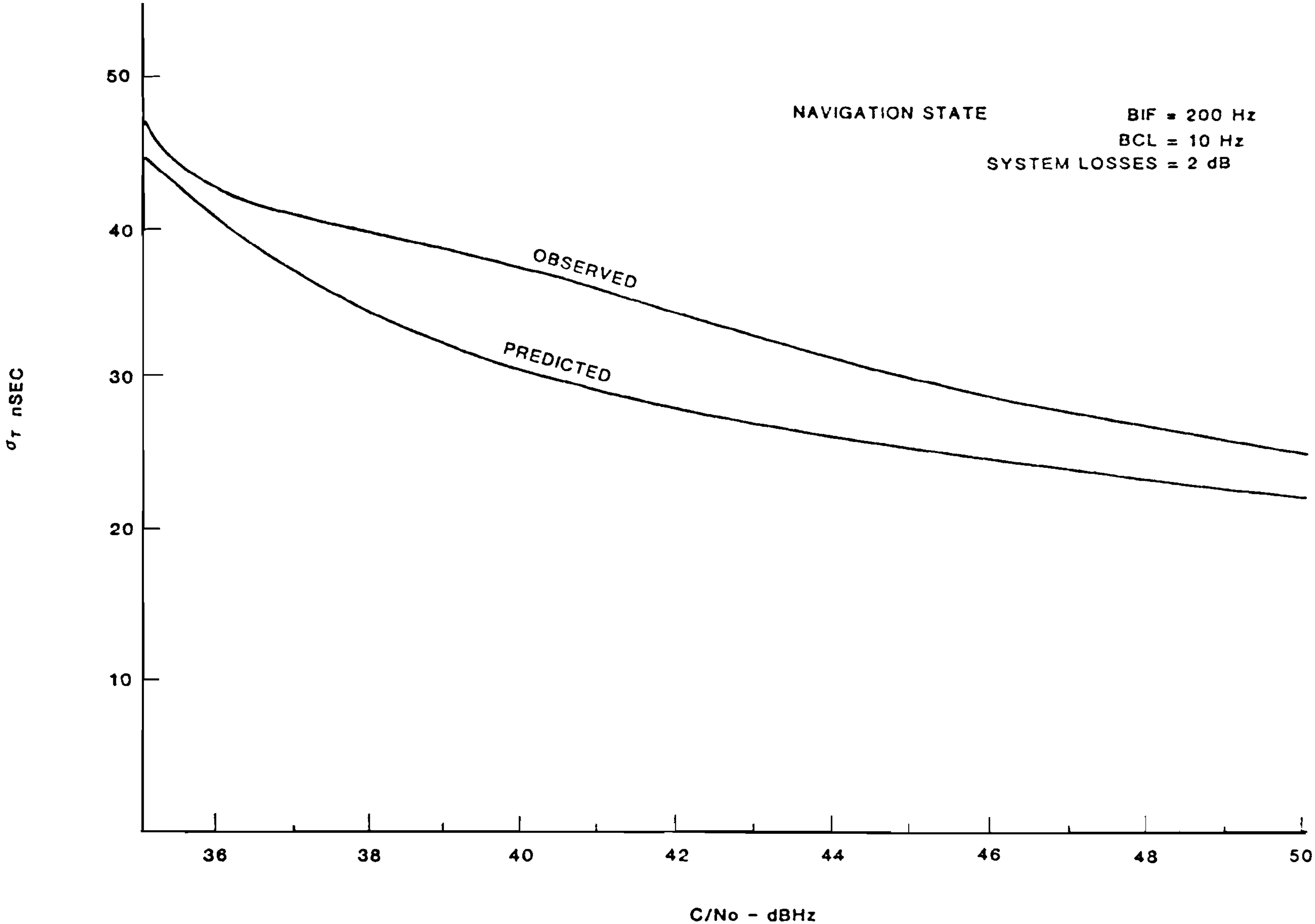

FIG. 4-27. COMPARISON OF THEORETICAL AND MEASURED RECEIVER CODE LOOP PERFORMANCE

TABLE 4-4

COMPARISON OF THEORETICAL AND MEASURED RECEIVER PERFORMANCE

Characteristic	Predicted	Measured
Minimum Acquisition C/N_o BIF - 1000 Hz BL - 10 Hz L - 2 dB	35.7 dB Hz	35 dB Hz
Nav Loss of Lock BIF - 200 Hz BL - 10 Hz L - 2 dB	31.5 dB Hz	33 dB Hz

TABLE 4-5

USER RECEIVED POWER FOR C/A CODE ONLY

	Satellite Overhead (at Zenith)	Satellite at Elevation Angle of 5°
Satellite Transmitter Power (dBw)	14.25	14.25
RF Loss (dB)	1.0	1.0
Antenna Polarization Loss (dB)	0.25	0.25
Antenna Gain	15.0	12.0
Satellite ERP (dBw)	28.0	25.0
Path Loss (dB)	182.5	184.2
Atmospheric Absorption (dB)	-	0.8
Power at User Antenna (dBw)	-154.5	-160.0
Receiver noise (dBw (4 dB noise Figure)	-200	-200
Receiver C/No (dBHz)	45.5	40.0

It is evident from Fig. 4-25 that the measured C/N_0 values were greater than expected. The mean C/N_0 for elevational angles greater than 15° was 47.8 dB-Hz, 2.3 dB greater than the 45.5 dB-Hz prediction for a zenith aspect It was postulated that the additional power was due to excess satellite transmit power, excess receiver antenna gain, and excess sensitivity in the receiver preamplifier.

To verify this a calculation of the expected received C/N_0 and link margin referred to the preamplifier input was made, as shown in Table 4-6, and plotted in Fig. 4-25. It is apparent that for satellite number 6 the link has about 2 dB additional margin, due probably to excess satellite radiated power. Also, the variations in C/N_0 were examined and found to be generally consistent with the ripple in the volute antenna patterns.

4.2.3 Static Acquisition Performance

Initial laboratory tests using the tower mounted volute antenna indicated that the T and E Equipment meets the Time to First Fix Requirements of 6 minutes maximum when the receiver is initialized with current almanac data.

The sequence of events in a representative static acquisition is shown in Table 4-7.

4.2.4 Static Position Accuracy and Stability

Tests were conducted to characterize the static accuracy and stability performance. Test data, obtained using the tower-mounted antenna, was collected and analyzed. Results from a representative 26-minute test conducted on 19 November 1982 using five GPS satellites were:

a. RMS horizontal error: 93 feet

b. RMS vertical error: 104 feet

A scatter-plot of the static test results is shown in Fig. 4-28.

A static test was also conducted on 9 May 1983 using a later version of the GPS position software. This version of the position software (Version 3.0) included the capability of navigating with three GPS satellites and the baro-altimeter. The RMS horizontal error for this run, lasting 63 minutes, was 95 feet, nearly the same as the five-satellite case. Although this version of the software was not flight tested, the basic capability for three-satellite navigation was demonstrated.

TABLE 4-6

EXPECTED LINK MARGIN

Elevation Angle (degrees)	Minimum user Receive Power[1] (dBw)	Correction for Actual Atmospheric Loss[2]. (dB)	Correction for Measured EDCR Volute Antenna Gain[3] (dB)	Net C/N_o (3 dB Noise Figure)[4] (db Hz)	Link Margin for 35 dBz Acquisition Threshold (db)
5	-160.0	+1.50	-2.0	40.5	5.5
10	-159.7	+1.74	0	43.0	8.0
20	-159.0	+1.86	+1.9	45.8	10.8
40	-158.0	+1.92	+1.2	46.0	11.0
60	-158.8	+1.94	+0.4 (est)	44.5	9.5
90	-160.0	+1.95	-0.4 (est)	42.5	7.5

1. From Rockwell ICD-GPS-200, May 81. (Assumes 2 dB atmospheric loss).
2. Digital Communications by Satellite, Spilker Page 171.
3. GPS-QTL-4-8, page 10.
4. The nominal noise figure for the EDCR is 4 dB. The actual noise figure present during the characterization measurement was 3 dB.

TABLE 4-7

STATIC ACQUISITION EXAMPLE

Event	Time (Minutes : Seconds)
Start	0
Satellite 4 acquired	0:32
Satellite 6 acquired	1:55
Satellite 5 acquired	2:49
Satellite 8 acquired	3:56
First Internal Fix	4:00
Transition Mode Started	5:00
Fix Sent to Navigation Software	5:05
Navigation Mode Started	5:11

GPS STATIC TEST
19 NOV 82
1747 - 1803 GMT
FIVE SATELLITES VISIBLE

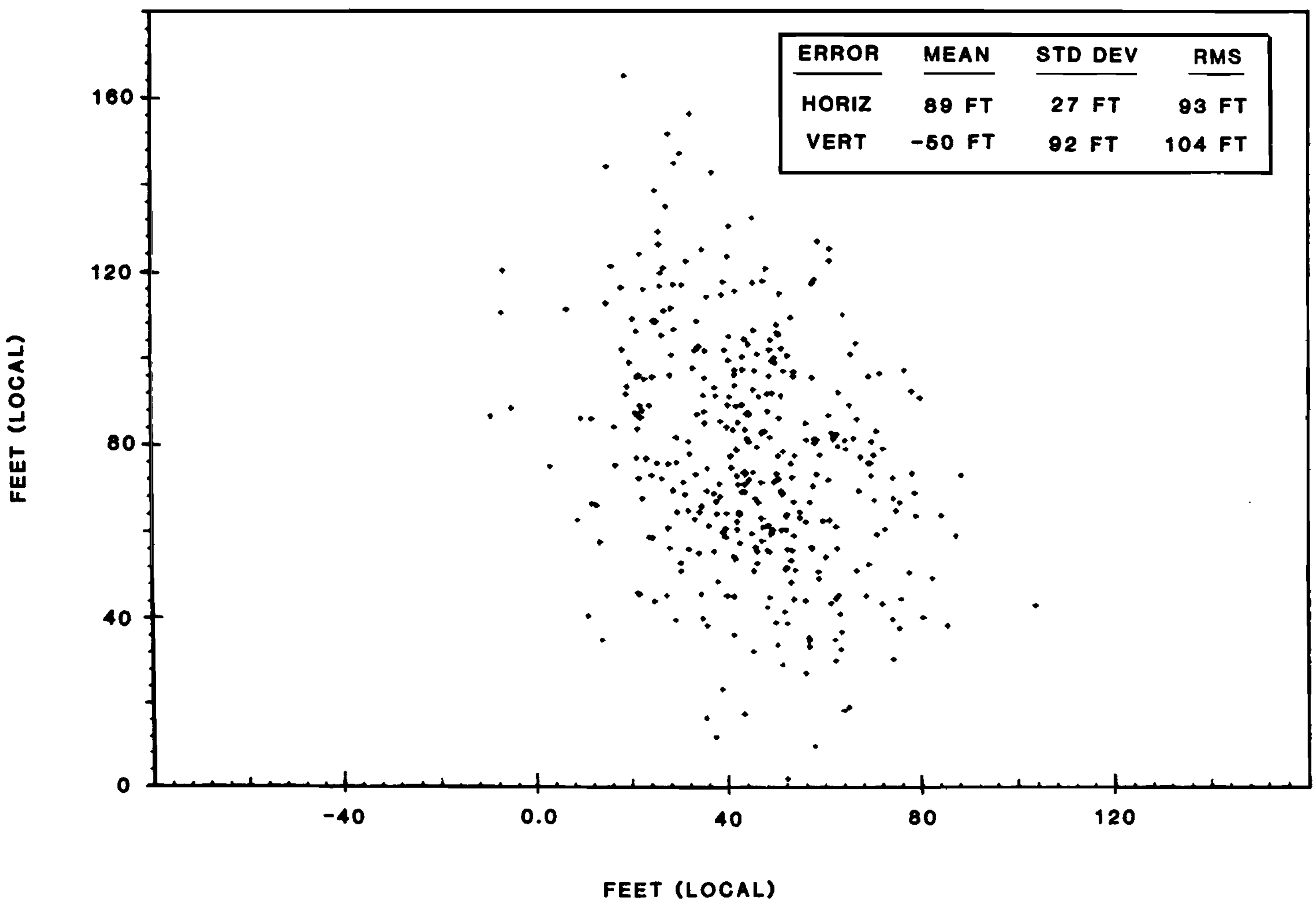

FIG. 4-28. GPS STATIC TEST, 19 NOV 82

4.2.5 Interference Effects

Static tests conducted in the Aerocommander indicate that the UHF radios, VOR receivers, ATC transponder and DME did not appear to interfere with the operation of the preamp and receiver channels. There was no observed effect on the operation of the aircraft avionics when the GPS receiver was operated.

In addition, a simulation of interference effects in the Rockwell Aerocommander test aircraft was carried out for the FAA by the DoD Electromagnetic Compatibility Analysis Center (ECAC). The ECAC study showed that the Aerocommander avionics would not interfere with the operation of the GPS receiver for the particular antenna configuration used in the tests [Ref. 12].

4.2.6 Performance Monitoring

The performance monitoring features described in Section 3.5.6 were verified during static tests. Features verified include the receiver fault monitoring via receiver firmwave diagnostics and receiver-position processor interface fault detection via the Position Software.

4.3 Flight Tests

During the course of the GPS test and evaluation project, a total of 25 flights were made during which a total of 33 hours of flight data was collected. A variety of flights were conducted at a total of seven different airports as listed in Table 4-8. These tests measured system performance during takeoffs, landings, approaches and turns. The tests conducted for airports in Massachusetts and southern New Hampshire were within the range of MODSEF surveillance.

The flight test program was divided into engineering and operational phases. The engineering tests were conducted primarily to determine the effect of aircraft dynamics and link margin on the accuracy and reliability of the GPS navigation system. The operational tests were conducted to determine the performance of the system under a variety of conditions typical of general aviation use and to verify the compatibility of the system with conventional air navigation systems.

4.3.1 Engineering Flight Tests

A total of 14 engineering test flights were made during which a total of 16.5 hours of data was collected. These flights were made over the six-month period lasting from June to December of 1982. Position software development continued over this period, so that most of the effort was directed at assessing the accuracy of the system in various dynamic situations, such as level flight, turns, climbing and descent. At the beginning of December, 1982, the position software was frozen at version 2.1, which was used for all subsequent engineering and operational flight tests.

TABLE 4-8

AIRPORTS FOR GPS FLIGHT TESTS

Airport	Location	Test Takeoff	Test Landing	Low-Approach	MODSEF Surveillance
Hanscom Field	Lexington, MA	X	X	X	Yes
Gardner Municipal	Gardner, MA			X	Yes
Logan International	Boston, MA	X	X	X	Yes
Boire Field	Nashua, NH			X	Yes
Manchester Airport	Manchester, NH	X	X	X	Yes
Burlington International	Burlington, VT	X	X		No
Dulles International	Washington, DC	X	X		No

4.3.1.1 Engineering Tests with Preliminary Position Software

An engineering test using the preliminary position software was conducted on 28 October 82. The results of this test are included here to illustrate the benefit of tracking all satellites in view and to quantify the fade margin during steep turns.

In this test, the aircraft was initially in a holding pattern at the LOBBY intersection as shown in Fig. 4-29. After emerging from the holding pattern, the aircraft performed two 360° turns at a bank angle of 30°. The aircraft next was flown to intercept the Shaker Hills waypoint (SKR NDB) and then landed on runway 11.

Figure 4-30 shows the satellite visibilities during the 28 October 1982 flight. All five operational satellites were at least 10° above the horizon and SV5 had the lowest elevation angle, ranging from 18° to 25° during the run. Figure 4-31 shows the GDOP, HDOP and VDOP values during the flight. The HDOP and VDOP values are calculated relative to the local MODSEF coordinate system. The GDOP value ranged from 5.1 to 5.4.

During the flight, the aircraft was under continuous MODSEF surveillance, allowing the system navigation accuracy statistics to be computed by post-flight processing. The position accuracy statistics are calculated in two ways based on: 1) the position fixes generated every 2.2 seconds, and 2) the α-β tracker estimates generated once per second. The position fix statistics give the accuracy of the independent position fixes in the normal navigation mode. The tracker estimate statistics give the system accuracy as displayed to the pilot using linear extrapolation between position fixes.

The position accuracy statistics for the 28 October flight are shown in Table 4-9. For this perliminary version of the position software, the horizontal error from the α-β tracker position estimate was 364 feet (95%). This horizontal error value easily meets the AC90-45A requirement for non-precision approach and is better than the 500 ft (95%) goal for straight and level flight. The rms horizontal error was 211 feet, which also meets the FRP requirements for non-precision approach.

The portion of the 28 October 1982 flight containing the 30° bank angle turns are shown in Figs. 4-32a and 4-32b. As shown in Table 4-10 the 95% horizontal position estimate error was 429 feet, a factor of two better than the 1000 ft 95% accuracy goal during 30° bank turns. Figures 4-33a and 4-33b show the horizontal and vertical errors versus time during the 30° bank turns for the position fixes and the trackes estimates. Figure 4-34 shows the measured carrier-to-noise-density (C/N_0) ratios during the 30° bank turns for the five visible satellites. Note that SV5 drops below the 33 dB-Hz loss-of-lock threshold at 390 sec and 515 sec. These two occasions correspond to the times when the aircraft was banked away from the satellite. From Fig. 4-30, the satellite elevation was about 20° so that the satellite was at -10° elevation angle with respect to the GPS antenna.

X-Y plot: GPS a/c in MODSEF local system

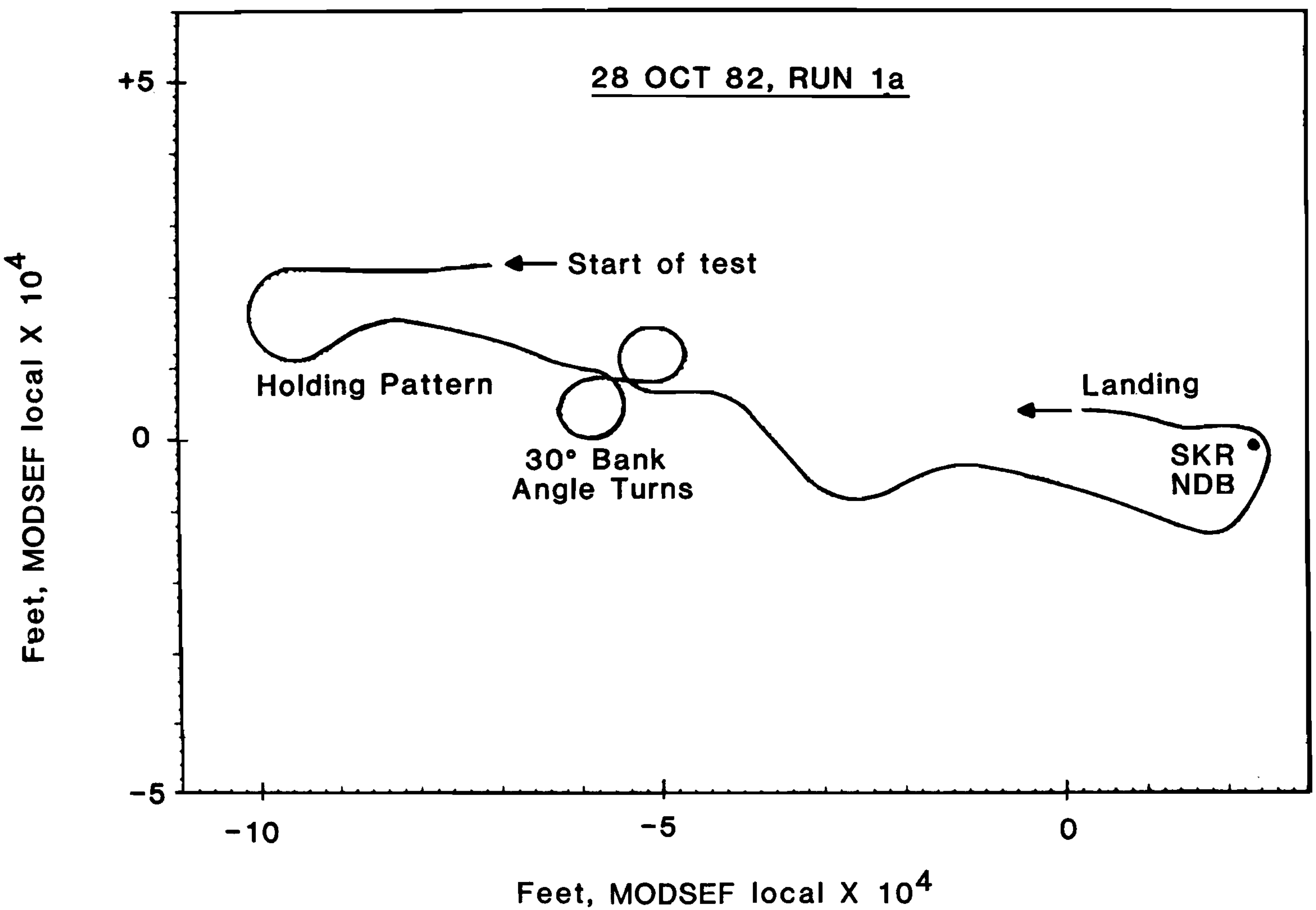

FIG. 4-29. TEST FLIGHT RUN 1a, 28 OCT 82

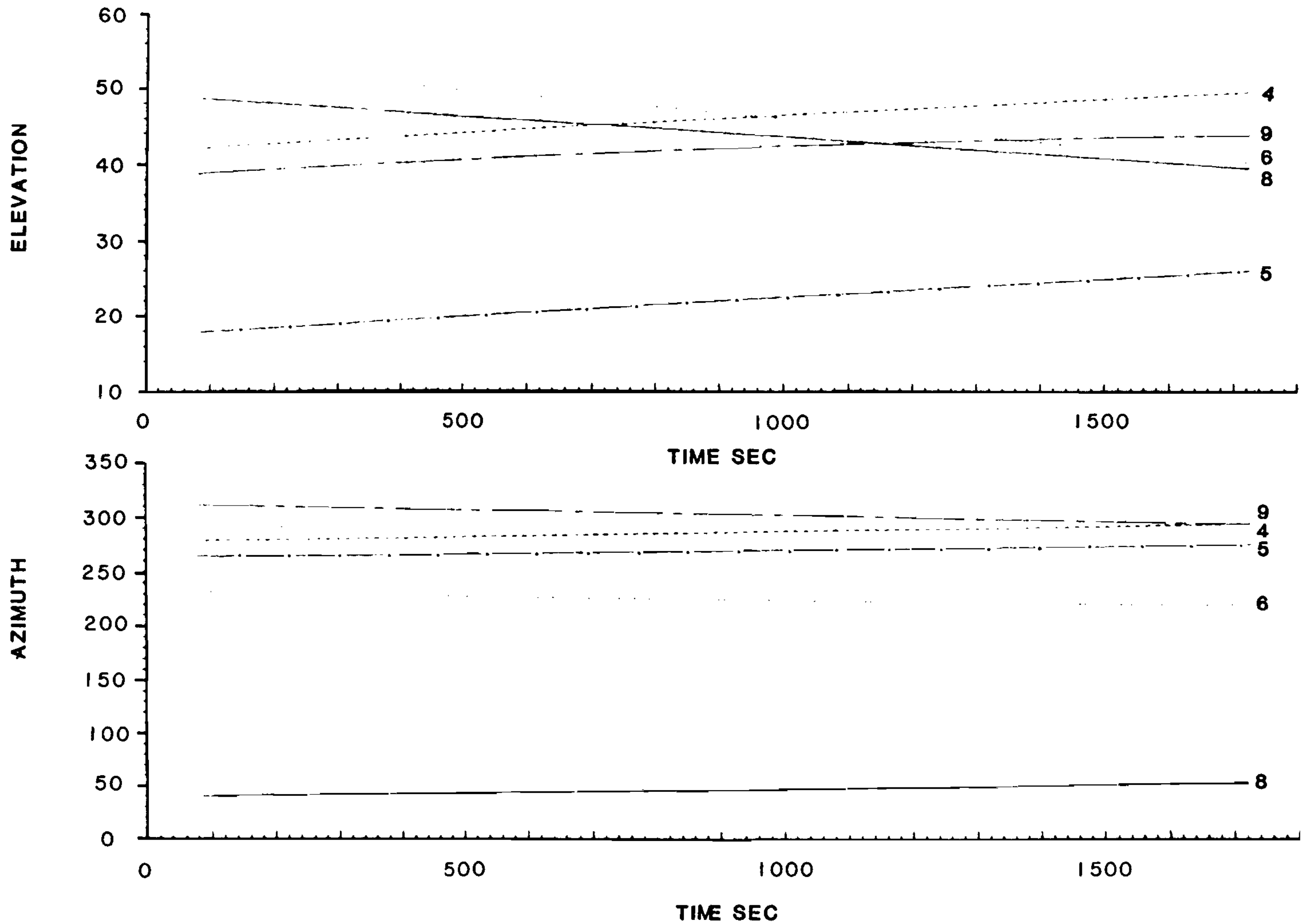

FIG. 4-30. SATELLITE VISIBILITIES FOR RUN 1a, 28 OCT '82

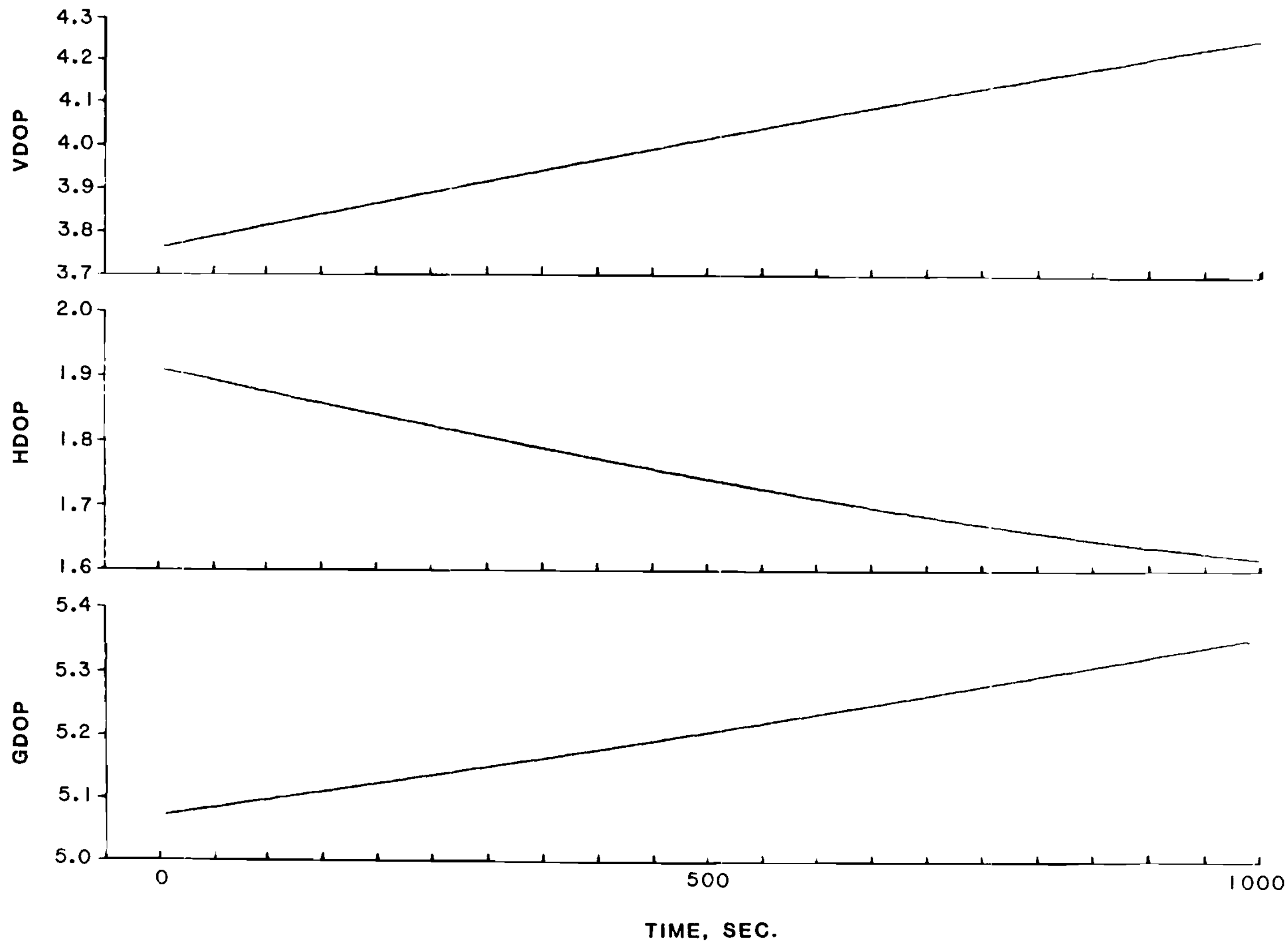

FIG. 4-31. DILUTION-OF-PRECISION, 28 OCT 82 FLIGHT

TABLE 4-9

POSITION ACCURACY STATISTICS FOR RUN 1a, 28 OCTOBER 1982

Position Fixes:

Error	Mean	Standard Deviation	RMS	95%
Horizontal	130	111	171	276 ft
Vertical	185	100	210	375 ft

Tracker Estimates:

Error	Mean	Standard Deviation	RMS	95%
Horizontal	128	168	211	364 ft
Vertical	194	126	231	423 ft

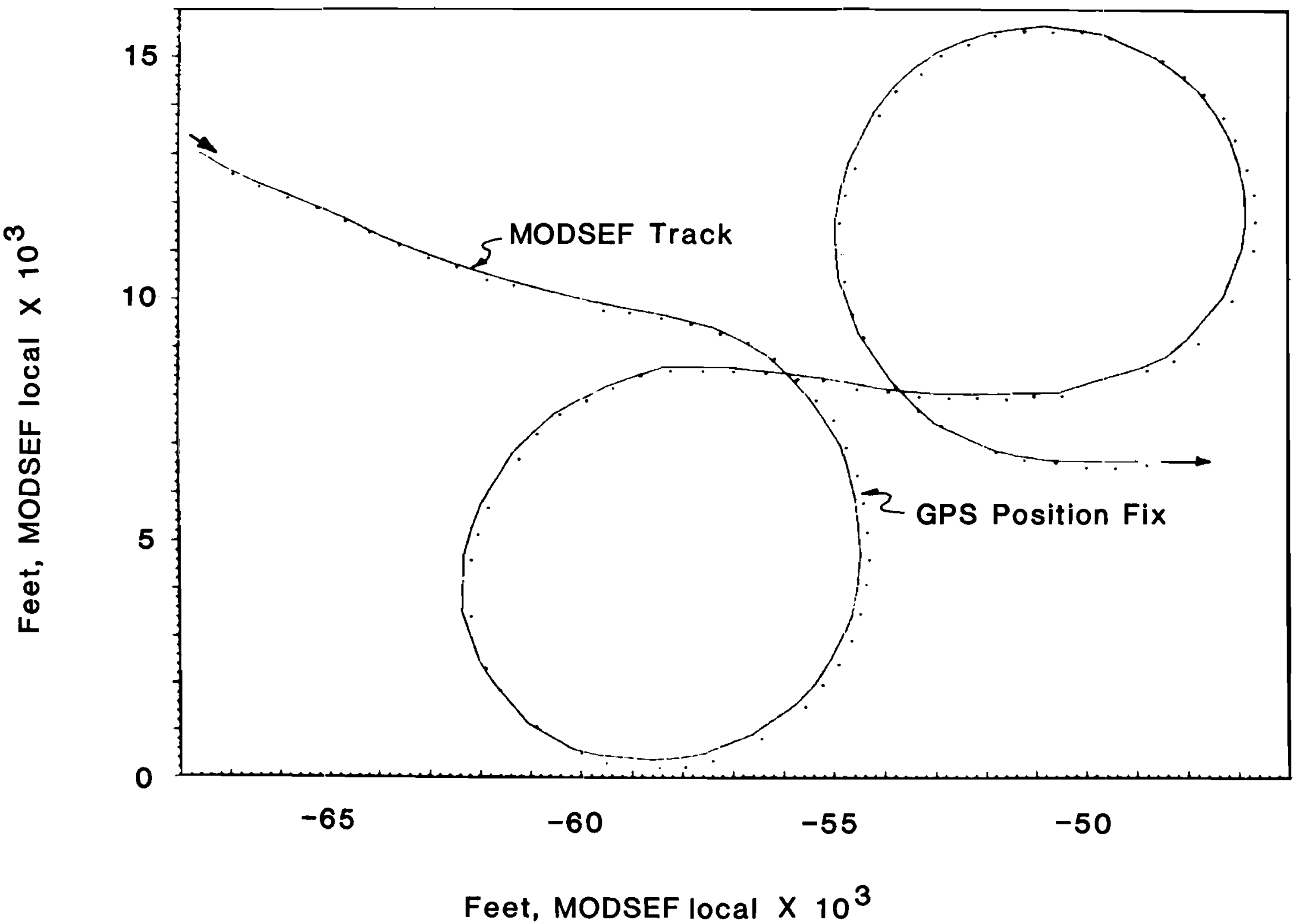

FIG. 4-32a. POSITION FIX PERFORMANCE, 30° BANK TURN

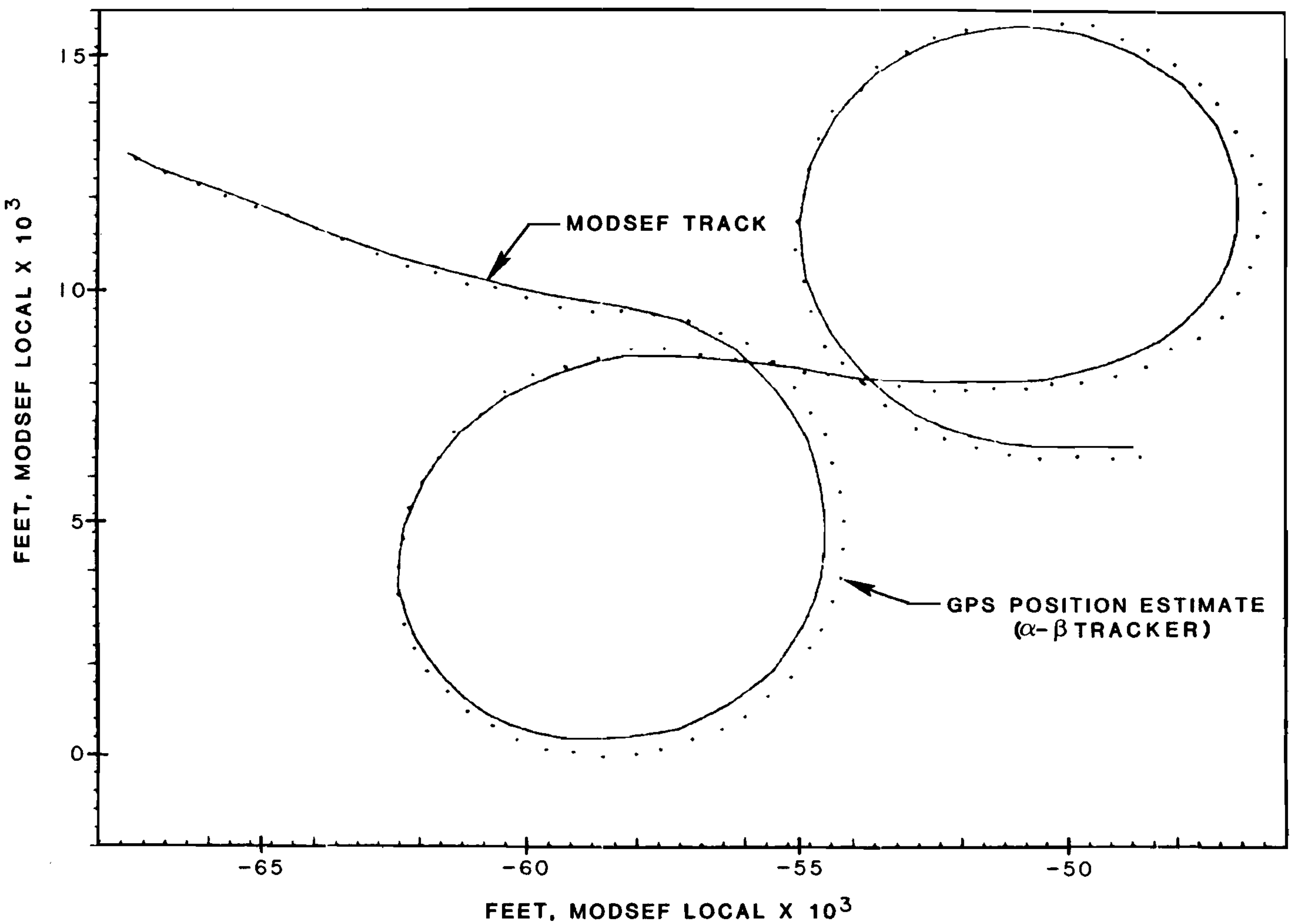

FIG. 4-32b. POSITION ESTIMATE PERFORMANCE, 30° BANK TURN

TABLE 4-10

POSITION ACCURACY STATISTICS FOR 30° BANK ANGLE TURNS

Position Fixes:

Error	Mean	Standard Deviation	RMS	95%
Horizontal	181	54	189	245 ft
Vertical	166	104	196	322 ft

Tracker Estimates:

Error	Mean	Standard Deviation	RMS	95%
Horizontal	182	201	271	428 ft
Vertical	191	135	234	423 ft

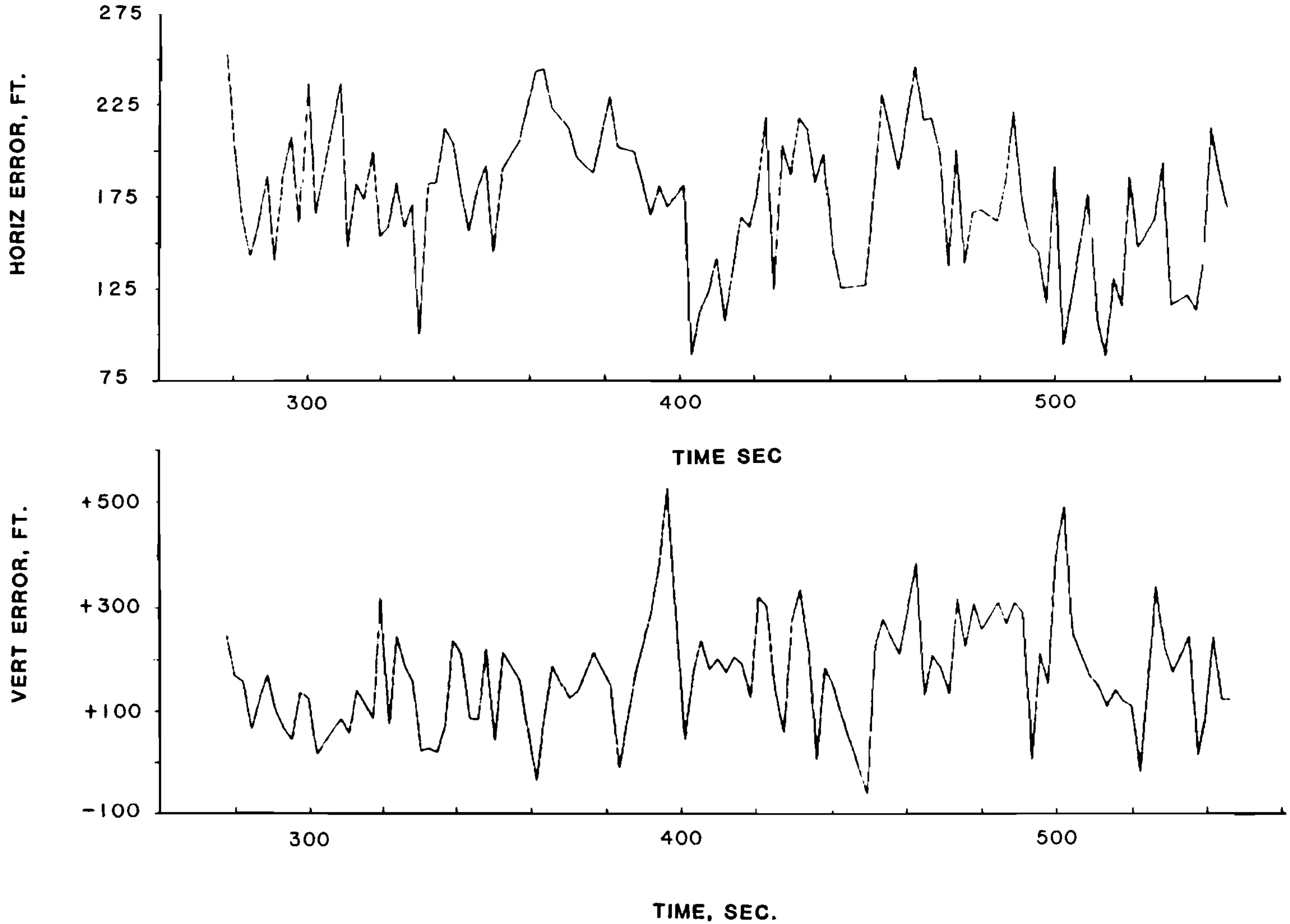

FIG. 4-33a. POSITION FIX ERROR DURING 30° TURNS

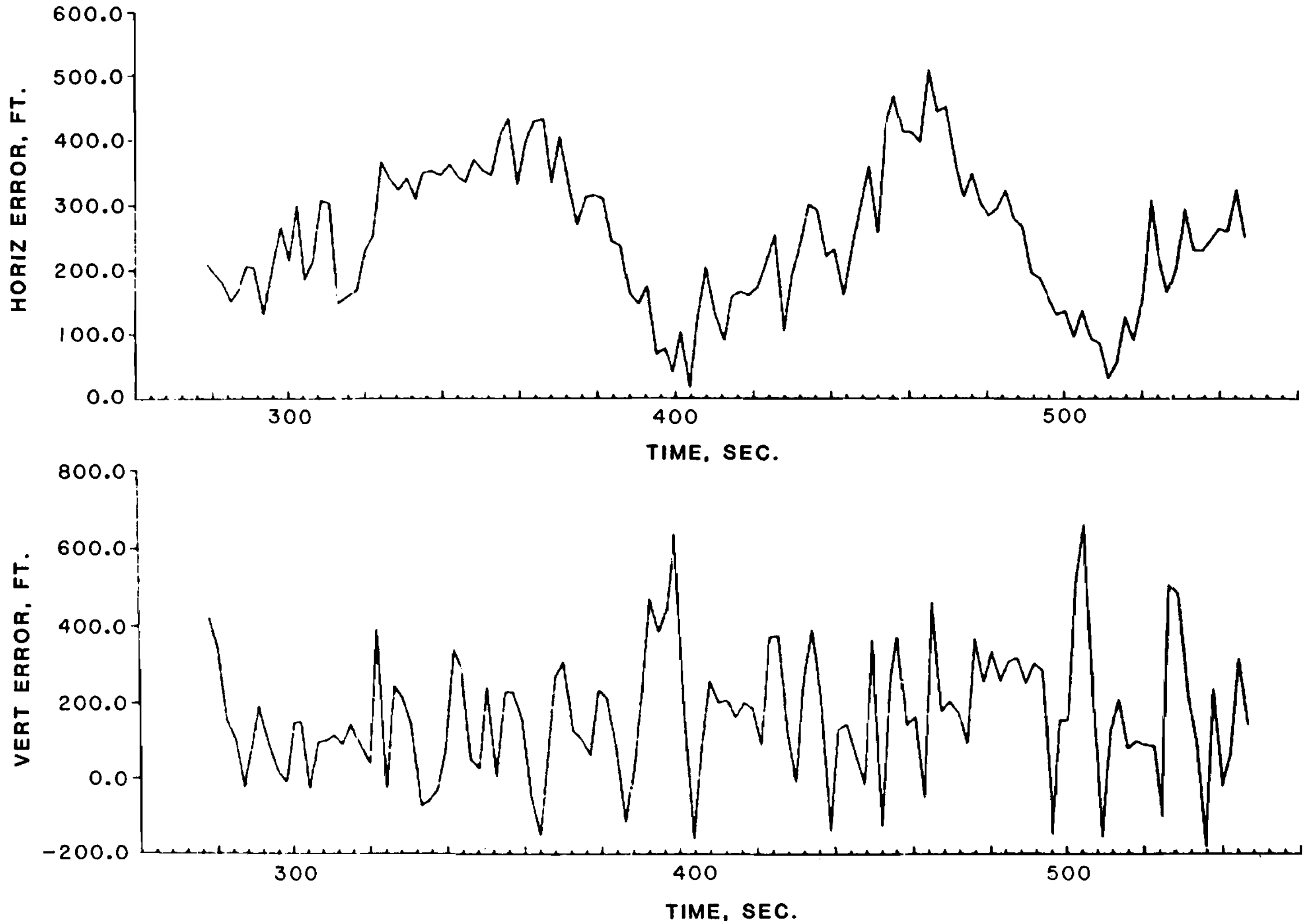

FIG. 4-33b. POSITION ESTIMATE ERROR DURING 30° TURNS

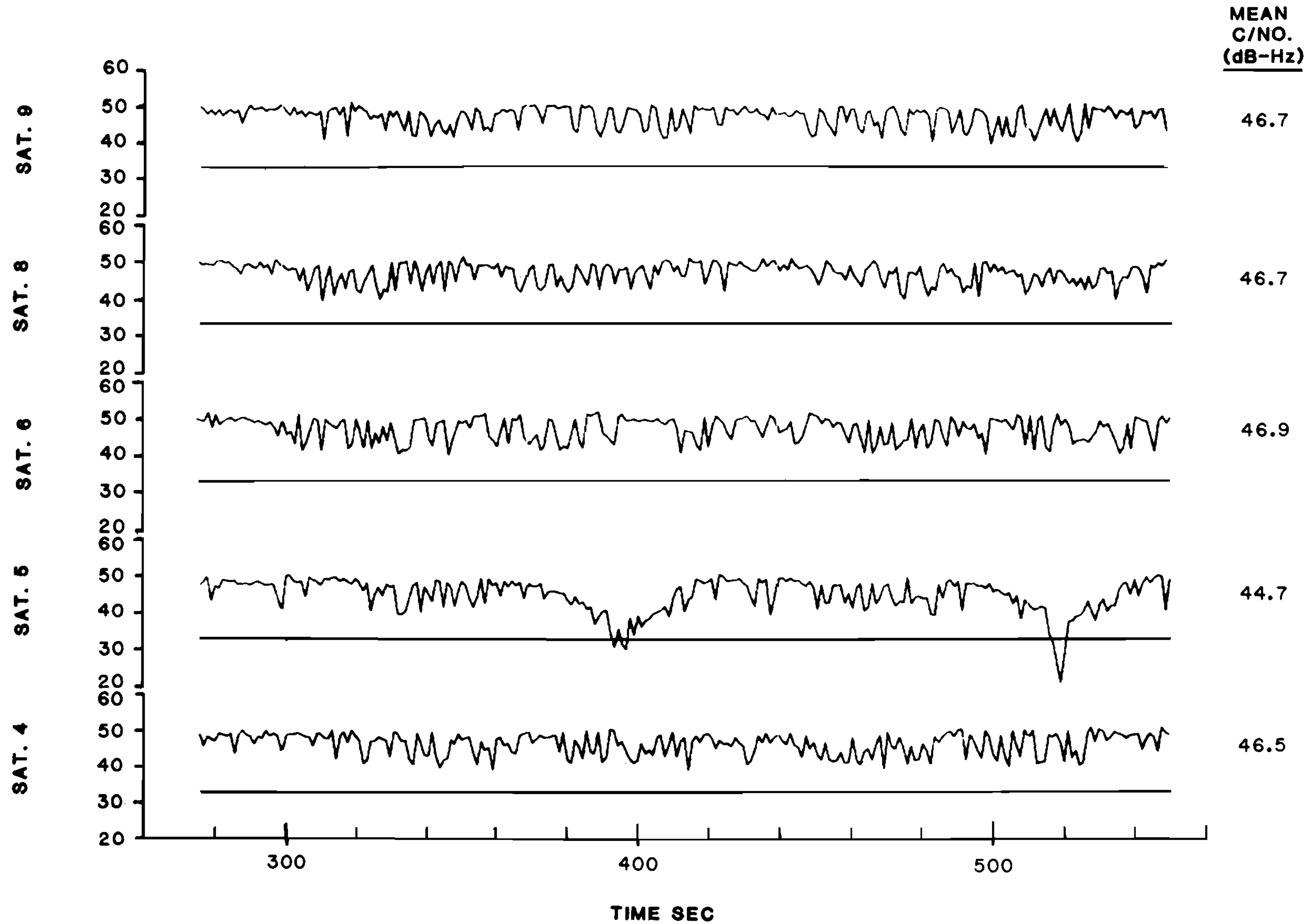

FIG. 4-34. SATELLITE C/No DURING 30° TURNS

According to the GPS antenna gain characteristic of Fig. 4-14, changing the elevation angle from +20° to -10° causes an 8 dB drop in antenna gain. This loss in antenna gain would drop the satellite C/No from the mean value of 44.7 dB-Hz to 36.7 dB-Hz. Since the C/No value for SV5 dropped to less than 33 dB-Hz during portions of the turn, it seems likely that shielding from the wings, engine nacelle and propellers occurred in addition to the antenna loss.

A significant conclusion from the 30° bank turn example is the importance of tracking all visible satellites rather than a subset of four SVs. Despite the momentary drop of SV5, there were always at least four satellites in track during the turn. As a result, the position solution was maintained continuously throughout the turn.

The results from the flight tests using the preliminary position software can be summarized. First, the accuracy of the GPS navigator exceeded the requirements of AC90-45A for two-dimensional area navigation in the enroute, terminal and non-precision approach modes. Second, the system maintained the position solution during 30° bank turns. Finally, it is seen that the system can maintain continuous position updates during momentary outages due to a satellite fade if adequate satellite coverage is provided.

4.3.1.2 Engineering Tests with Final Position Software

The position software was frozen at version 2.1 at the beginning of December, 1982. The remaining engineering flight tests were conducted with this software version. The aim of these tests were to: 1) measure the accuracy improvement in the version 2.1 software, 2) verify performance during takeoffs and landings, 3) examine the behavior of the α-β tracker and 4) determine the possible effect of multipath on system performance.

4.3.1.2.1 Accuracy Tests

To illustrate the accuracy performance achieved using the final version of the position software, the Hanscom flight shown in Fig. 4-35 was selected. The flight was one of several touch-and-go landings performed on 12 December 1982 at runway 29 and the results are summarized in Table 4-11. For this flight segment lasting about ten minutes, the rms horizontal error was 104 feet and the 95% horizontal error was 175 feet. It should also be noted that the 95% vertical error in this case was 215 feet, which marginally meets the vertical navigation requirements of AC90-45A shown in Table 2-3. The horizontal and vertical errors for the 12 December 1982 flight segment are also shown in Figs. 4-36a and 4-36b for the position fixes and the tracker estimates, respectively. The two large horizontal errors at about 150 sec into the run are due to misses in the MODSEF surveillance rather than GPS errors; these artifacts do not significantly affect the error statistics.

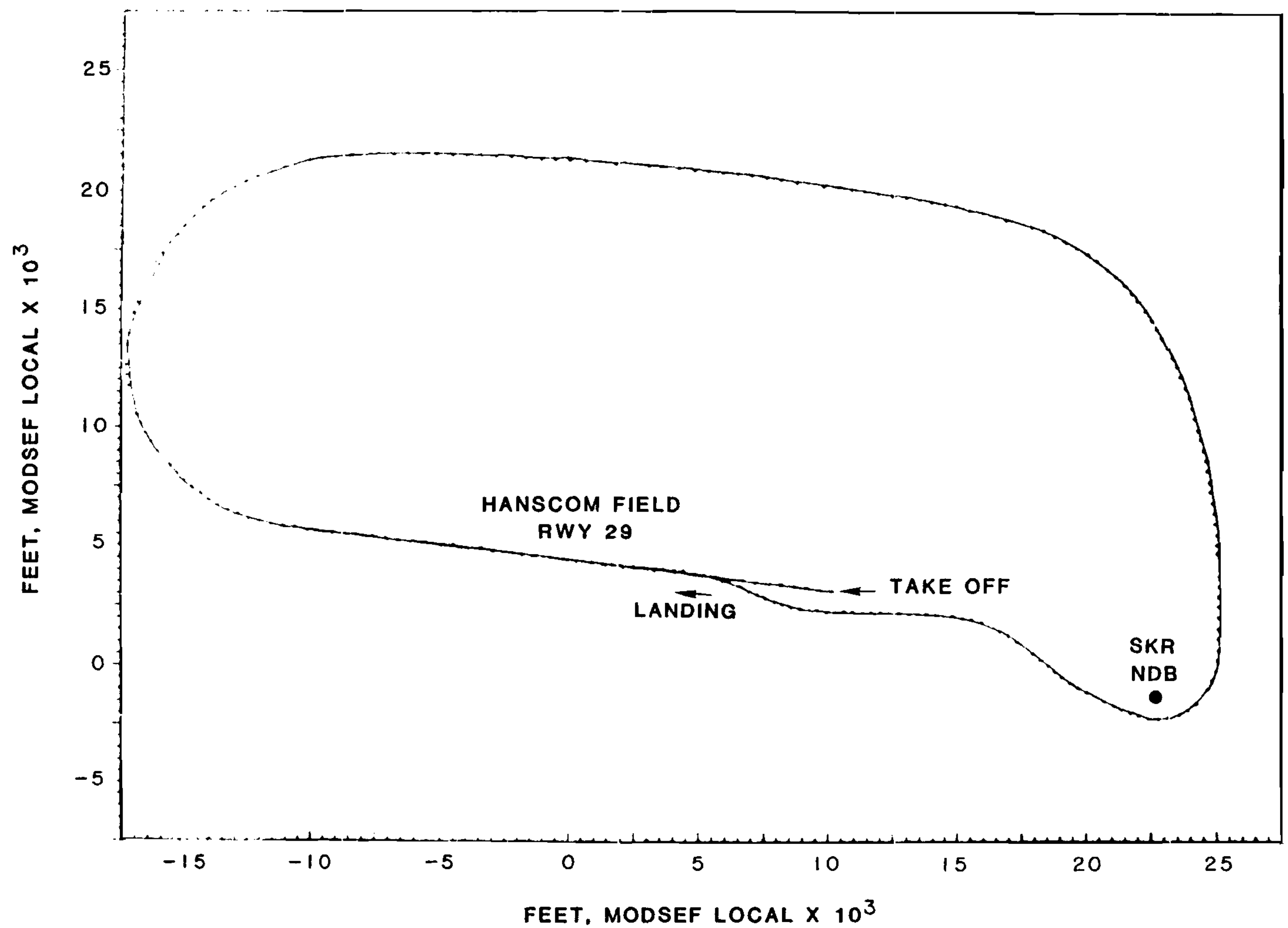

FIG. 4-35. FLIGHT TEST, 21 DEC 82

TABLE 4-11

POSITION ACCURACY STATISTICS, 21 DECEMBER 1982 TEST

Position Fixes:

Error	Mean	Standard Deviation	RMS	95%
Horizontal	34	57	66	112 ft
Vertical	65	49	81	162 ft

Tracker Estimates:

Error	Mean	Standard Deviation	RMS	95%
Horizontal	34	98	104	175 ft
Vertical	87	65	108	215 ft

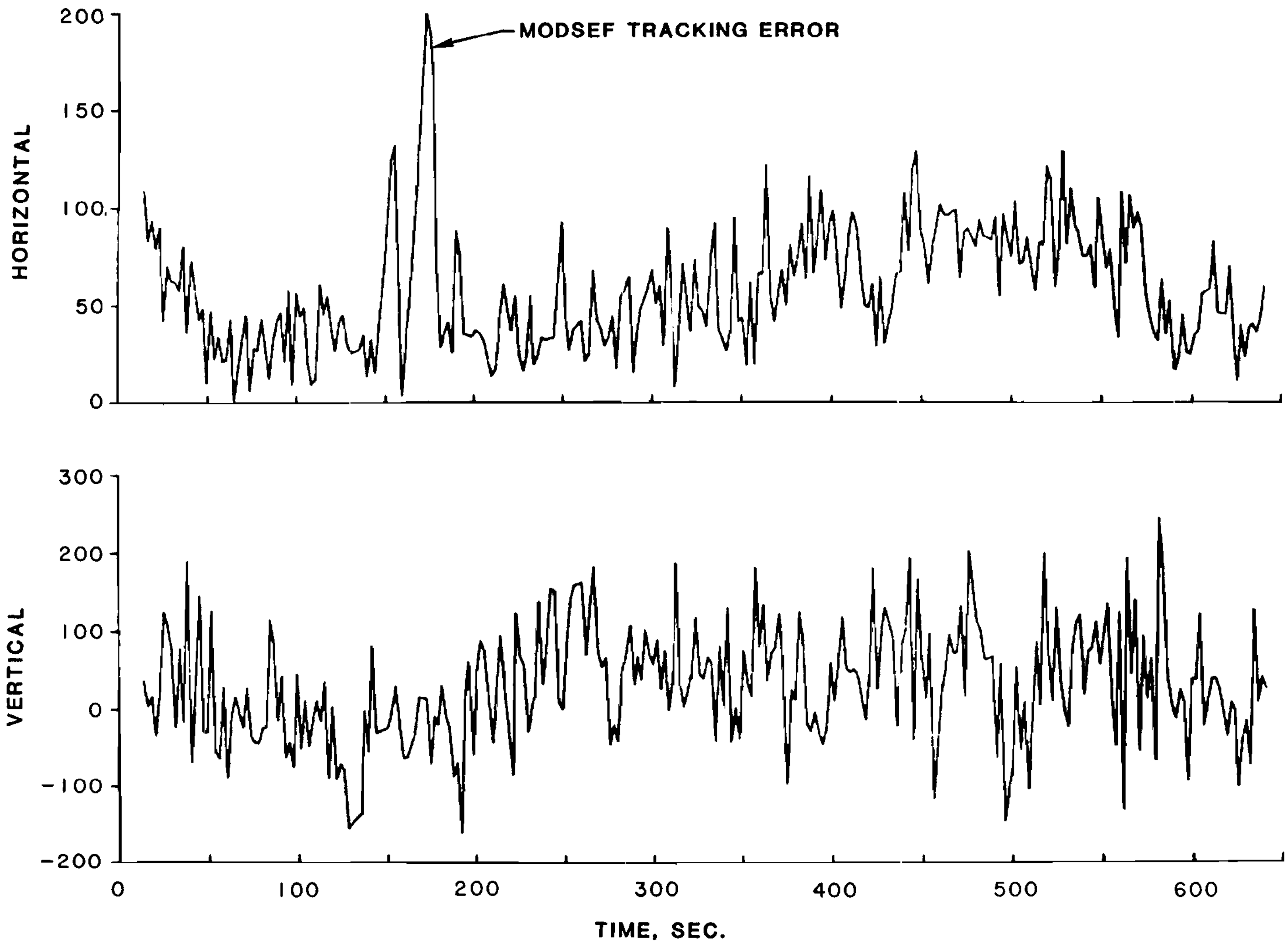

FIG. 4-36a. POSITION FIX ERRORS, 21 DEC 82 FLIGHT TEST

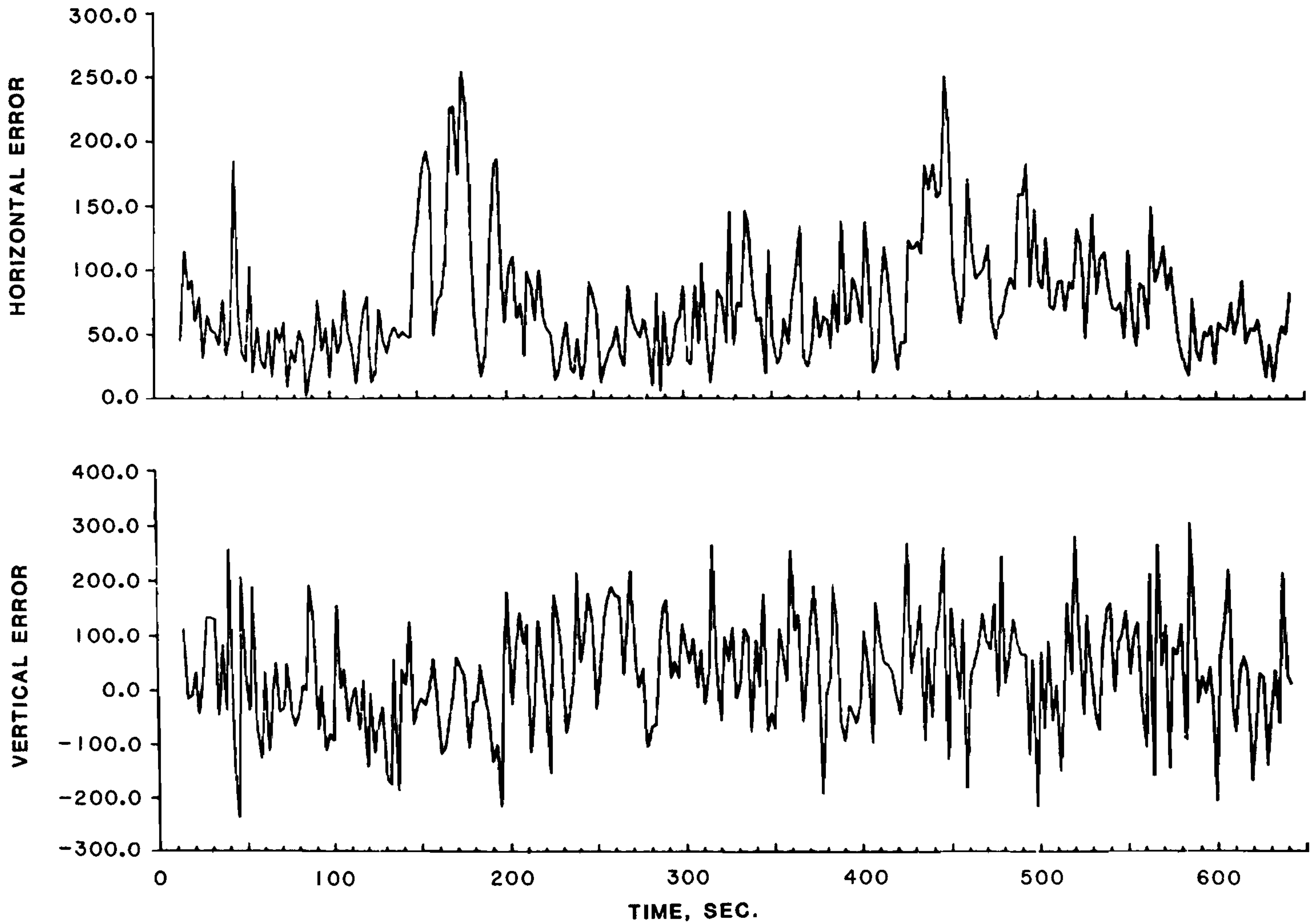

FIG. 4-36b. POSITION ESTIMATE ERRORS, 21 DEC 82 FLIGHT TEST

Figure 4-37 shows the pseudo-range residuals for the 21 December 1982 flight. The pseudo-range residuals denote the difference between the measured pseudo-range and the calculated range based on the α-β tracker position estimate. Note that the magnitudes of the residuals increase for roughly 100 seconds starting at about 400 seconds into the run. This time interval corresponds to the sharp turn during the flight near the Shaker Hills waypoint (SKR NDB).

The pseudo-range residuals increase during turns because of the behavior of the α-β tracker. The tracker projects the last position estimate forward to the next position fix time, assuming that the aircraft is moving in a straight line at constant velocity. Because acceleration is not modelled, the tracker position estimate error increases during a turn. As a result, the pseudo-range residuals also increase, forcing the position solution algorithm to apply larger corrections to the position estimate in order to produce the position fix.

4.3.1.2.2 Tracker Performance

As a further illustration of the effect of the α-β tracker on the pseudo-range residuals during turns consider the flight segment of Fig. 4-38. In this test, a series of five 360° turns was made at 15° to 20° bank angle. Figure 4-39 shows the pseudo-range residuals for this test. It is readily apparent from the plot that the five-turn series causes a variation in the pseudo-range residuals of about $\pm$ 100 feet. It may be further noted that the residuals for SV8 vary in the opposite sense from the other satellites; this behavior stems from the fact that SV8 is west of the aircraft while the rest of the satellites lie to the east.

4.3.1.2.3 Multipath Tests

Tests were also conducted to determine if multipath effects could be observed. In one multipath test the aircraft was flown over the ocean on a generally south-westerly course while descending from 1500' to 500' in altitude and then climbing back to 2500'. The satellite elevation angles during this test ranged from 25° to 55°. The flight profile was selected in order to maximize multipath effects, which should vary according to altitude. The sea state was calm, also promoting maximum multipath magnitude. The ground path and altitude profile for the test are shown in Figs. 4-40 and 4-41, respectively. The satellite visibilities are shown in Fig. 4-42a.

The pseudo-range residuals for the test are shown in Fig. 4-42b. It can be seen that the residuals do not change in character throughout the test. There is a bias in the SV9 residuals of about 50 feet, but this bias does not change with altitude.

It was concluded from this test that multipath effects were not significant for satellites of 25° elevation angle or greater. There were no effects discovered in any of the flight tests that could be attributed to multipath.

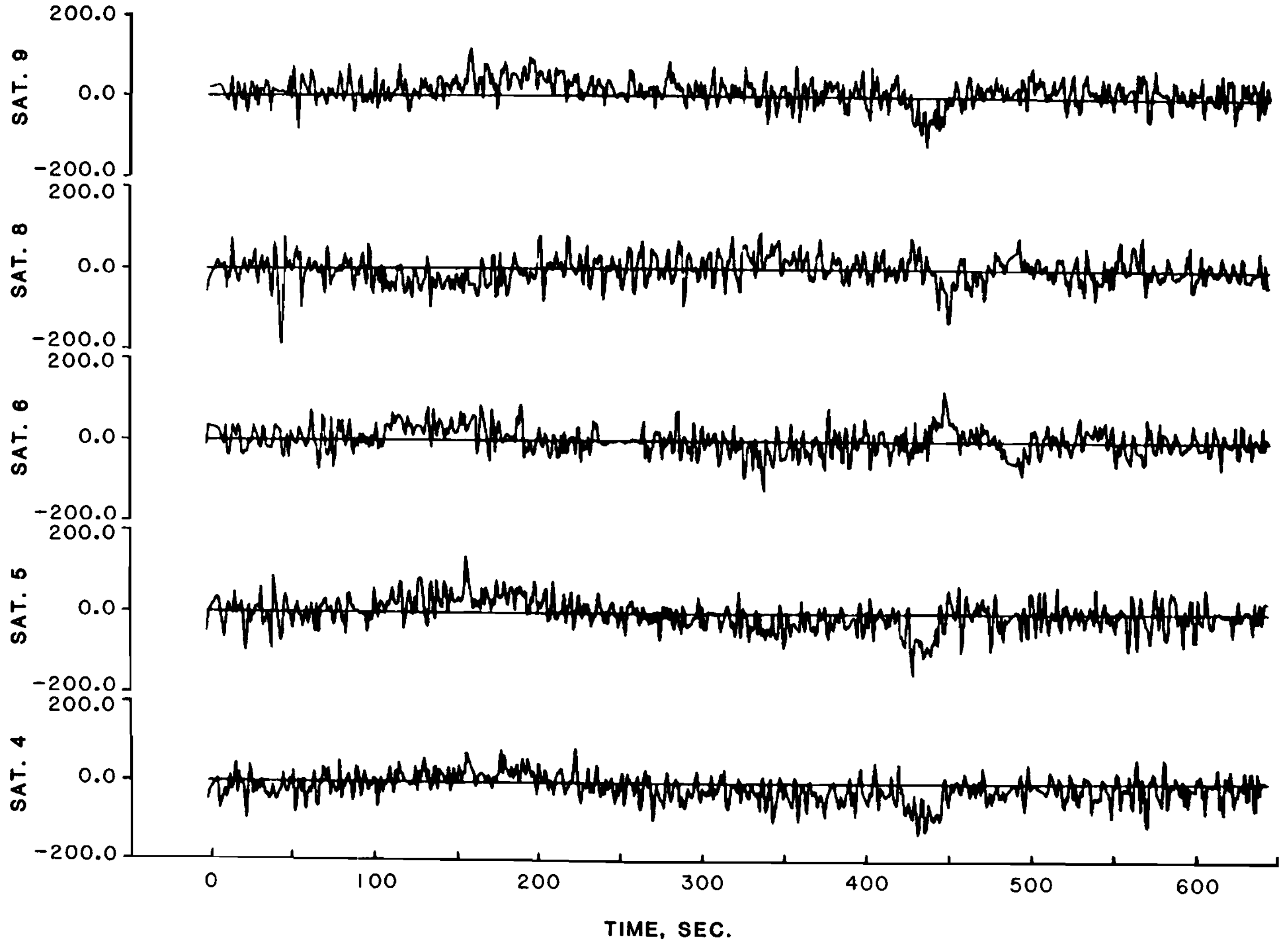

FIG. 4-37 PSEUDO-RANGE RESIDUALS, 21 DEC 82 FLIGHT TEST

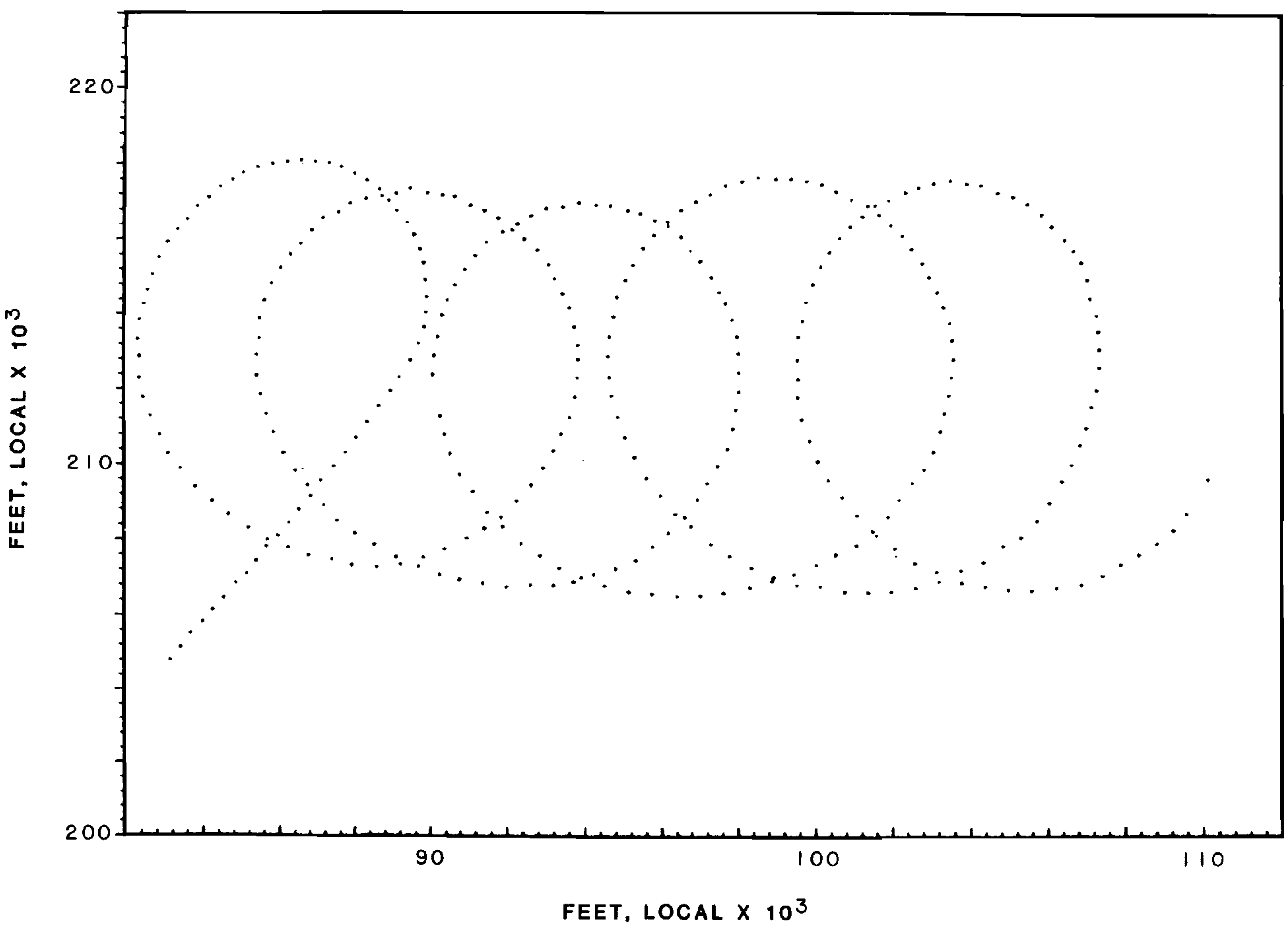

FIG. 4-38. FIVE 360° TURN SERIES, 25 JAN 83

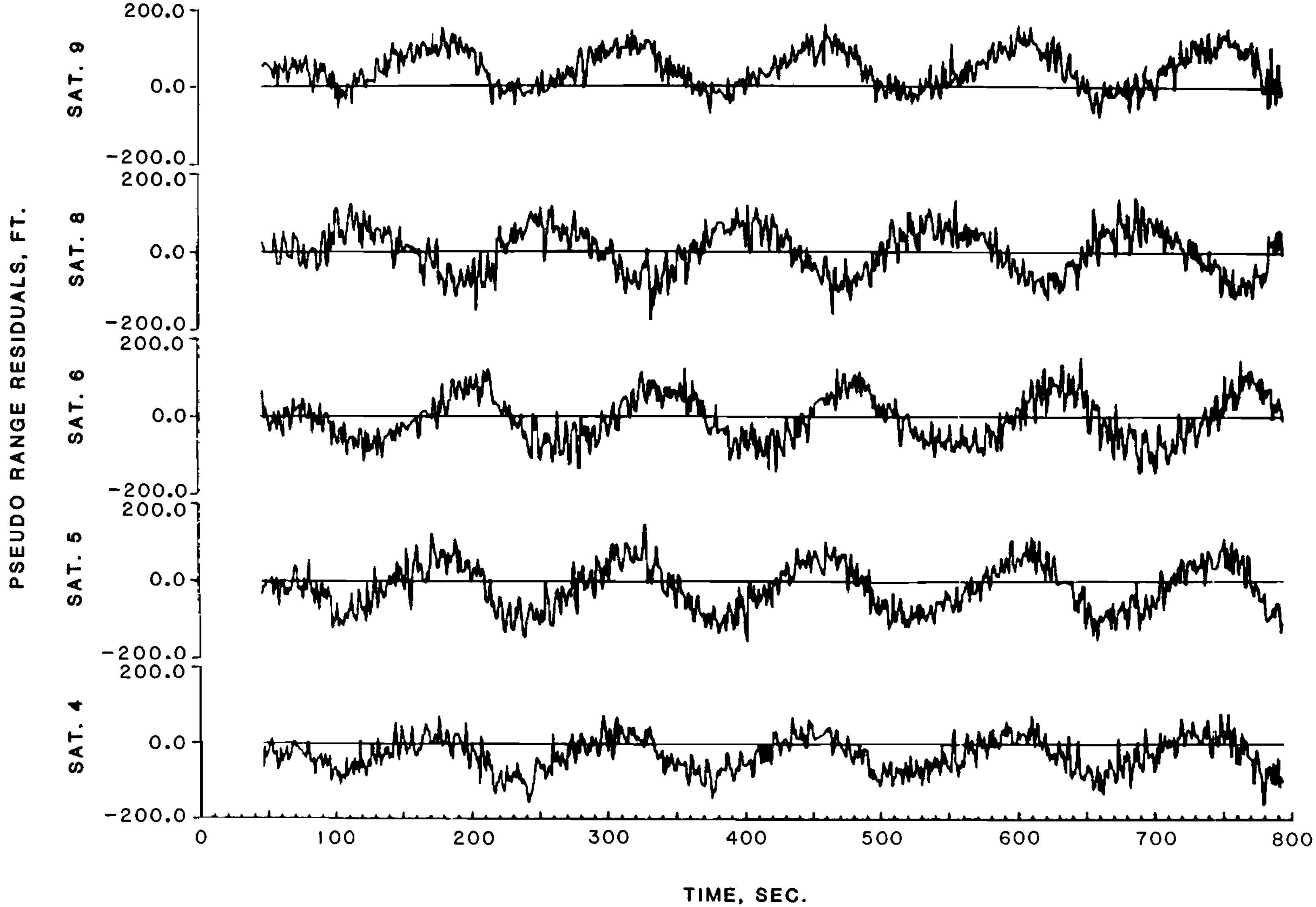

FIG. 4-39. PSEUDO RANGE RESIDUALS FOR FIVE 360° TURNS

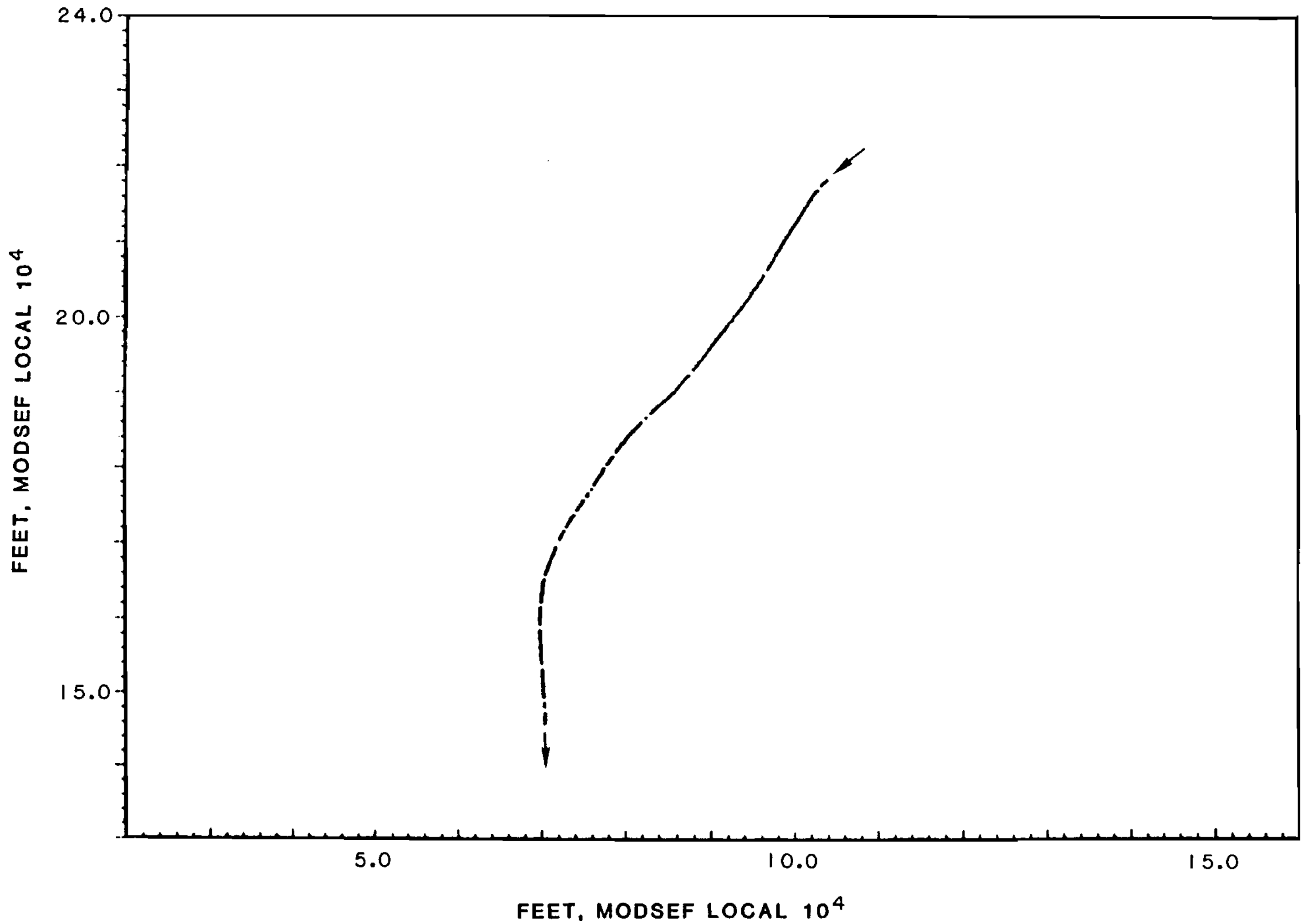

FIG. 4-40. GROUND TRACK FOR MULTIPATH TEST, 25 JAN 83

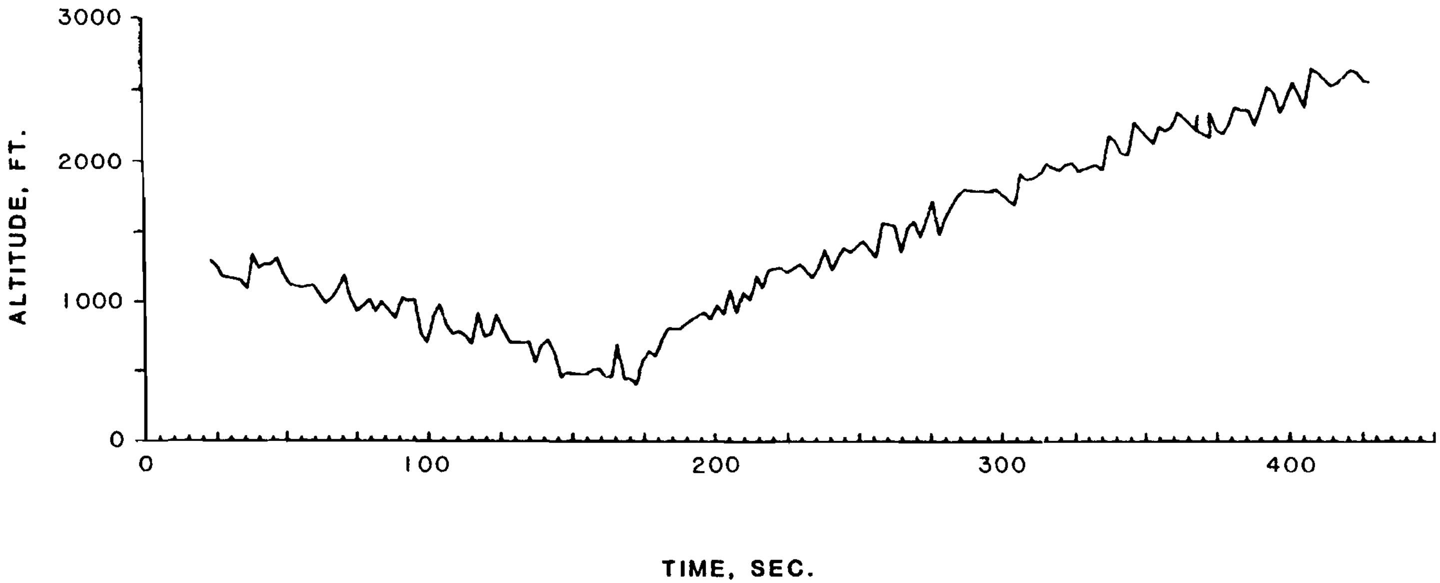

FIG. 4-41. ALTITUDE PROFILE FOR MULTIPATH TEST, 25 JAN 83

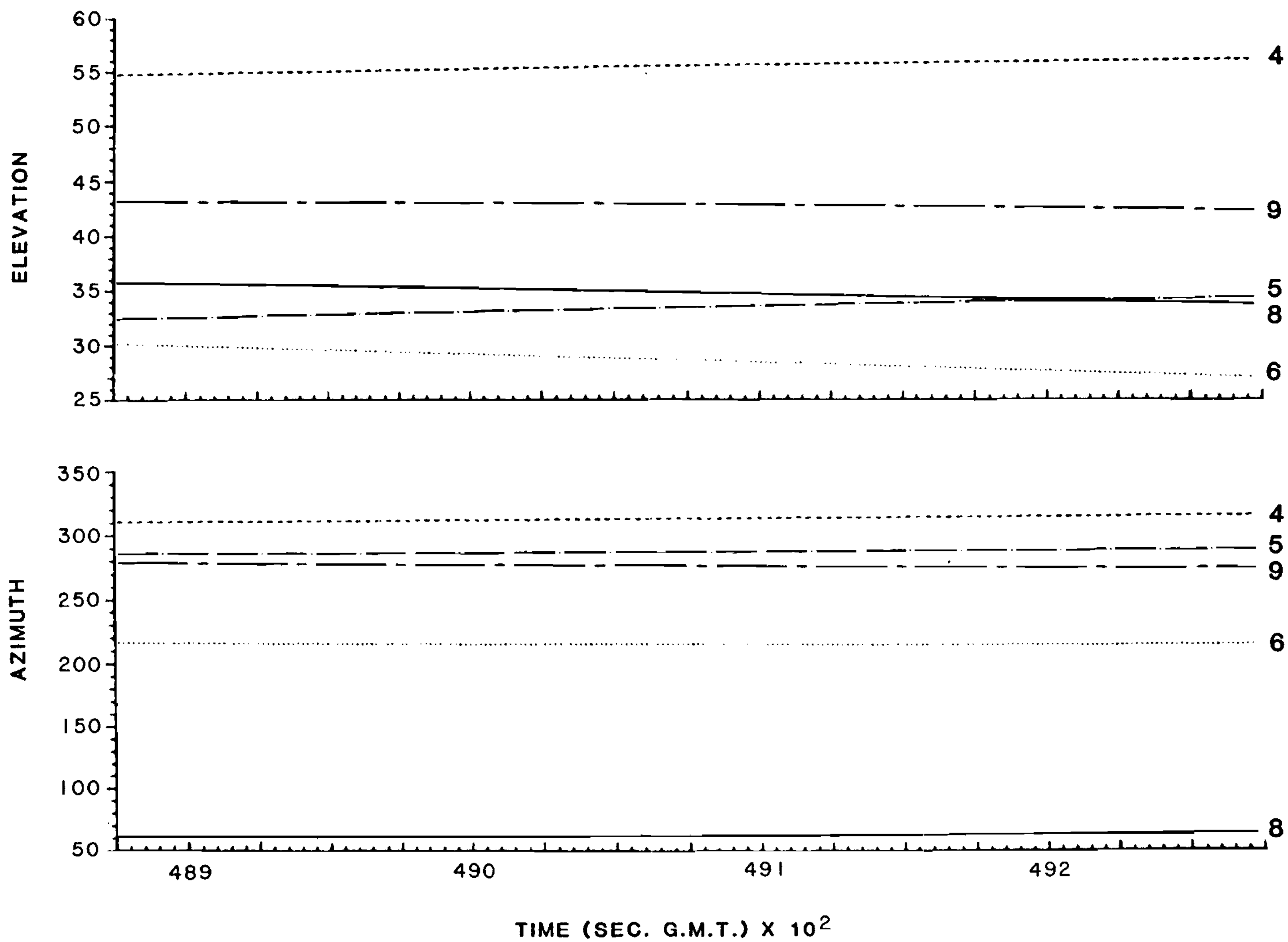

FIG. 4-42a. SATELLITE VISIBILITIES FOR MULTIPATH TEST, 25 JAN 83

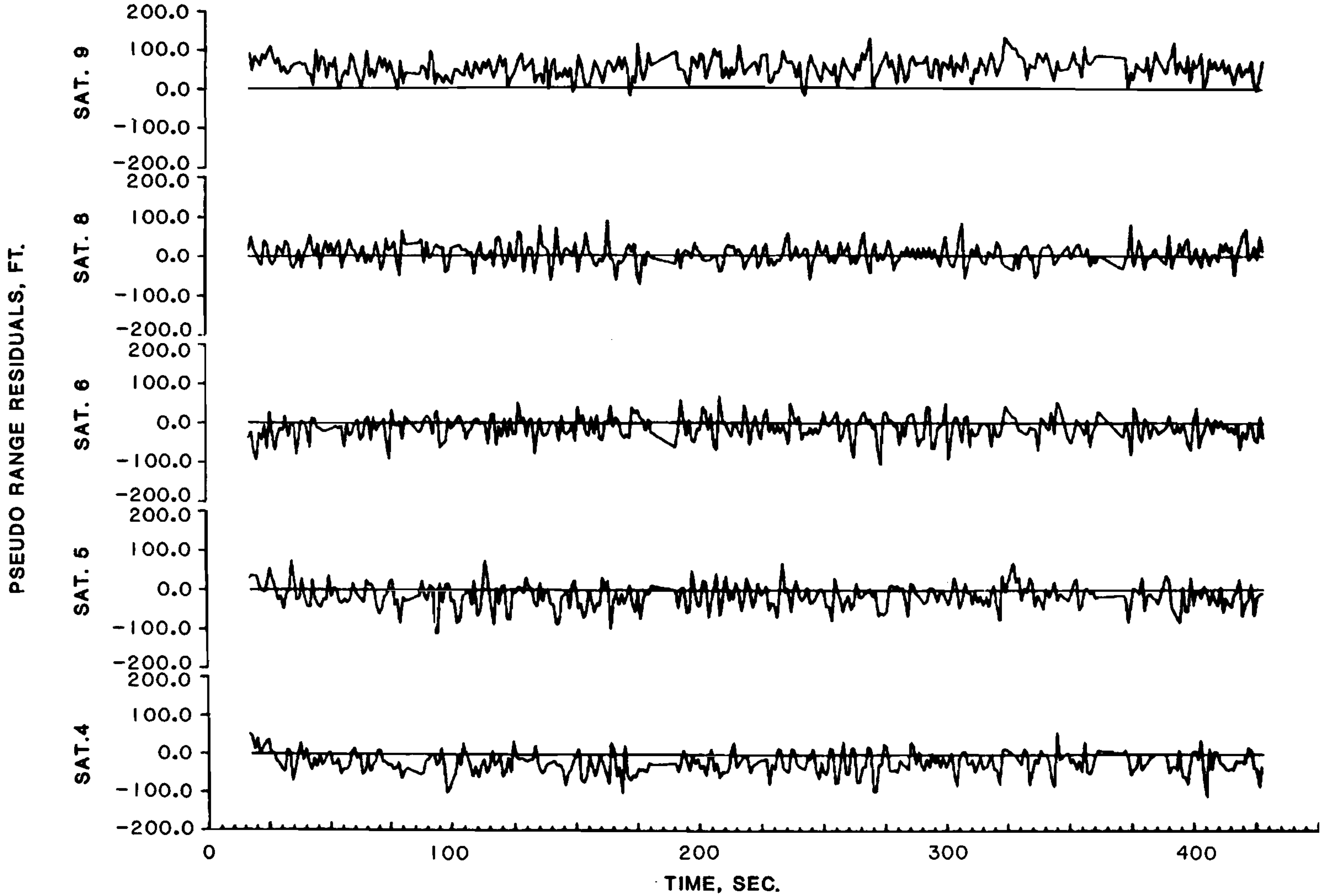

FIG. 4-42b. PSEUDO RANGE RESIDUALS FOR MULTIPATH TEST, 25 JAN 83

4.3.1.3 Summary of Engineering Test Results

Based on the engineering tests, several conclusions were reached. First, the accuracy of the GPS system exceeds the requirements of AC90-45A for two-dimensional area navigation in the enroute, terminal and non-precision approach modes. As expected, the system accuracy was not sufficient to meet all of the requirements of AC90-45A for precision (three-dimensional) ILS-type landings, although the performance was surprisingly close to meeting some of those requirements. The GPS accuracy also met the projected requirements for non-precision approach as stated in the Federal Radio Navigation Plan. Finally, the system performance exceeded the project goals for level and 30° bank turns.

The second conclusion from the engineering tests was that the system is not unacceptably affected by aircraft dynamics. The ability of the system to maintain position updates throughout 30° bank angle turns was demonstrated. It was also shown that the system maintained continuous position updates during momentary satellite outages during a turn.

A third conclusion was that the α-β tracker performance is adequate even though it does not attempt to model vehicle acceleration. Given the low airspeed and limited dynamics of general aviation aircraft, the use of the linear tracker appears justified. The test results show that the system accuracy remains well within the horizontal accuracy requirements of AC90-45A.

A final conclusion from the engineering tests was that multipath interference did not appear to have a significant effect on system performance Despite specific tests designed to produce multipath effects, no pseudo-range errors occurred which could be attributed to multipath.

4.3.2 Operational Flight Tests

Upon completion of the engineering flight tests, a series of operational flights were conducted to test the performance of the system as an area navigator. These operational tests were conducted in three different areas representing various airport types likely to be encountered by general aviation aircraft. The areas were:

- Burlington International Airport - Burlington, Vt.
- Logan International Airport - Boston, MA.
- Hanscom Field - Lexington - Manchester Airport - Manchester, NH.

The tests at the Burlington, Vt. airport were designed to determine if a GPS navigator can operate in an area surrounded by mountainous terrain. The tests at Logan International were made to verify that GPS can be operated at an urban airport adjacent to large buildings. The flights in the Hanscom Field/Manchester Airport area were designed to verify the correct performance of the GPS navigation system in typical general aviation operations.

4.3.2.1 Burlington, Vt. Tests

The approach patterns to Burlington International airport are shown in Fig. 4-43. There are two non-precision approaches to the airport: an NDB approach to Runway 15 and a VOR approach to Runway 1. The airport is located between two mountain ranges, the Green Mountains at about 20 miles to the east and the Adirondack Mountains at about 25 miles to the southwest.

For the Burlington operational tests, the GPS test aircraft was flown from Hanscom Field in Massachusetts to Burlington International on 27 January 1983. A series of non-precision approaches were made using both the VOR and NDB approach procedures. Both the BTV VOR and the BT NDB were entered as waypoints in the GPS navigation software for this purpose.

4.3.2.1.1 Enroute Performance

During the first portion of the test flight, the aircraft was enroute to the Burlington VOR from Hanscom Field as shown in Fig. 4-44. At the beginning of run 2a the aircraft was 70 nautical miles away from the VOR on the 151° radial. At the altitude the aircraft was flying (4250 feet), the VOR-DME was unusable for ranges greater than 30 nm on this radial.

Figure 4-45 shows the altitude and ground speed for run 2a as estimated by the position software. Fig. 4-46 shows the GPS satellite azimuth and elevation during the run. Note that only four satellites were visible during this period. The satellite carrier-to-noise-density values are shown in Fig. 4-47. Note at the beginning of the run that SV9 has a C/N_0 about 5 dB lower than the other SVs. At this time, SV9 was at 8° elevation angle, but still had a substantial loss-of-lock margin of about 12 dB.

The pseudo-range residuals for 2a are shown in Fig. 4-48. The residuals are seen to remain small, typically less than $\pm$ 50 feet, over most of the run. There are, however, three instances where the residuals became large: once for SV9 and twice for SV4. Analysis of the data showed that these perturbations occured when the position software was unable to collect a valid pseudo-range measurement from the receiver. Due to an apparent software bug, the failure to collect a valid measurement caused the next measurement to be improperly time-tagged. The improper time-tagging, in turn, caused the range to the satellite to be calculated incorrectly. The incorrect range calculation then caused the pseudo-range residual to be in a error by about 500 feet.

It is significant that a pseudo-range error of this magnitude has only a small effect on the navigation accuracy; this is due to two reasons. First, the error is short-term, lasting for a maximum of two navigation cycles. Second, the batch least-squares method minimizes the effect of large residuals on the position fix. In this case, the 500 foot residual error caused a position fix error of only about 100 feet. A position estimate error of this magnitude is not discernable on the pilot course deviation display. It should also be noted that pseudo-range reasonableness check in the position software rejects any residual greater than 1000 feet, preventing a bad position fix from being generated.

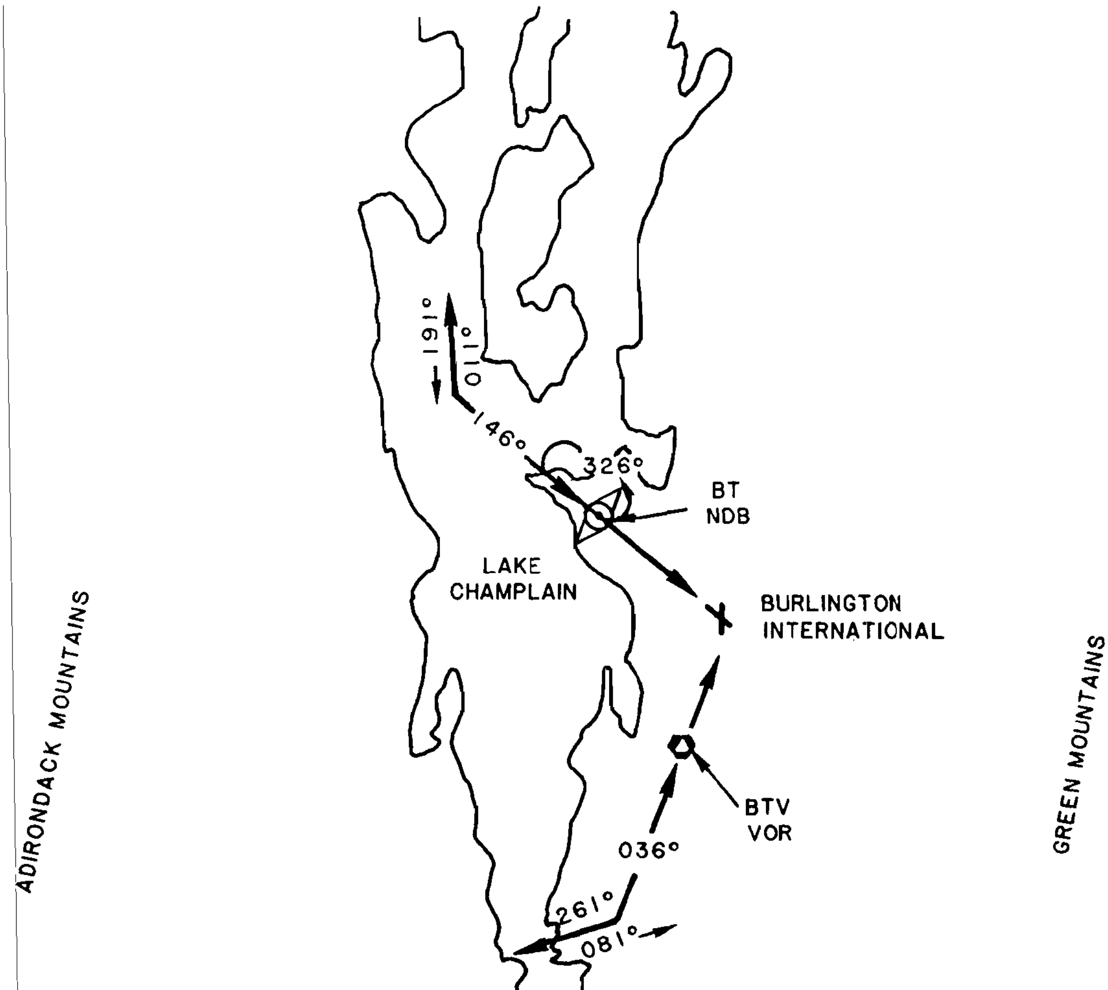

FIG. 4-43. BURLINGTON, VT APPROACHES: NDB RWY 15 AND VOR RWY 1

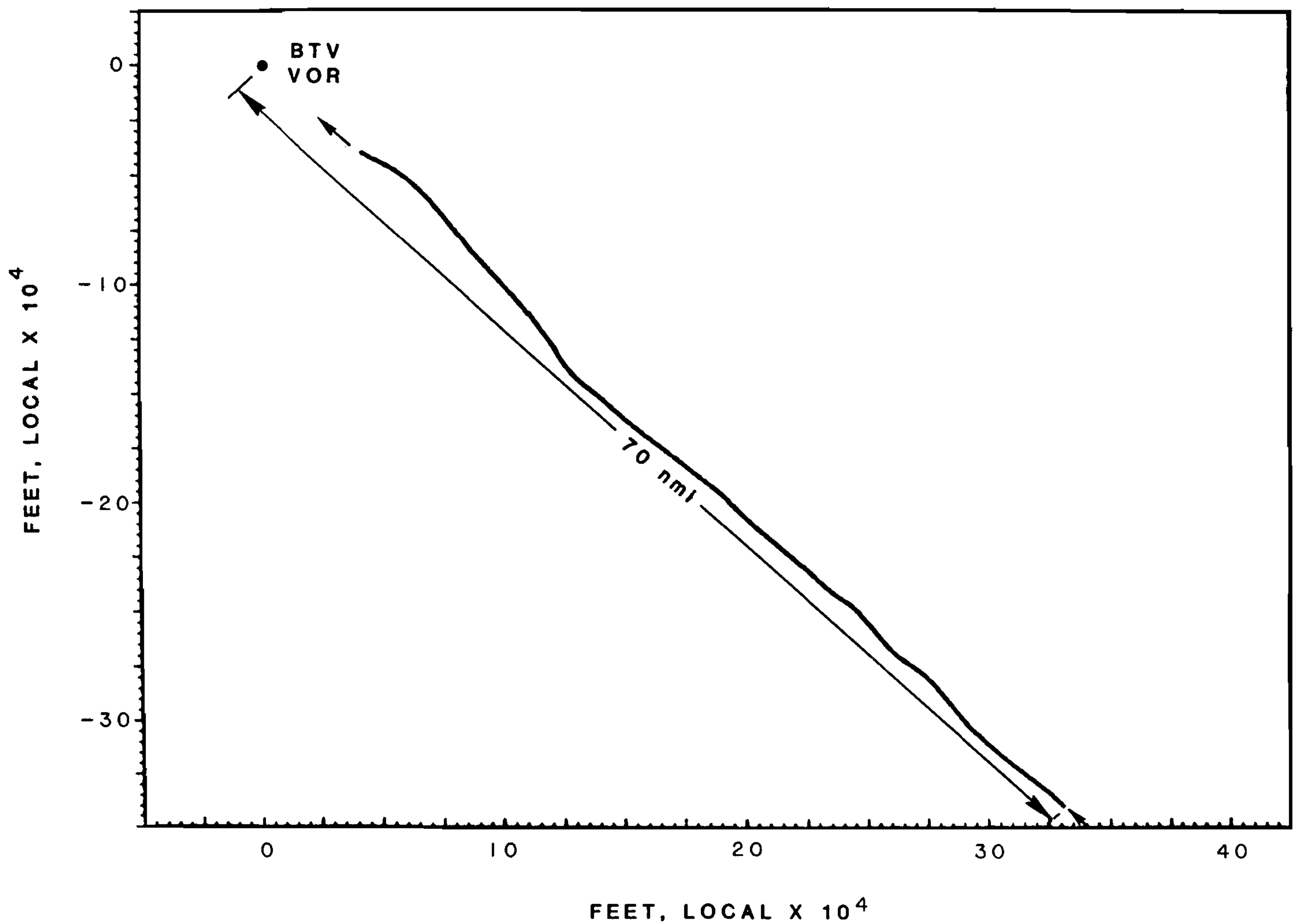

FIG. 4-44. BURLINGTON, VT OPERATIONAL TEST, RUN 2a 27 JAN 83

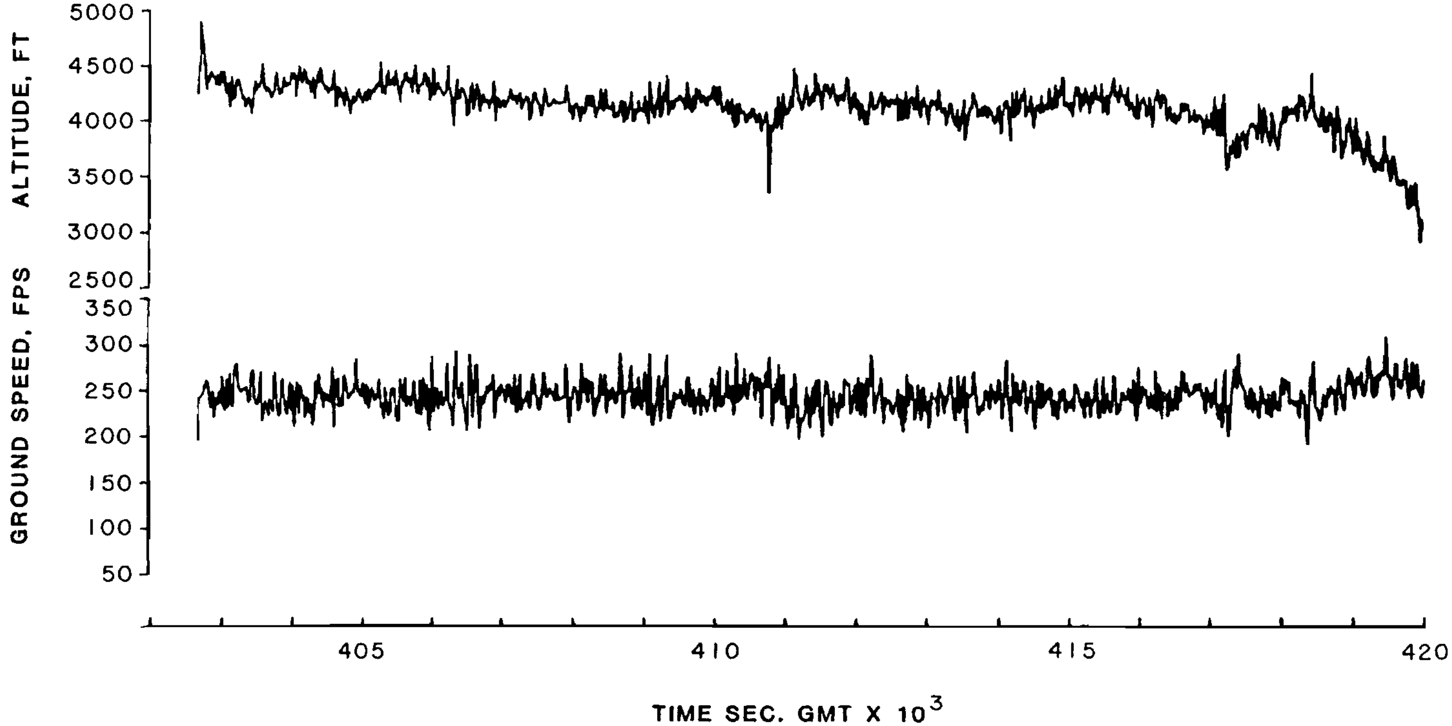

FIG. 4-45. ALTITUDE AND GROUND SPEED, RUN 2a, 27 JAN 83

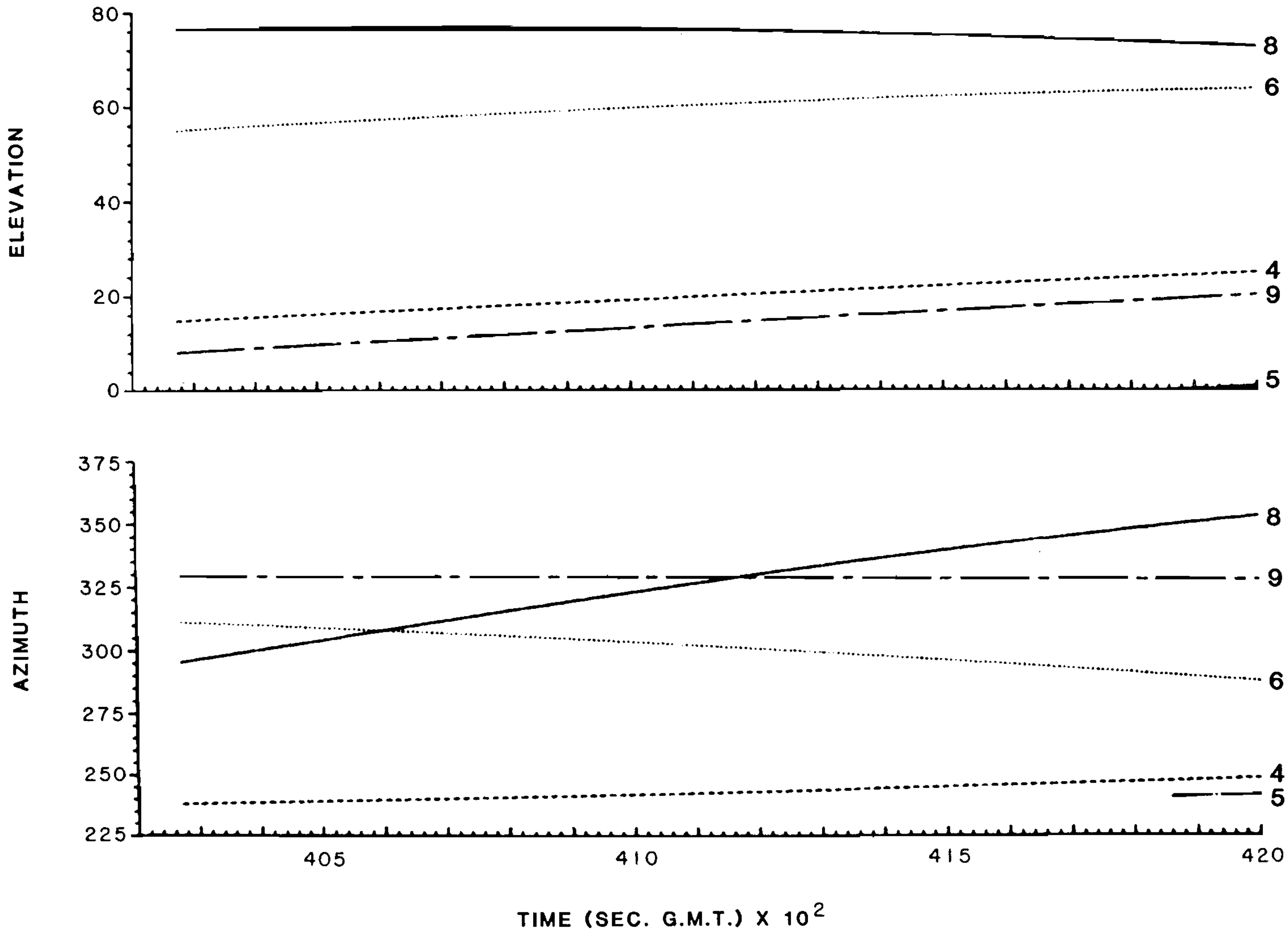

FIG. 4-46. GPS SV POSITIONS

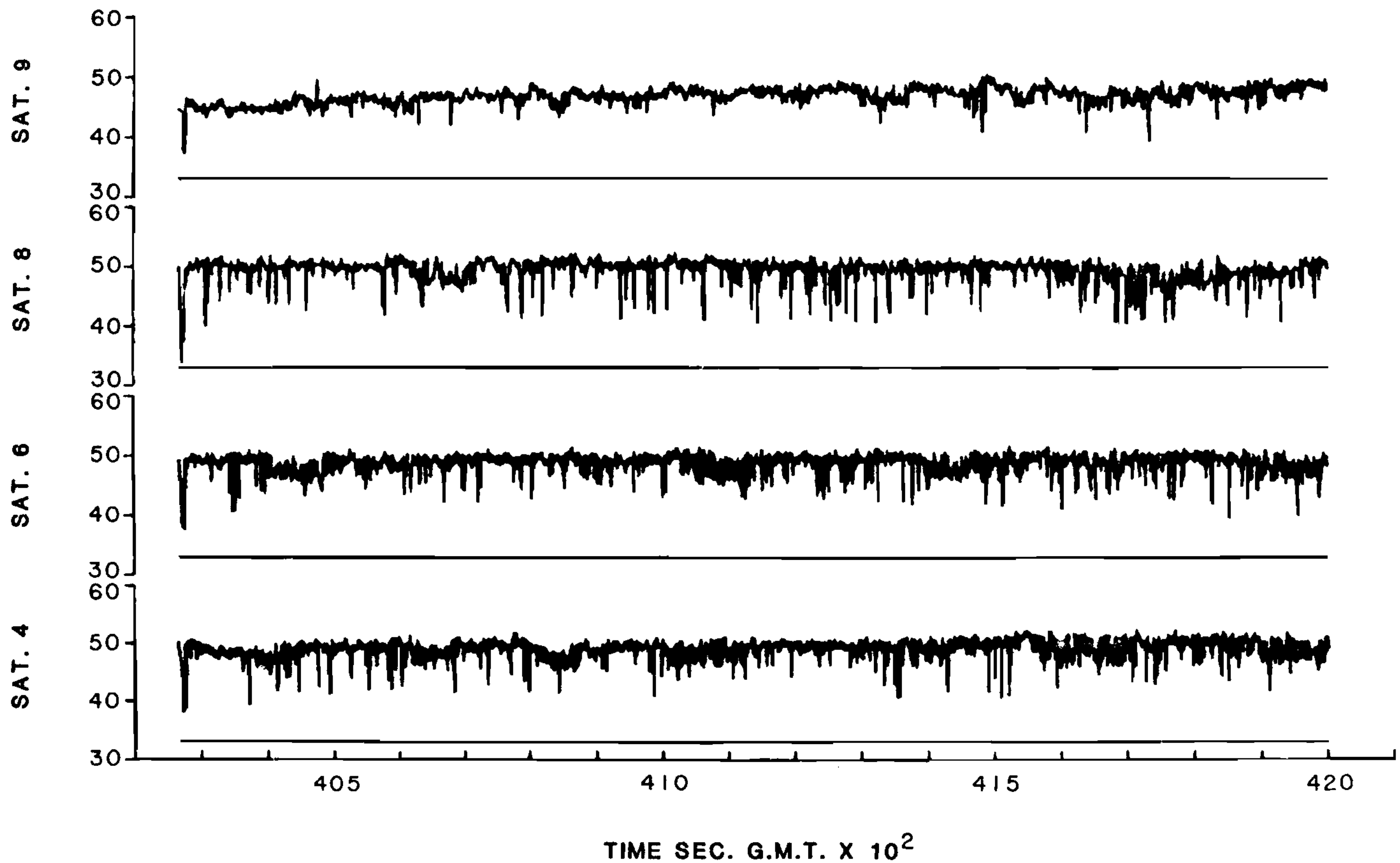

FIG. 4-47. SATELLITE C/NO. VALUES, RUN 2a, 27 JAN 83

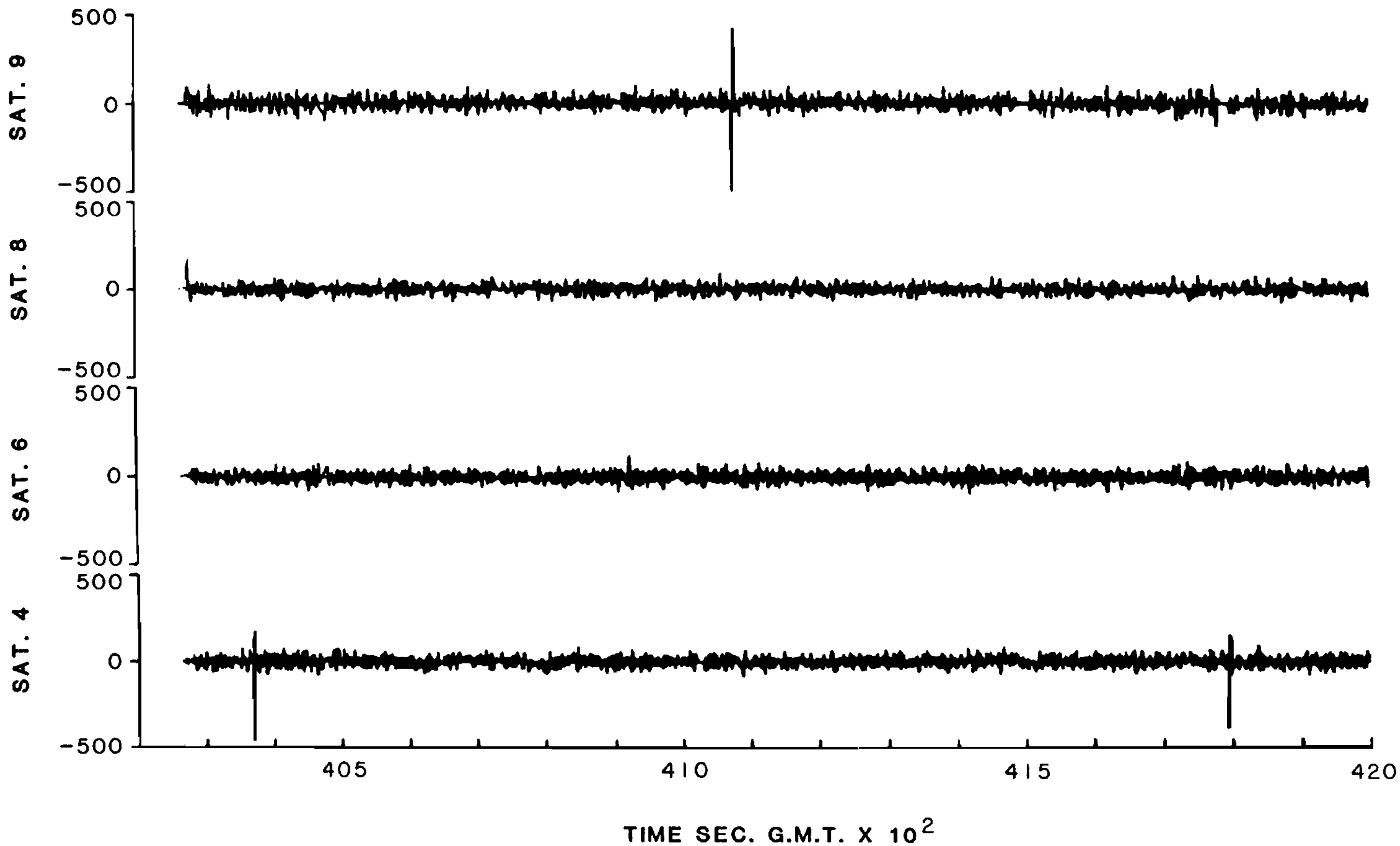

FIG. 4-48. PSEUDO RANGE RESIDUALS, RUN 2a, 27 JAN 83

The results of this test show the ability of the GPS system to perform enroute navigation in mountainous terrain with a minimum set of four satellites. It is of particular interest that the GPS was able to significantly outperform VOR in this mountainous area. GPS was able to provide equivalent navigation service 70 nmi away from the VOR while the VOR itself is unusable at ranges greater than 30 nmi. This performance advantage of GPS results from the fact that the GPS satellites are above the horizon, while VOR is ground-based and much more susceptible to terrain blockage.

4.3.2.1.2 VOR Approach

Runs 2b and 3b consist of non-precision VOR approaches to the Burlington airport. Figure 4-49 shows the ground track for run 2b. The aircraft first intercepted the VOR on the 151° radial, then proceeded outbound on the 216° radial and performed a procedure turn. After intercepting the VOR on the 36° radial, the aircraft was then flown to the field for a low approach at runway 33. Some gaps will be noted in the ground track; the gaps are due to data recording problems rather than interruptions in the position solution.

Figure 4-50 shows the altitude and ground speed profiles for run 2b. Figure 4-51 shows the satellite visibilities for the run. Although five satellites are shown, this run was still navigating with four satellites (SVs 4,6,8 and 9). The satellite C/N_0 values are shown in Fig. 4-52. It is seen that the satellite signal strength drops by as much as 10 dB in some turns, but always remains above the 33 dB-Hz loss-of-lock threshold. Figure 4-53 shows the pseudo-range residuals; note the increases in the residuals corresponding to the turns. There are also some large residuals at the end of the run for SV4; these jumps result from the software bug previously described.

The ground track for run 3b is shown in Fig. 4-54. For this run, the aircraft intercepted the VOR then flew the 216° outbound radial and made the procedure turn as before. After intercepting the VOR, an OBS setting of 36° from the waypoint was flown. It was found, however, that this resulted in a 42° course from the waypoint, taking the aircraft to the east of the end of runway 33. Because of air traffic control considerations, a right downwind approach was then flown to runway 15 and a landing made for refueling.

Post-flight analysis revealed an error in the navigation software which had the result of biasing the OBS setting by 6°, explaining the incorrect course of 42° commanded by the navigation software. This error was corrected for subsequent operational flight tests.

Figure 4-55 shows the altitude and ground speed profiles for run 3b. Note that during the last portion of the run, the aircraft is on the ground and taxiing around the airport. The satellite visibilities are shown in Fig. 4-56. All five satellites were in track during this run, including SV5 which was initially at 10° elevation angle. The satellite C/N_0 values are shown in Fig. 4-57. Note that SV5, the low elevation angle satellite, was dropped on two occasions during the run. These occasions correspond to the procedure turn and the base leg turn, at which times the aircraft was banked

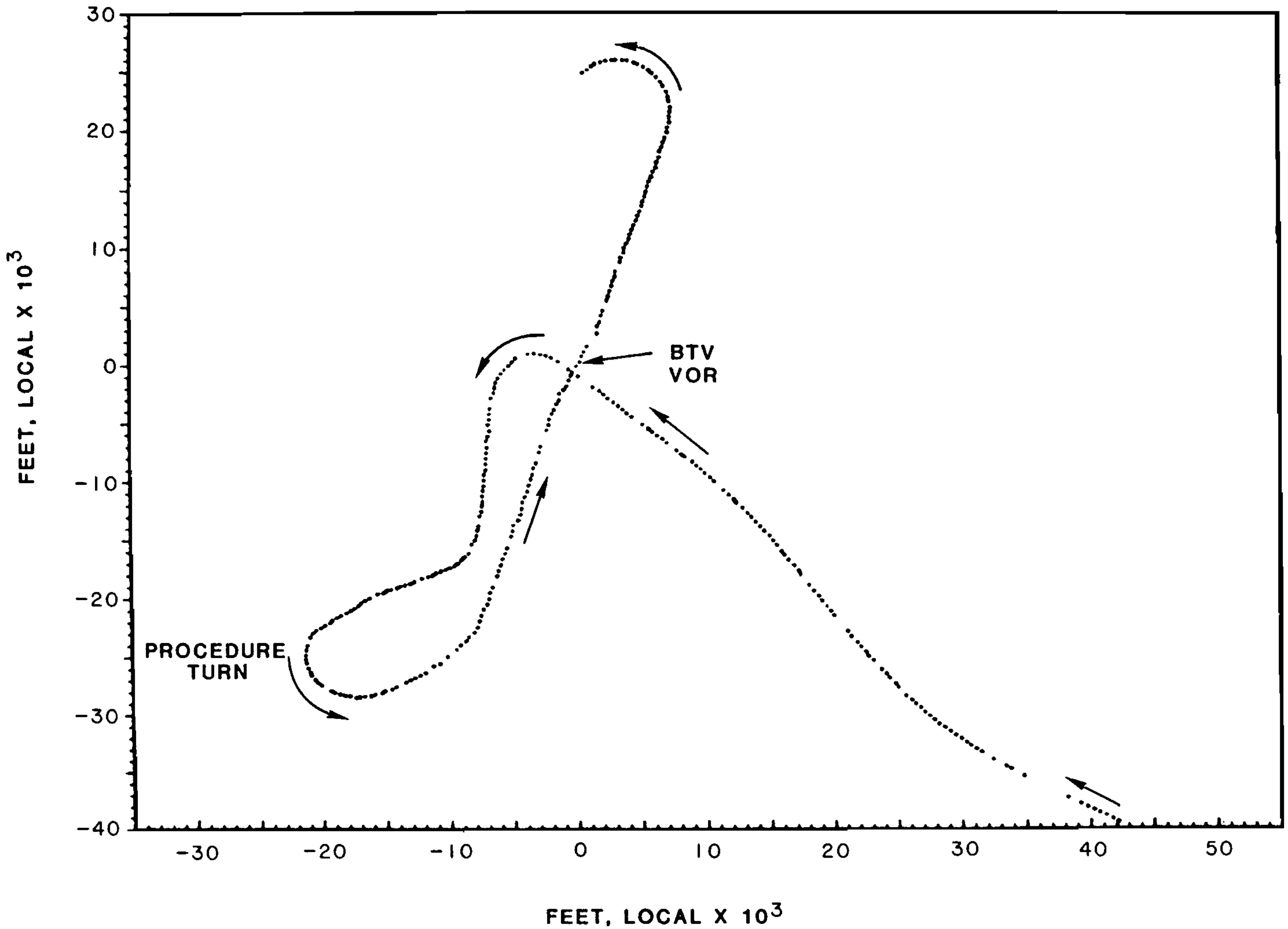

FIG. 4-49. BURLINGTON, VT VOR APPROACH, 27 JAN 83

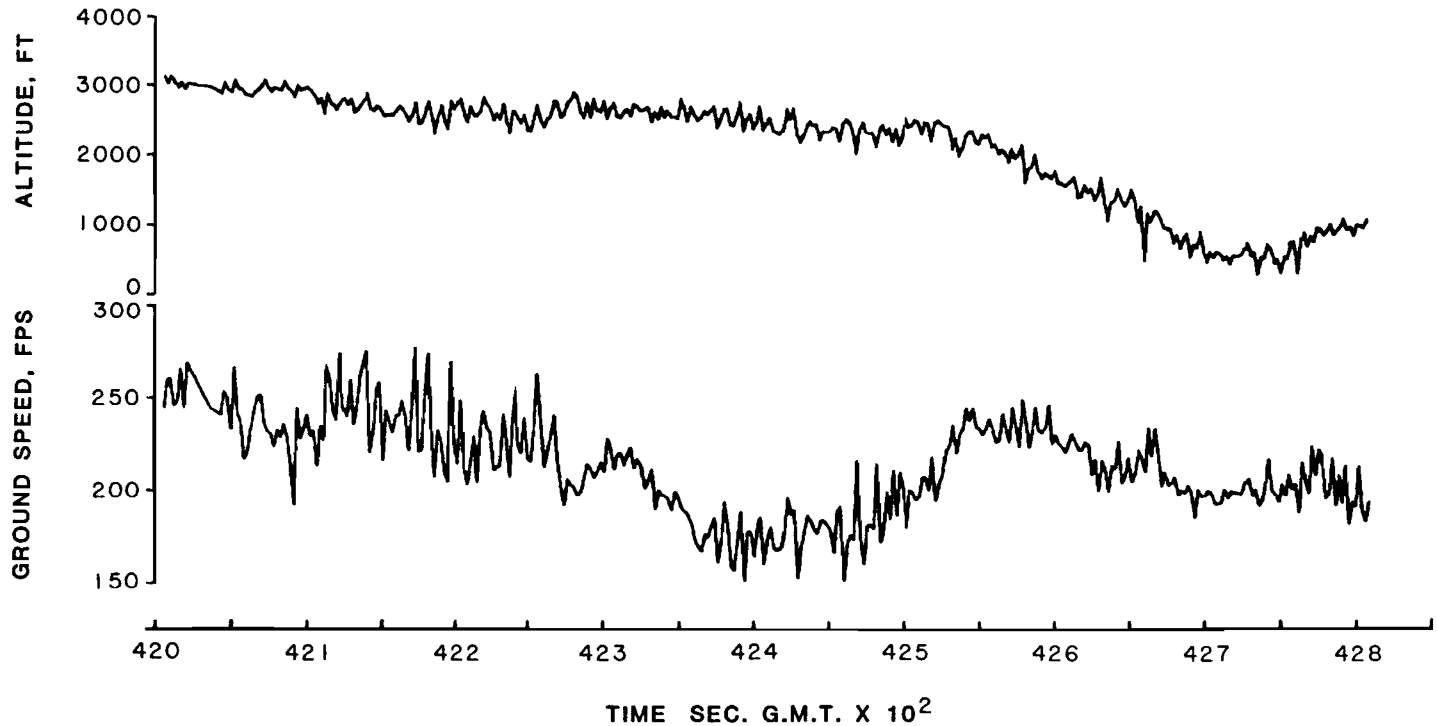

FIG. 4-50. ALTITUDE AND GROUND SPEED, RUN 2b, 27 JAN 83

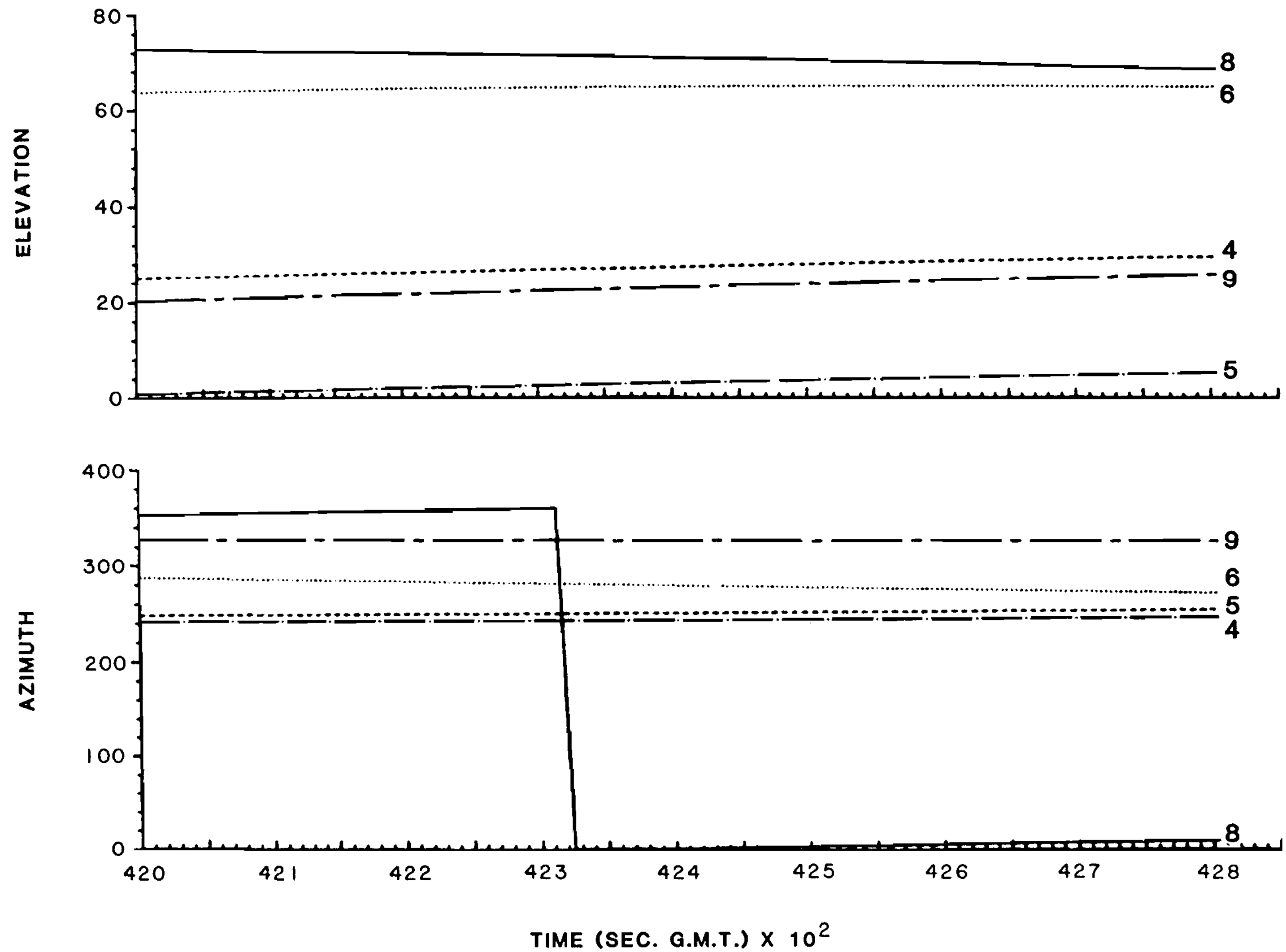

FIG. 4-51. SATELITE VISIBILITIES, RUN 2b, 27 JAN 83

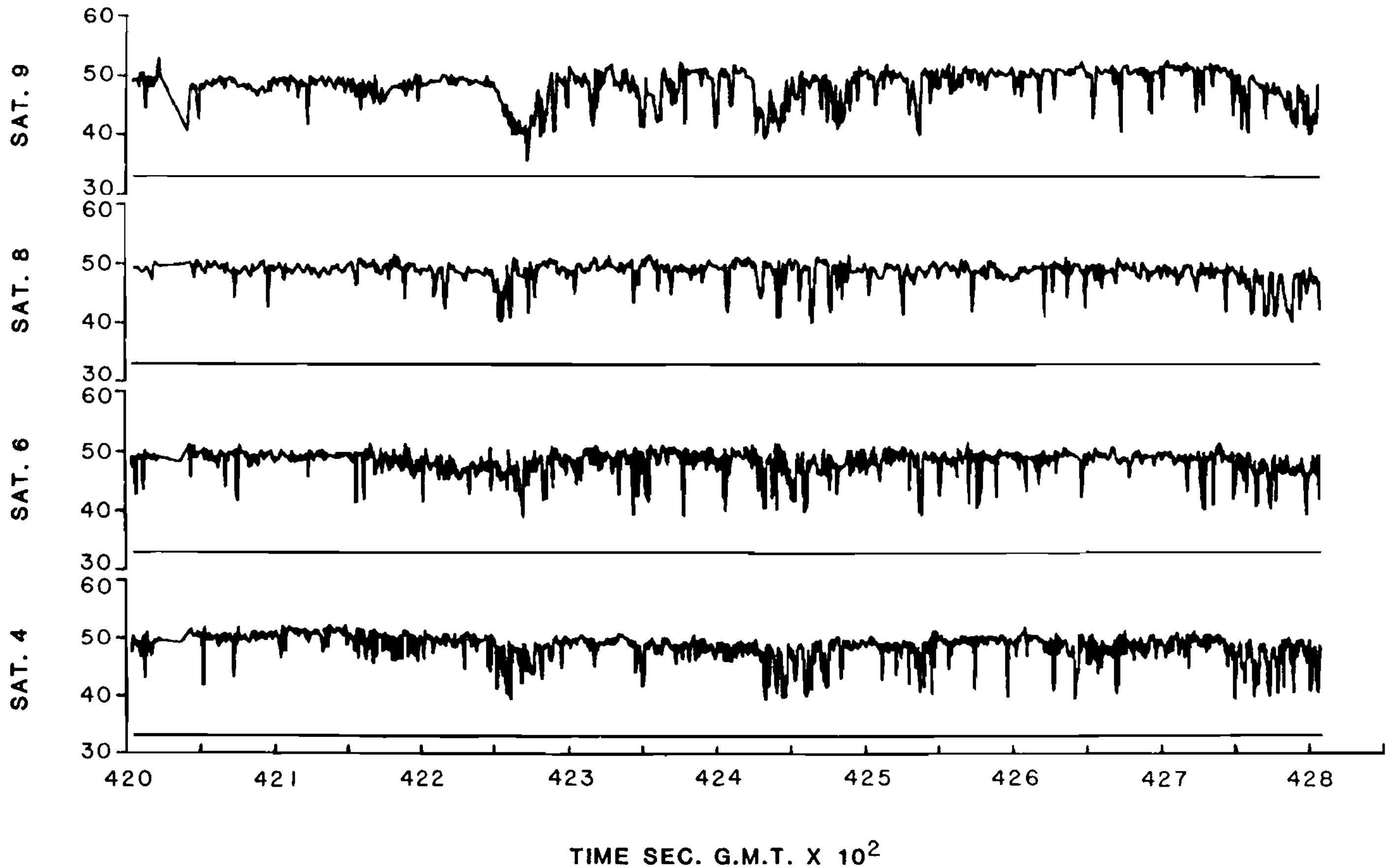

FIG. 4-52. SATELITE C/NO. VALUES, RUN 2b, 27 JAN 83

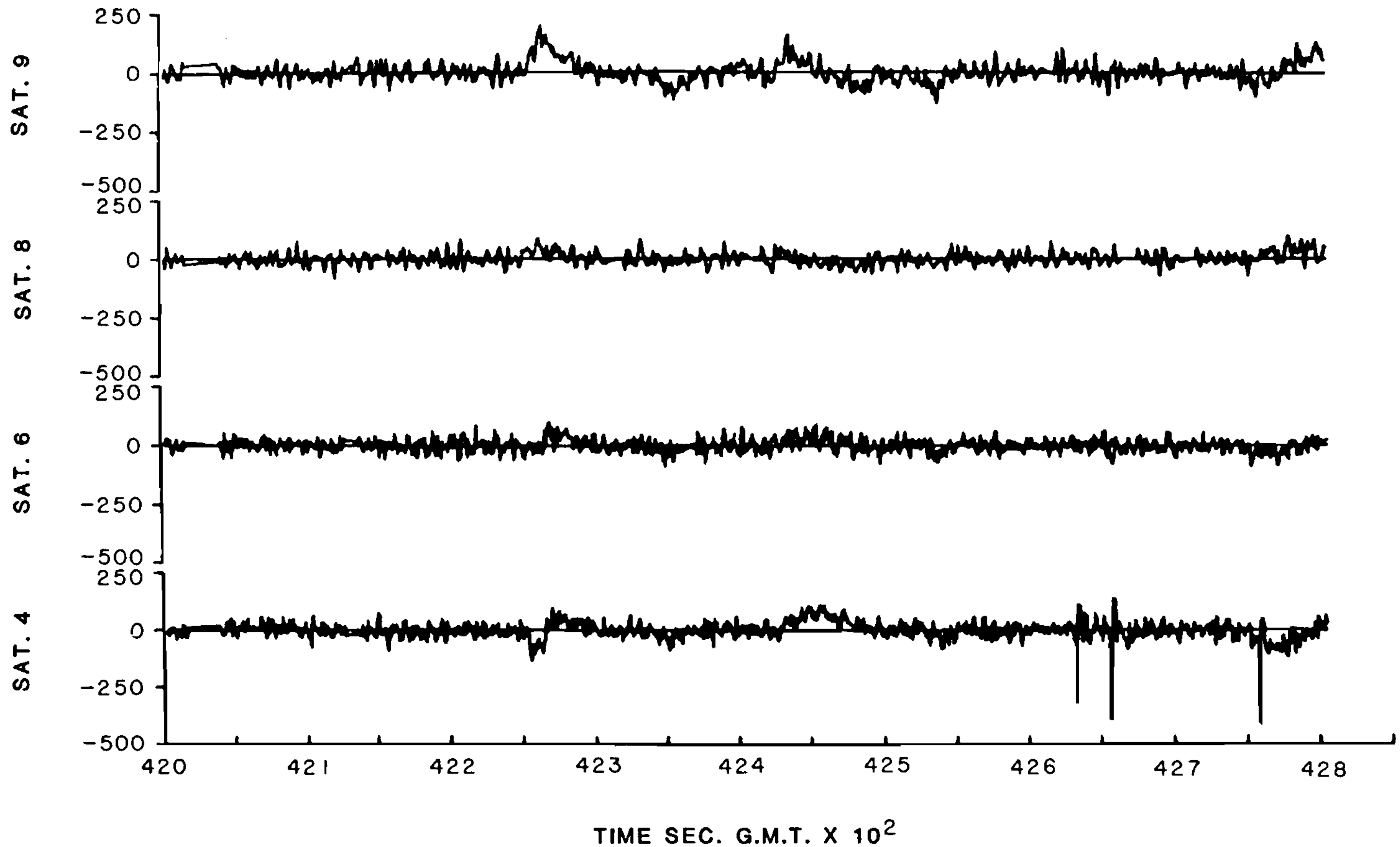

FIG. 4-53. PSEUDO-RANGE RESIDUALS, RUN 2b, 27 JAN 83

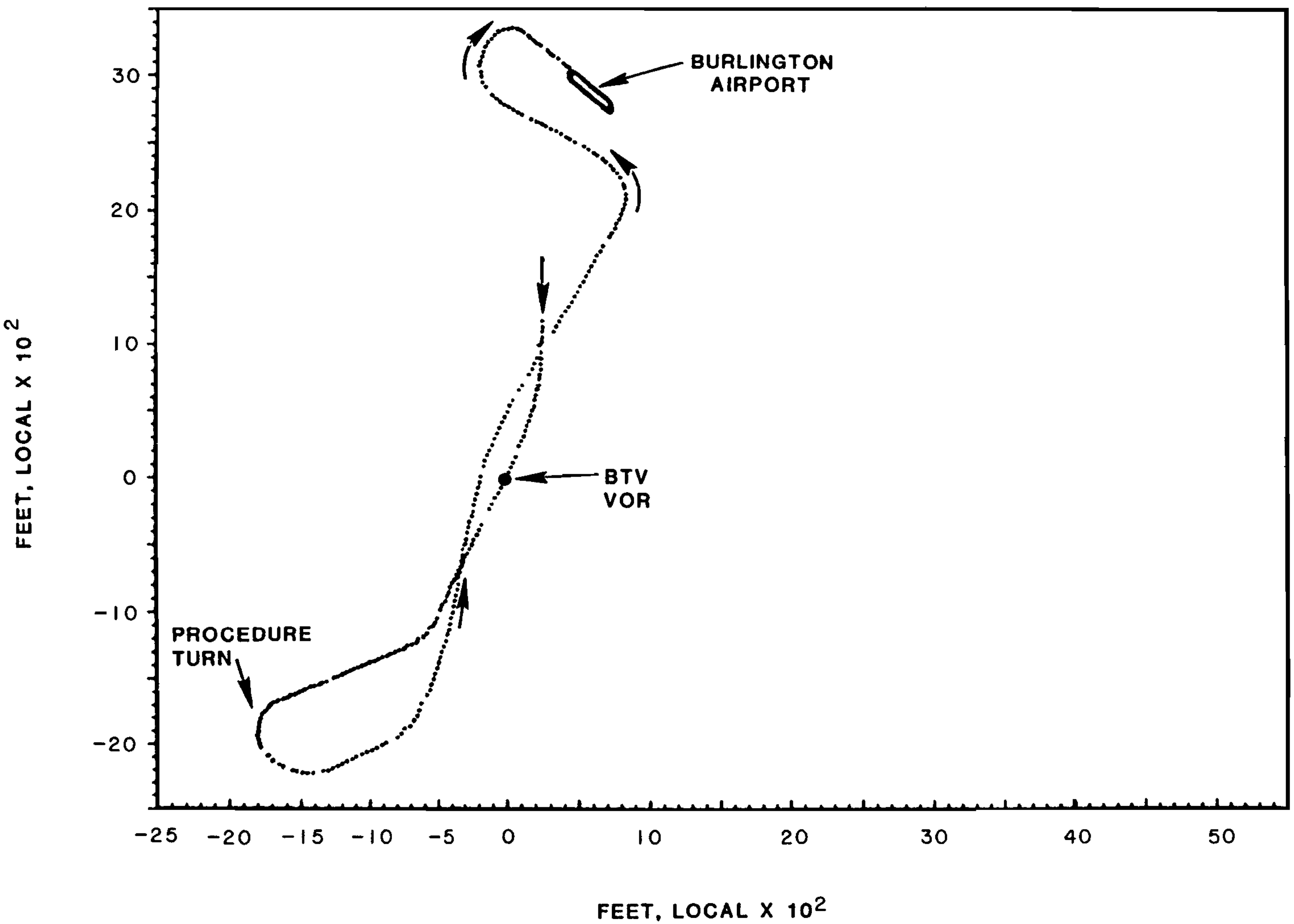

FIG. 4-54. BURLINGTON, VT VOR APPROACH, RUN 3b, 27 JAN 83

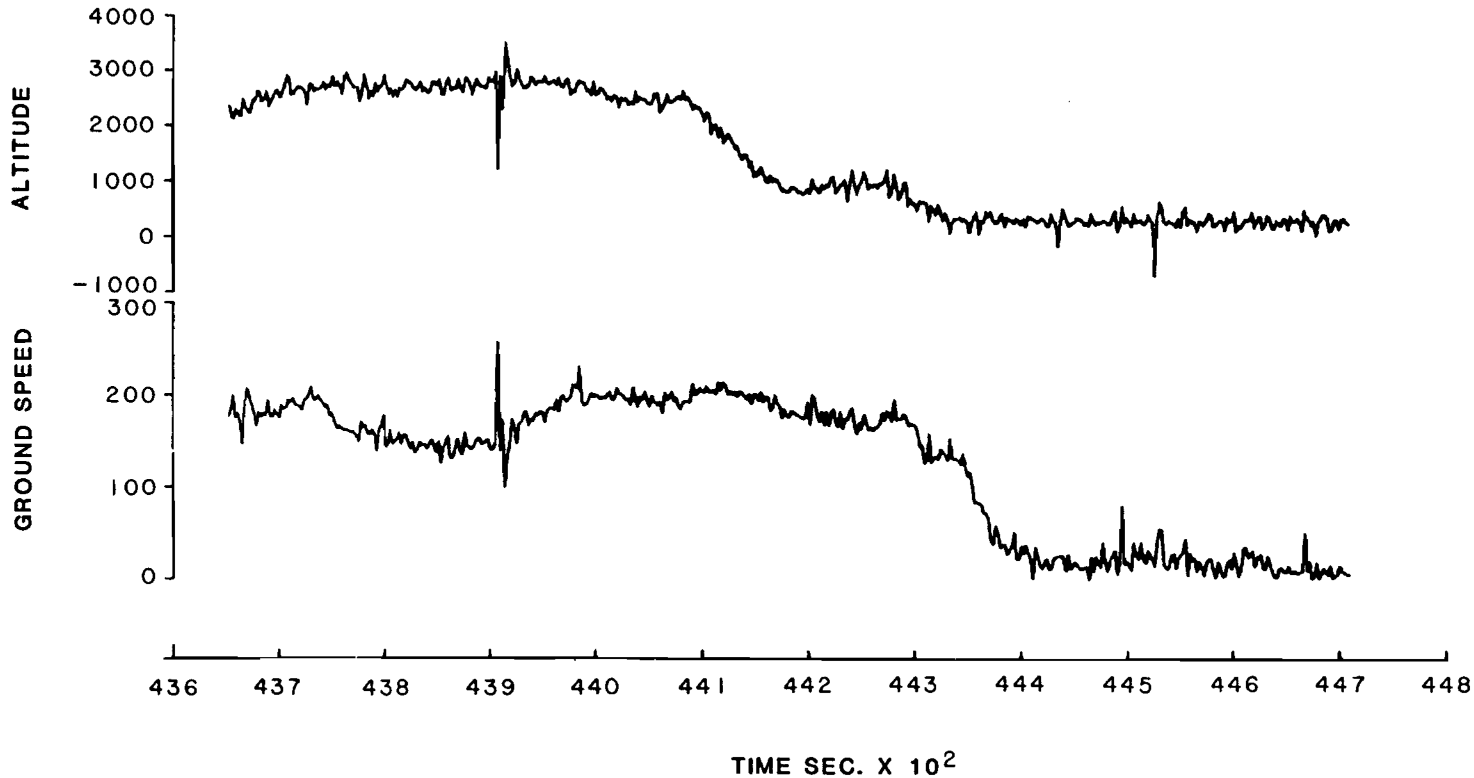

FIG. 4-55. ALTITUDE AND GROUND SPEED, RUN 3b, 27 JAN 83

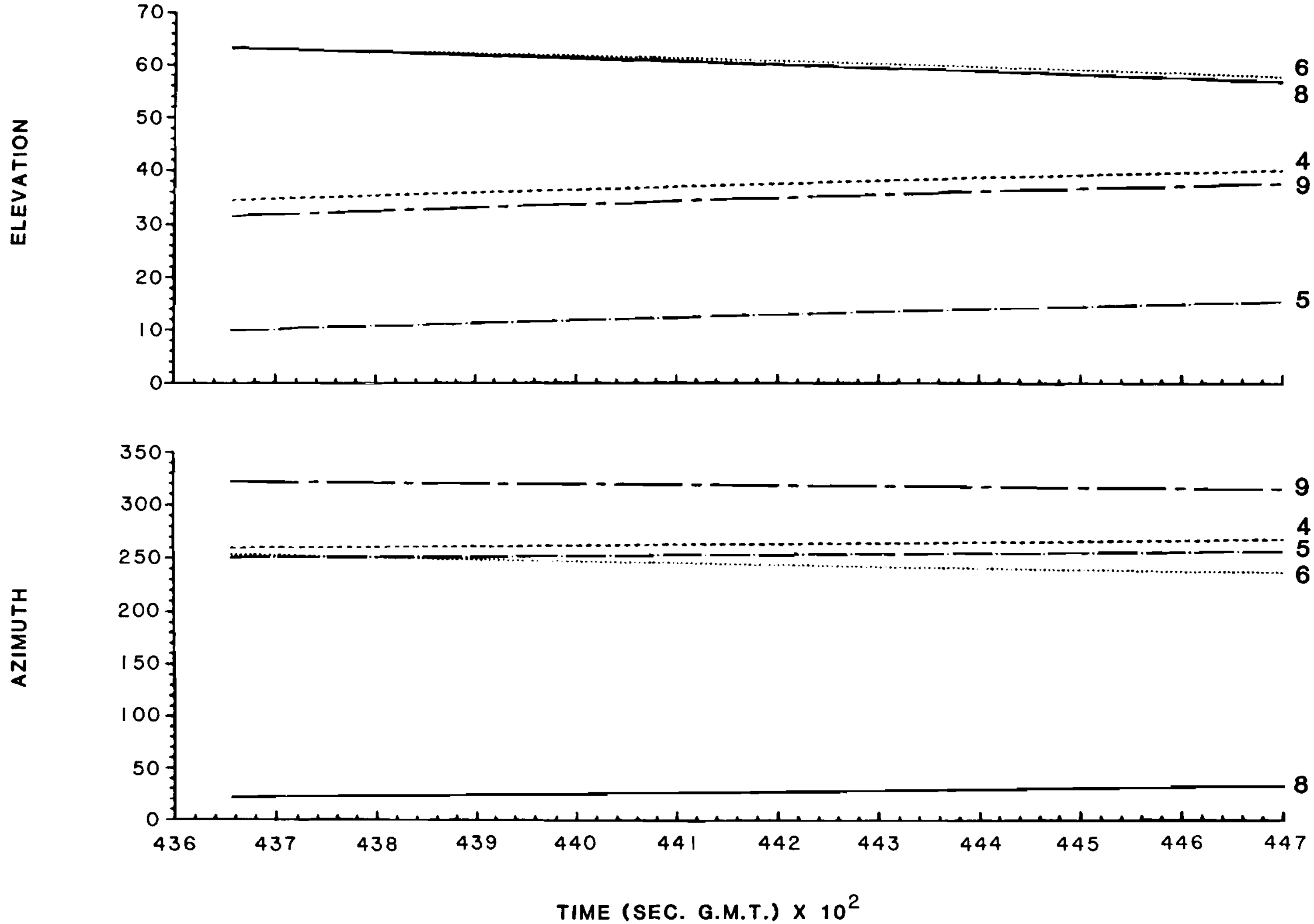

FIG. 4-56. SATELLITE VISIBILITIES, RUN 3b, 27 JAN 83

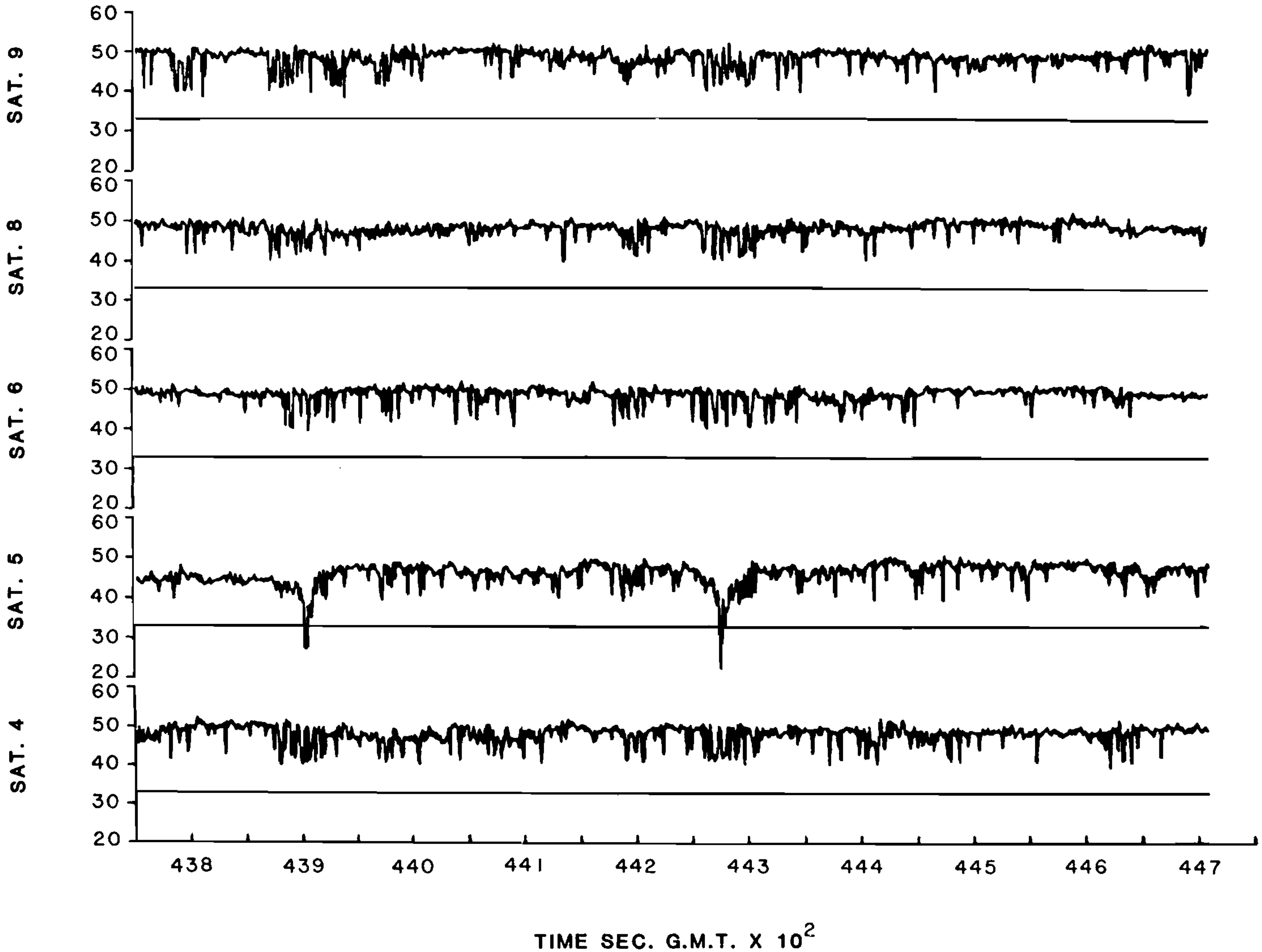

FIG. 4-57. SATELLITE C/NO. VALUES, RUN 3b, 27 JAN 83

away from SV5. The position solution is maintained continuously in these cases, however, since the other four satellites remained in track. This example again illustrates the importance of tracking all visible satellites rather than the minimum set of four.

Figure 4-58 shows the pseudo-range residuals for run 3b. It can be seen from the figure that there are a number of jumps in the pseudo-range residuals. Except for the two cases in which SV5 suffered a loss of lock, the jumps are all due to the position software problem discussed earlier. In this run, the position software appears to occasionally fail to collect a valid pseudo-range measurement before it is overwritten by the receiver with the next measurement. This problem is symptomatic of a lack of available CPU time in the position processor. The lack of CPU time is attributable in part to the large amount of engineering data being recorded by the system. The data recording function introduces an overhead which would not be present in a production system.

It can also be noted from Fig. 4-58 that there is a substantial bias (~75 feet) on the SV4 residuals and a smaller bias in the opposite direction on SV6. The source of this bias is not known, but it may be due to aging ephemeric data from SV4. Unlike the other satellites, SV4 was operating on a crystal oscillator because its atomic clocks had failed. Consequently, SV4's clock drift is not well modelled by the ephemeric data from the satellite. The bias is clearly not due to multipath because it does not vary with altitude, remaining constant throughout the run.

The results of runs 2b and 3b show that GPS can be used to simulate a VOR approach in a mountainous area. Furthermore, despite a position software bug that introduced pseudo-range jumps, the system maintained reliable operation throughout standard-rate turns even during the temporary loss of a low-angle satellite. Also, the system kept a low (10°) elevation angle satellite in track during level flight.

4.3.2.1.3 NDB Approach

The ground track for two NDB approaches to runway 15 (run 4) is shown in Fig. 4-59. For this run, the aircraft took off from runway 15 and proceeded outbound on the 326° radial from the NDB. After a procedure turn, the aircraft made a non-precision approach on the 146° radial. A missed approach was executed on advice from air-traffic control and a second approach initiated. At this point, the run terminated due to a momentary aircraft electrical power interruption.

The altitude and ground speed profiles for run 4 are shown in Fig. 4-60. The satellite visibilities are shown in Fig. 4-61. Figure 4-62 shows the measured satellite C/N_0 values for the turn. Note the large number of losses of lock for SV6 during the run. Examining the satellite elevation, aircraft altitude and topography of the region, it is clear that these dropouts are not due to terrain blockage. Examination of the data shows that SV6 was dropped once temporarily during the takeoff due an aircraft power surge. Lock was reestablished for the satellite in the first SV6 dwell slot in the navigation cycle but not in the second. As a result, the satellite C/N_0 estimates for the second dwell slot are not reliable, but were inadvertenly plotted.

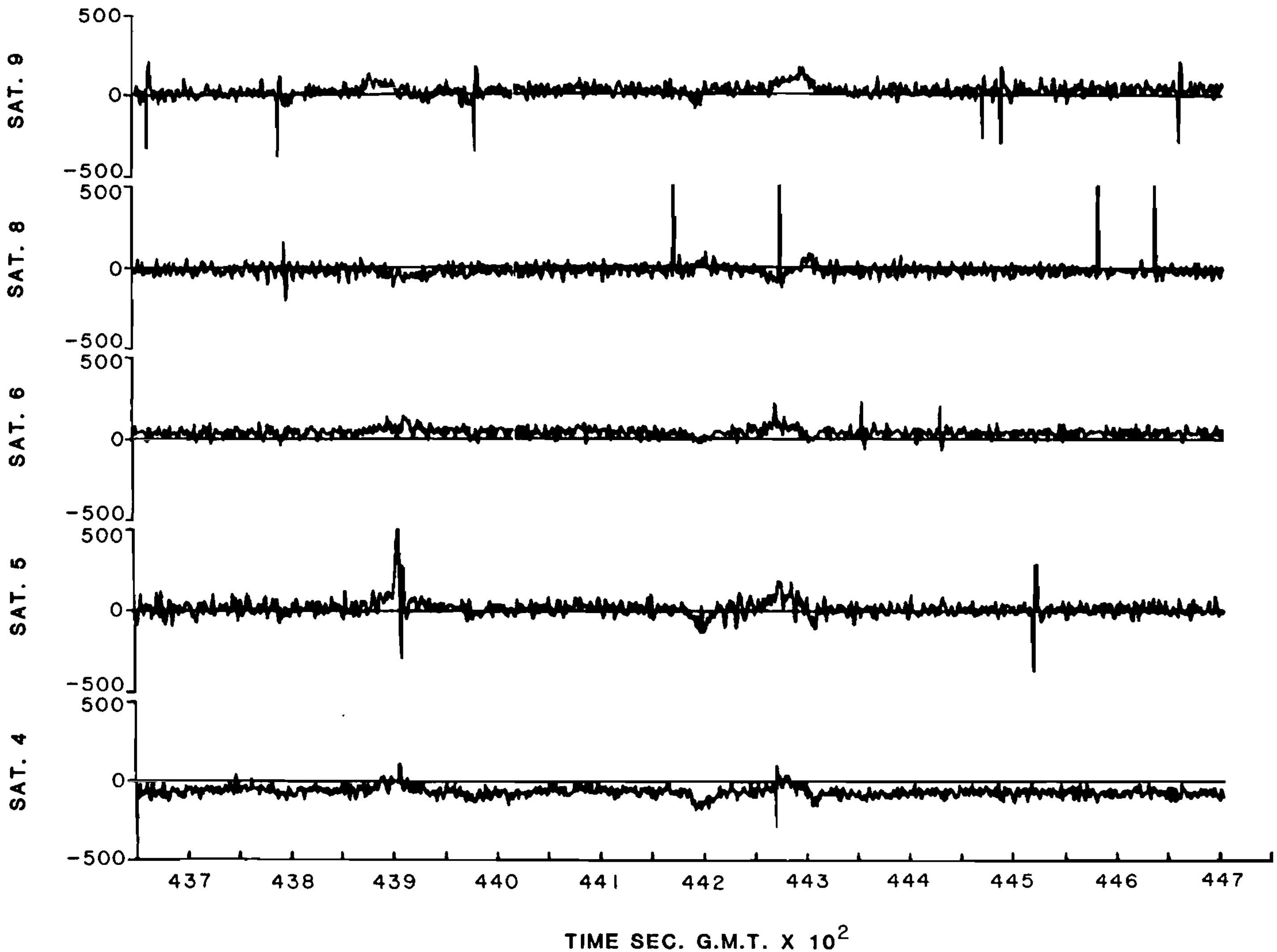

FIG. 4-58. PSEUDO-RANGE RESIDUALS, RUN 3b, 27 JAN 83

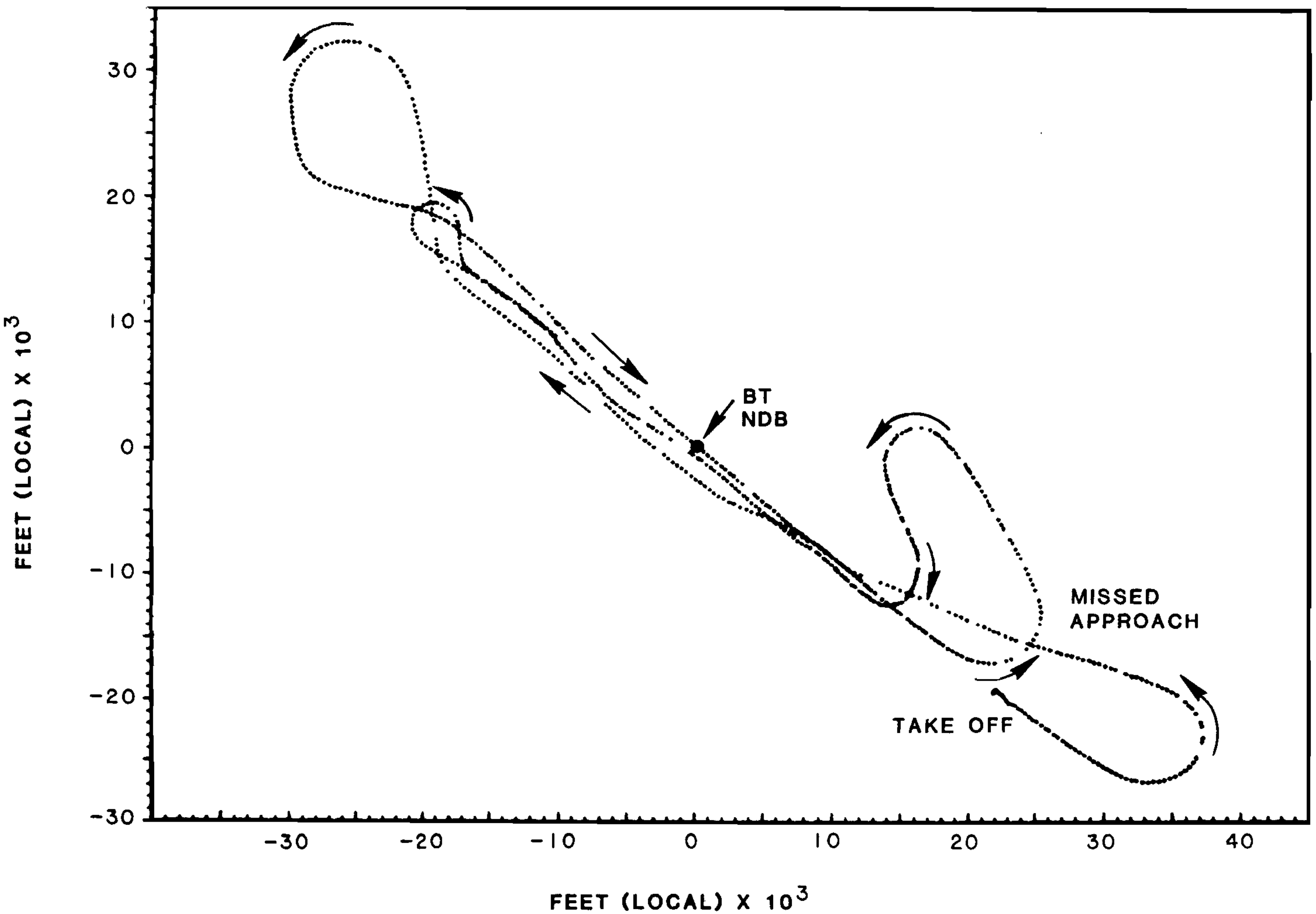

FIG. 4-59. BURLINGTON, VT NDB APPROACH, RUN 4, 27 JAN 83

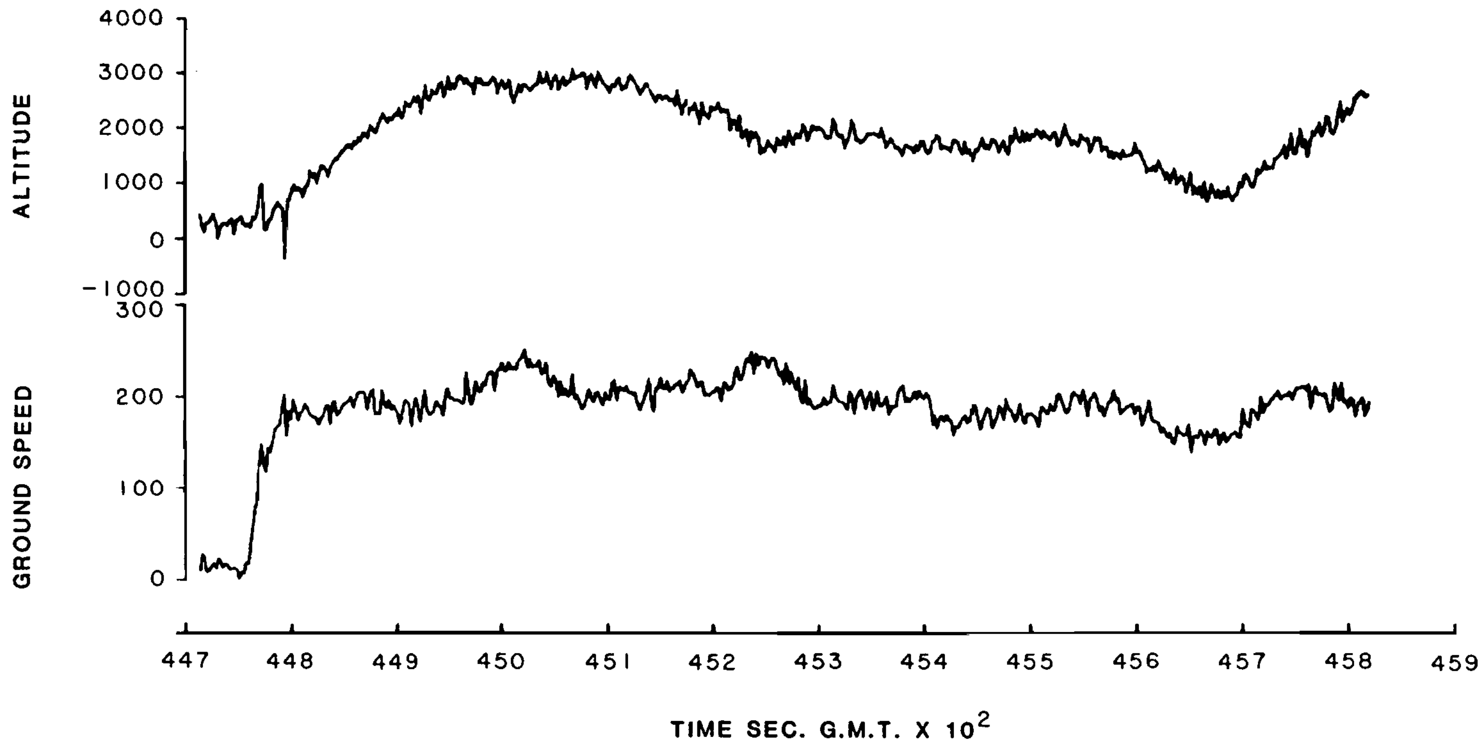

FIG. 4-60. ALTITUDE AND GROUND SPEED, RUN 4, 27 JAN 83

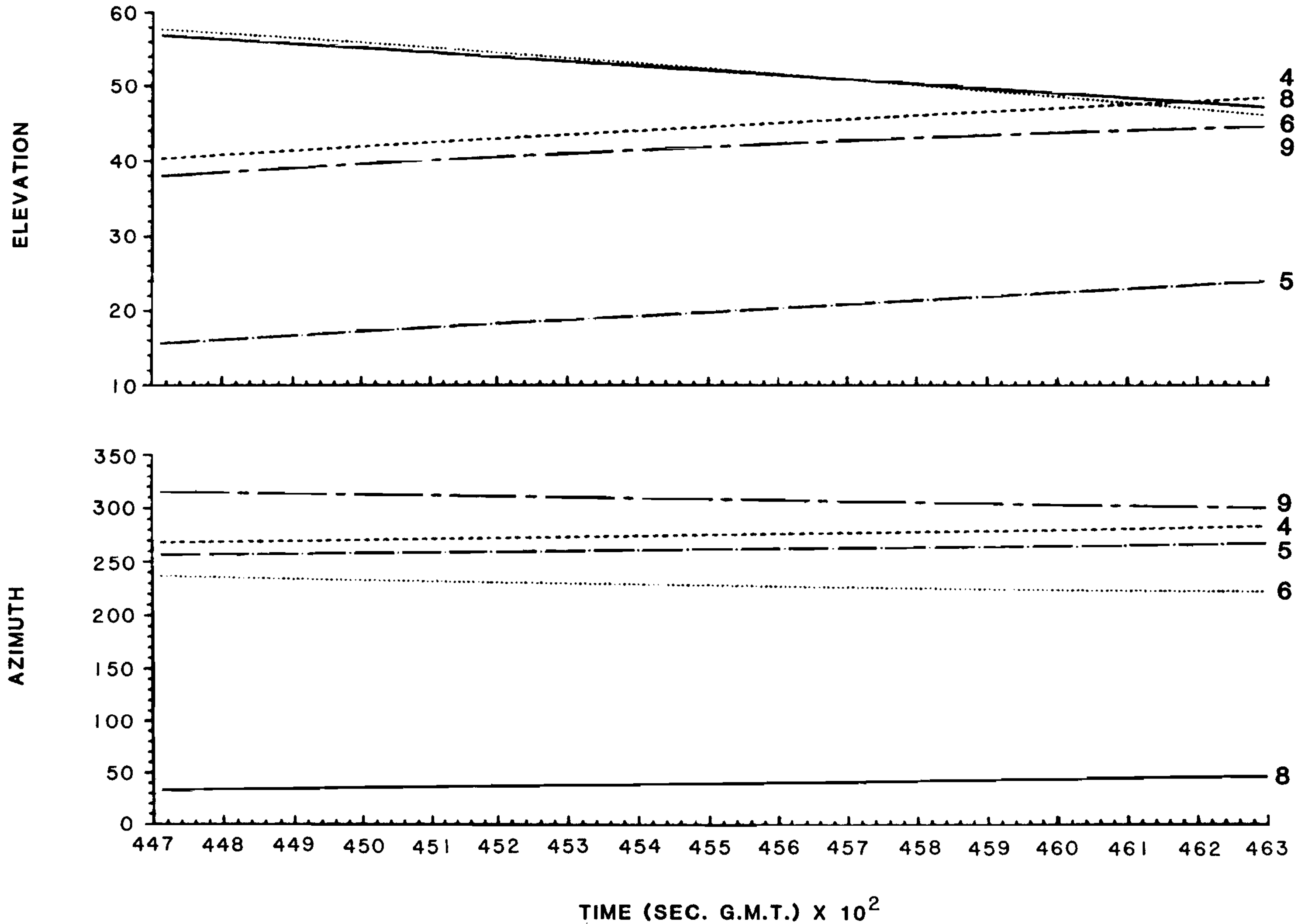

FIG. 4-61. SATELLITE VISIBILITY, RUN 4, 27 JAN 83

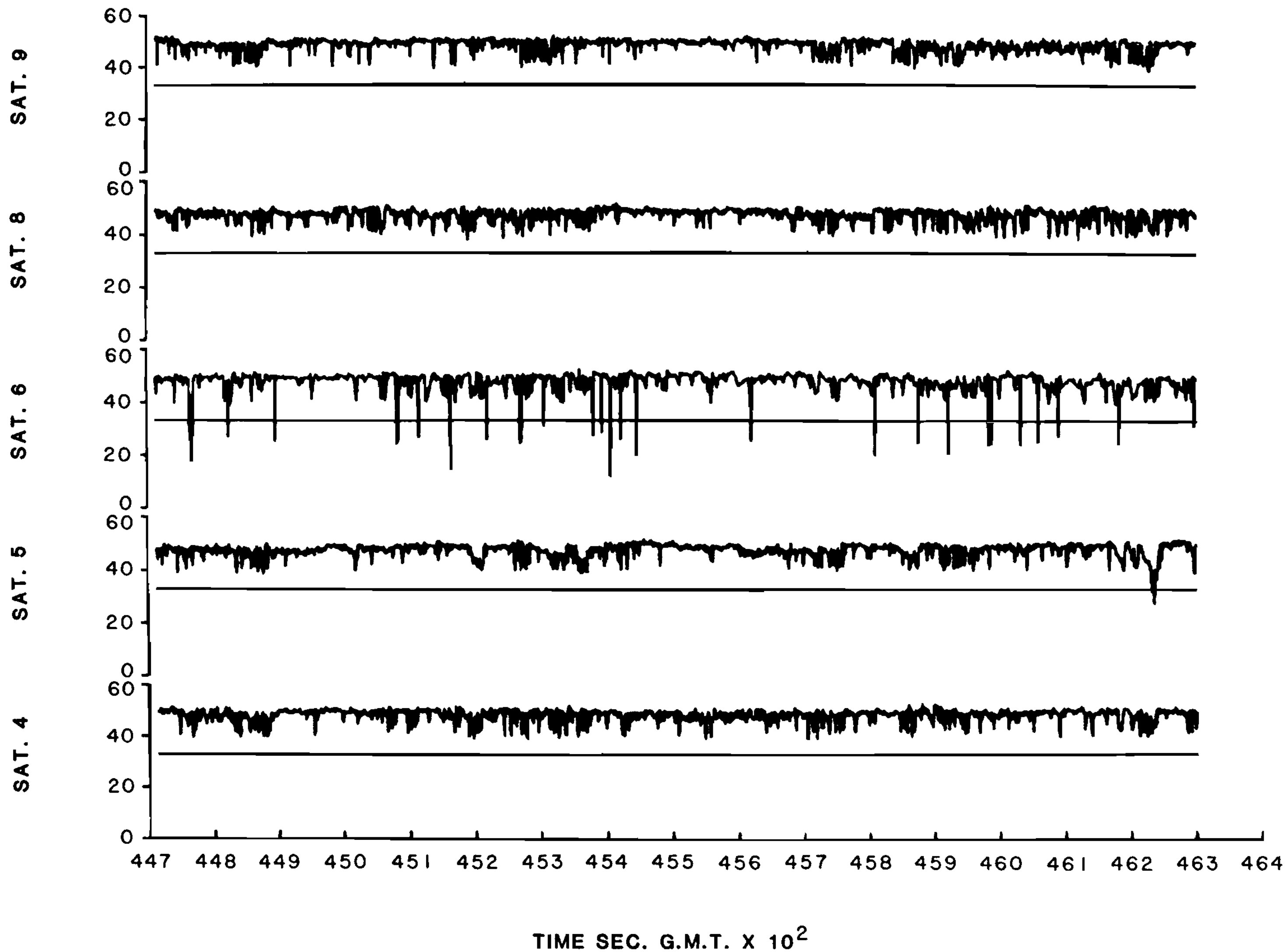

FIG. 4-62. SATELLITE C/NO. VALUES, RUN 4, 27 JAN 83

It should be noted that the verison 2.1 position software does not contain a provision for replacing failed satellites in the navigation mode dwell cycle. This provision was built into version 3.0 software which was not completed in time to support flight testing. Had the satellite replacement feature been installed, the position software would have been able to reestablish lock in the second SV6 dwell slot. It should be noted that the satellite replacement feature, while not flight tested, was validated for version 3.0 in laboratory tests.

The pseudo-range residuals for run 4 are shown in Fig. 4-63. The residuals are similar to those for run 3. Again note that SV4 had a negative bias and SV6 had a positive bias. The SV6 positive bias is probably due to the batch least-squares position fixing algorithm attempting to minimize the negative bias on SV4 due to its less accurate clock.

The results for run 4 are seen to be similar for the VOR approaches. It is seen that the GPS system functioned well on the NDB approach in this mountainous region.

4.3.2.2 Logan International Tests

Operational GPS test flights were made into Logan International airport at Boston, MA on 25 January 1983 and 28 January 1983. The number of flights into Logan was limited by difficulty in obtaining ATC clearances into the airport during the satellite visibility period, which coincided with time of high air traffic density. However, enough experience was gained at Logan to verify successful operation of the GPS system at this large, busy urban airport.

Figure 4-64 shows the ground track recorded by the GPS system during run 2 on 25 January 1983. The test aircraft approached the LYNDY waypoint (a non-directional beacon site) from the northeast. After intercepting the waypoint, the aircraft began a non-precison approach to runway 22. Upon landing, the aircraft taxiied to the end of runway 22R and took off. After intercepting the MILTT waypoint (also an NDB site), the aircraft turned to the northwest and departed the Logan area. Throughout the run, the GPS system maintained all five satellites in track and supplied continuous position updates. (Note: the gaps in the ground track shown in Fig. 4-64 are due to data recording dropouts).

Figure 4-65 shows the altitude and ground speed recorded by the GPS system during the Logan run. As seen in the figure, the middle part of the run was spent taxiing around the airport. During the time the aircraft was taxiing, there were numerous airport buildings and large aircraft in the immediate vicinity. Figure 4-66 shows the satellite visibilities for the run. Note that four of the satellites are to the west of the airport, towards the downtown Boston area, and the remaining satellite is to the east, towards the ocean. Figure 4-67 shows the dilution-of-precision values for the run as calculated in post-processing. As seen in the figure, the GDOP varied from about 6.3 to 6.7 during the run.

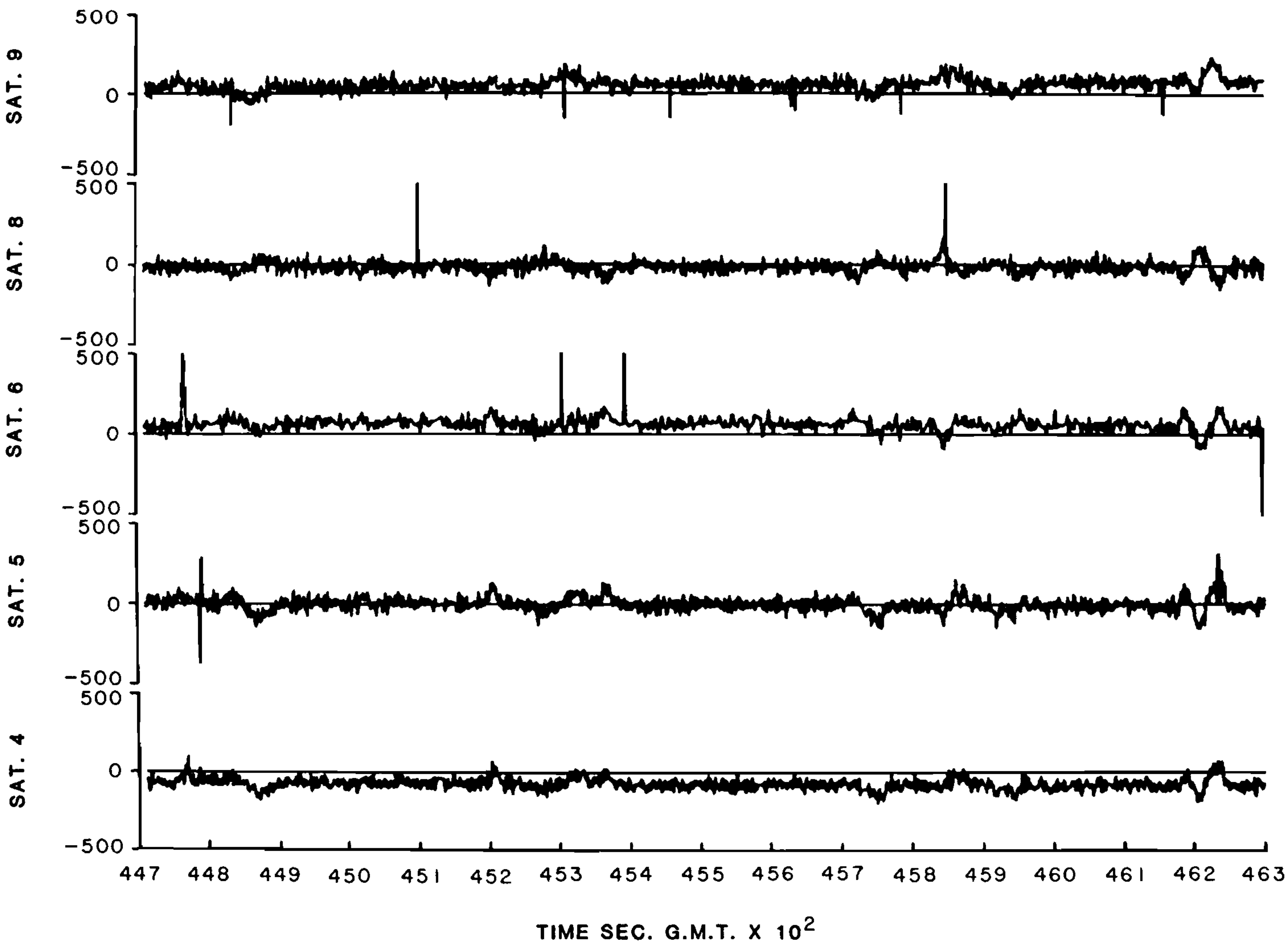

FIG. 4-63. PSEUDO-RANGE RESIDUALS, RUN 4, 27 JAN 83

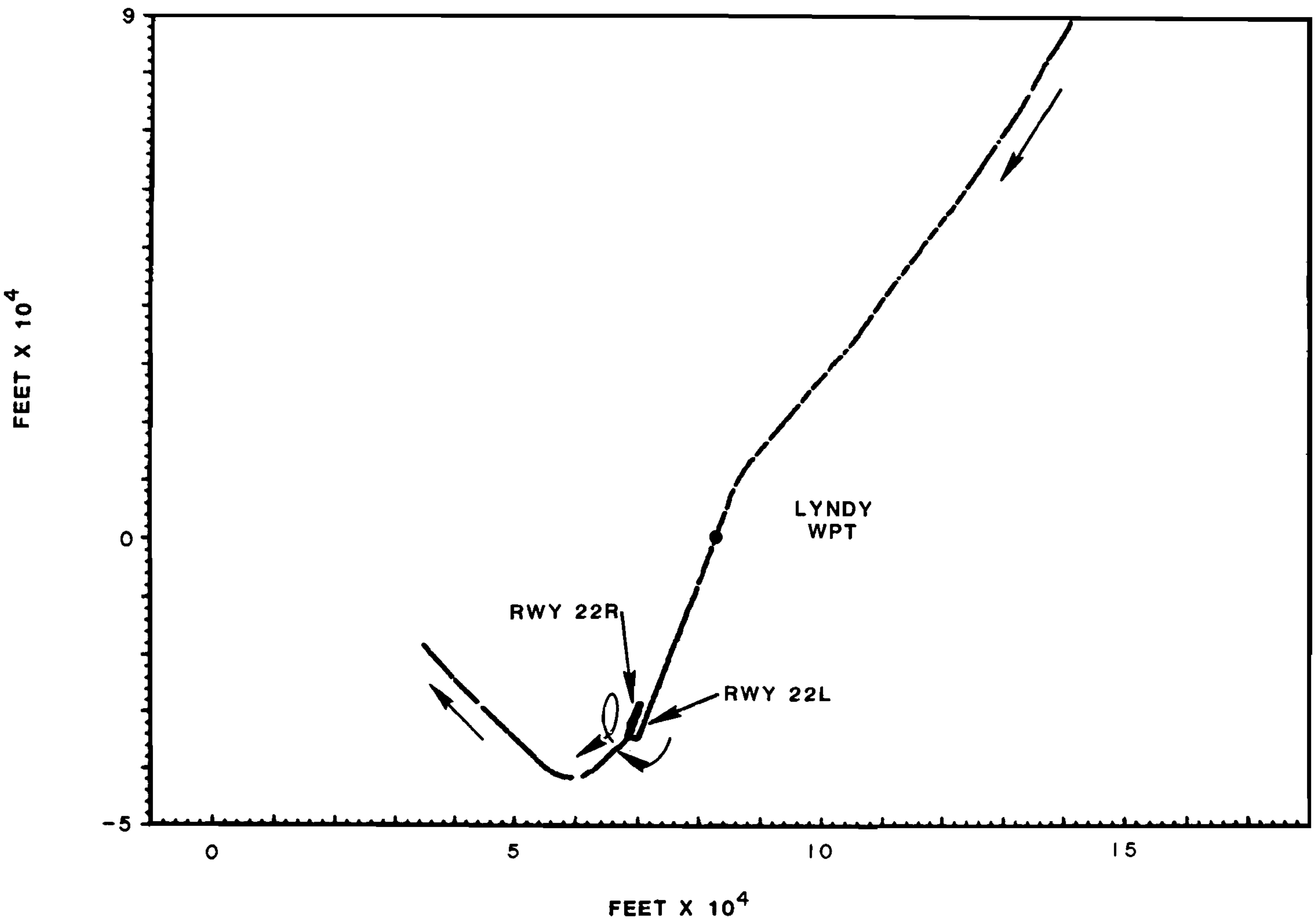

FIG. 4-64. LOGAN INTERNATIONAL TEST, 25 JAN 83, RUN 2

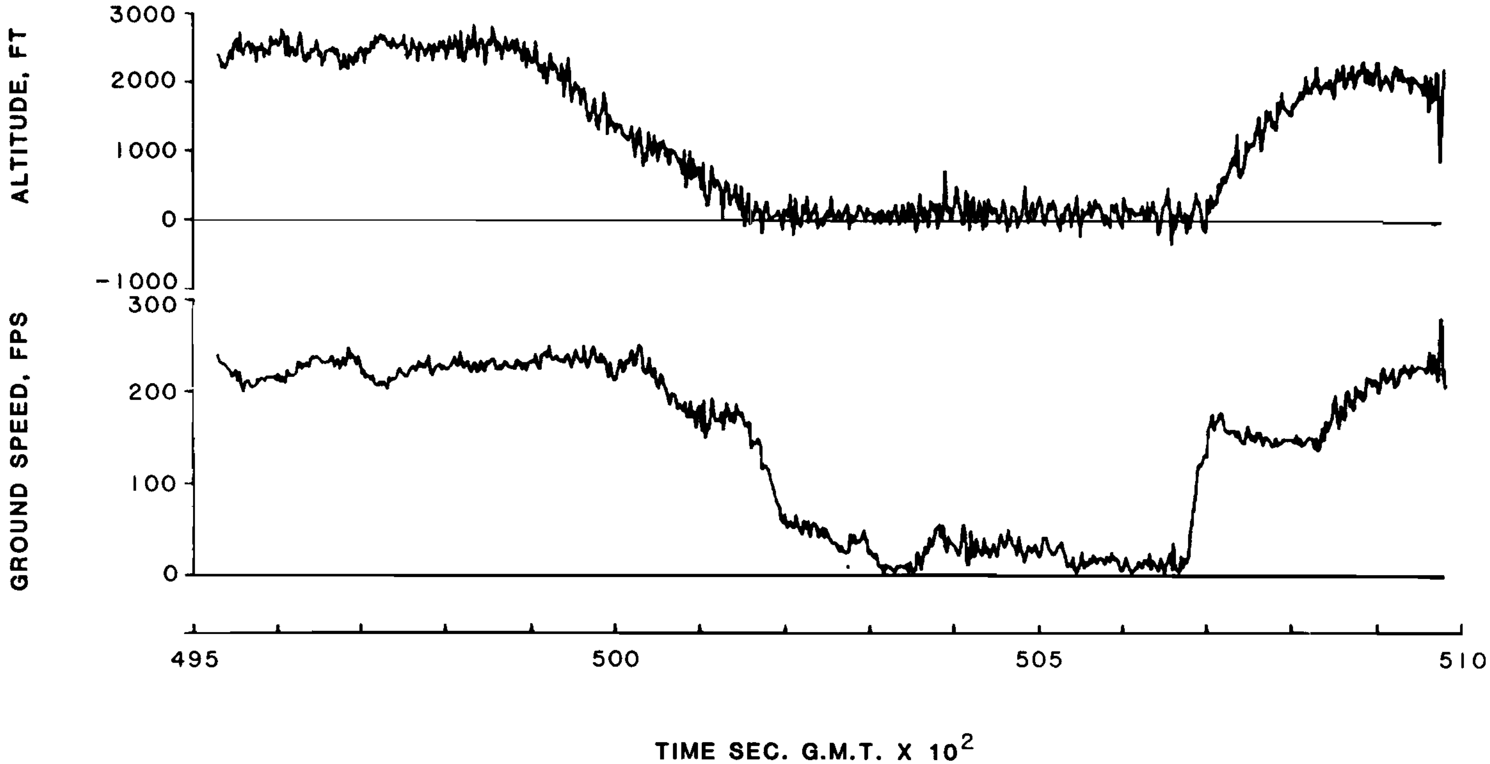

FIG. 4-65. ALTITUDE AND GROUND SPEED, 25 JAN 83, RUN 2

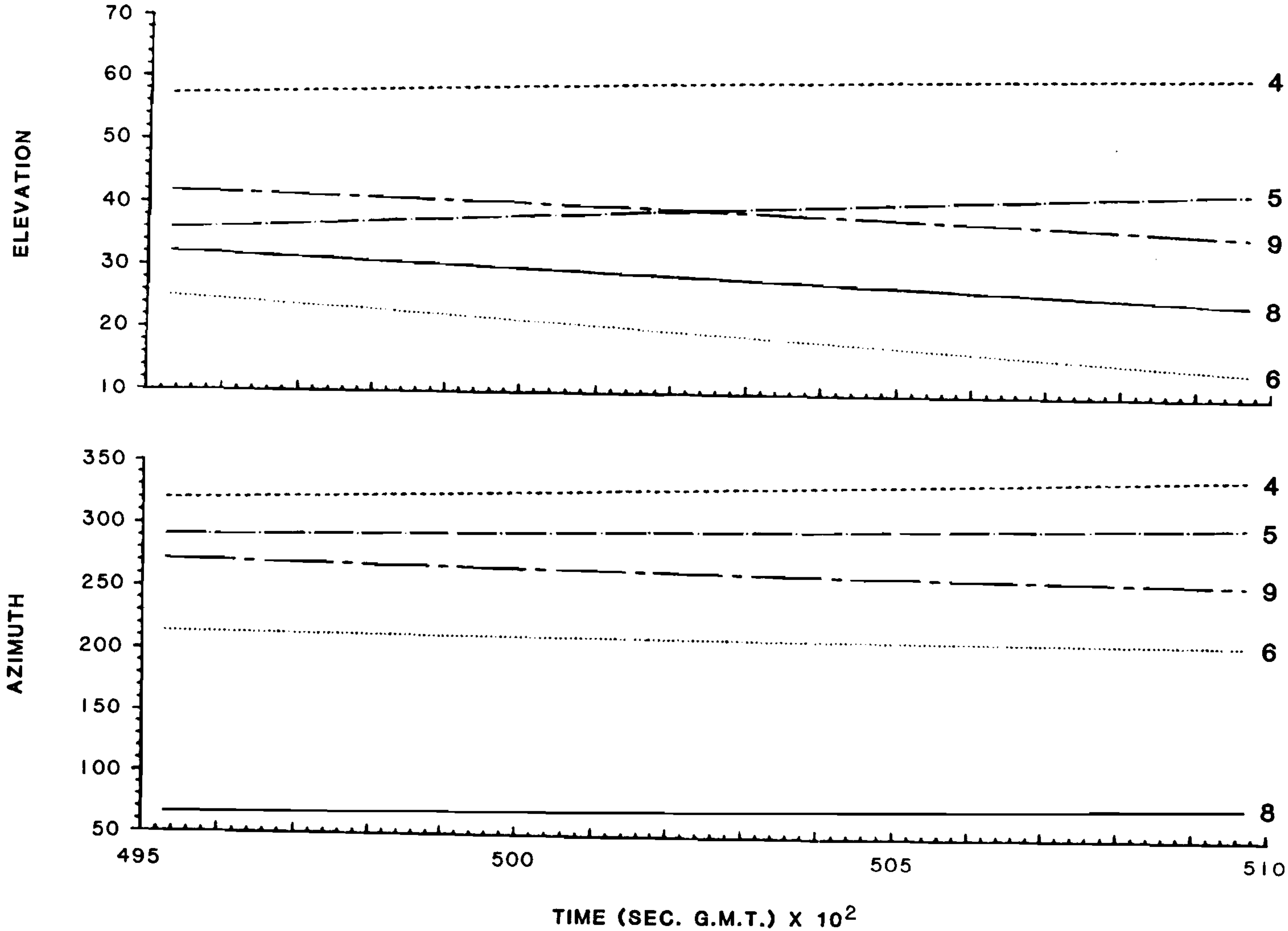

FIG. 4-66. SATELLITE VISIBILITY, 25 JAN 83, RUN 2

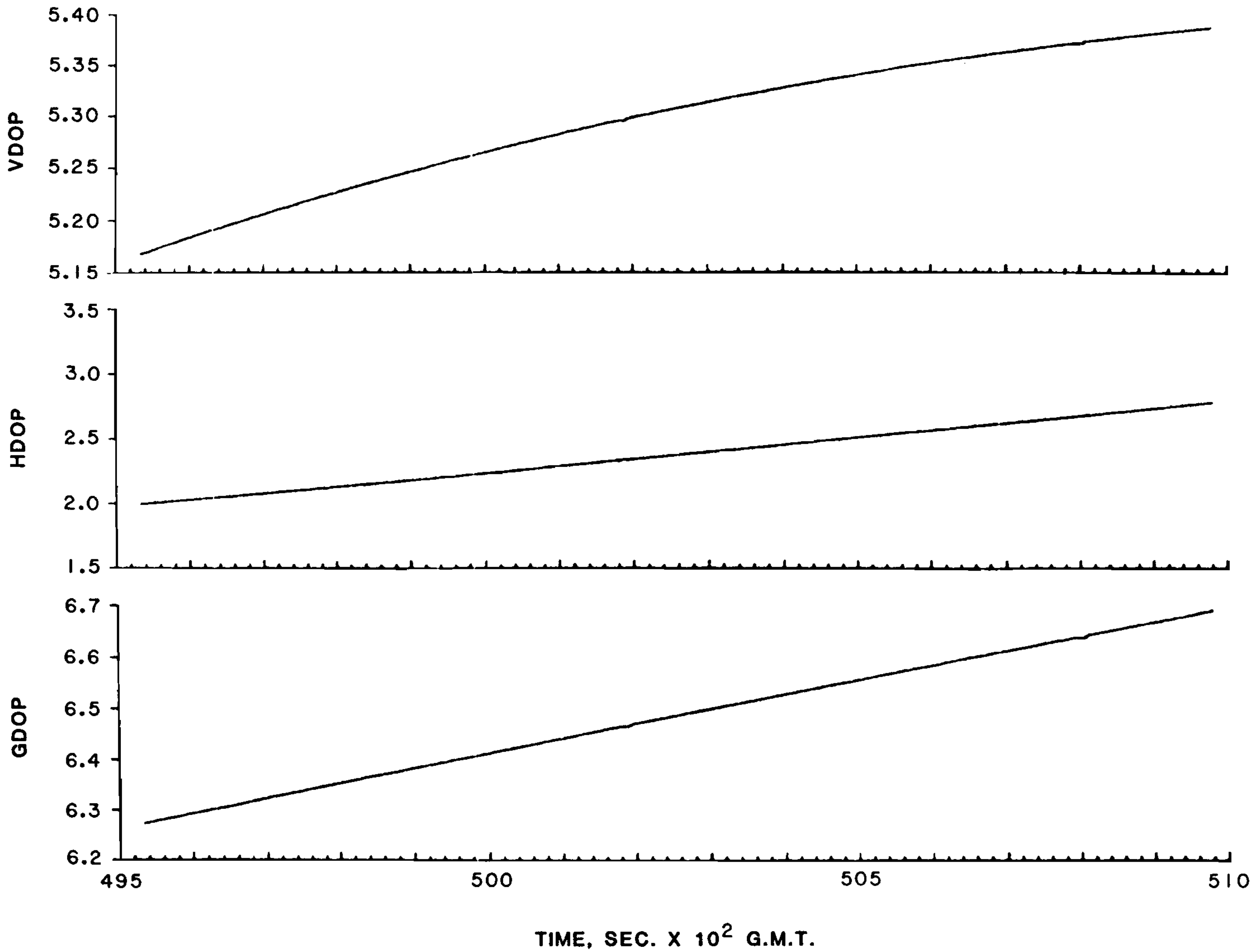

FIG. 4-67. DILUTION-OF-PRECISION, 25 JAN 83, RUN 2

The satellite C/N_0 values are shown in Fig. 4-68. All of the satellite C/N_0 values remained well above the 33 dB-Hz loss-of-lock threshold, although SV6 dropped substantially (about 10 dB) during the turn after takeoff from runway 22 R. The drop in C/N_0 is not surprising since the aircraft banked away from SV6 during the turn.

It is significant that the GPS system kept the satellites in track continuously while taxiing despite the buildings and large aircraft near to the GPS aircraft. Although blockage of the satellite signal is probable when the aircraft is immediately adjacent to a building, significant blockage did not occur on the taxiways or runways.

The pseudo-range residuals for the 25 Janaury 1983 run are shown in Fig. 4-69. The residuals showed no jumps of the kind seen earlier, indicating that the position software was always able to collect pseudo-range measurements from the receiver. Note the positive bias (+75 feet on SV9 and negative bias (-50 feet) on SV5. As explained earlier, these biases appear to be due to old ephermeric data transmitted by the satellites.

A second test flight was made at Logan International on 28 January 1983. Figure 4-70 shows the ground track for a low-approach and departure from runway 4L. The altitude and ground speed profiles for the flight are shown in Fig. 4-71. After departing the runway, the aircraft made a turn to the northwest prior to intercepting the LYNDY waypoint on instructions from air traffic control. The aircraft then departed the Logan area for Hanscom Field.

The satellite C/N_0 values for the 28 January 1983 Logan run are shown in Fig. 4-72. The run was made late in the satellite visibility window, so that only four satellites were available for navigation. Nonetheless, the GPS system was able to provide continuous navigation updates throughout the run. The pseudo-range residuals for the run are shown in Fig. 4-73. Note the positive change in the SV8 residual and negative changes in the SV5 and SV9 residuals corresponding to the initial turn in the run. Again, this behavior is explained by the satellite positions: SV8 was to the east while SV5 and SV9 were to the west. SV4 was more to the north and the aircraft velocity in that direction changed little.

The Logan runs demonstrated that GPS can be used for non-precision approach into a large urban airport. It was also found that the GPS system was able to maintain navigation service while on the taxiways and runways under conditions that generally render VOR/DME systems inoperable. It should be cautioned that these observations apply to the GPS system while in navigation mode; the lock threshold is 2 dB higher (less sensitive) for the acquisition mode. Also, some satellite signals are likely to be blocked when the aircraft is parked next to a large building such as a passenger terminal. Nonetheless, the satellite C/N_0 margins appear quite acceptable once the aircraft is out on the taxiways.

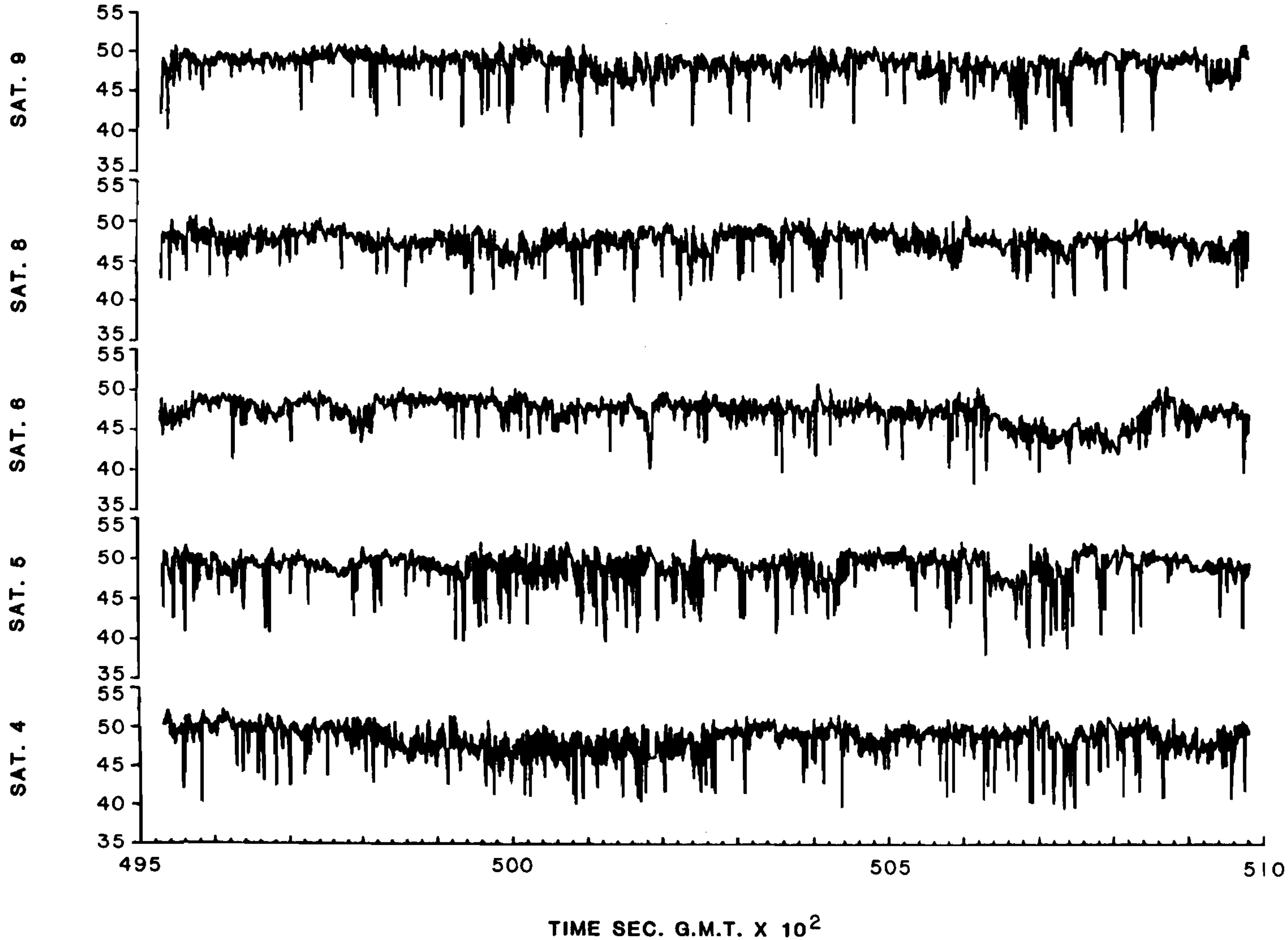

FIG. 4-68. SATELLITE C/NO., 25 JAN 83, RUN 2

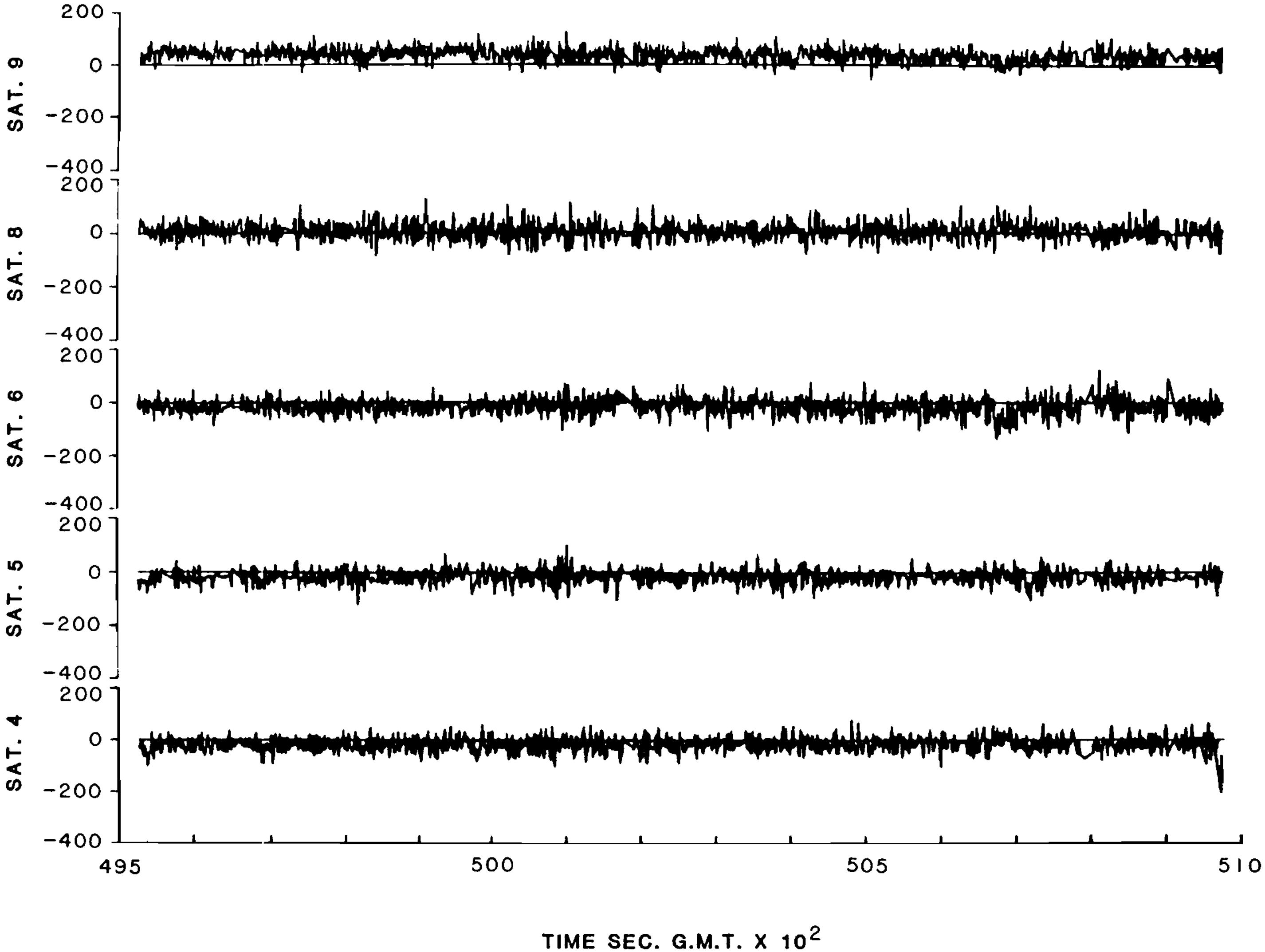

FIG. 4-69. PSEUDO-RANGE RESIDUALS, 25 JAN 83, RUN 2

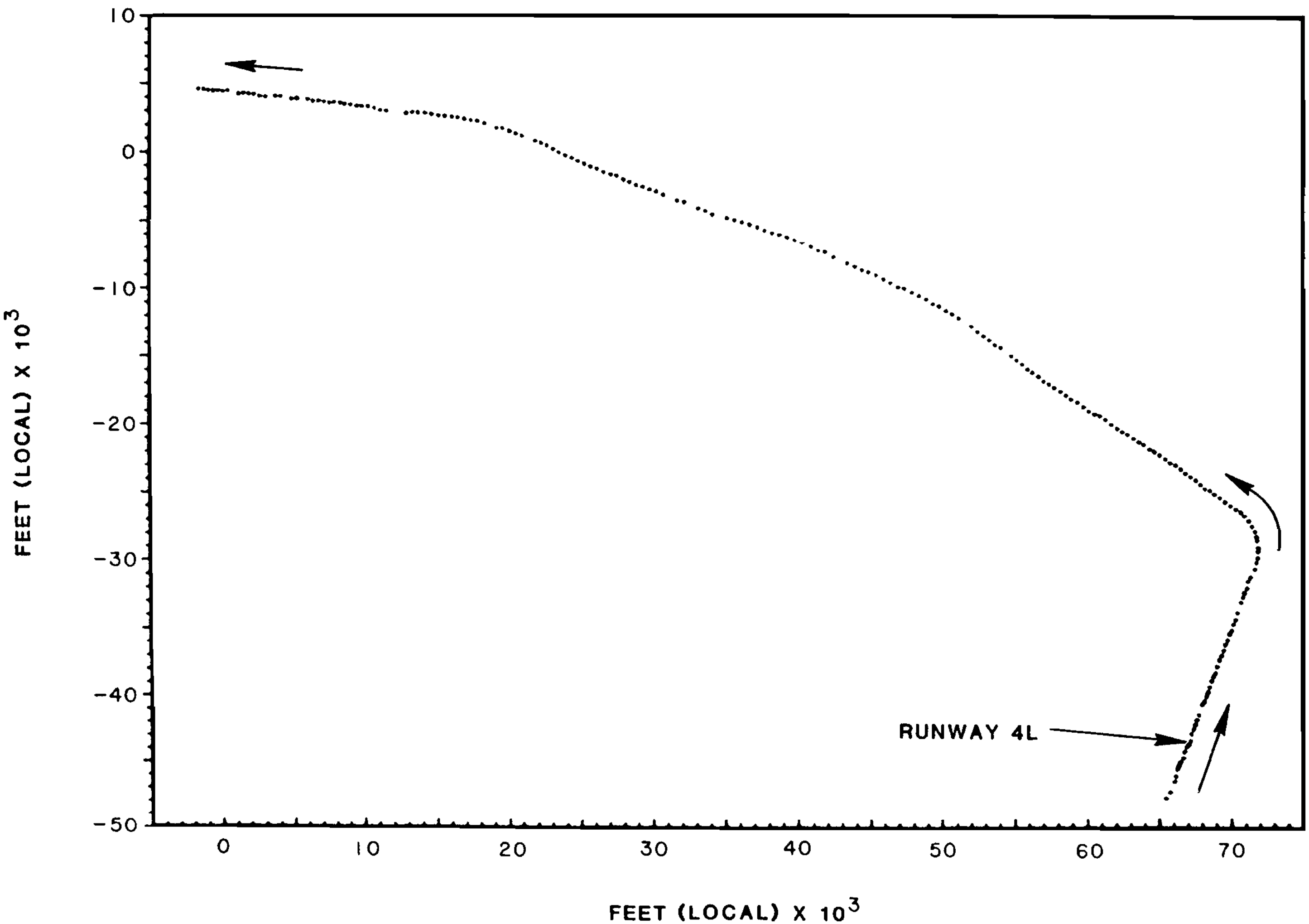

FIG. 4-70. LOGAN INTERNATIONAL, 28 JAN 83

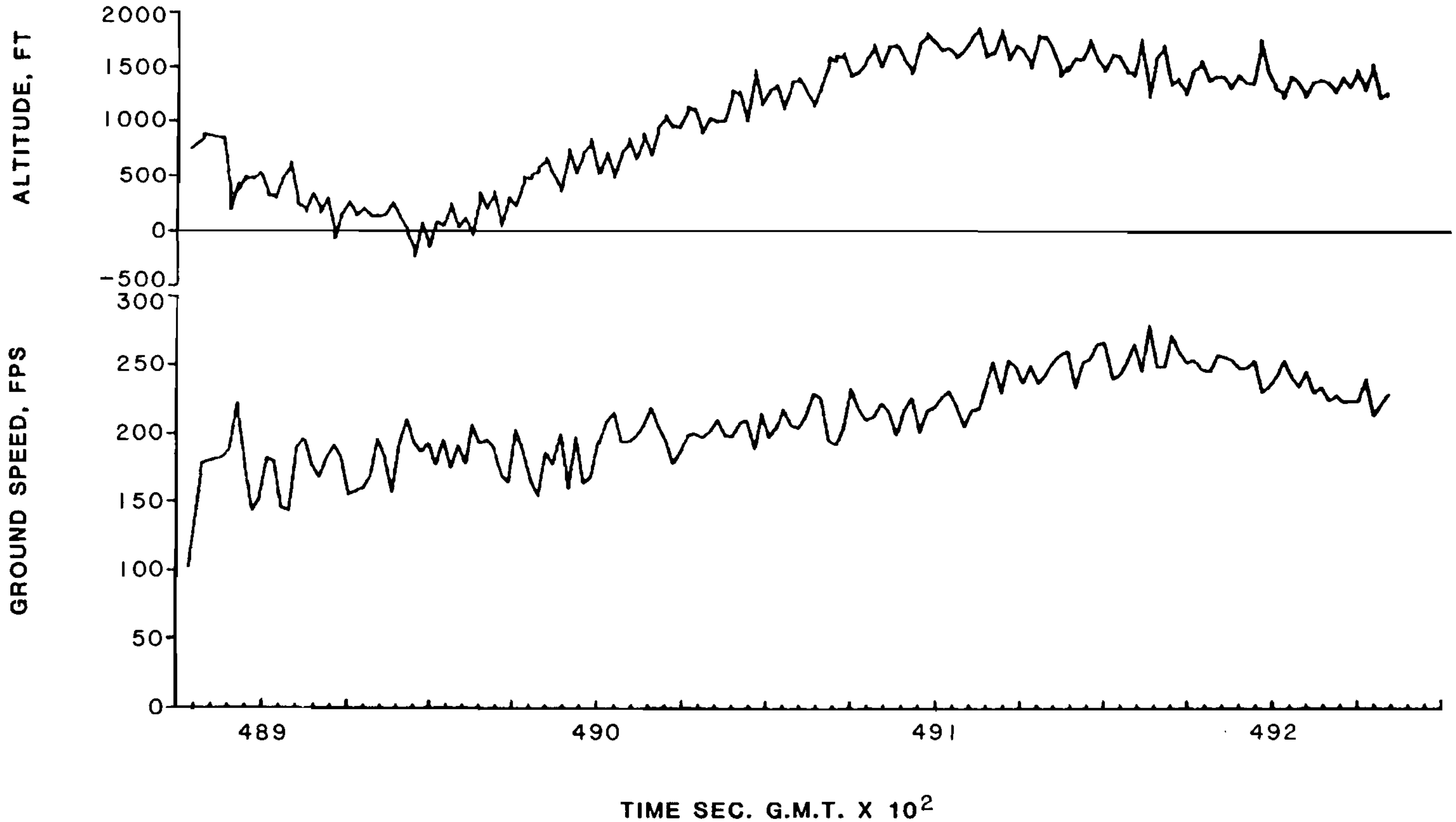

FIG. 4-71. ALTITUDE AND GROUND SPEED, 28 JAN 83, RUN 2a

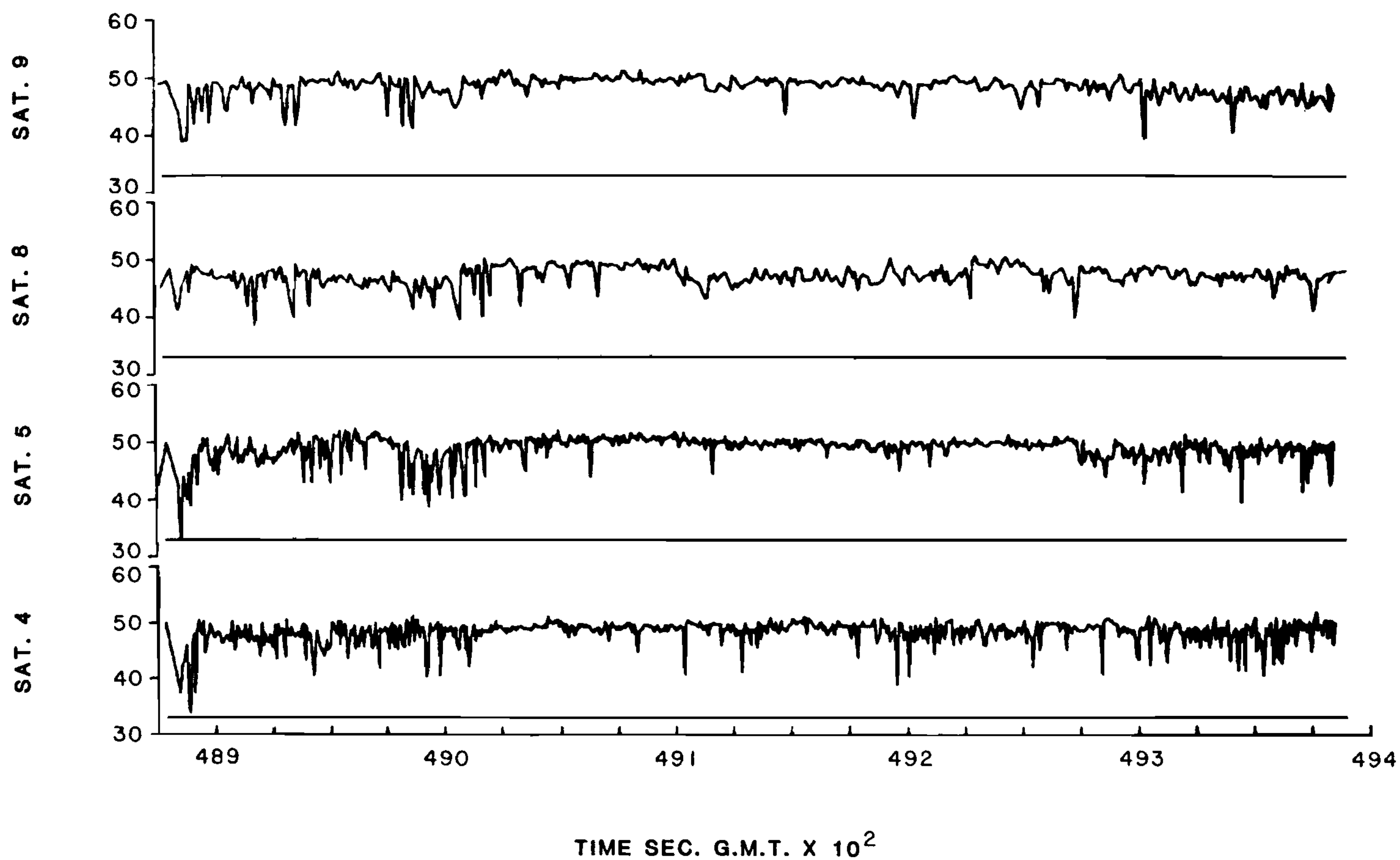

FIG. 4-72. SATELLITE C/NO., 28 JAN 83, RUN 2a

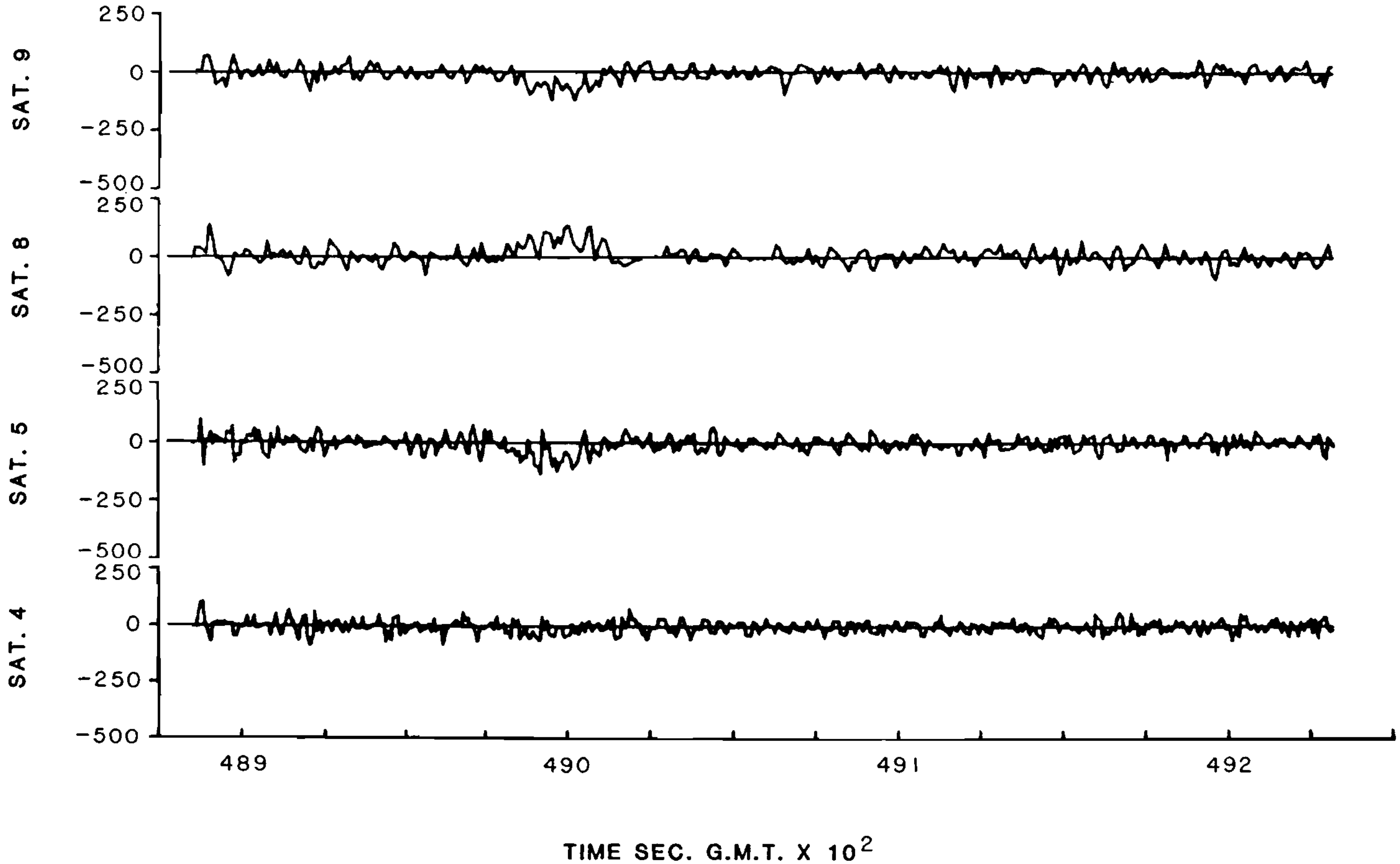

FIG. 4-73. PSEUDO-RANGE RESIDUALS, 28 JAN 83, RUN 2a

4.3.2.3 Hanscom Field/Manchester Airport Tests

4.3.2.3.1 25 January 1983 Test

The final set of operational tests were made in the vicinity of Hanscom Field at Lexington, MA and Manchester Airport at Manchester, NH. The purpose of these tests was to verify the use of GPS as a navigation system in typical general aviation operations. Figure 4-74 shows the GPS-generated ground track of such a flight into Manchester Airport on 25 January 1983. In this case the aircraft was flown north until the 337° radial to the MHT VOR waypoint was intercepted. The aircraft was then flown on the radial, intercepting the waypoint and descending for a landing at runway 35.

The altitude and ground speed profiles for the flight are shown in Fig. 4-75. As seen in the figure, a substantial disturbance occured in the navigation updates just prior to landing. Analysis of the test data showed that this disturbance was caused by an incorrect position fix calculation. The calculation was incorrect because the position software failed to collect valid measurements from the receiver in both SV4 dwells and a pseudo-range from the previous navigation cycle was included in the position fix calculation due to a position software error. The system corrected the position error on the next cycle, 2.2 seconds later.

It should also be noted that the magnitude of the change in the position fix was greater than a thousand feet, so that the fix should have been declared invalid by the position software. However, the limits on position fix changes were unrealistically high in the Version 2.1 software used for the test, so that the fix was passed on to the α-β tracker. Despite this fact, the disturbance was sufficiently damped out such that it was not operationally significant.

The satellite visibilities for the 25 January 1983 run are shown in Fig. 4-76. Note that SV6 was successfully tracked down to 4° elevation angle, below the nominal 5° elevation angle mask. Even more surprising, the aircraft was on the ground at the time. Figure 4-77 shows the satellite C/N_0 values for run. Note that SV6 is dropped for a short time, just before landing, but is brought back into track. Shortly afterward, SVs 4,5,8 and 9 are also dropped but tracking is immediately recovered.

Figure 4-78 shows the pseudo-range residuals. The jump in the SV4 residual was caused by the incorrect position fix, as previously discussed. The other two jumps occur in SV8 and are caused by the temporary loss of tracking for that satellite.

4.3.2.3.2 4 February 1983 Test

For subsequent operational tests in the Hanscom Field/Manchester Airport area, a standard test scenario was developed as shown in Fig. 4-79. For this scenario, the aircraft departs from Hanscom Field, runway 11, and is flown to the Shaker Hills NDB waypoint (SKR 4). After intercepting the waypoint, the

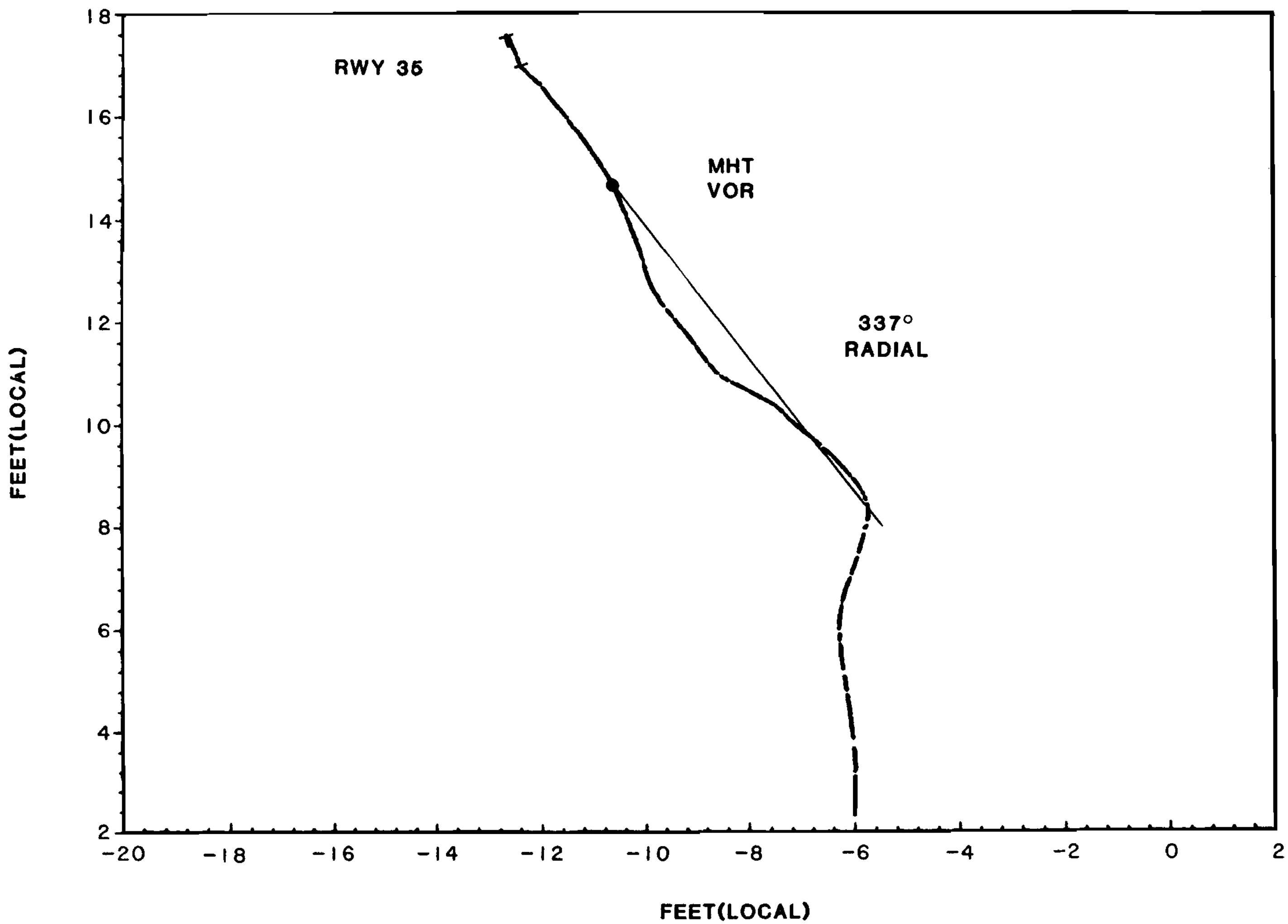

FIG. 4-74. MANCHESTER AIRPORT, 25 JAN 83, RUN 3

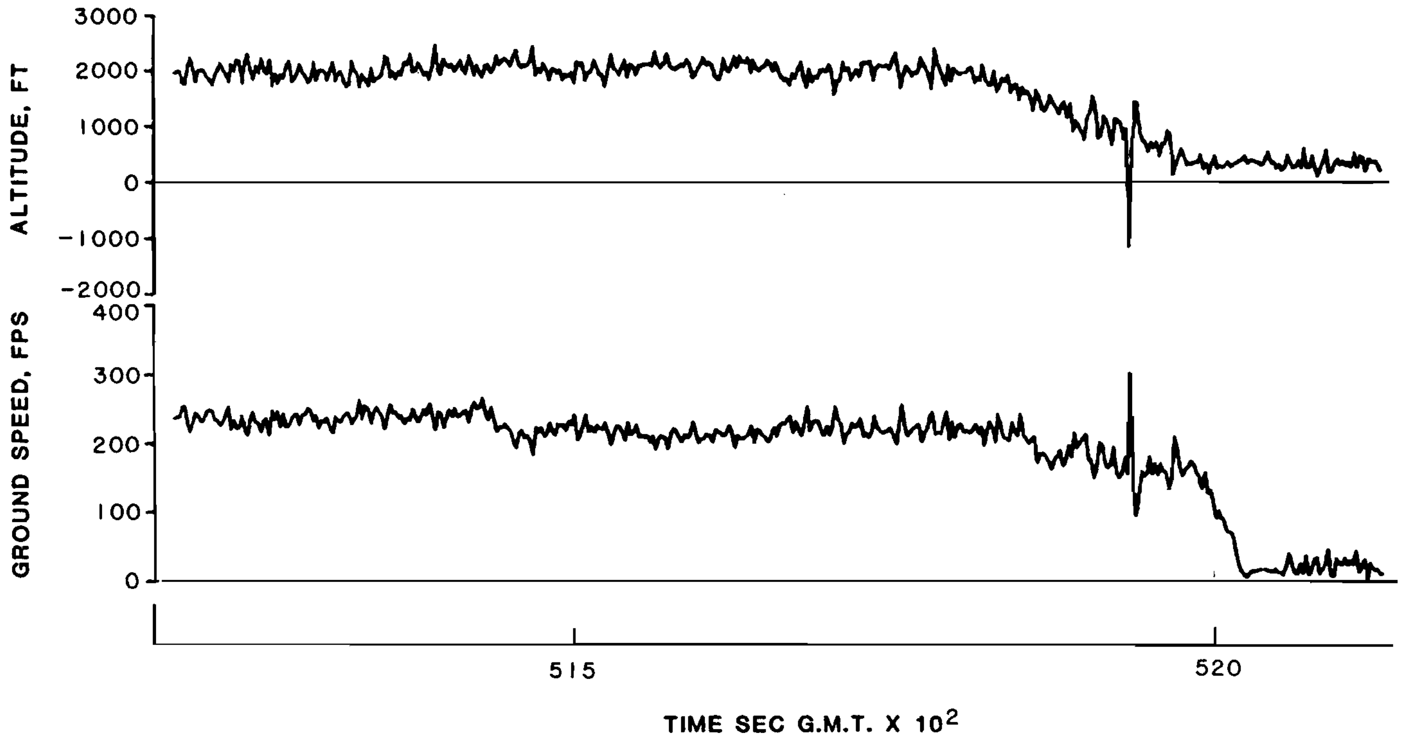

FIG. 4-75. ALTITUDE AND GROUND SPEED, 25 JAN 83, RUN 3

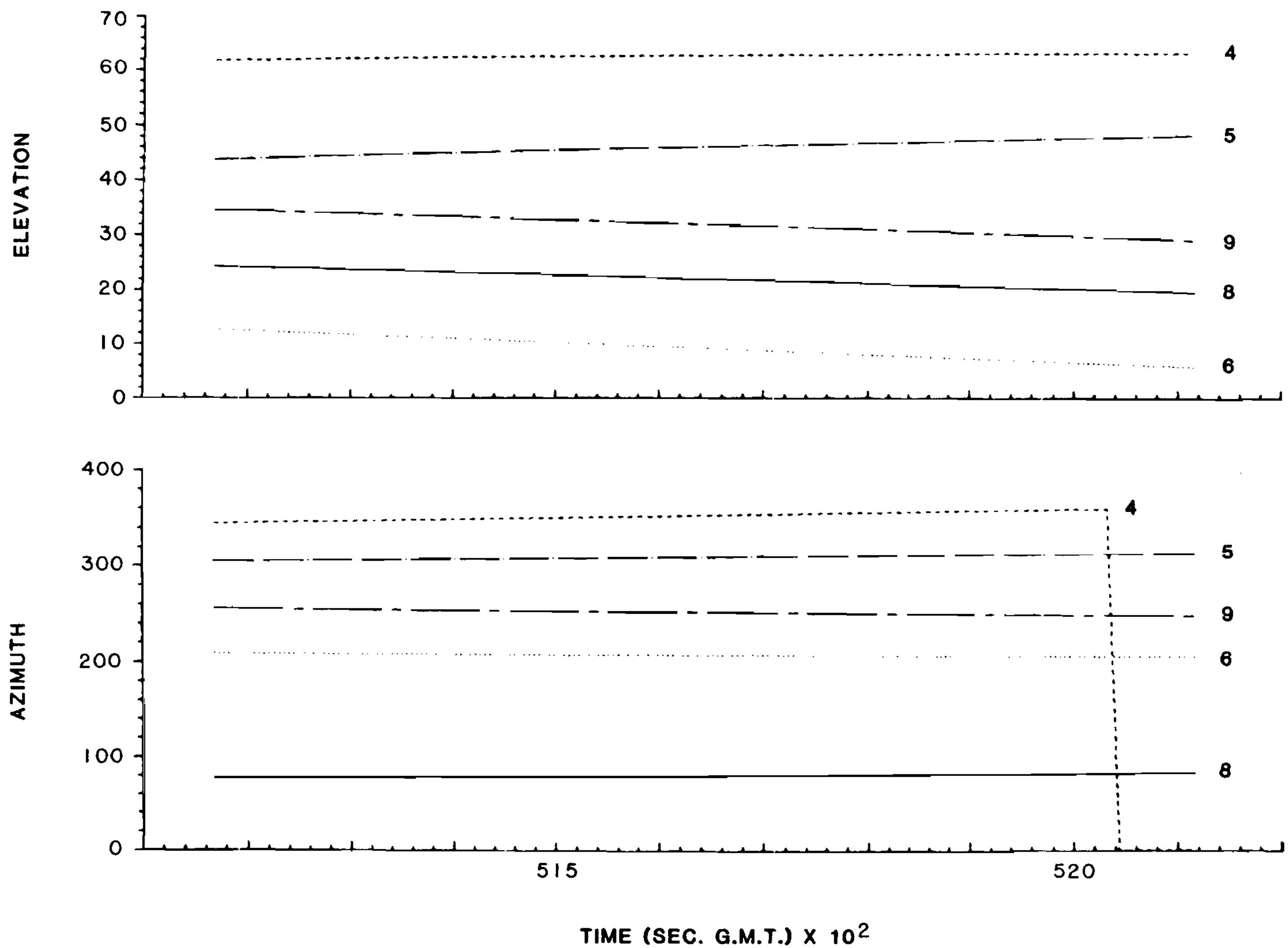

FIG. 4-76. SATELLITE VISIBILITIES, 25 JAN 83, RUN 3

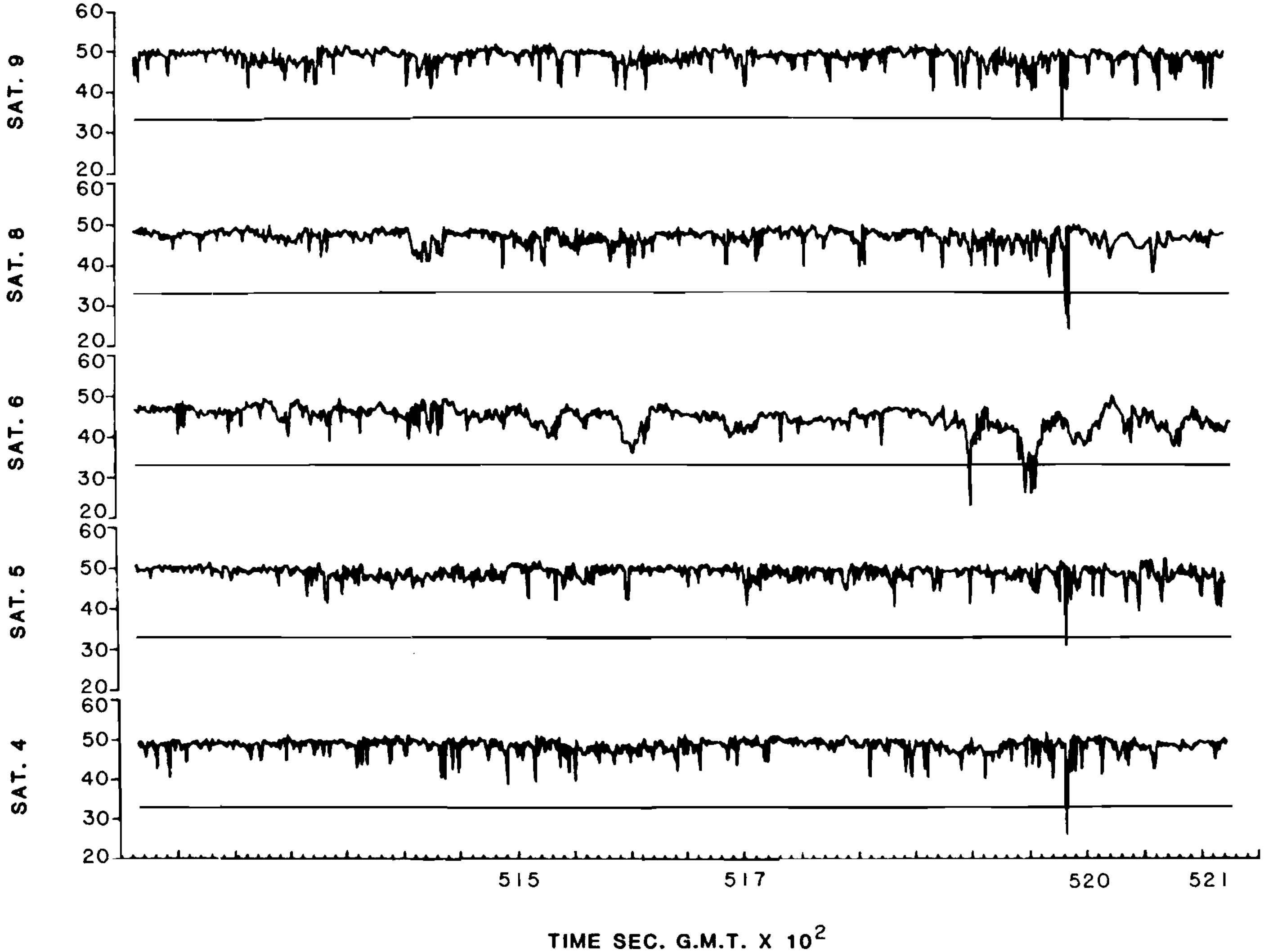

FIG. 4-77. SATELLITE C/NO., 25 JAN 83, RUN 3

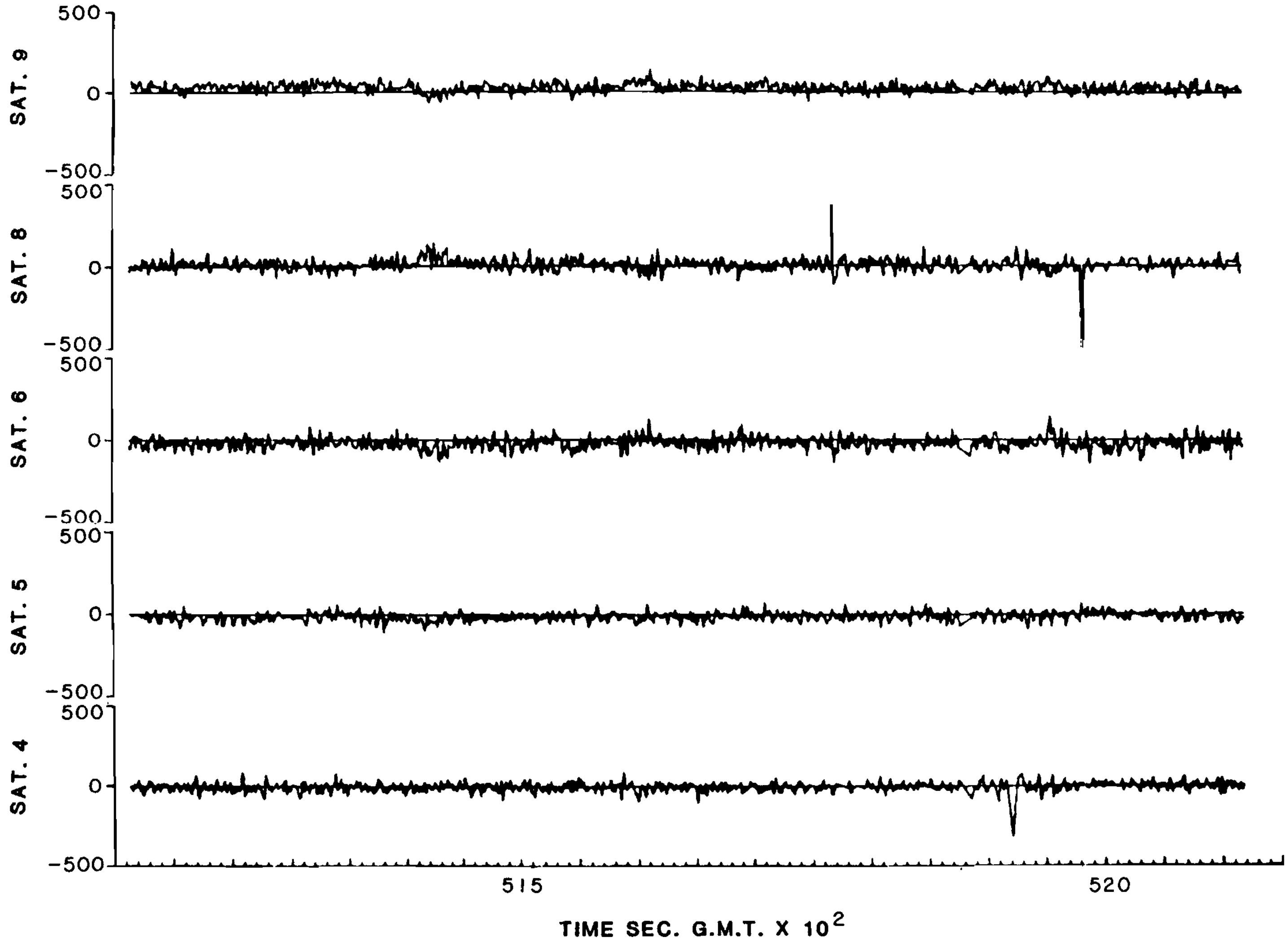

FIG. 4-78. PSEUDORANGE RESIDUALS, 25 JAN 83, RUN 3

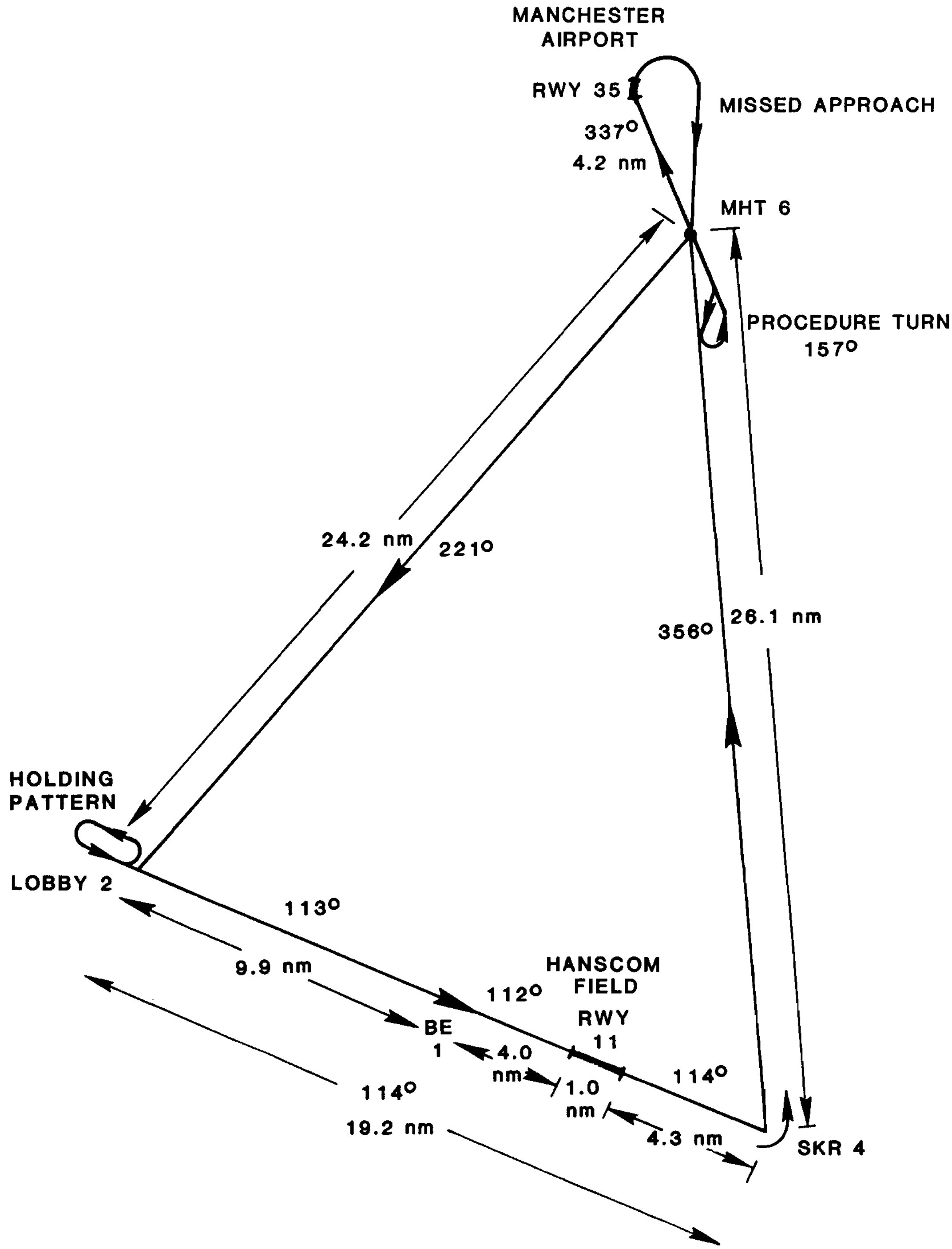

FIG. 4-79. TEST SCENARIO FOR HANSCOM FIELD/MANCHESTER AIRPORT OPERATIONAL FLIGHTS

aircraft then intercepts the 356° radial to the Manchester VOR waypoint (MHT 6). After overflying the Manchester waypoint, the aircraft is turned to 157° outbound, performs a procedure turn and turns inbound on the 337° radial. Upon intercepting the waypoint again, the aircraft begins the descent to runway 35. A missed approach is then performed with the Manchester waypoint as the Missed Approach Point (MAP).

After overflying the Manchester waypoint again, the aircraft departs on the 221° radial for the LOBBY intersection waypoint (LOBBY 2). The aircraft enters a holding pattern at LOBBY, then departs on the 113° radial for the Bedford NDB waypoint (BE 1). The descent to runway 11 at Hanscom Field begins after the Bedford waypoint is overflown. The aircraft then lands at Hanscom or performs a low-approach to start another circuit of the course.

The ground track for Run 1a on 4 February 1983 is shown in Fig. 4-80. The test aircraft was under continuous MODSEF surveillance commencing just before the aircraft reached the SKR waypoint and ending as the aircraft left the LOBBY waypoint. As can be seen from the figure, the aircraft was successfully navigated to the selected waypoints using the GPS system. On the Shaker Hills to Manchester leg, the pilot maintained the course indicated by the system fairly closely, but departed from the GPS course on the Manchester to LOBBY leg due to ATC traffic advisories. The altitude and ground speed profiles for the run are shown in Fig. 4-81.

The satellite visibilities for Run 1a are shown in Fig. 4-82 and the dilution-of-precision calculations are given in Fig. 4-83. Figure 4-84 shows the satellite C/N_0 values during the run and Fig. 4-85 shows the pseudo-range residuals.

Since the test aircraft was under MODSEF surveillance during the run the system accuracy could be determined by post-flight processing. Figure 4-86a shows the horizontal and vertical position fixing error as a function of time. There are several large horizontal errors shown in the figure; analysis of the data shows that the large values are instances in which the MODSEF facility failed to track the aircraft. These spurious errors do not substantially affect the error statistics. The horizontal and vertical error in the GPS position estimate (tracker output) is shown in Fig. 4-86b.

Table 4-12 shows the position accuracy statistics for Run 1a. The horizontal accuracy of the tracker estimates is seen to be well within the system performance requirements and goals.

In order to examine the behavior of the system during a turn, the holding pattern section of Run 1a was expanded as shown in Figs. 4-87 and 4-88. The MODSEF radar track is plotted with the GPS position fixes in Fig. 4-87 and with the tracker estimates in Fig. 4-88. The horizontal and vertical errors for the position fixes and tracker estimates are shown in Figs. 4-89 and 4-90, respectively. As seen in Fig. 4-87 and 4-89 the horizontal position fix error does not build up during the turns, and the only major discrepancies between the GPS position fixes and the radar track appear to be MODSEF tracking errors. Note in particular that during Turn 3 the horizontal position fix error remains less than 150 feet throughout the turn.

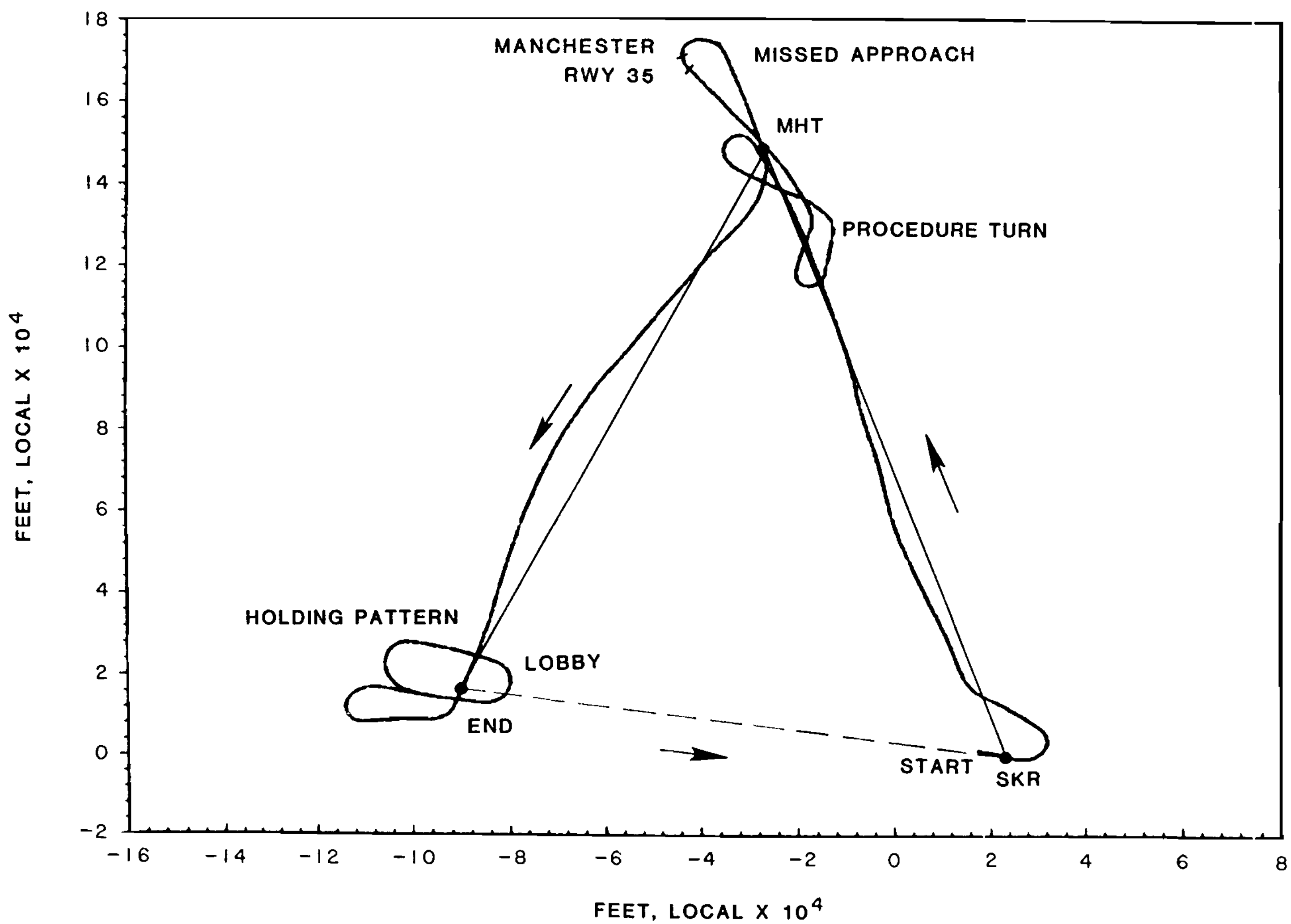

FIG. 4-80. OPERATIONAL TEST, 4 FEB 83, RUN 1a

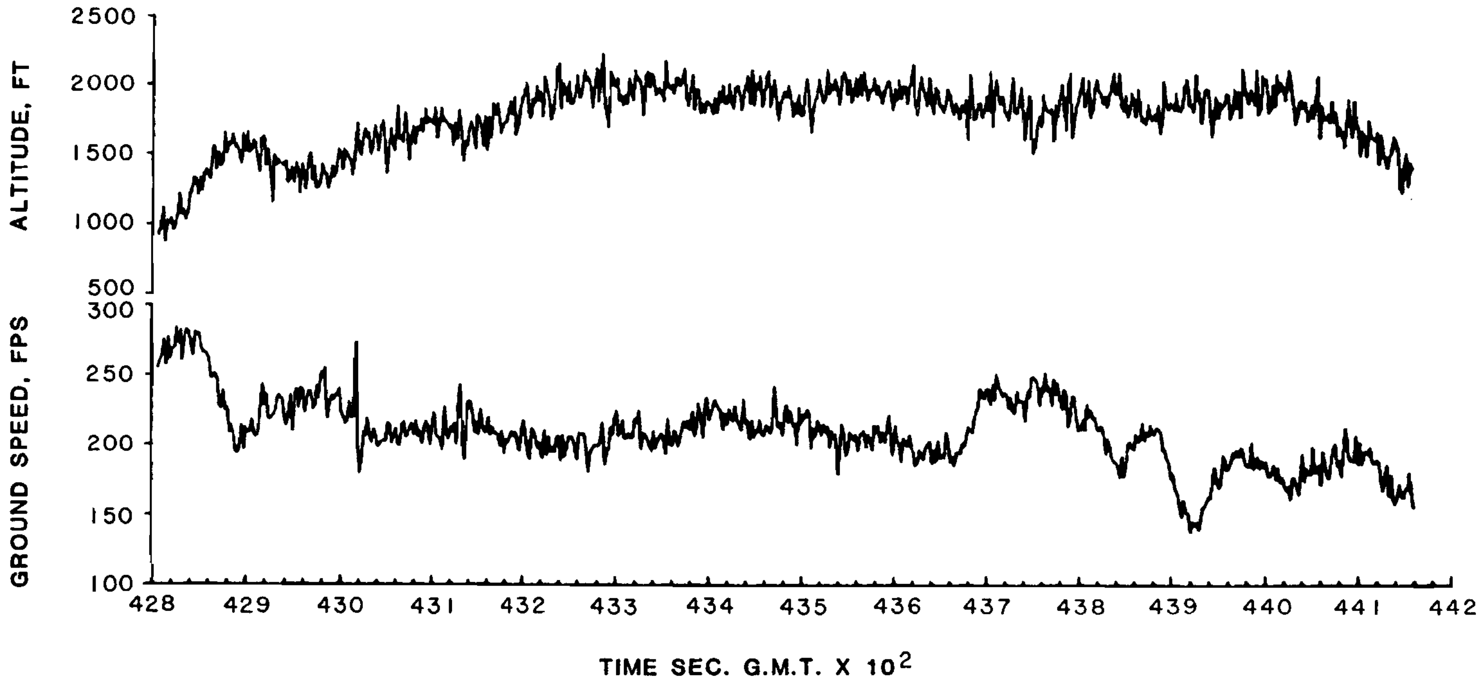

FIG. 4-81. ALTITUDE AND GROUND SPEED, 4 FEB 83, RUN 1a, (PAGE 1 OF 2)

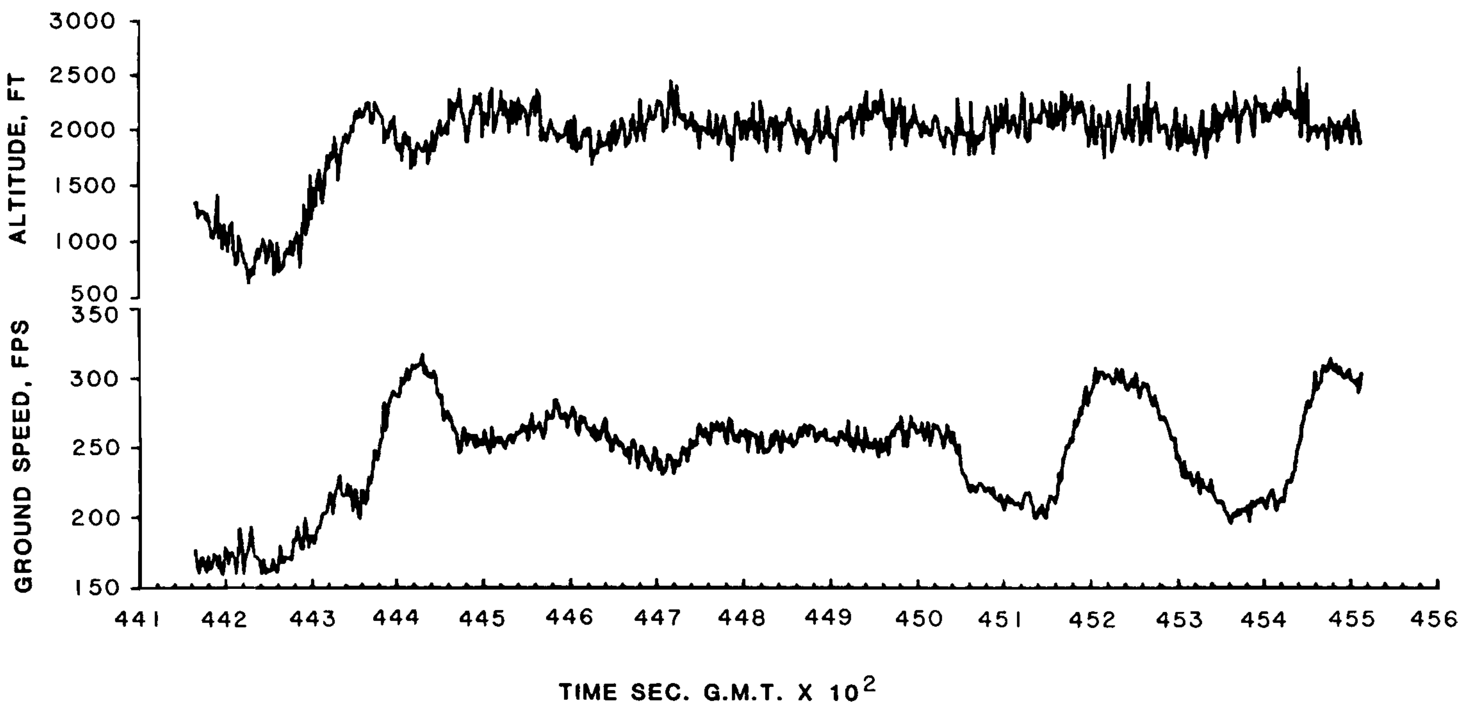

FIG. 4-81. ALTITUDE AND GROUND SPEED, 4 FEB 83, RUN 1a, (PAGE 2 OF 2)

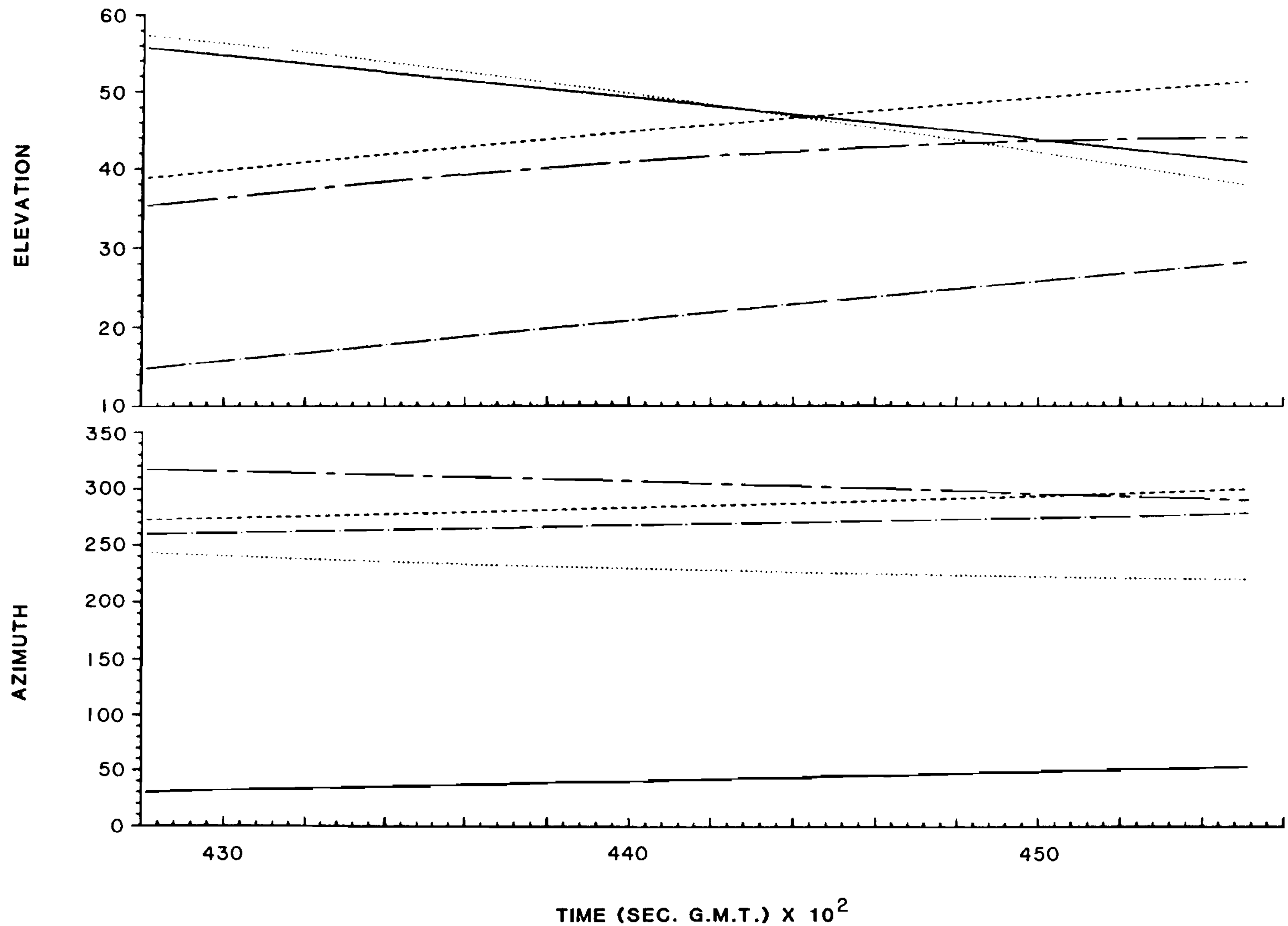

FIG. 4-82. SATELLITE VISIBILITIES, 4 FEB 83, RUN 1a

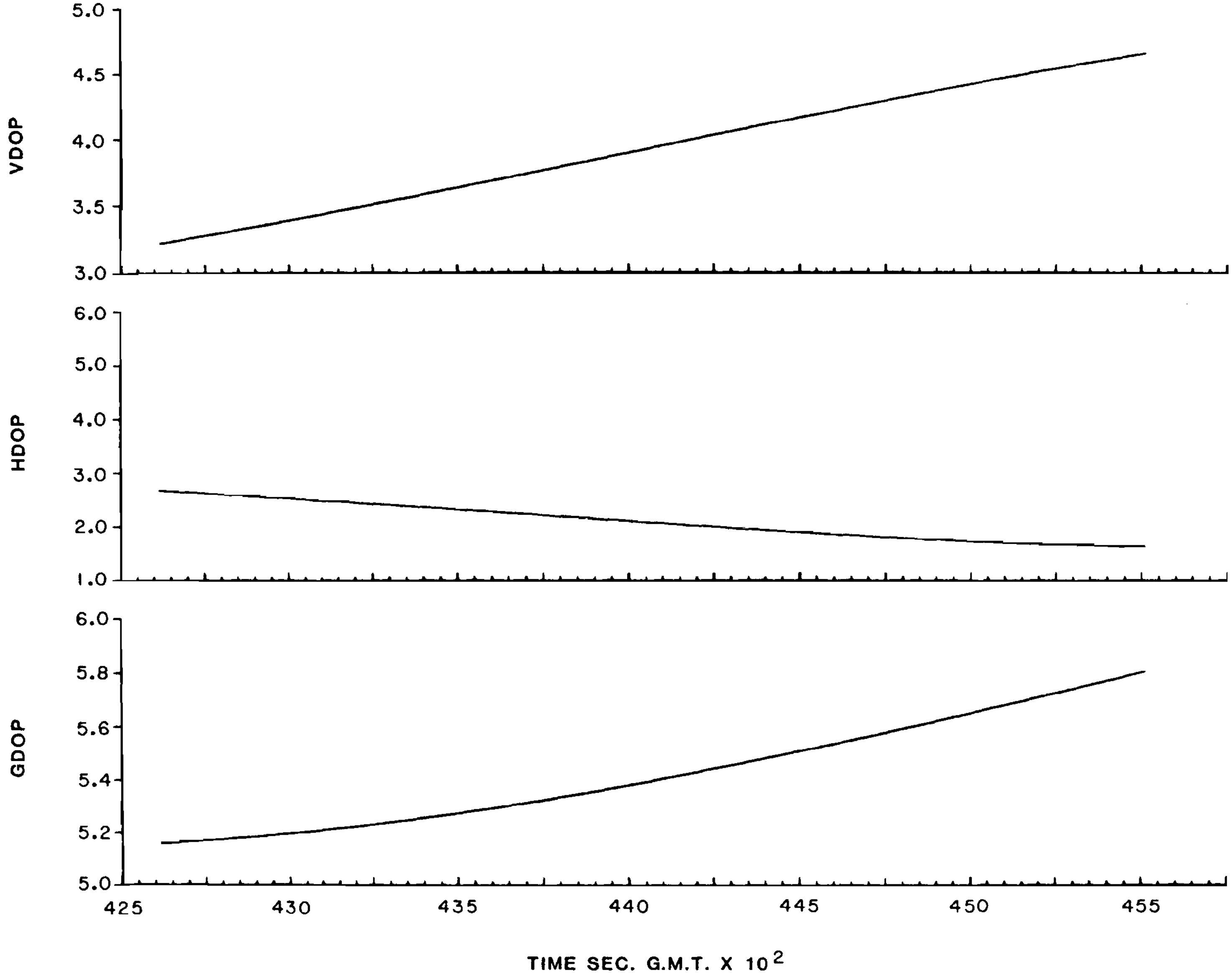

FIG. 4-83. DILUTION OF PRECISION, 4 FEB 83, RUN 1a

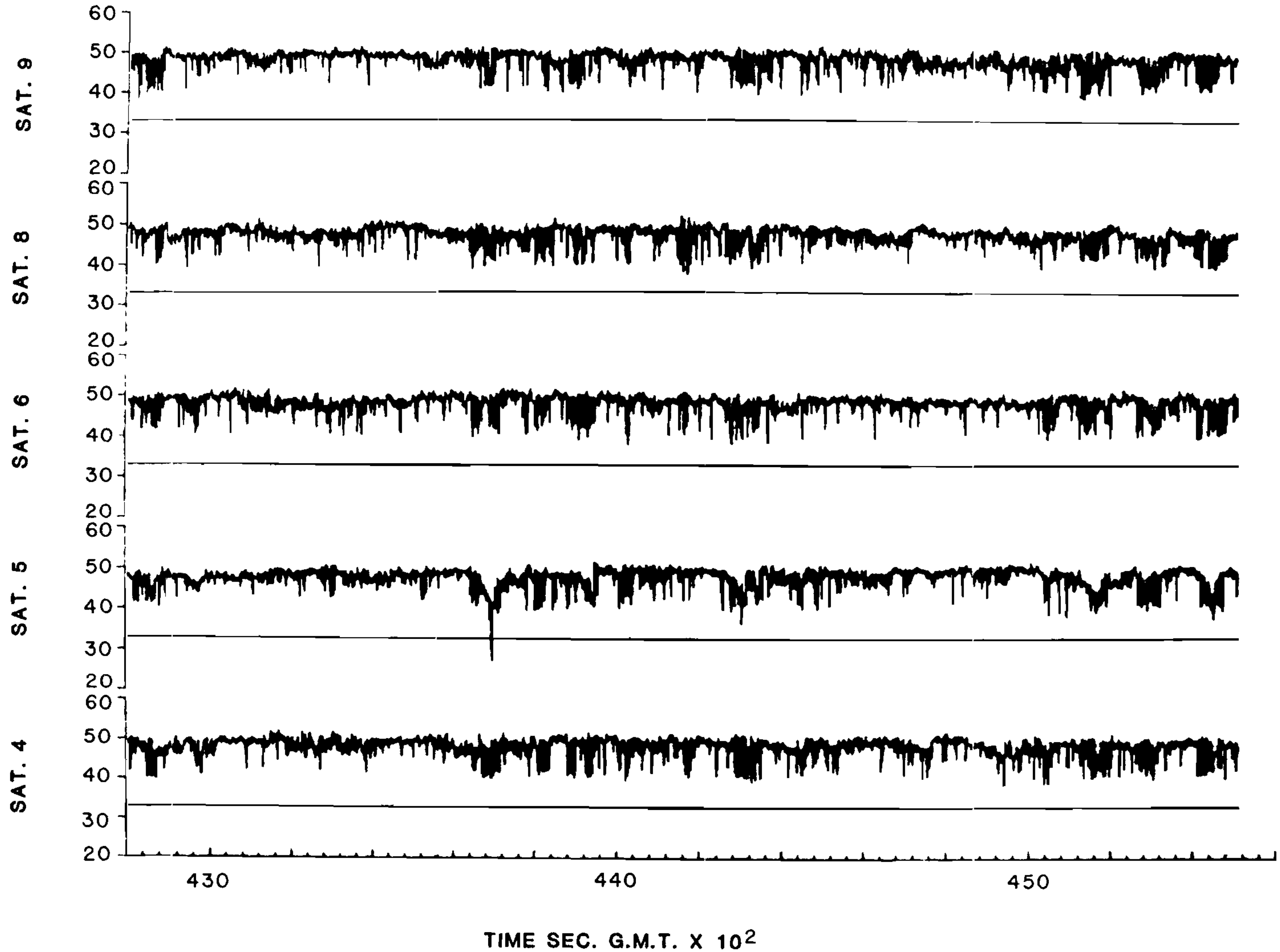

FIG. 4-84. SATELLITE C/NO., 4 FEB 83, RUN 1a

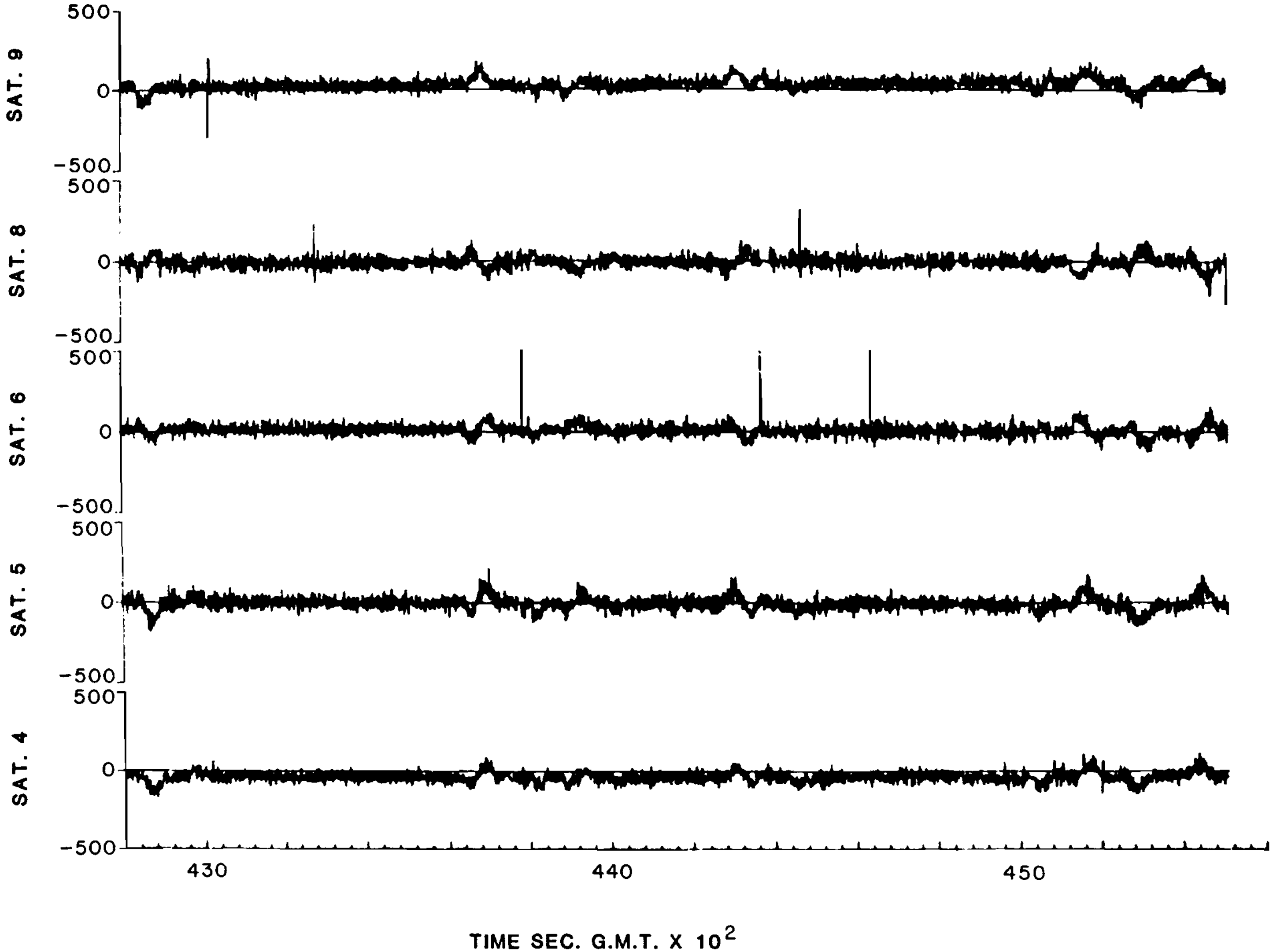

FIG. 4-85. PSEUDORANGE RESIDUALS, 4 FEB 83, RUN 1a

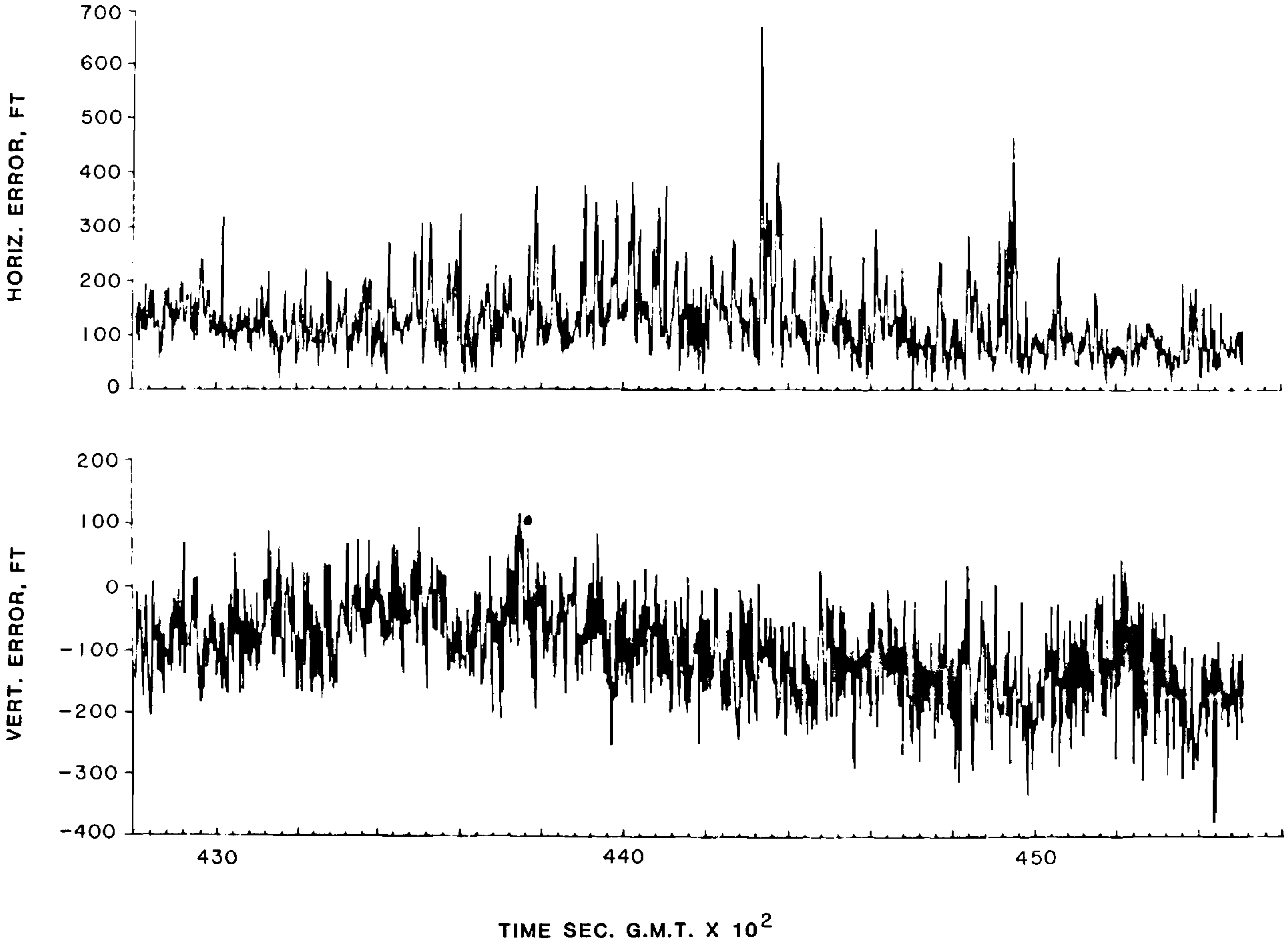

FIG. 4-86a. POSITION FIX ERROR, 4 FEB 83, RUN 1a

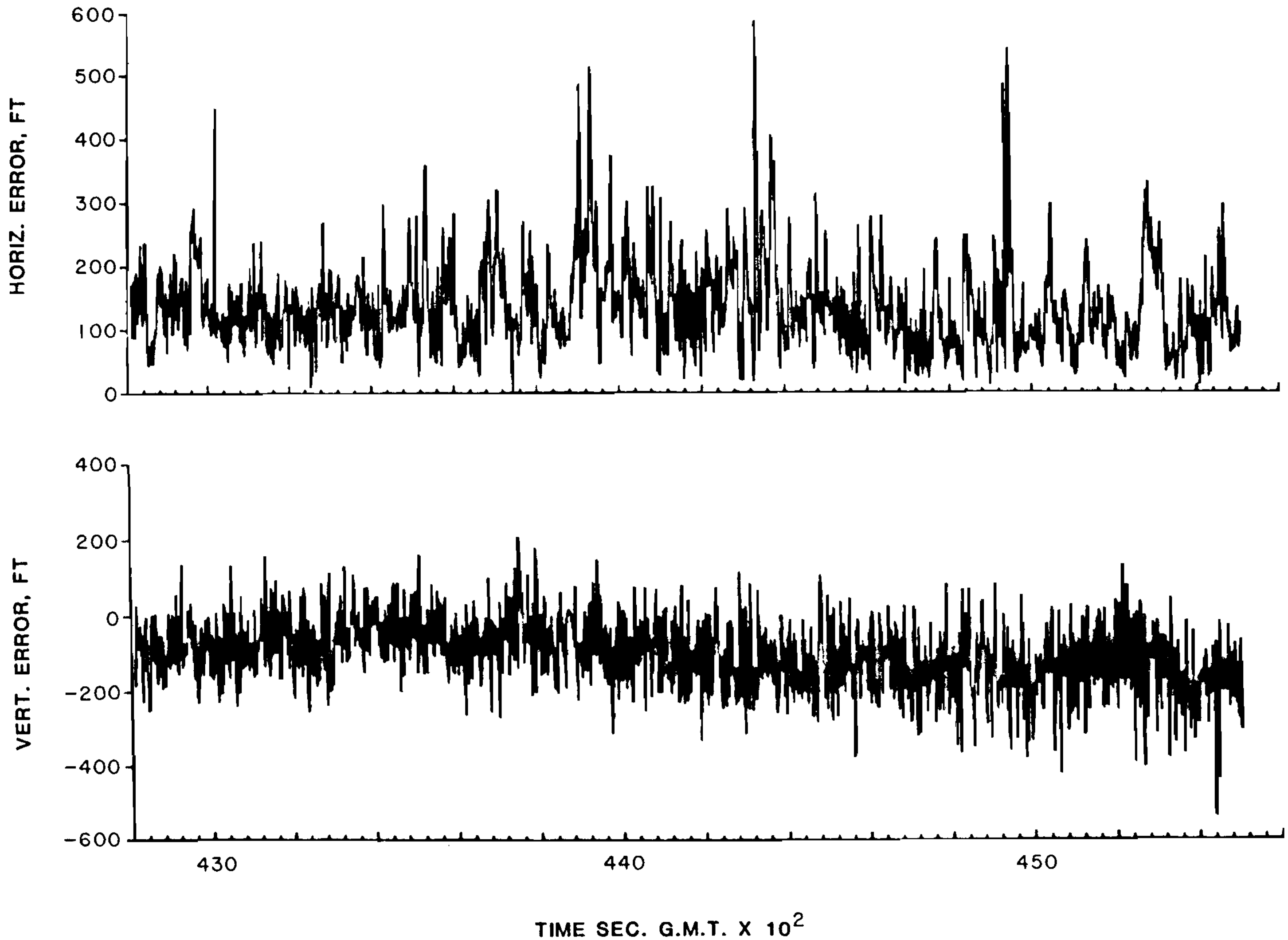

FIG. 4-86b. POSITION ESTIMATE ERROR, 4 FEB 83, RUN 1a

TABLE 4-12.

POSITION ACCURACY STATISTICS,

4 FEBRUARY 1983, RUN 1A

(42806 - 45511)

Position Fixes:

Error	Mean	Standard Deviation	RMS	95%
Horizontal	78	121	144	257 ft
Vertical	104	68	124	221 ft

Tracker Estimates:

Error	Mean	Standard Deviation	RMS	95%
Horizontal	76	134	154	268 ft
Vertical	114	82	140	260 ft

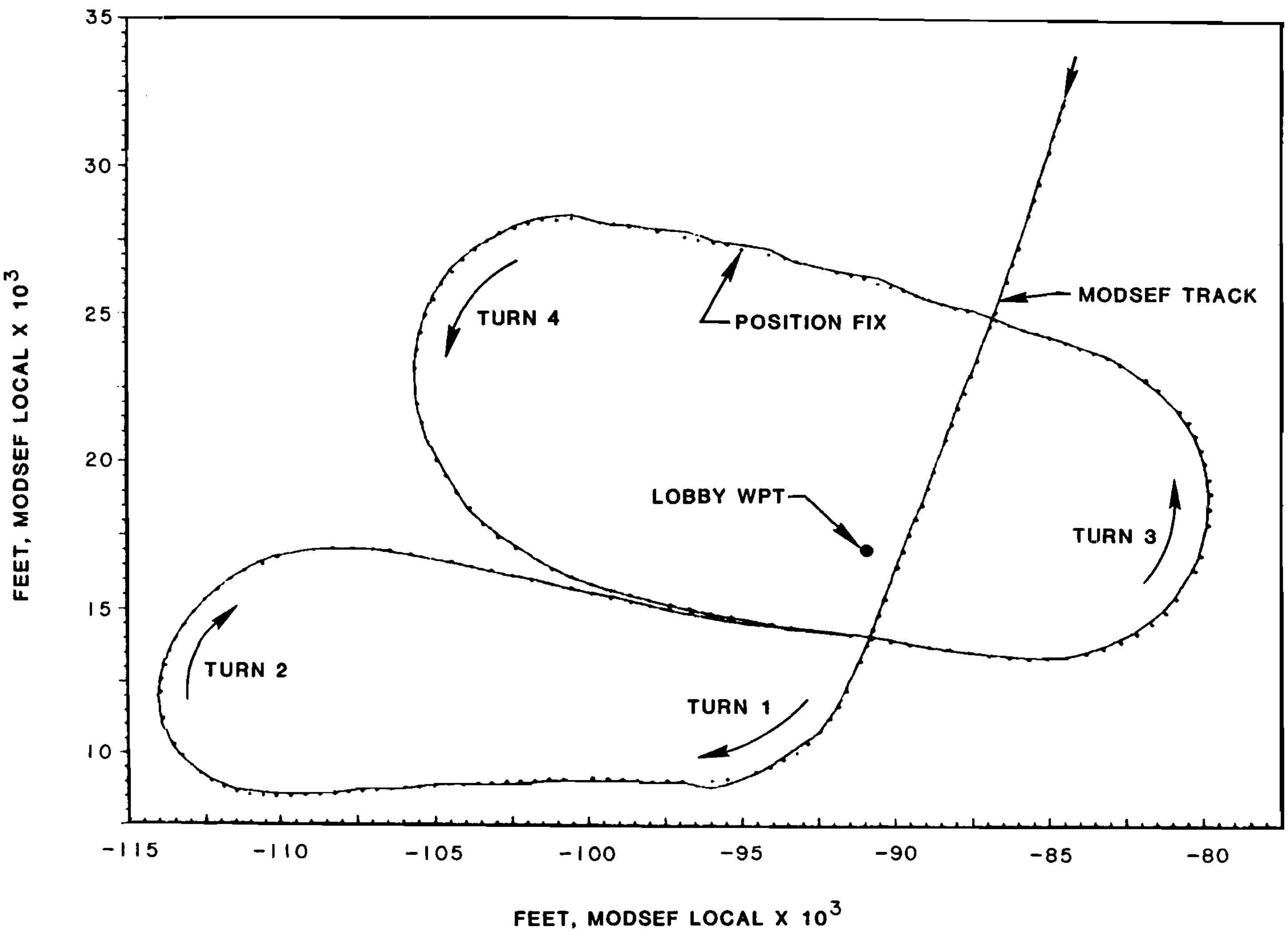

FIG. 4-87. HOLDING PATTERN, 4 FEB 83, RUN 1a: POSITION FIXES

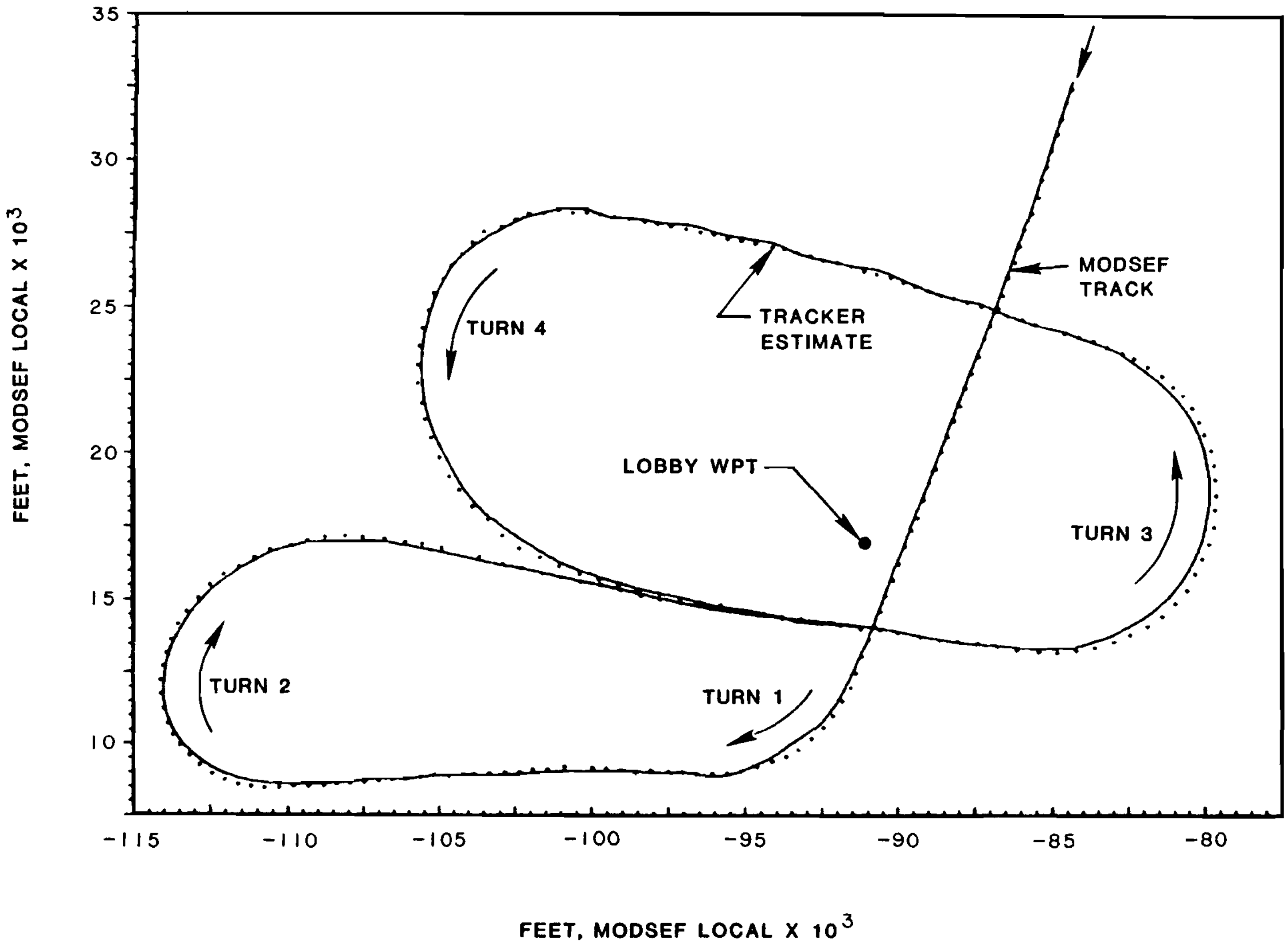

FIG. 4-88. HOLDING PATTERN, 4 FEB 83, RUN 1a: TRACKER ESTIMATES

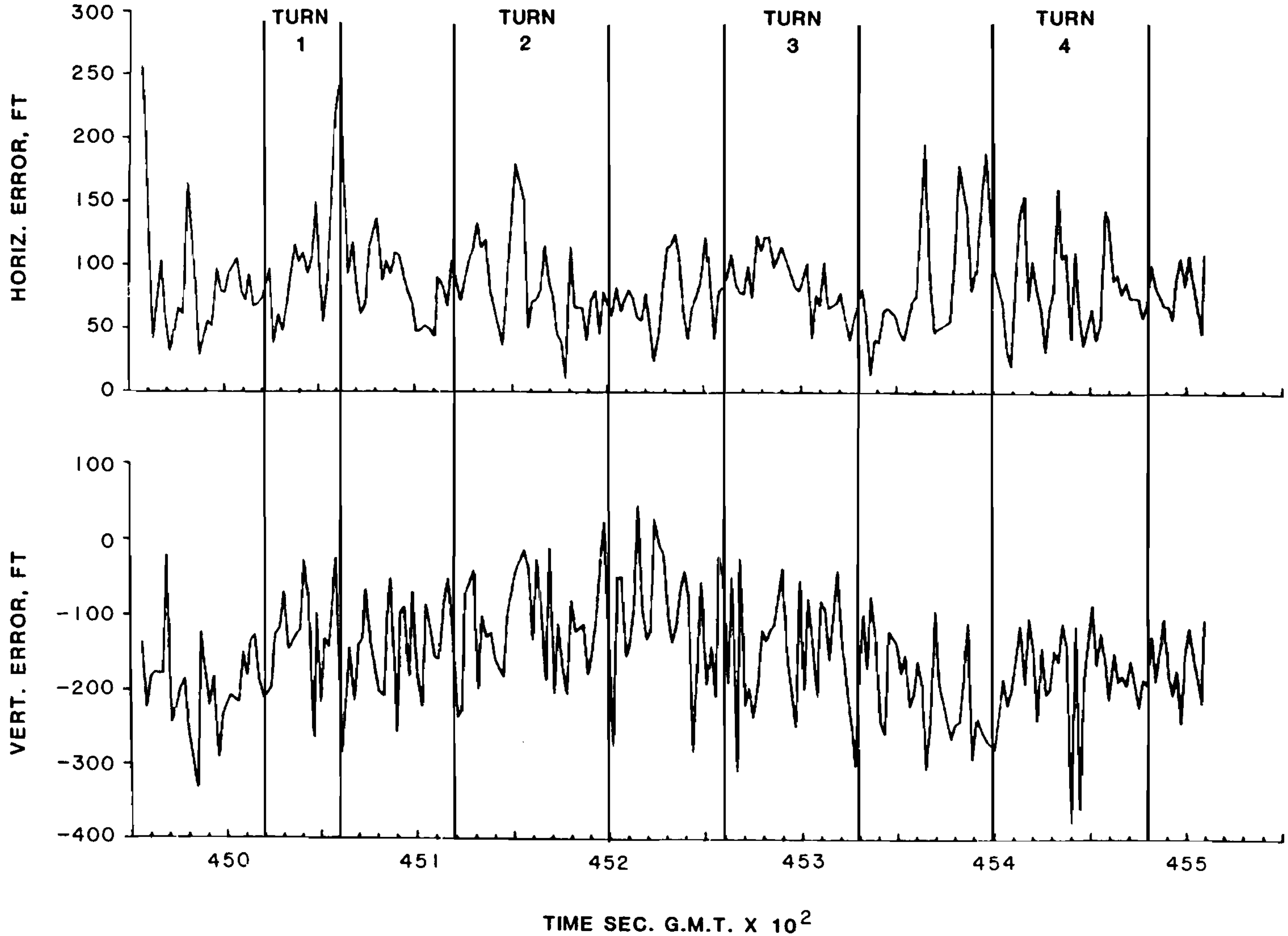

FIG. 4-89. POSITION FIX ERRORS FOR HOLDING PATTERN, 4 FEB 83, RUN 1a

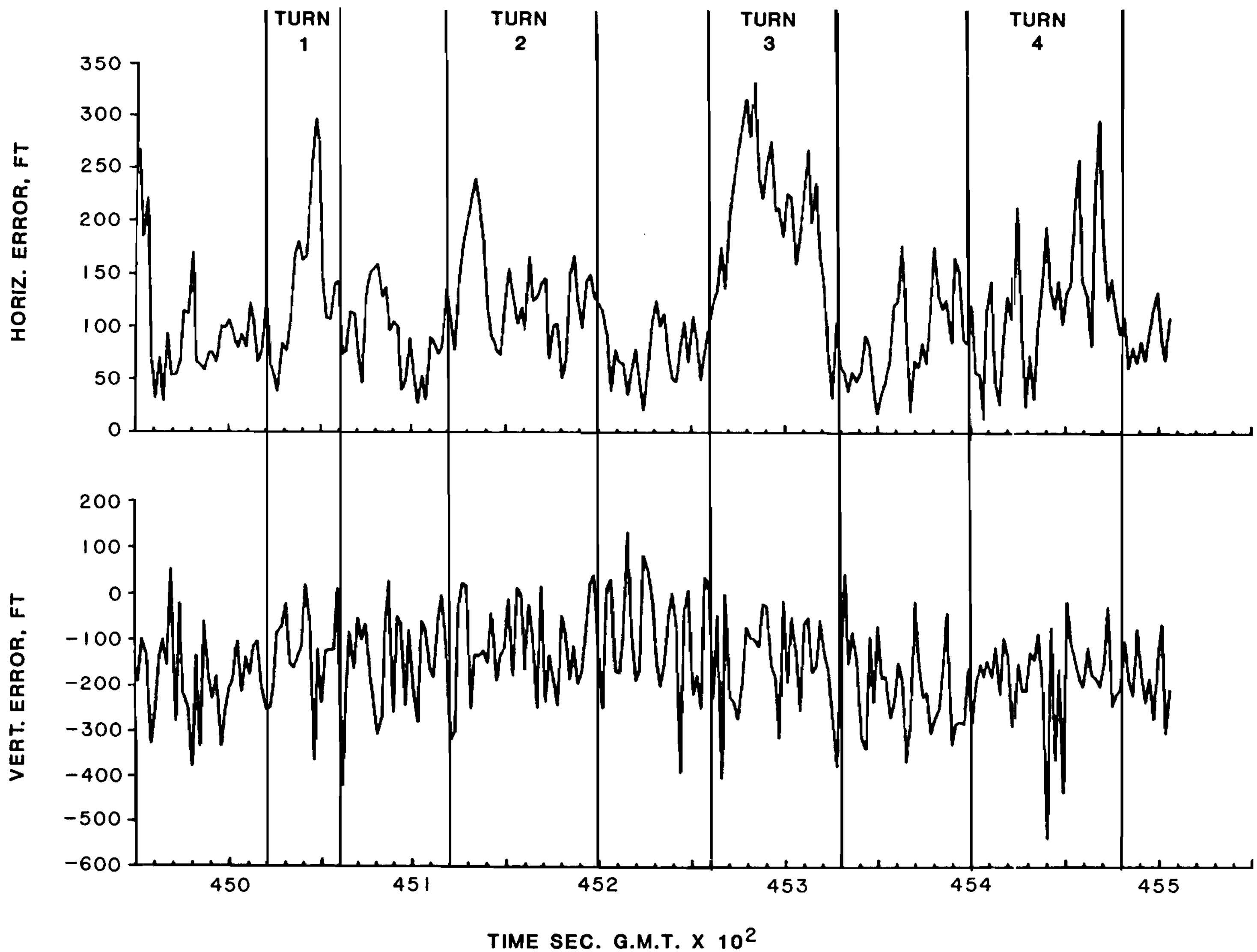

FIG. 4-90. TRACKER ESTIMATE ERROR FOR HOLDING PATTERN, 4 FEB 83, RUN 1a

Figures 4-88 and 4-90 show the performance of the tracker in the holding pattern. It is seen that a considerable bias error occurs in the tracker estimates during some of the turn segments. This bias error is especially noticeable in Turn 3 where the horizontal error increases to as much as 300 feet. A possible explanation for the increased bias error in Turn 3 can be obtained from Fig. 4-91 which shows the altitude and ground speed profile for the holding pattern. It is seen that the ground speed was about 300 feet per second (180 kts) at the beginning of Turn 3 but declined to 200 fps by the end of the turn 60 seconds later. Because this deceleration is unmodelled, the tracker tended to overestimate the distance traveled between fixes at the beginning of the turn. As the ground speed declined, the errors in Turn 3 also declined. By contrast, the ground speed was low at the start of Turn 4 but increased during the turn; consequently, the horizontal errors tended to increase during the turn.

The position error statistics for the holding pattern are shown in Table 4-13. The horizontal error of the tracker estimates is clearly well within the system requirements and goals.

Run 1b on 4 February 1982 was similar to Run 1a, except that a low approach was made at Manchester airport and the aircraft was flown back to the Bedford NDB (BE 1) waypoint instead of the LOBBY waypoint. The accuracy statistics were similar to Run 1a.

4.3.2.3.3 9 February 1983 Test

A second operational test of the type conducted on 4 February 1983 was made on 9 February 1983. Figure 4-92 shows the ground track for Run 1a. For this test, the aircraft took off from Hanscom Field runway 29 (instead of runway 11) due to prevailing wind conditions. After departing the runway, the aircraft was turned 180° toward the Shaker Hills NDB (SKR). The remainder of the run was made according to the test scenario of Fig. 4-79. The gap in the ground track after the turn at the SKR NDB is due to an inadvertent interruption in the data recording; the GPS navigation updates were continuous throughout the run. The altitude and ground speed profile of the run is shown in Fig. 4-93.

The satellite visibilities are shown in Fig. 4-94. Although the visibilities for all five satellites are shown, only four satellites (SVs 4,5,6 and 8) were used for navigation during the run. Despite this the system maintained continuous navigation updates for a period of nearly two hours. The dilution-of-precision calculations for Run 1a are shown in Fig. 4-95. Note that the GDOP for the run is higher than that for the test of 4 February 1983 due to the use of only four satellites.

The horizontal and vertical position fix error versus time is shown in Fig. 4-96. The corresponding data for the tracker estimates is shown in Fig. 4-97. It should be noted that the MODSEF radar tracking data did not start until time = 43085 sec due to difficulties with the radar system; the start of the radar tracking is indicated in Fig. 4-92. The accuracy statistics for the run are summarized in Table 4-14. These statistics compare favorably to the 4 February data.

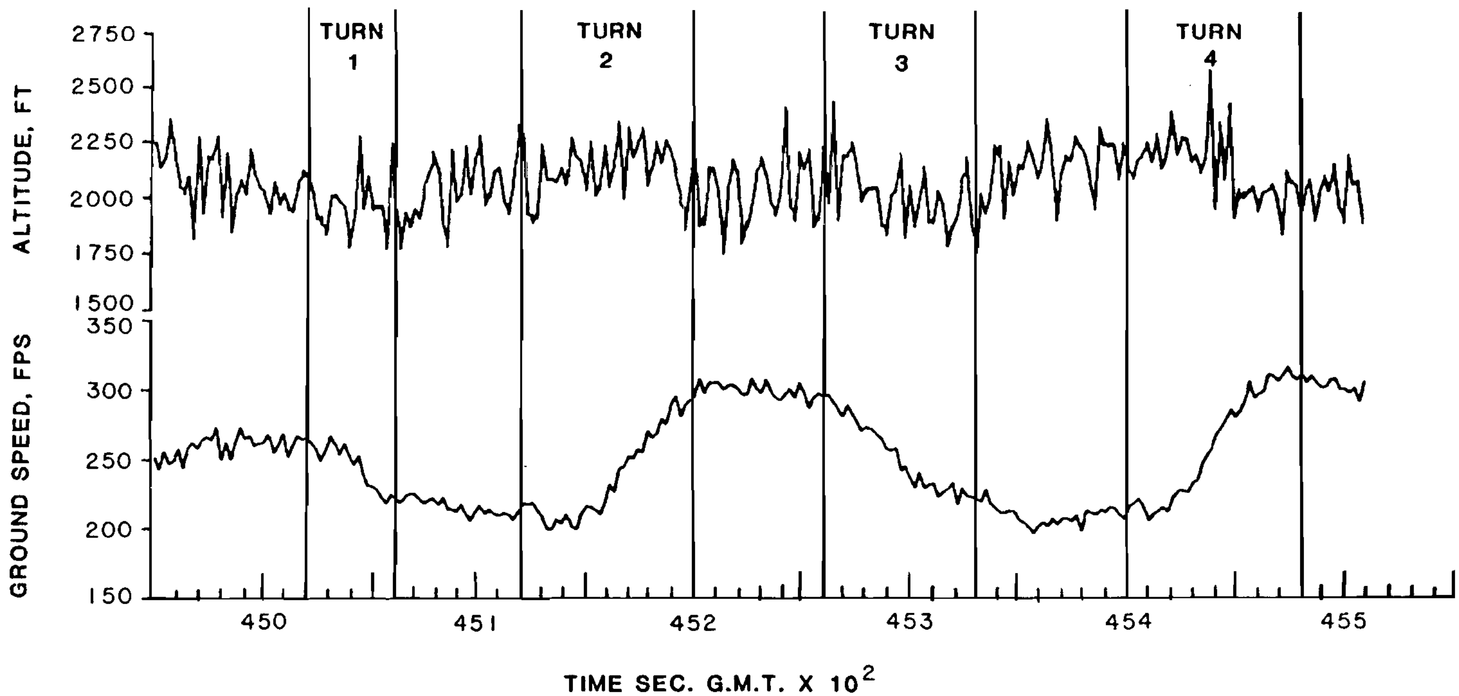

FIG. 4-91. ALTITUDE AND GROUND SPEED FOR HOLDING PATTERN, 4 FEB 83, RUN 1a

TABLE 4-13.

POSITION ACCURACY STATISTICS FOR HOLDING PATTERN

4 FEBRUARY 1983, RUN 1A

Position Fixes:

Error	Mean	Standard Deviation	RMS	95%
Horizontal	55	75	93	155 ft
Vertical	151	73	198	277 ft

Tracker Estimates:

Error	Mean	Standard Deviation	RMS	95%
Horizontal	49	49	70	253 ft
Vertical	157	98	185	331 ft

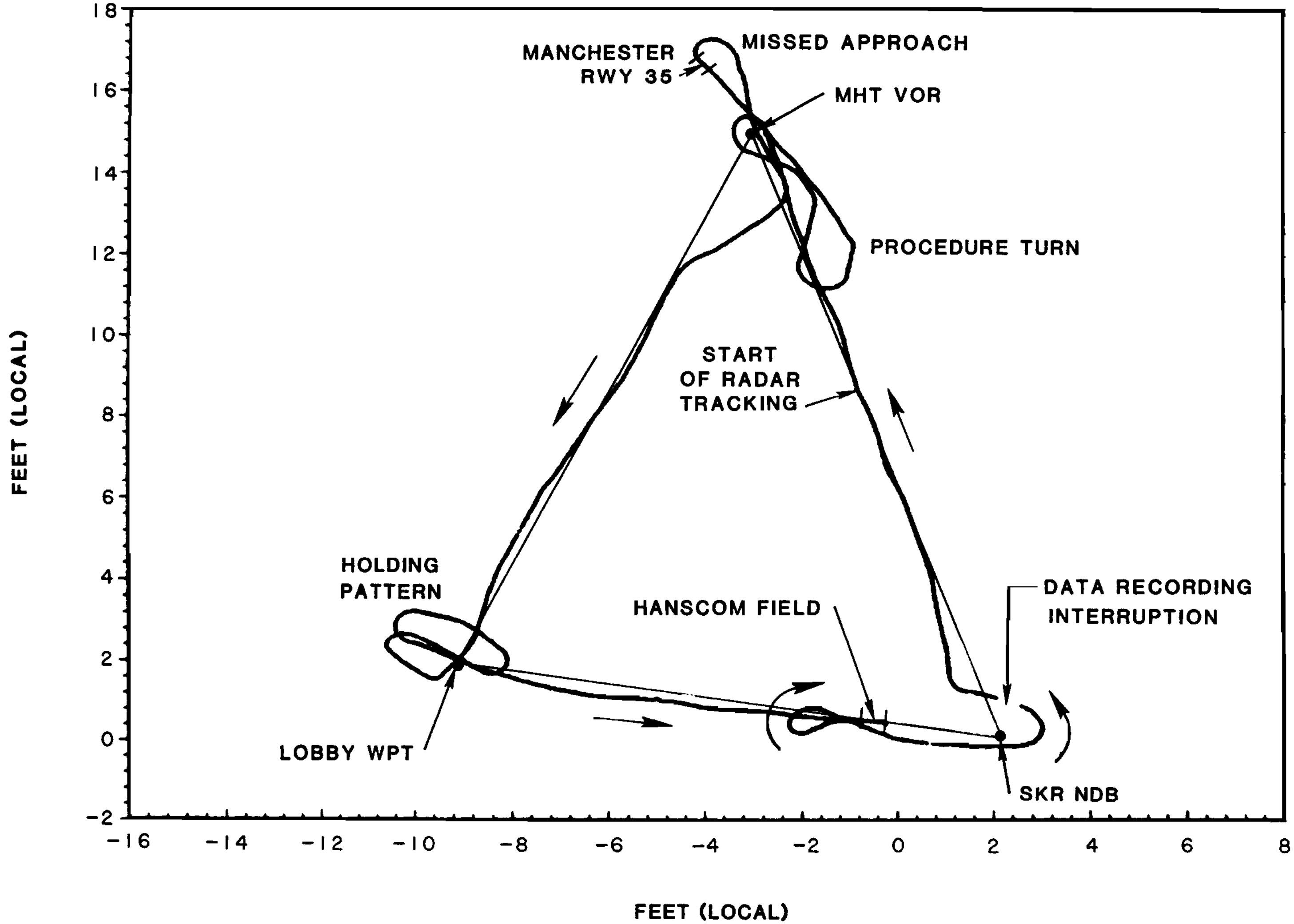

FIG. 4-92. OPERATIONAL FLIGHT TEST, 9 FEB 83, RUN 1a

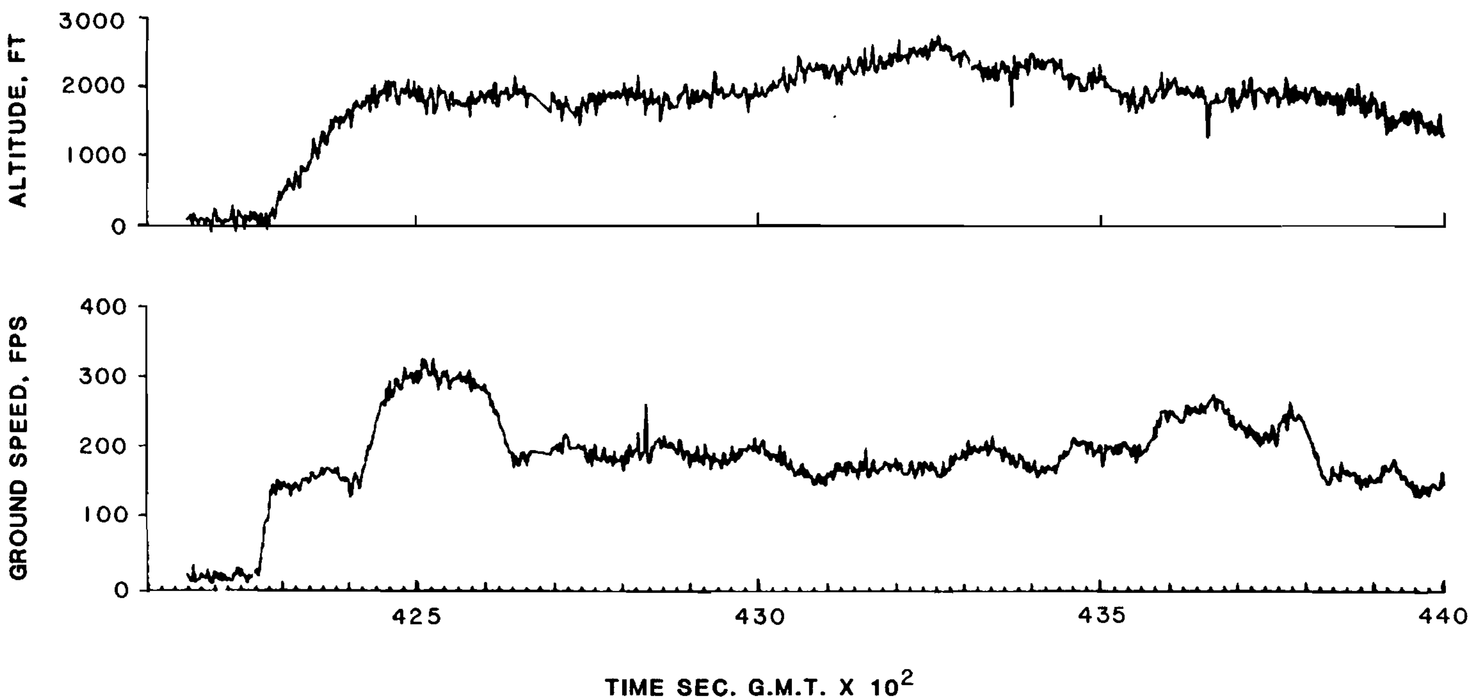

FIG. 4-93. ALTITUDE AND GROUND SPEED, 9 FEB 83, RUN 1a (1 OF 2)

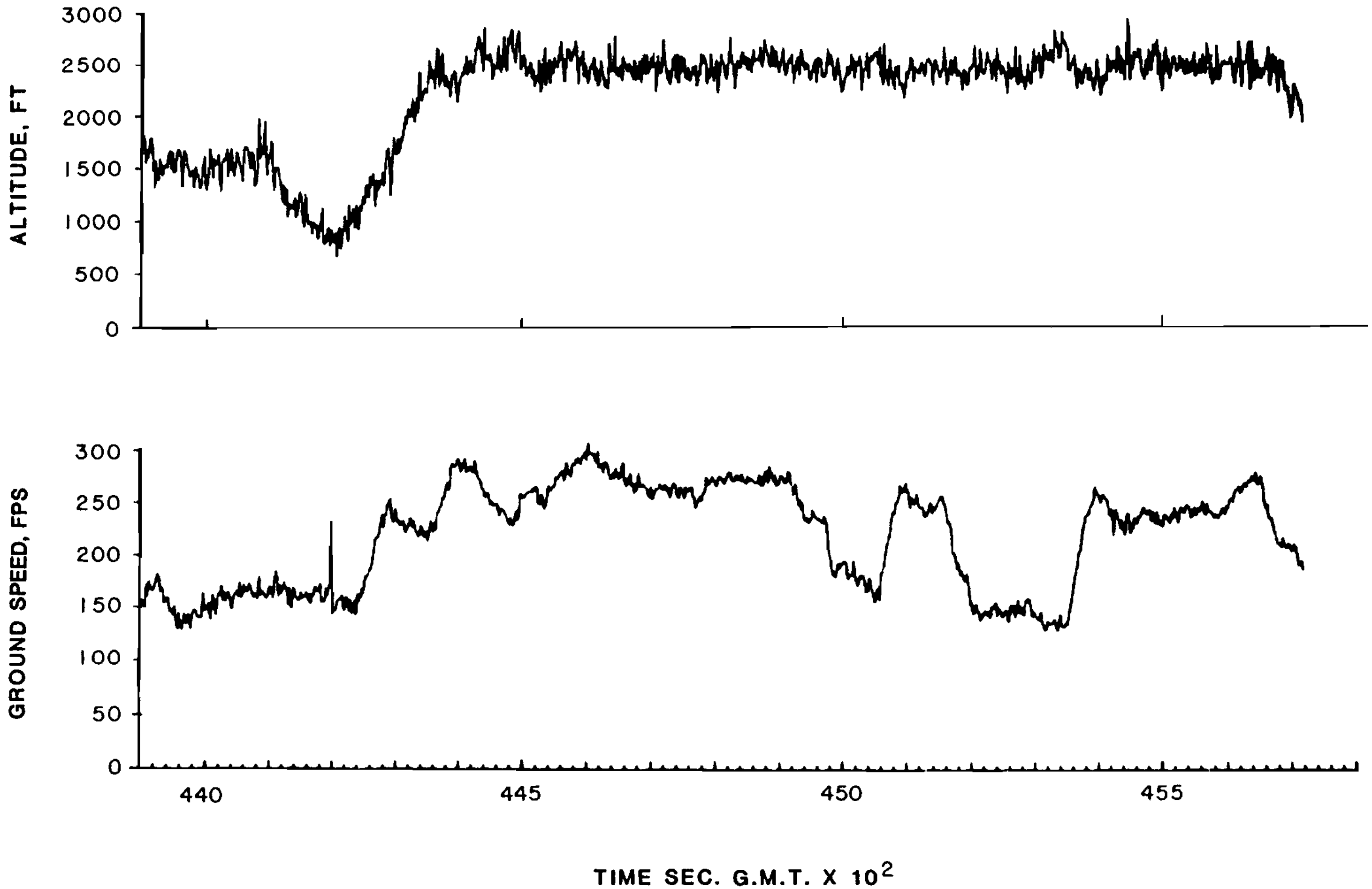

FIG. 4-93. ALTITUDE AND GROUND SPEED, 9 FEB 83, RUN 1 (2 OF 2)

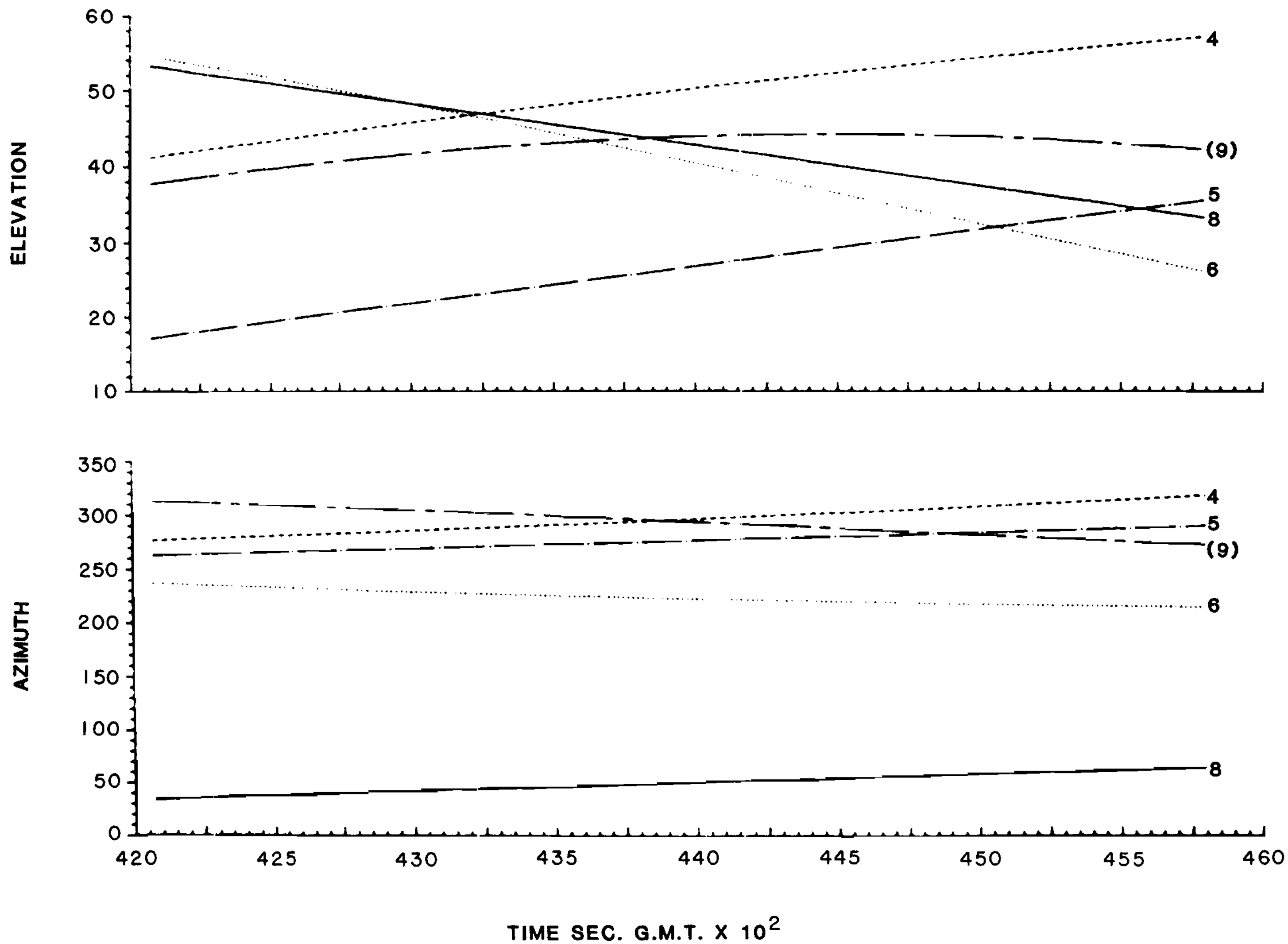

FIG. 4-94. SATELLITE VISIBILITIES, 9 FEB 83, RUN 1a

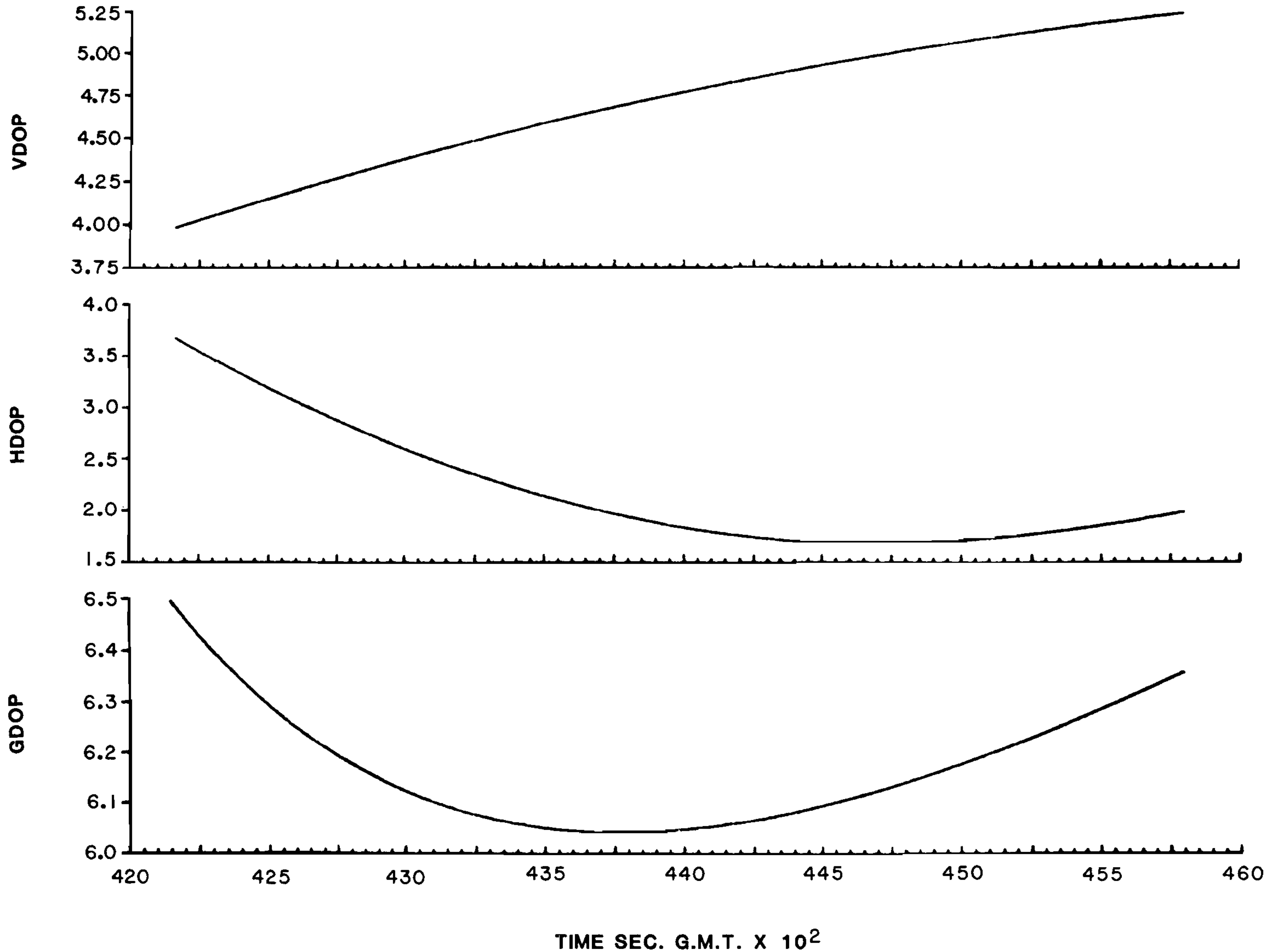

FIG. 4-95. DILUTION OF PRECISION, 9 FEB 83, RUN 1a

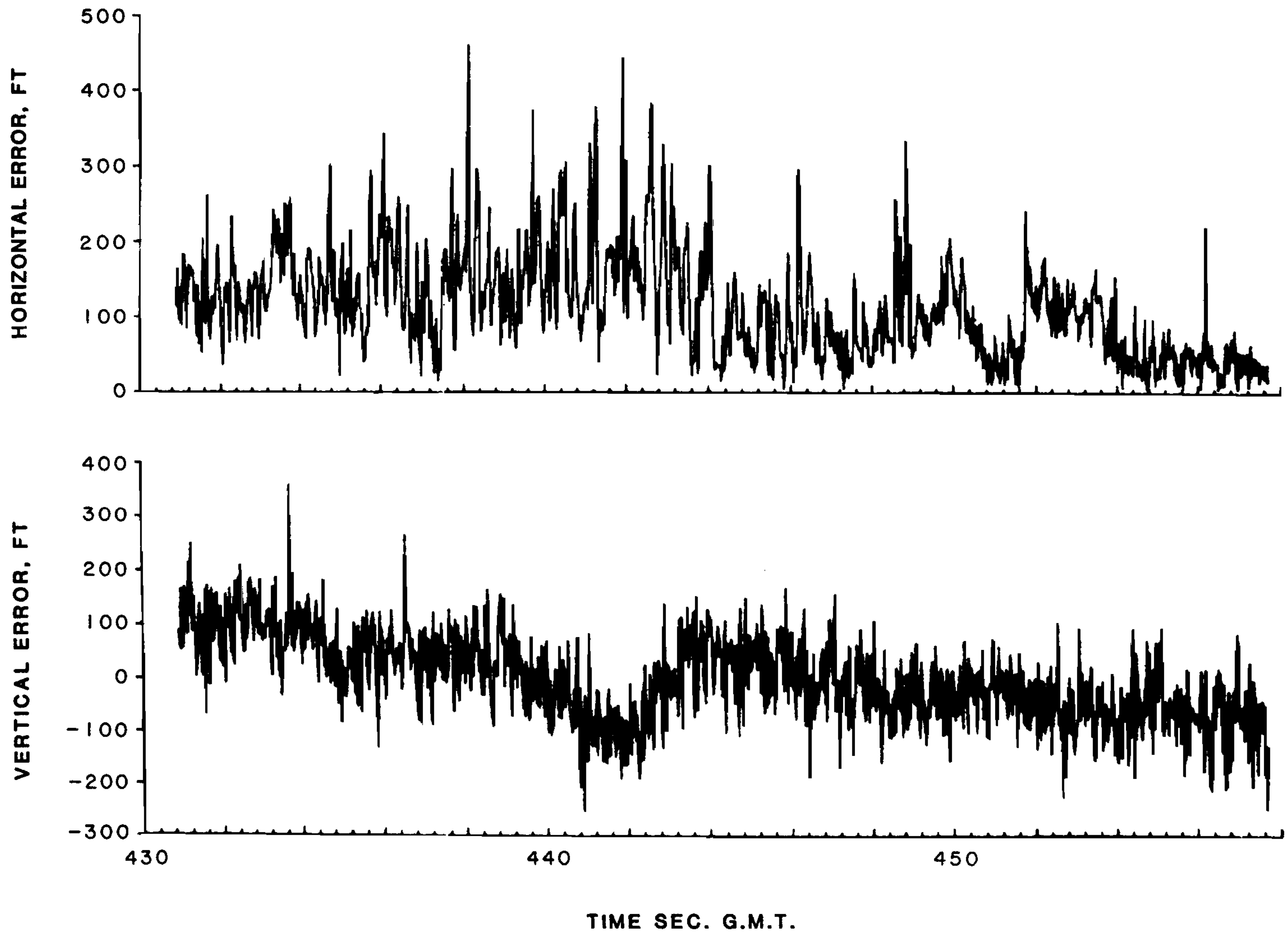

FIG. 4-96. POSITION FIX ERROR, 9 FEB 83, RUN 1a

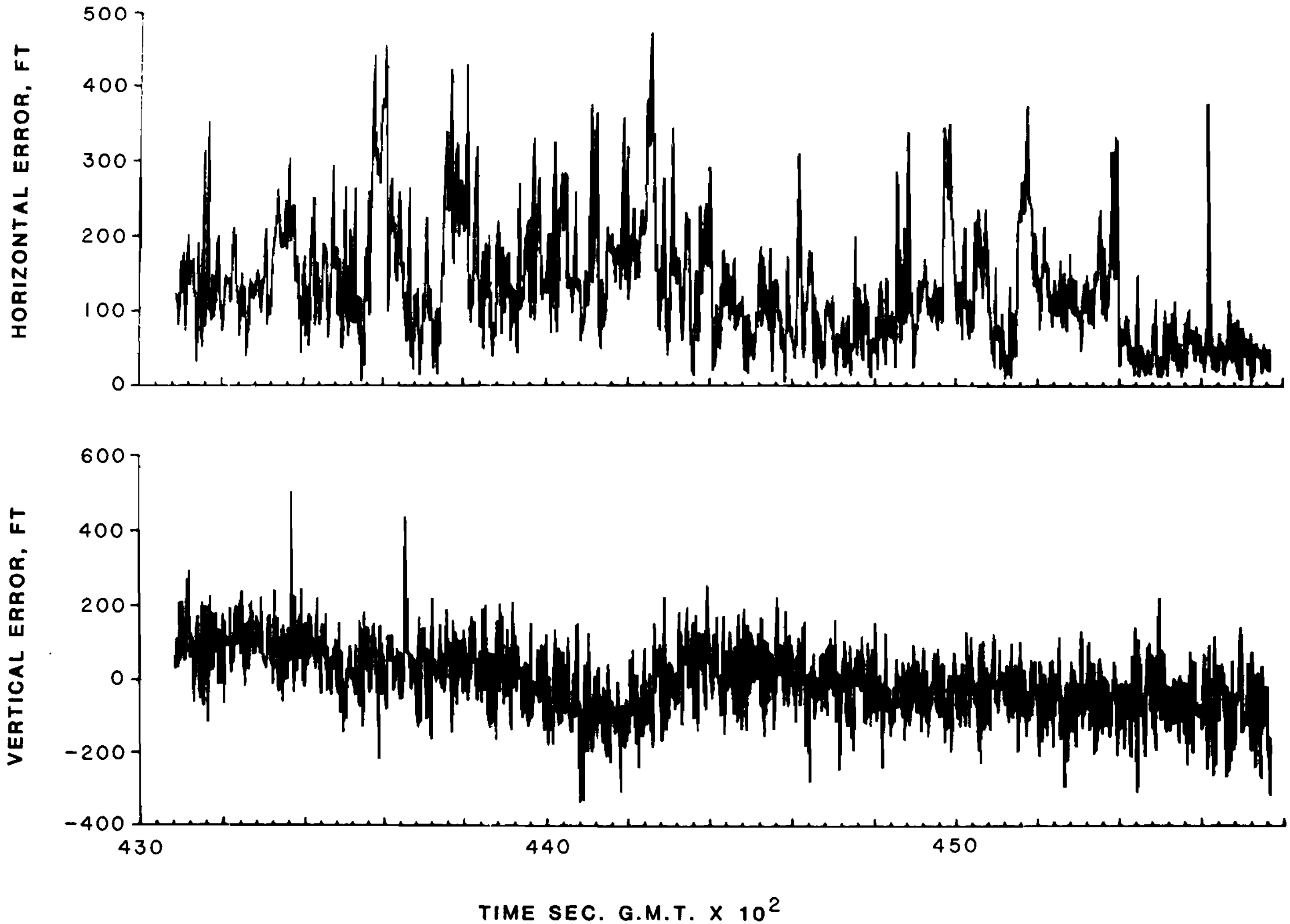

FIG. 4-97. TRACKER ESTIMATE ERROR, 9 FEB 83, RUN 1a

TABLE 4-14.

POSITION ACCURACY STATISTICS FOR 9 FEBRUARY 1983

RUN 1A (43085 - 45770)

Position Fixes:

Error	Mean	Standard Deviation	RMS	95%
Horizontal	73	112	134	260 ft
Vertical	68	48	83	158 ft

Tracker Estimates:

Error	Mean	Standard Deviation	RMS	95%
Horizontal	73	135	154	299 ft
Vertical	84	62	105	198 ft

At the end of run 1a, the aircraft had completed one complete circuit around the test course so a second circuit as started (run 1b) as shown in Fig. 4-98. The aircraft made a low-approach at 500 feet over Hanscom Field and proceeded to the Shaker Hills waypoint. The run terminated near the LOBBY waypoint when SV6 dropped below the 5° elevation angle mask. The altitude and ground speed profiles for run 1b are shown in Fig. 4-99.

The satellite visibilities for run 1b are shown in Fig. 4-100. Again note that SV9, although included in the figure, was not used for navigation. Note also at the end of the run that SV6 had dropped below the nominal 5° elevation angle mask. The dilution-of-precision values for the run are shown in Fig. 4-101.

Figure 4-102 shows the satellite C/N_0 values for the latter portion of run 1b. Note that the SV6 C/N_0 value at the end of the run is above the 33 dB-Hz loss-of-lock threshold. The satellite C/N_0 does drop below the threshold several times during the initial turn of the holding pattern but the satellite is quickly re-established in track on each occasion.

The horizontal and vertical position fix error vs. time is shown in Fig. 4-103. The corresponding tracker estimate error is shown in Fig. 4-104. The position accuracy statistics are summarized in Table 4-15. In general, the position accuracy is seen to be less for run 1b than Run 1a; however, the GDOP has also become larger in the latter run as seen from Fig. 4-101.

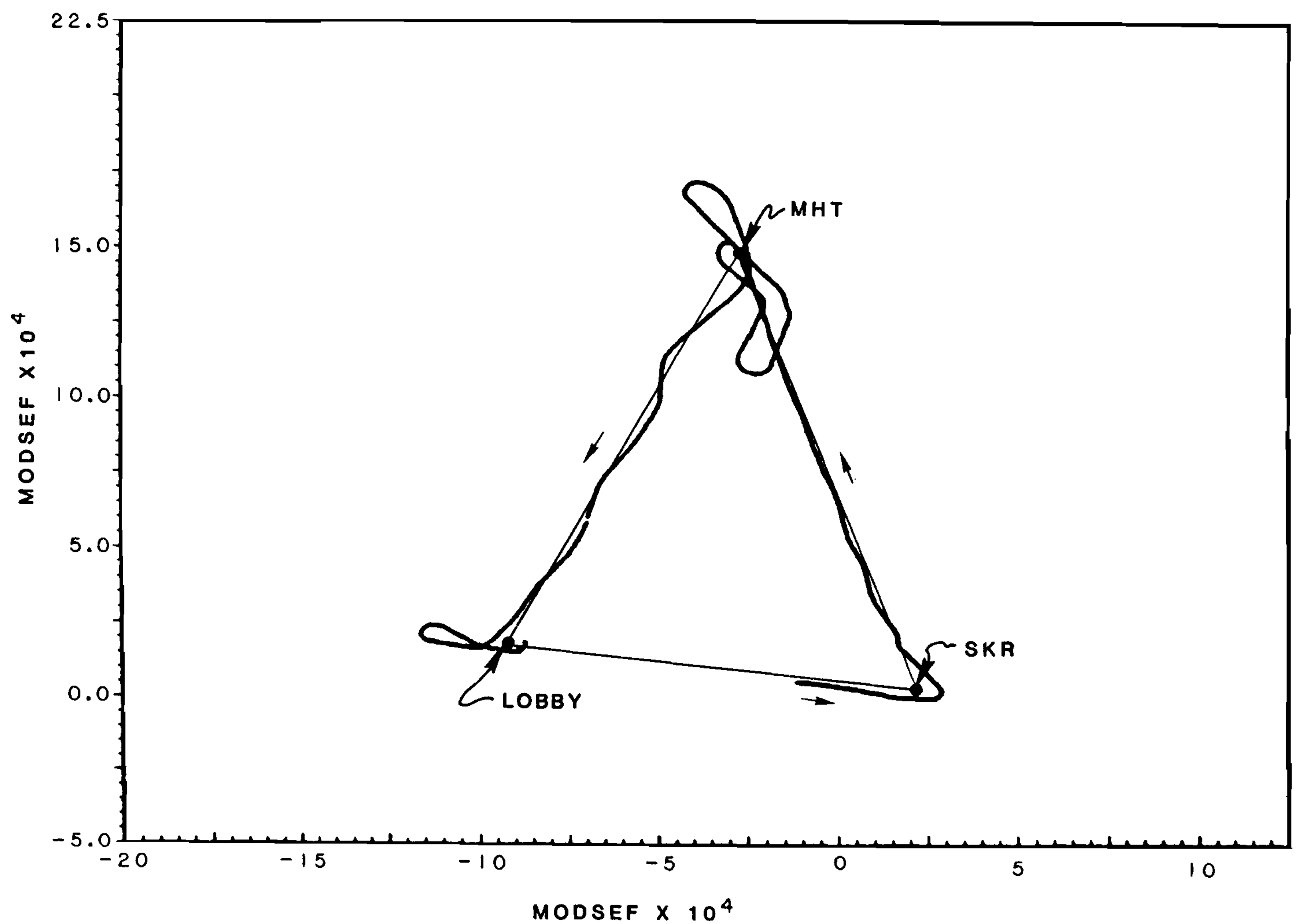

FIG. 4-98. OPERATIONAL TEST, 9 FEB 83, RUN 16

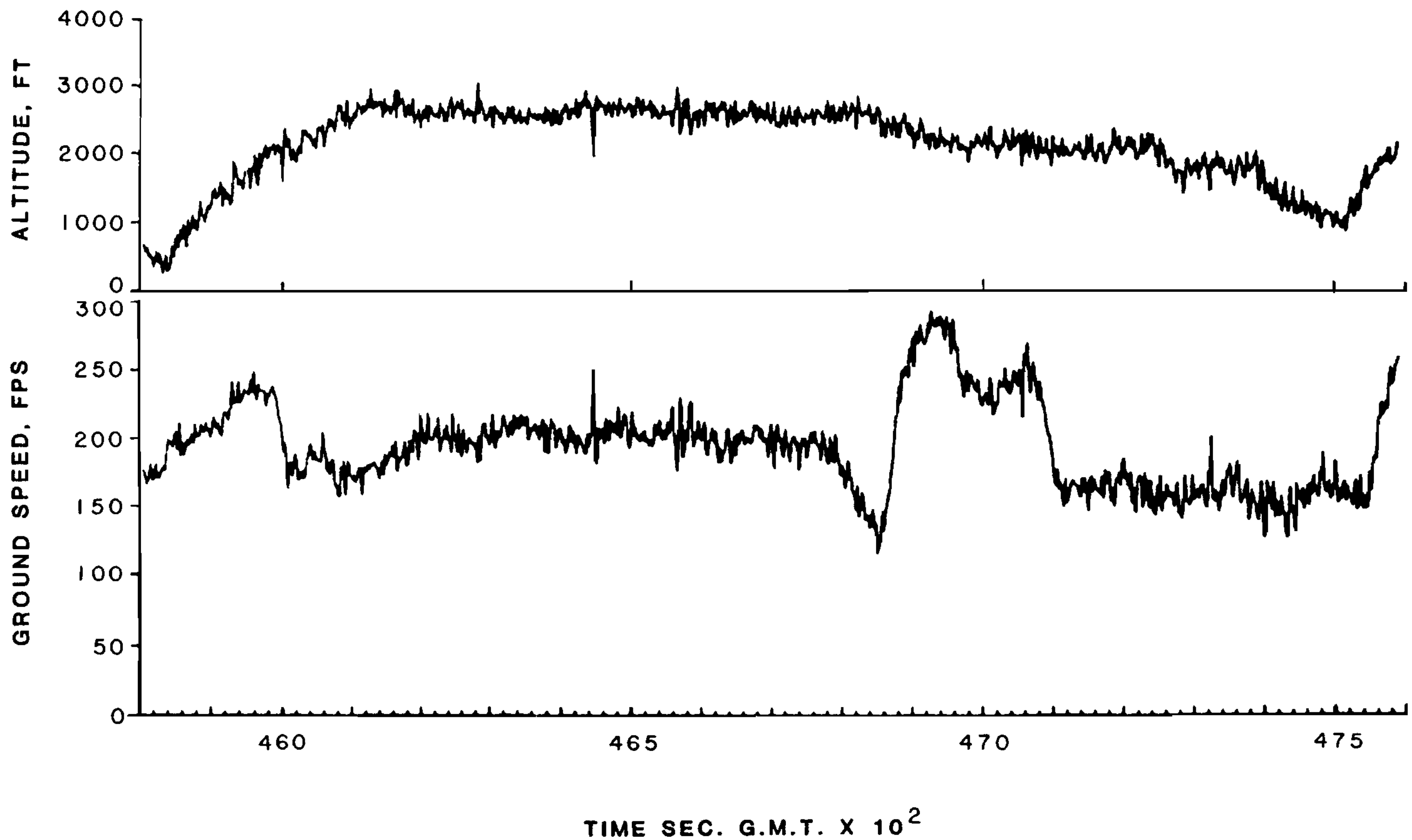

FIG. 4-99. ALTITUDE AND GROUND SPEED, 9 FEB 83, RUN 1b (1 OF 2)

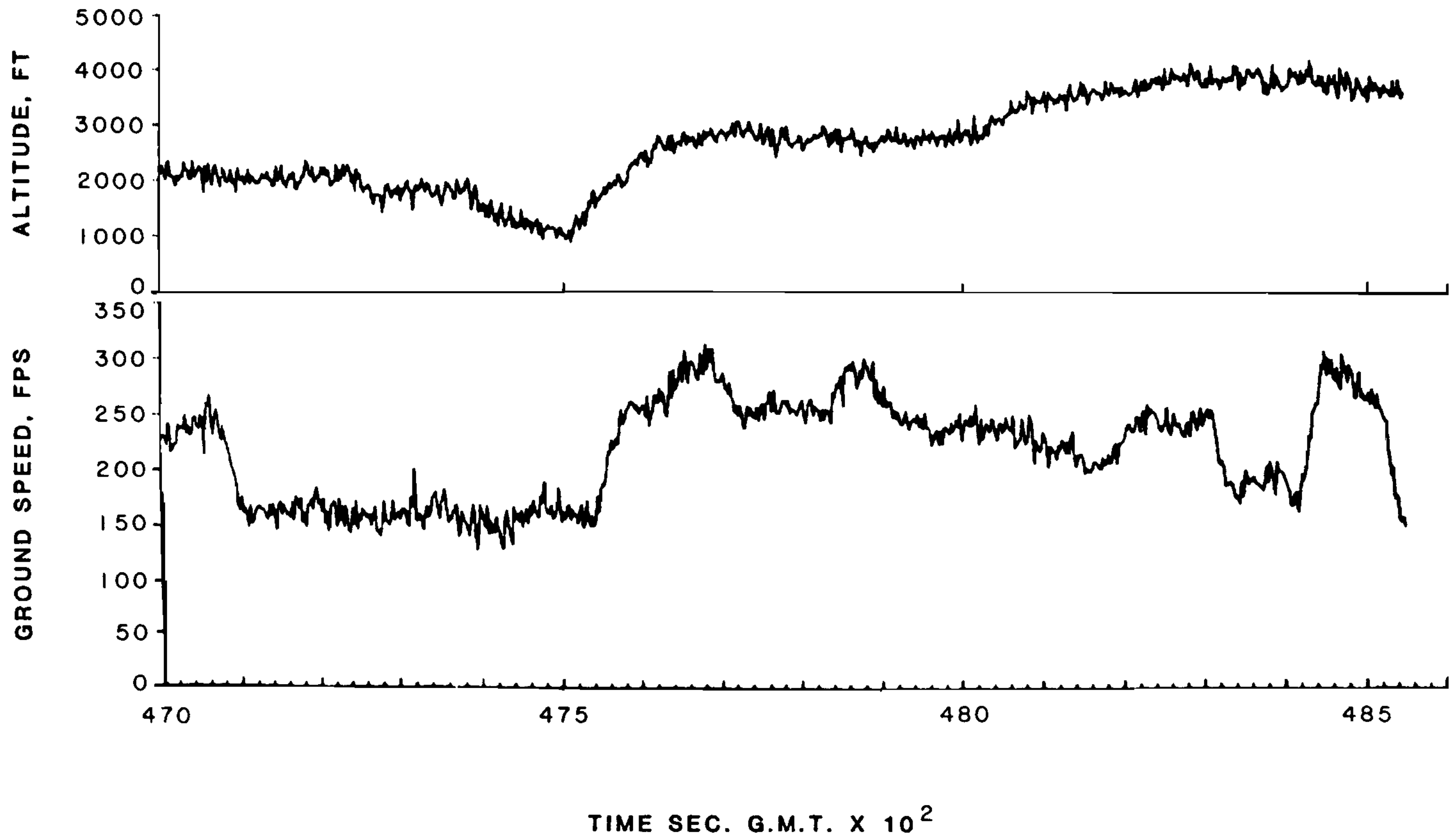

FIG. 4-99. ALTITUDE AND GROUND SPEED, 9 FEB 83, RUN 1b (2 OF 2)

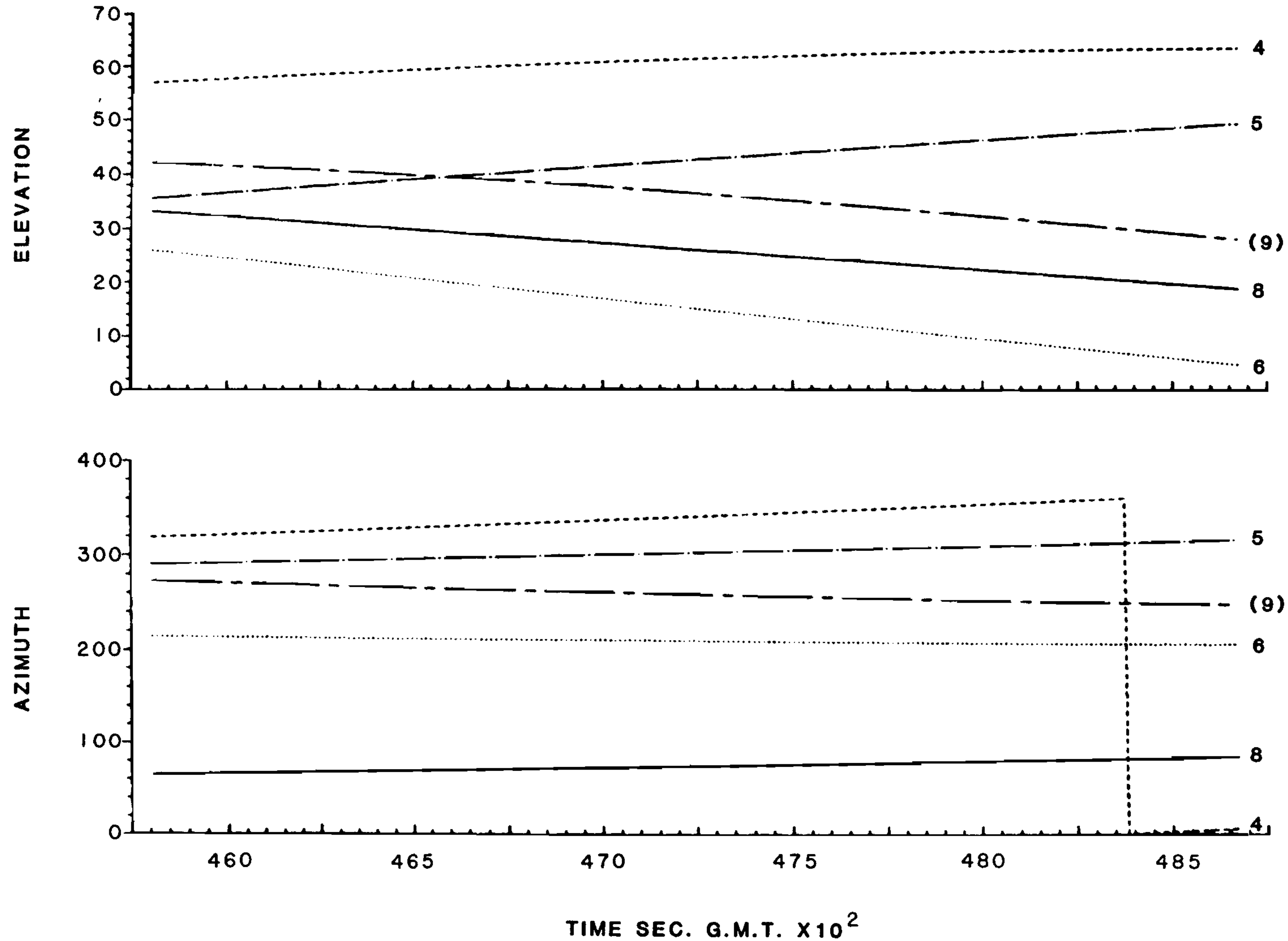

FIG. 4-100. SATELLITE VISIBILITIES, 9 FEB 83, RUN 1b

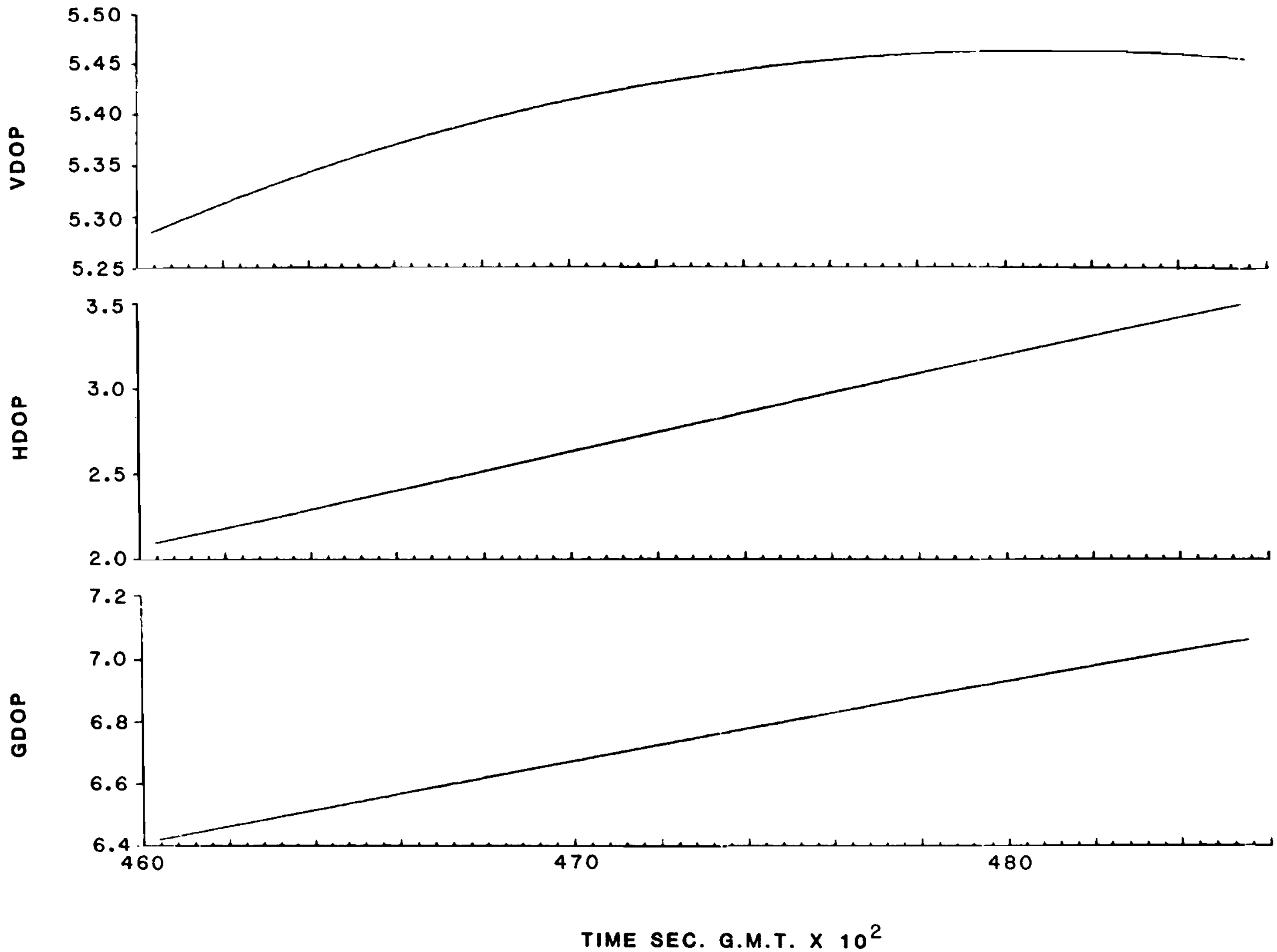

FIG. 4-101. DILUTION-OF-PRECISION VALUES, 9 FEB 83, RUN 1b

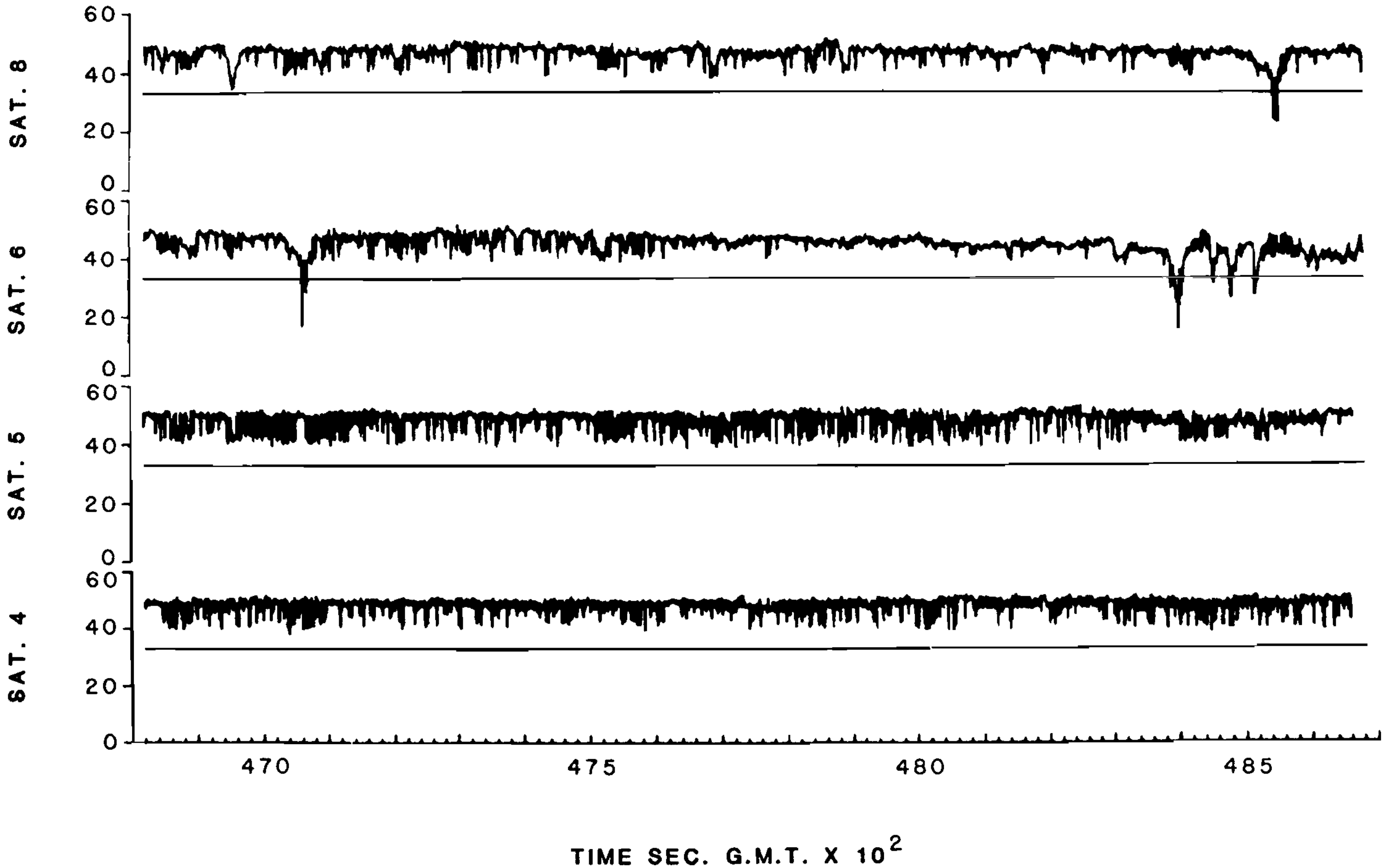

FIG. 4-102. SATELLITE C/NO. VALUES, 9 FEB 83, RUN 1b

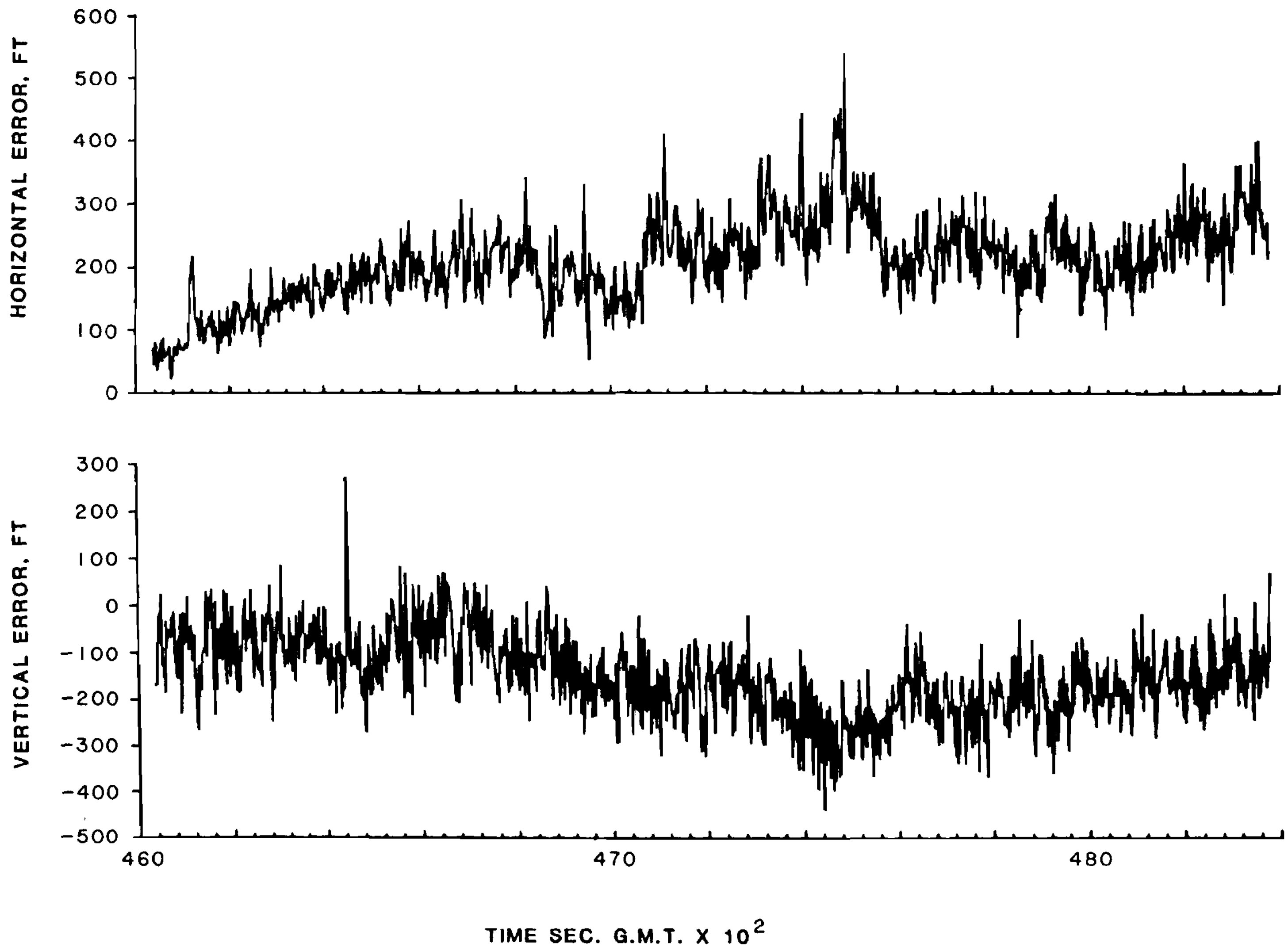

FIG. 4-103. POSITION FIX ERROR, 9 FEB 83, RUN 1b

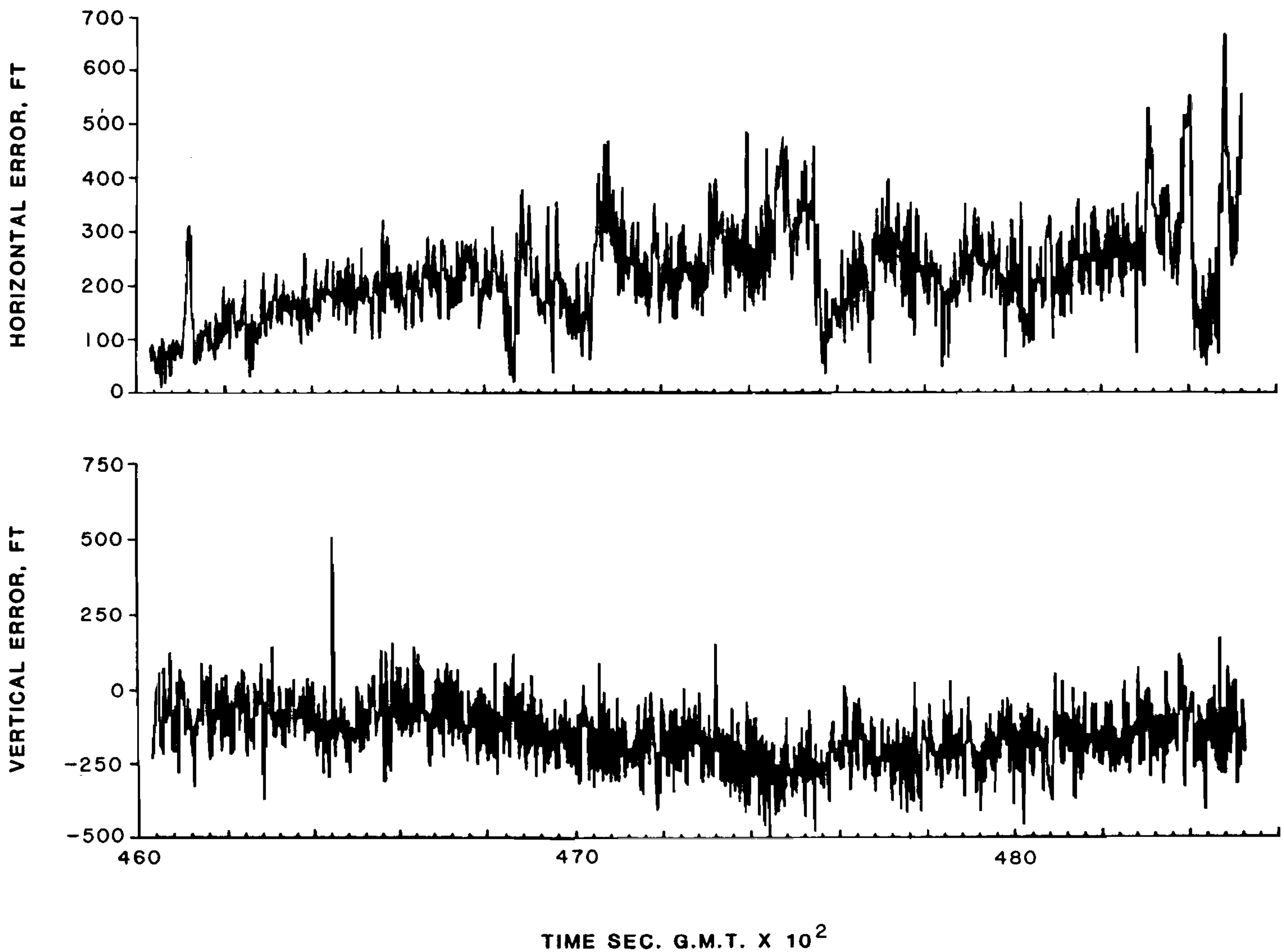

FIG. 4-104. TRACKER ESTIMATE ERROR, 9 FEB 83, RUN 1b

TABLE 4-15.

POSITION ACCURACY STATISTICS FOR 9 FEBRUARY 1983

RUN 1B (46030 - 48580)

Position Fixes:

Error	Mean	Standard Deviation	RMS	95%
Horizontal	185	117	219	322 ft
Vertical	153	83	174	293 ft

Tracker Estimates:

Error	Mean	Standard Deviation	RMS	95%
Horizontal	191	142	238	378 ft
Vertical	159	97	186	329 ft

4.3.2.4 Summary of Operational Flight Test Results

The operational flight tests demonstrated the use of the GPS C/A code navigator in mountainous terrain, at a large urban airport and in typical general aviation operations. The position accuracy for the operational flight tests in the Hanscom Field/Manchester Airport is summarized in Table 4-16. These statistics combine the results from 4 February 1983 (Run 1a), 9 February 1983 (Runs 1a and 1b) and 10 February 1983 (Run 2) into a single run lasting 2.7 hours. As seen from the table, the 95% horizontal accuracy of the tracker estimates was 333 feet, which easily meets the 0.3 nm accuracy requirement of AC90-45A for two-dimensional area navigation. This performance also essentially meets the proposed 328 foot (95%) accuracy requirements of the Federal Navigation Plan for non-precision approach.

The operational flight tests also demonstrated the compatibility of the GPS system with current air navigation practices and procedures. The test pilots responded favorably to the operation of the system, noting in particular that the GPS navigator gave a more stable cross-track deviation indication for non-precision approach than that provided by a VOR receiver. It was also noted that the GPS could obtain the course and distance to a selected waypoint while on the ground, a feature not always available with a conventional RNAV unit due to VOR coverage.

It was found that the GPS system was able to maintain navigation in the mountainous area near the Burlington, VT Airport and in the vicinity of large buildings at Logan International Airport. The system was able to maintain satellites in track to elevation angles as low as 5°, even when on the ground.

The system was generally able to maintain satellites in track during turns with only temporary loss of lock. The system was able to recover from the temporary loss of satellite without a substantial effect on the system position accuracy. It was seen that the horizontal position accuracy was maintained when the system was forced to navigate with three satellites during the temporary loss of one satellite in a turn.

TABLE 4-16.

POSITION ACCURACY STATISTICS FOR OPERATIONAL FLIGHT TESTS

4-10 FEBRUARY 1983

Position Fixes:

Error	Mean	Standard Deviation	RMS	95%
Horizontal	98	143	174	305 ft
Vertical	103	78	129	242 ft

Tracker Estimates:

Error	Mean	Standard Deviation	RMS	95%
Horizontal	98	161	189	333 ft
Vertical	115	93	148	277 ft

5.0 FUNCTIONAL REQUIREMENTS OF A GENERAL AVIATION RECEIVER

The results of testing the GPS Tests and Evaluation System evaluation of the GPS T and E equipment indicate that a general aviation GPS navigator should satisfy the following functional requirements:

5.1 General Requirements

5.1.1 Reliability

The GPS navigation system encompassing the user equipment, satellite vehicles and ground support equipment, must have a combined reliability equal to or surpassing that of alternative navigation systems. The GPS user equipment must therefore provide navigation data without operationally significant outages due to fades or multipath, assuming that the NAVSTAR constellation provides acceptable coverage.

5.1.2 Integrity

The GPS navigation system must not provide misleading information under any conditions of operational significance. It is therefore necessary that the GPS receiver continually monitor its own performance and indicate to the pilot when the navigation information displayed is no longer in compliance with the accuracy requirements.

Further, provisions must be incorporated to allow the pilot to verify that the navigation information is accurate using either built-in test equipment, an auxiliary test system, or a procedural check.

5.1.3 Compatibility

The GPS navigation system must provide a pilot interface which is compatible with existing air navigation systems.

5.2 Technical Requirements

5.2.1 Link Margin

The GPS receiver link margin, for all satellites above 5° elevation angle and with nominal effective radiated power, should be at least 3 dB during acquisition and at least 6 dB once a satellite is in track. These margins assume the aircraft is in level flight.

5.2.2 Startup

The receiver should automatically acquire and track all visible satellites.

5.2.3 Time-to-First-Fix

The receiver should automatically provide a first fix to the navigation display within 6 minutes of power on, unless the set has not been operated for longer than one month.

5.2.4 Continuous Navigation Solutions

The GPS receiver should provide position estimates or related navigation data derived from all satellites in view, to the navigation display at a 1 Hz rate.

5.2.5 Position Estimation

The position estimation algorithm should substitute a synthetic altitude (coast) if the HDOP, computed each fix interval, becomes unacceptably high, or if the number of satellites drops temporarily to three.

5.2.6 Performance Monitor

The performance monitor should perform the following tests:

Test	Action
Test satellite health data.	Delete unhealthy satellites.
Test pseudo-range for consistency with previous measurement or present prediction.	Do not use inconsistent values in the position estimator.
Test position estimation variance.	Set NAV FLAG to notify pilot of bad data if variance exceeds threshold.
Maintain coast timer.	Set NAV FLAG to notify pilot of bad data if coast time > T where T is selected so that an aircraft maneuver will not cause an error greater than the applicable FAA accuracy requirement.

References

1. HQ Space Division (AFSC), GPS Status Meeting, 4-6 June 1980.
2. J.C. Hansen etal, "NAVSTAR GPS Civil Applications Study", Final Report, INTRADYN (June 1979), SAMSO TR-79-63.
3. "Design Study of a Low Cost Civil Aviation GPS Receiver System", Magnavox (December 1979), NASA Contractor Report 159176.
4. FAA Advisory Circular 90 - 45A, February 21, 1975.
5. "Federal Radionavigation Plan", DOD - No. 4650.4 p. 11, Department of Transportation and Department of Defense, (July 1980).
6. Rockwell International, "NAVSTAR GPS Space Segment/Navigation User Interfaces," ICD-GPS-200, May 27, 1981.
7. B.D. Elrod and F.D. Natali, Stanford Telecommunications, Inc., "Investigation of a Preliminary GPS Receiver Design for General Aviation", STI/E-TR-8022, July 1978.
8. Aerospace Corporation, "Effects of Multipath on Coherent and Non Coherent PRN Ranging Receiver", TOR-0073 (3020-03)-3, May 1973.
9. General Dynamic Electronic Division, "Multipath Analysis", DRB D9000540B, Rev. 1 (February 1974).
10. General Dynamics, "Proposal for NAVSTAR GPS, Vol. 2, User System Segment, Technical Discussion, P3631007, June 1974.
11. "Cost Development of the Dual Channel GPS Navigator for General Aviation Applications", FAA Report EM-82-27, August 1982.
12. "EMC Analysis of the Civil-Use GPS Receiver on Four Specific Aircraft Configurations," DoD Electromagnetic Compatibility Analysis Center, ECAC-CR-82-048, April 1982 (Draft Report).

APPENDIX A

POSITION ESTIMATION ALGORITHM

The receiver software uses a least-squares fix which operates by batch processing a set of up to ten GPS pseudo-range measurements that are sequentially obtained by the receiver. The algorithm produces a new fix every 2.2 seconds. The algorithm is outlined in Figs. A-1 and A-2.

The algorithm begins by referencing all 10 measurements to a common time by utilizing the pseudo-range rate estimates derived from the receivers AFC loop, i.e,

$$PR_k(t_r) = PR_k(t_k) + \dot{PR}_k(t_k)\cdot[t_r - t_k]$$

where

t_r = common reference time

t_k = is the measurement time of the k-th satellite and

PR_R and $\dot{PR}_R$ are the pseudo-range and pseudo-range rate for the k-th satellite.

The common reference time is selected to be the mid point of the 2.2 second measurement batch interval in order to minimize prediction errors. Since the AFC loop has a tracking error standard deviation of 7 Hz (equivalent to a range rate of 4.1 feet per second), the measurement error contributed by the translation process is ≃ 4 feet, one-sigma.

The pseudo-range measurements are then corrected for propagation delay effects using the models shown in Table A-1.

Referring to Figure A-1, let $\underline{r}$ = (x,y,z) denote the user position vector in ECEF (earth-centered, earth-fixed) coordinates and let $\underline{p_i} = (x_i, y_i, z_i)$ denote the position vector of the i-th GPS satellite. The pseudo-range measurements are scalars given by:

$$m_i = |\underline{r} - \underline{p_i}| + \tau \qquad (1)$$

where τ is the receiver clock bias, normalized by the speed of light to units of distance. Equation (1) is expanded results in a Taylor series about the estimated user position, $\hat{r}$, and estimated receiver clock time $\hat{t}_r = t + \hat{\tau}$.

The equation is then linearized by neglecting all but first-order terms:

$$\Delta m_i = \frac{\partial m_i}{\partial \underline{r}} \Delta \underline{r} + \frac{\partial m_i}{\partial t} \Delta b \qquad (2)$$

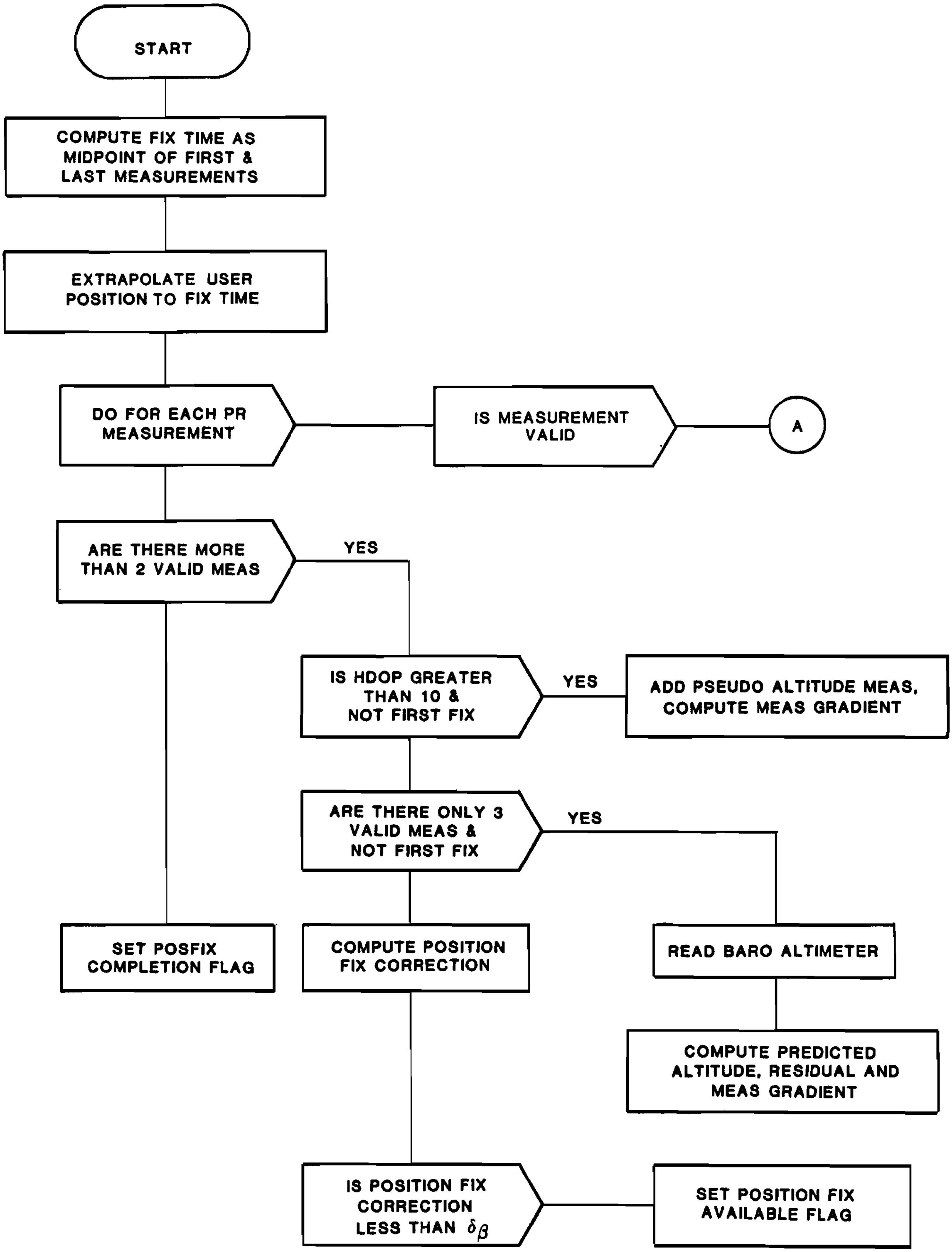

FIG. A-1. POSITION FIX ALGORITHM

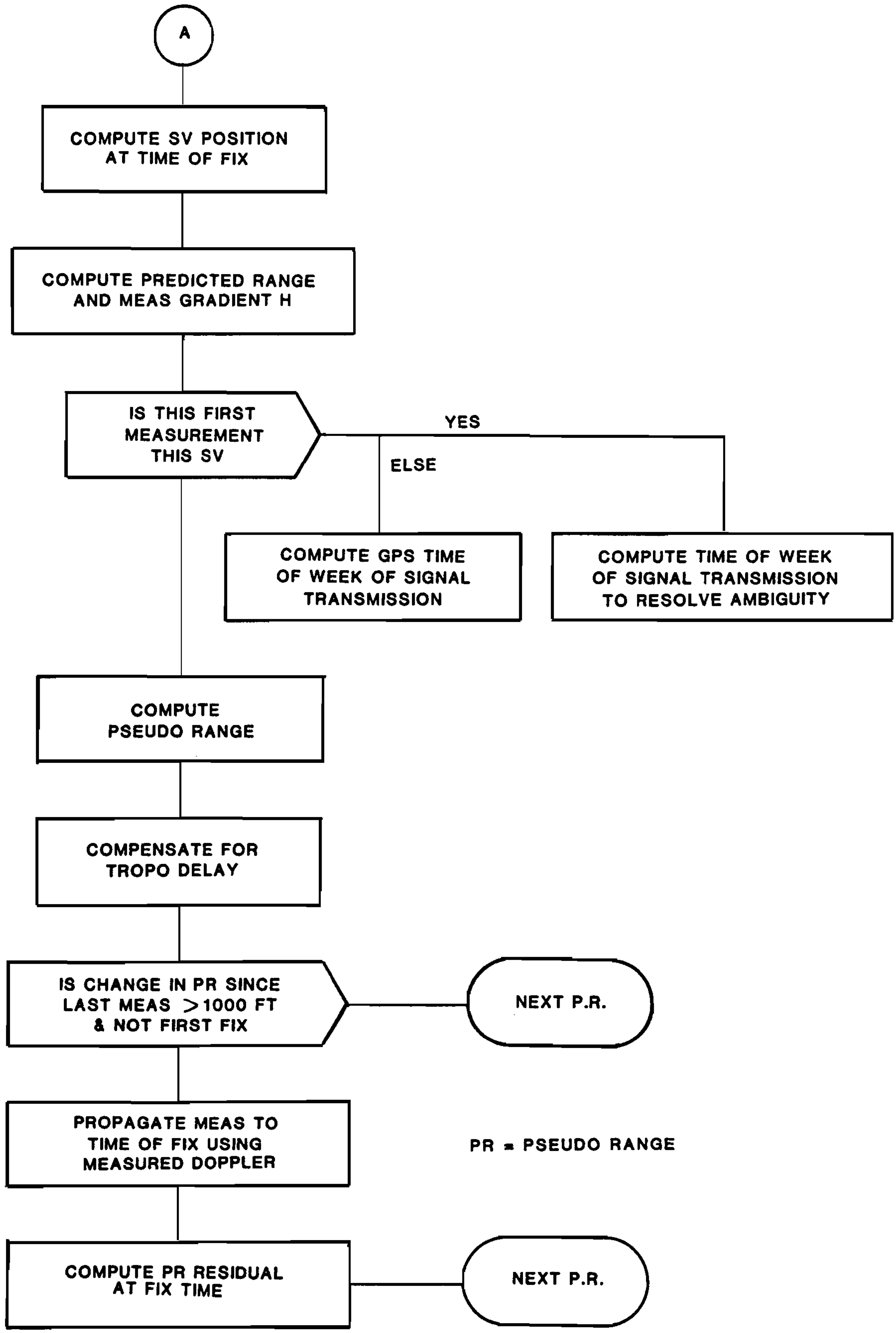

FIG. A-1. POSITION FIX ALGORITHM (CONT.)

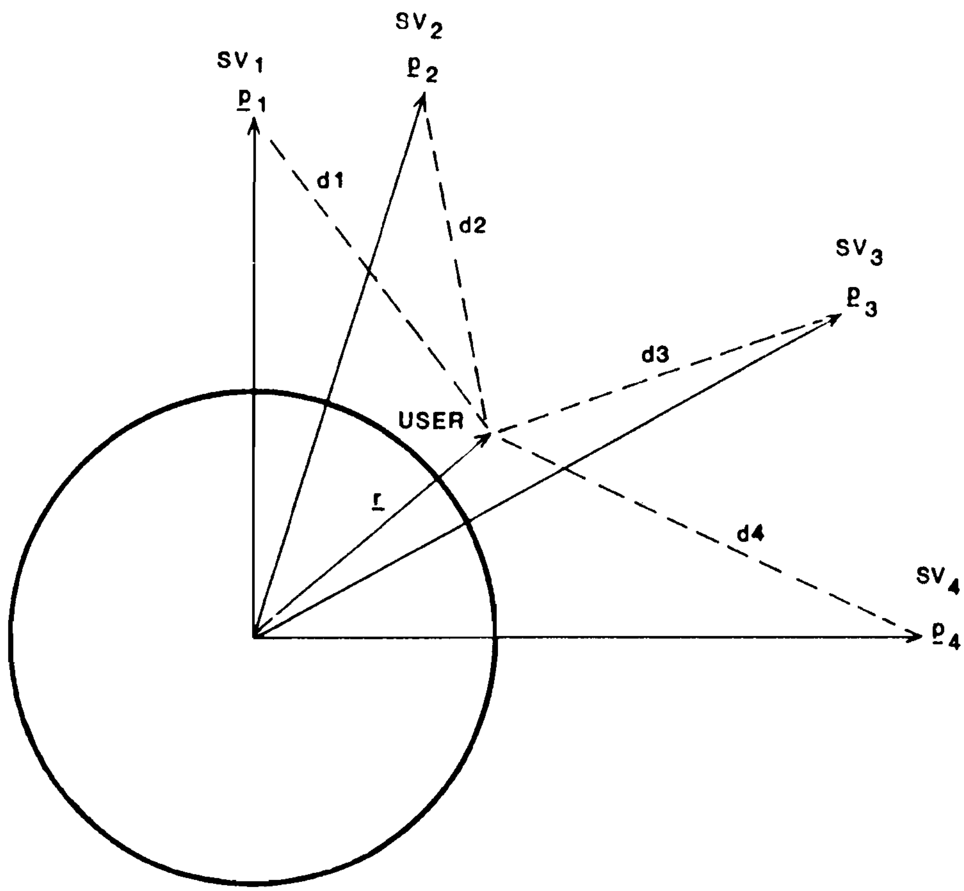

FIG. A-2. GPS POSITION FIXING GEOMETRY

TABLE A-1. SIGNAL PROPAGATION DELAY COMPENSATION MODELS

IONOSPHERIC [MODEL NOT IMPLEMENTED]

$$\hat{\varepsilon}_{IONO} = \theta(E)\left[d_1 + d_2 \cos\left(2\pi \left(\frac{t-14}{24}\right)\right)\right] \text{ (feet)}$$

$\theta = 1$, $E = 90°$, $\theta \approx 3$, $E = 5°$

E = elevation angle to the satellite

d_1 and d_2 are data base parameters

t is local time in hours

TROPOSPHERIC

$$\hat{\varepsilon}_{TROPO} = \frac{K}{\text{SinE}}\, e^{-h/h_s} \text{ (feet)}$$

$K = N_o h_s$

N_o = Sea level refractivity

h = estimated altitude

h_s = Exponential scale height (22500 ft above mean earth radius)

h = estimated altitude

E = satellite elevation angle

where $\Delta\underline{r} = \hat{r} - r$ and $\Delta b = \hat{t}_r - t_r = \hat{\tau} - \tau$. The Δm_i are the residual pseudo-range errors due to the user position estimate error, $\Delta\underline{r}$, and receiver clock bias estimate error, Δb. Rewriting equation (1), we have:

$$m_i = \left[(x-x_i)^2 + (y - y_i)^2 + (z - z_i)^2\right]^{1/2} + t_r - t$$

thus

$$\Delta m_i = \frac{(x - x_i)}{|\underline{r} - \underline{p}_i|} \Delta x + \frac{(y - y_i)}{|\underline{r} - \underline{p}_i|} \Delta y + \frac{(z - z_i)}{|\underline{r} - \underline{p}_i|} \Delta z - \Delta b$$

$$= [h_{i1}, h_{i2}, h_{i3}, -1] \bullet \left[\frac{\Delta r}{\Delta b}\right]$$

where the h_{ij} are the direction cosines from satellite i to the user position.

When N measurements are available ($N \geq 4$), Δm in matrix form becomes:

$$\Delta\underline{m} = H \bullet \left[\frac{\Delta r}{\Delta r}\right]$$

$$= H \bullet \Delta\underline{S}$$

where H is an N x 4 matrix and $\Delta\underline{m}$ is an N-dimensional vector. Solving for $\Delta\underline{S}$:

$$\Delta\underline{S} = \frac{\Delta r}{\Delta b} = (H^T H)^{-1} H^T \Delta\underline{m} \qquad (3)$$

In the special case of N=4, then $(H^T H)^{-1} H^T = H^{-1}$.

The resulting values of $\Delta\underline{r}$ and Δb are used to correct the previous user position and clock bias estimates to produce new estimates for the next measurement cycle.

The batch-processing method allows the data for all satellites in view to be utilized to produce a position fix, and obviates the need for a satellite selection algorithm, since the position fix utilizing all N satellites will have better GDOP than any subset of four of the satellites. Furthermore, it can be shown that the residual error is minimized in the least-squares sense by equation (3), under the linearity assumption of equation (2).

APPENDIX B

POSITION ESTIMATION FILTER

The position estimates developed by the algorithm described in Appendix A are processed by a filter (tracker) before they are released to the navigation software.

An alpha-beta fixed gain filter was selected following a study of tracker alternatives. The filter operates on X, Y, Z and t to produce X, Y, Z, $\dot{X}$, $\dot{Y}$, $\dot{Z}$, t and $\dot{t}$. The velocity gain is related to the position gain by $\beta = \sigma^2/(2-\sigma)$. Figure B-1 shows the general flow for the tracker.

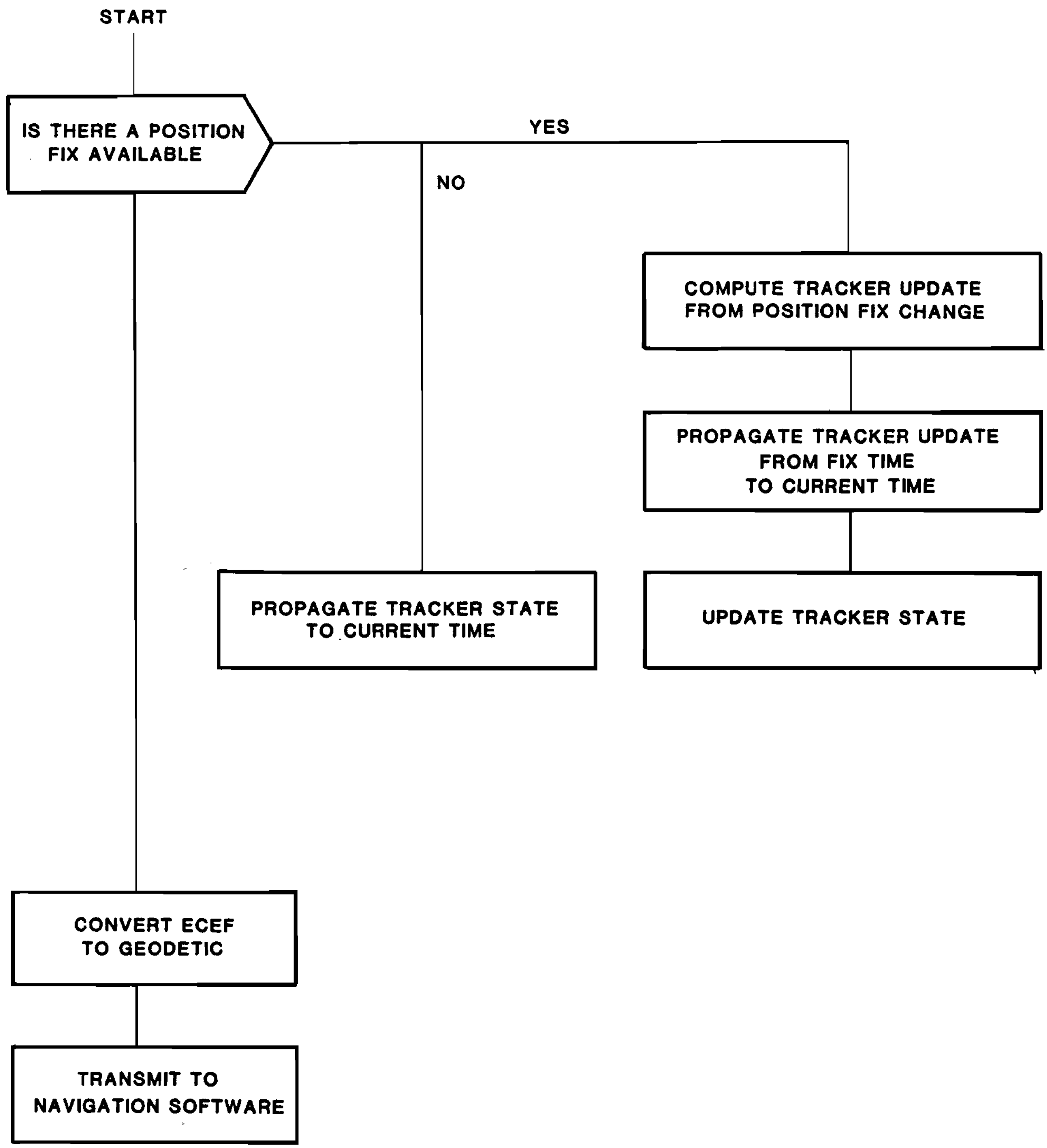

FIG. B-1. POSITION ESTIMATION TRACKER

APPENDIX C

COORDINATE CONVERSION ALGORITHM

In order to compare the actual aircraft position, as estimated by the Mode S Facility, with recorded GPS T&E position estimates it is necessary to to convert the GPS estimate coordinates to Mode S Facility local coordinates. The latter is described in the following paragraphs.

The three coordinate systems of concern are: (1) earth centered earth fixed (ECEF), (2) local, and (3) geodetic. The ECEF system is a Cartesian coordinate system fixed to the earth and defined such that the z-axis points toward the North pole, the x-axis points out along the intersection of the Greenwich meridian and the equator, with the y-axis chosen to complete a right-handed coordinate system. A local system is constructed so that the x-axis points east, the y-axis points north and the z-axis points "up". The geodetic coordinates consist of longitude, latitude, and altitude above sea level.

Conversions between these coordinate systems depend on the model used for the surface of the earth. For this effort the WGS-72 model was selected. WGS-72 is an ellipsoid of revolution whose semi-major (equatorial) radius is 6378135.0 meters, and whose semi-minor (polar) radius is 6356750.5 meters.

Conversion from local coordinates to ECEF (and inversely) requires a rotation and a translation. (The rotation, in effect, aligns the coordinate axes and the translation displaces the origin). If P is a point whose coordinates in the local system are expressed as the three-vector quantity $\nu = (x,y,z)$, then its coordinates in ECEF, $V = (X,Y,Z)$ are given, in general, by:

$$V = R\nu + D \qquad [1]$$

where R is a 3x3 rotation matrix and D is the ECEF three-vector coordinate of the origin of the local system. The inverse conversion, is given by

$$\nu = R^T (V - D) \qquad [2]$$

where R^T is the transpose of R (which is equal to its inverse).

To state the transformation between a local system and ECEF coordinates, let θ be the longitude, λ be the geodetic latitude and λ' be the geocentric latitude of the local coordinate system. Then the rotation matrix is given by:

$$R = \begin{vmatrix} -\sin\theta & -\cos\theta\sin\lambda & \cos\theta\cos\lambda \\ \cos\theta & -\sin\theta\sin\lambda & \sin\theta\cos\lambda \\ 0 & \cos\lambda & \sin\lambda \end{vmatrix} \qquad [3]$$

To compute D, we need to consider the following geometry:

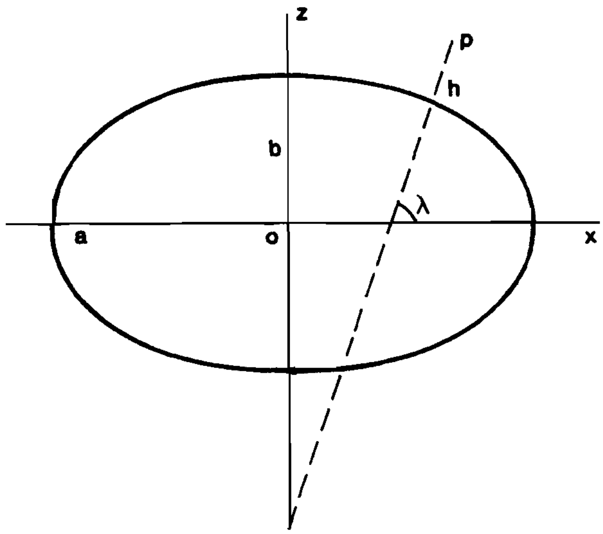

Let a be the equatorial radius, b be the polar radius, and $\varepsilon^2 = \frac{a^2 - b^2}{a^2}$ be the numerical eccentricity. From the equation for an elipse, $\frac{X^2}{a^2} + \frac{Z^2}{b^2} = 1$ it can be shown that:

$$D_z = [d(1-\varepsilon^2) + h] \sin \lambda$$

$$D_x = (d + h) \cos \lambda \cos \theta \qquad [4]$$

$$D_y = (d + h) \cos \lambda \sin \theta$$

where:

$$d = \frac{a}{\sqrt{1-\varepsilon^2 \sin^2 \lambda}}$$

and h is the height (altitude) of the local system. Thus equations [3] and [4] convert local coordinates to ECEF coordinates.

Using R and D, conversion from local coordinates to ECEF coordinates and back can be accomplished. If, for example, the coordinates of a satellite are given in a horizon system (azimuth, elevation, and slant range) these coordinates can be converted to local x,y,z and then to ECEF. A difficulty arises, however, when converting the Mode S Facility reported position of a target to its own local coordinates. The difficulty arises because target reports give altitude rather than elevation angle. Because of this, the local z-axis coordinate of the target is not directly known, but must be computed, and the computation depends upon the model of the earth. The exact solution using an ellipsoid model of the earth involves solving a fourth order equation. A simple spherical model allows a direct calculation and in practice has shown to be accurate to 0.1 meters to a range of 30 nm. The geometry and result is shown below.

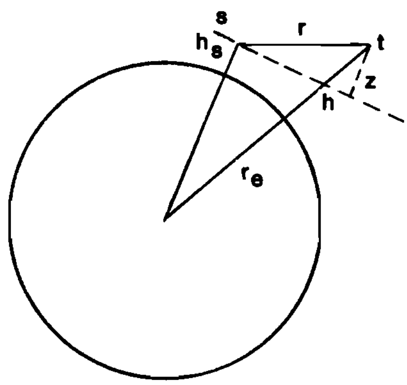

$$z = \frac{h^2 - h_s^2 + 2(h-h_s)\, r_e - r^2}{2(r_e + h_s)}$$

where:

h is the reported altitude,

h_s is the altitude of the local system,

r is the slant range, and

$r_e = \frac{a+b}{2}$ is the average earth radius.

☆ U. S. GOVERNMENT PRINTING OFFICE: 198400700-000--54